UNIVERSITE DE STRASBOURG

ECOLE DOCTORALE DES SCIENCES DE LA VIE ET DE LA SANTE

THESE

Présentée pour obtenir le grade de

Docteur de l'Université de Strasbourg

Discipline : Sciences du Vivant- Aspects Moléculaires et Cellulaires de la Biologie

Spécialité : Immunologie

Par

Estelle Hess

RANK and the regulation of lymph node and skin homeostasis

Directeur de Thèse: Dr Christopher Mueller

Soutenance publique le 13 Septembre 2011

Membres du jury

Rapporteur externe :   Pr Burkhard Ludewig

Rapporteur externe :   Dr Rachel Golub

Examinateur :   Dr Bernardo Reina

Membre invité :   Dr Sylviane Muller

Acknowledgments

I am grateful to the members of my jury, Pr Burkard Ludewig (Institute of Immunobiology, Kantonsspital St Gallen, Swiss), Dr Rachel Golub (Institut Pasteur, Paris), Dr Bernardo Reina (IGBMC, Strasbourg) for accepting to evaluate this work.

Je remercie le Dr Sylviane Muller, directrice de l'unité Immunologie et Chimie thérapeutiques (UPR9021), de m'avoir accueillie dans son laboratoire et d'avoir accepté de participer à mon jury.

Je tiens à exprimer tout particulièrement mes remerciements à mon directeur de thèse, le Dr Christopher Mueller, pour avoir encadré mon travail pendant ces 5 années passées à l'ICT. Même si j'ai parfois eu du mal à te suivre dans ta revendication du droit pour les scientifiques d'avoir des idées folles, tu as su te montrer disponible pour me soutenir et m'encourager pendant toutes ces années.

Merci à toi mon Schtroumpf couillon pour avoir été présent pendant 3 ans à mes côtés pendant les bons moments et aussi pendant les galères de manips. Nos discussions m'auront beaucoup manquées pendant ma fin de thèse.

Merci à toi Monique pour m'avoir aidée à gérer nos lignées de souris mais aussi pour ta bonne humeur et tous ces moments passés ensemble, autour d'un plateau repas ou pendant mes injections en tous genres !

Merci à toi Maya, tu auras toujours été là pour me donner des conseils et pour m'écouter dans les moments de galère quand mes manips n'en faisaient qu'à leur tête ! On a fait un petit bout de chemin depuis le Master 1 !

Merci à tous mes collègues actuels et passés de l'ICT avec qui j'ai apprécié de travailler pendant ces années. Raquel pour tous ces « spanish diner » et autres bons moments partagés ensemble pendant ton séjour à Strasbourg. Akkiz pour ta gentillesse, ta joie de vivre et ton sourire que je n'aurai vu que très rarement quitter ton visage. Marion pour tous tes précieux conseils de microscopiste avisée mais aussi pour nos discussion autour d'un ultramicrotome ou d'un cryostat. Hortense pour ta bonne humeur et pour tous nos délires schtroumpfesques. Julien pour ces moments partagés autour de pots de Macadamia Nut Brittle. Fred pour tes conseils scientifiques avisés et ta constante bonne humeur. Susana pour nos moments partagés en 138b. Pierre pour toutes nos discussion et ta passion pour la l'histoire et la philosophie des sciences. Merci aussi à Stef, Cristian, Paul, Hayet et tout ceux que j'oublie de citer ici.

Un grand merci à ma famille, à mes parents, à ma sœur et à la famille de Matt pour m'avoir encouragée tout au long de ce parcours initiatique qu'est la thèse sans toujours comprendre vraiment ce que je faisais avec cette molécule au nom étrange.

Merci à toi Matt pour m'avoir supporté dans tous les sens du terme ! Merci pour tes encouragements, tes conseils, ta patience, tes corrections anti-virgules intempestives… Tu es toujours là pour faire relativiser l'éternelle stressée que je suis. Me voilà presque arrivée au bout du parcours pour enfin te rejoindre au pays de la bière et de la frite !

Table of contents

Abstracts

List of abbreviations

Introduction

Abstract

The receptor activator of NF-κB (RANK) is known to control bone mass and development of the skin appendages. This, and its function in epithelial cell biology in general, incited us to investigate the role of RANK in skin and hair follicles (HFs). We show that mice deficient in RANK or RANK-ligand (RANKL) are unable to initiate a new growth phase of the hair cycle and display arrested epidermal homeostasis. Transgenic mice overexpressing RANK in the HF and administration of recombinant RANKL activate the hair cycle and epidermal growth. RANK is expressed by HF stem cells and RANKL is actively transcribed by the growing HF supporting a role of RANK-activation of stem cells for hair cycle entry.

In addition to its function in bone and skin, RANK is required for development of lymph nodes (LNs), a feature shared with lymphotoxin β receptor (LTβR). However, LTβR is further involved in the maintenance of LN organization, which had not been demonstrated for RANK. We therefore addressed the question of the function of RANK in LNs beyond development. For this, we took advantage of the transgenic mice overexpressing RANK in the HF, as they displayed a massive post-natal growth of skin-draining LNs. They displayed conserved proportions of hematopoietic and stromal cells, but an increase in the number of small B cell follicles. We showed that skin-derived RANKL induces LN stromal cell proliferation and expression of chemokines and adhesion molecules, resulting in the LN growth. This work highlighted an additional function for RANK-signaling in LNs, namely its control of LN plasticity, and underlines the importance of tissue-derived cues for secondary lymphoid organ homeostasis.

French abstract

Introduction

La protéine RANKL (Receptor Activator of Nuclear Factor-κB Ligand) est un membre de la superfamille du TNF (Tumor Necrosis Factor) qui se présente sous une forme membranaire homotrimérique pouvant être clivée et secrétée. La trimérisation de son récepteur membranaire RANK induit l'activation de multiples voies de signalisation, dont la voie NF-κB, Calcineurine/ NFAT (Nuclear Factor of Activated T cells), MAPK (Mitogen-Activated Protein Kinase) et PKB/Akt (Protéine Kinase B). Un deuxième récepteur soluble leurre, connu sous le nom d'ostéoprotégérine (OPG), permet d'inhiber l'interaction entre RANKL et RANK (Figure 1a). Ces trois protéines ont été décrites comme étant impliquées dans la communication entre cellules T et cellules dendritiques, dans la maturation des ostéoclastes (cellules spécialisées dans la résorption de la matrice osseuse) et dans la formation des glandes mammaires durant le processus de lactation. En plus de sa fonction dans la biologie des cellules dendritiques, la triade RANK-RANKL-OPG est également impliquée dans l'organogenèse des ganglions lymphatiques et dans l'induction de la tolérance immune, renforçant encore son rôle dans le système immunitaire (Figure 1b).
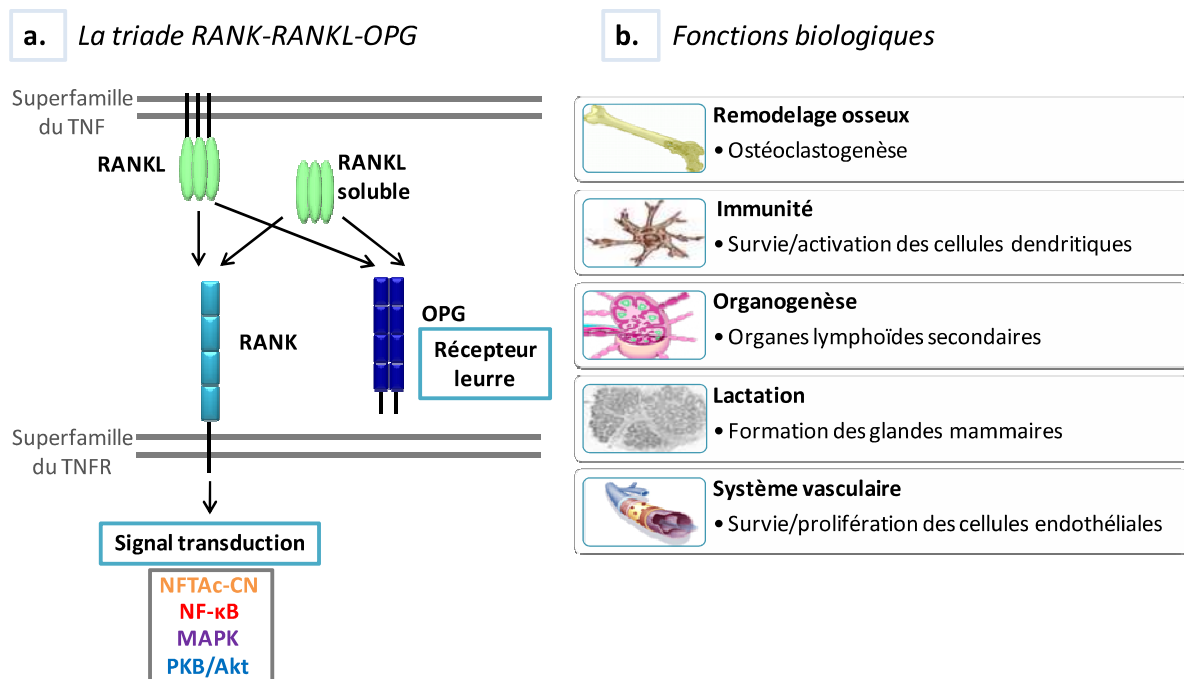
Figure 1 : La triade RANK, RANKL et OPG. Représentation schématique des interactions entre les membres de la triade RANK, RNALK et OPG (a), ainsi que de leurs fonctions biologiques (b).

Durant mon doctorat je me suis intéressée au rôle de RANK dans l'homéostasie de la peau et du ganglion lymphatique. En effet, RANK est impliqué dans la formation des appendices de la peau que sont les glandes mammaires et les dents. Le follicule pileux qui est un autre appendice de la peau est constamment remodelé par des cycles de phases alternées de croissance (anagen), de régression (catagen) et de repos (telogen) et une similitude est notable entre les mécanismes impliqués dans ces cycles et dans l'ostéoclastogenèse. A la vue du rôle de RANK et RANKL dans la biologie de nombreuses cellules épithéliales comme les cellules épithéliales mammaire, de la prostate, du thymus, ou encore de l'intestin, notre équipe s'est penchée sur l'étude du rôle potentiel de ces protéines dans le cycle du follicule pileux et dans le renouvellement constant des kératinocytes de l'épiderme (Figure 2a).

Vers de nouvelles fonctions pour RANK-RANKL-OPG :

a. dans la peau et son follicule pileux ?   **b. dans les ganglions lymphatiques?**
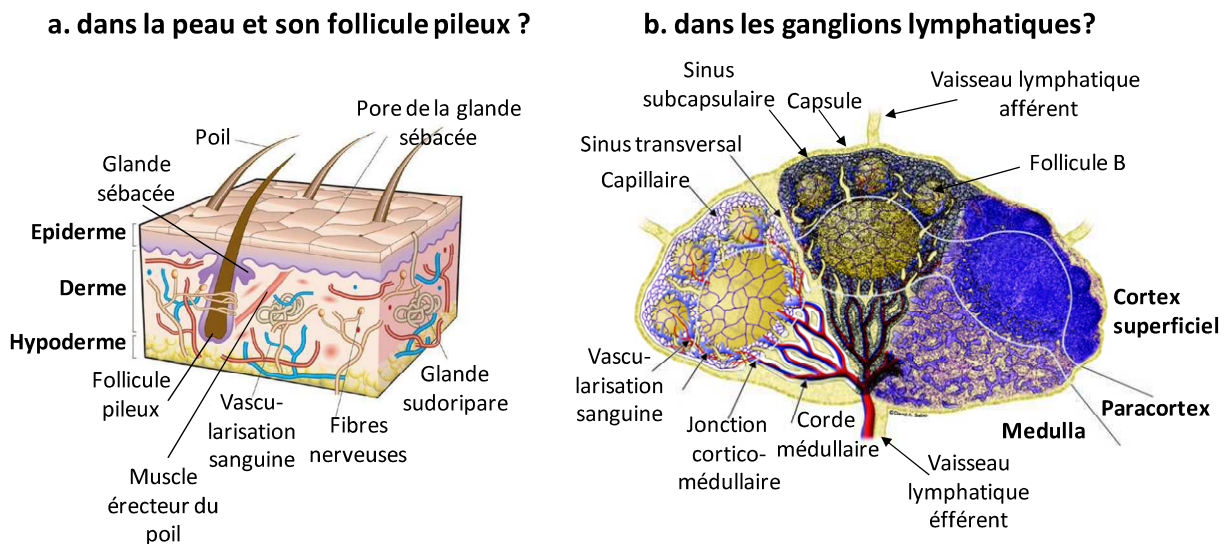
Figure 2 : Représentation schématique des structures de la peau(a) et des ganglions lymphatiques(b).

En parallèle, je me suis intéressée au rôle de RANK dans le ganglion lymphatique adulte. En effet, au cours de l'embryogenèse RANKL est requis pour la survie et/ou la prolifération des cellules induisant la formation des tissues lymphoïdes (LTics pour Lymphoïd Tissue inducer cells), néanmoins l'absence de ganglions chez les souris déficientes en RANK ou RANKL a compliqué l'étude de l'activité de ces protéines dans le ganglion adulte. Au cours du développement du ganglion, deux autres membres des familles du TNF et du TNFR sont requis : LTα1β2 (Lymphotoxin α1β2) et LTβR (LTβ Receptor). En l'absence de LTics ou de la voie de signalisation LTβR, les ganglions lymphatiques ne se développent pas. En plus de son rôle développemental, la voie LTβR est essentielle pour l'organisation des follicules B dans le ganglion adulte. De manière analogue, RANKL semble aussi être requis pour la formation des follicules B mais, contrairement à LTα1β2, les données

concernant RANK ne sont qu'indirectes. Ces similitudes de fonctions entre RANK et LTβR an niveau du développement et de l'architecture des follicules B, ainsi que le rôle de RANK dans la prolifération et la survie des cellules endothéliales laissent suggérer un possible rôle de RANK dans l'organisation et/ou l'homéostasie du ganglion adulte (Figure 2b).

Ainsi les objectifs durant ma thèse ont été d'élucider les fonctions de RANK dans l'homéostasie de la peau et du ganglion lymphatique adulte. Pour cela, j'ai étudié deux modèles murins, le premier étant une souris déficiente pour RANKL et le deuxième une souris sur-exprimant RANK sous le contrôle du promoteur S1008A (S100 calcium-binding protein A8) actif dans la lignée granulo-myéloïde et dans la peau (Figure 3).
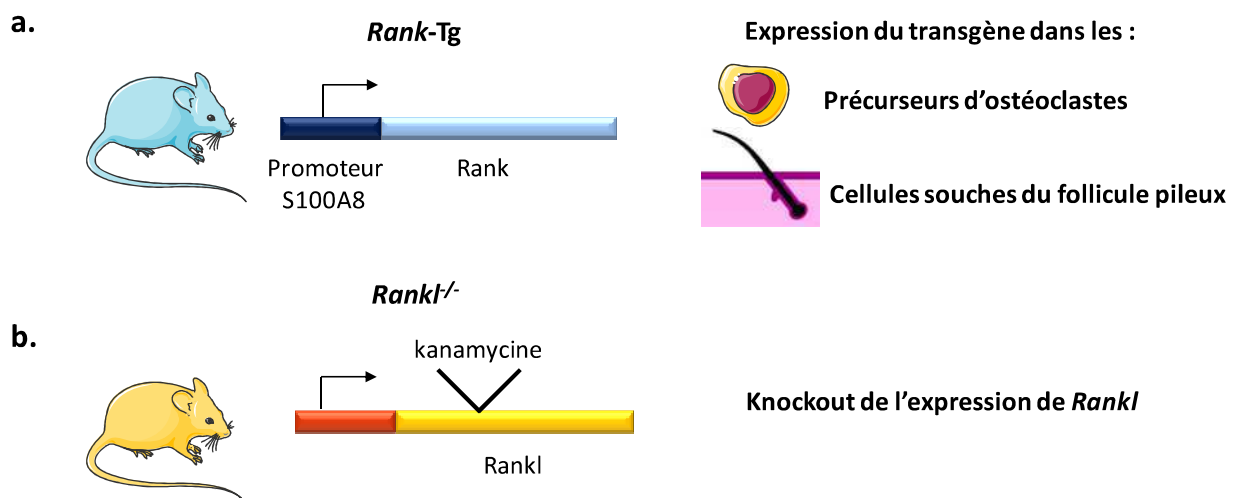
Figure 3 : Modèles murins utilisées pour l'étude de la fonction de la triade RANK-RANKL-OPG dans l'homéostasie de la peau et du ganglion lymphatique. Deux modèles ont été utilisés : une souris sur-exprimant la protéine RANK murine sous le contrôle du promoteur humain S100A8 (S 100 calcium binding protein A8) actif dans la lignée des précurseurs d'ostéoclastes et dans les cellules souches de la peau (a) et une souris dans laquelle l'expression de Rankl a été interrompu par l'insertion du gène codant pour la kanamycine.

Résultats

1.   RANKL régule le cycle du follicule pileux et l'homéostasie de l'épiderme

Nous avons montré que RANK est exprimée par les cellules souches du follicule pileux (Figure 4a). Durant la progression du cycle d'une phase de repos (telogen) vers l'anagen, l'expression d'OPG diminue alors que le niveau de RANKL augmente (Figure 4b).
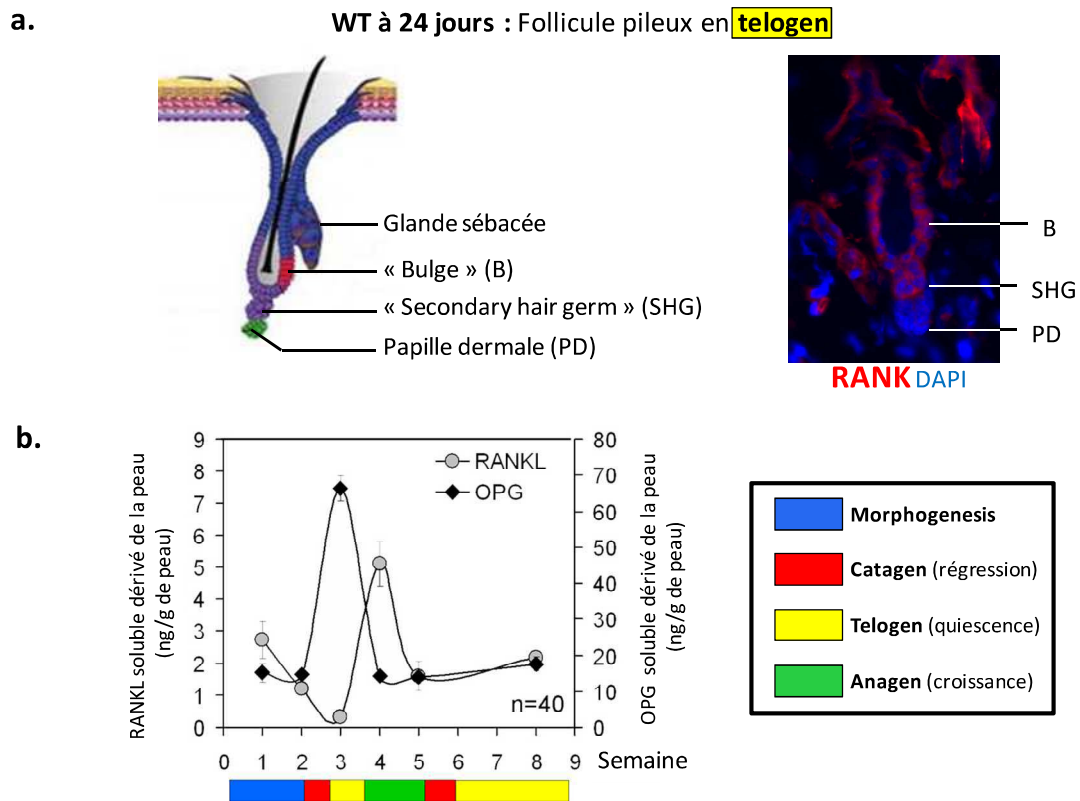
Figure 4 : Expression de RANK-RANKL-OPG dans la peau et son follicule pileux. Localisation de l'expression de RANK dans les cellules souches du follicules pileux par immunofluorescence sur coupes congelées de peau de souris WT âgées de 24 jours (a). Mesures par ELISA de RANKL et OPG solubles dans des cultures d'explants de peau aux jours indiqués chez des souris WT (b). (Des informations supplémentaires sur les protocoles utilisés peuvent trouver dans Duhéron et al. Proc Natl Acad Sci USA 2011 Mar 29;108(13):5342-7).

De plus, les souris déficientes pour RANKL présentent une morphogenèse des follicules pileux comparable à celle des souris sauvages, mais aucune phase de croissance du follicule pileux (anagen) n'a pu être observée chez ces souris (Figure 5a). La restauration du développement de l'anagen lors de la transplantation de peau de souris déficiente pour RANKL sur des souris *nude* a montré que les cellules souches du follicule pileux ne sont pas défectueuses. Ainsi, ces données nous ont permis de proposer un mécanisme dans lequel le niveau de RANKL, non associé à OPG, augmente durant la progression du cycle vers l'anagen, permettant la liaison de RANKL à RANK porté par les cellules souches et induisant leur activation. Cette hypothèse a été confirmé d'une part par l'entrée en

anagen de souris sauvages traitées par application de RANKL (Figure 5c). D'autre part le modèle murin transgénique pour RANK, surexprime RANK dans les cellules souches du follicule pileux et présente une entrée en anagen plus précoce, ainsi que de plus nombreux cycles, confirmant la fonction de RANK dans l'entrée en anagen (Figure 5b). Alors que les souris déficientes pour RANKL présentent un épithélium plus fin que les souris sauvages, celui de la souris transgénique pour RANK est plus épais que la souris sauvage (Figure 5d). Cet épaississement de l'épithélium est associé à une forte prolifération de kératinocytes basaux exprimant RANK endogène, alors que ces mêmes cellules chez les souris déficientes pour RANKL ne prolifèrent pas. Ceci nous a permis de suggérer que la protéine RANK active la prolifération des kératinocytes de l'épithélium.
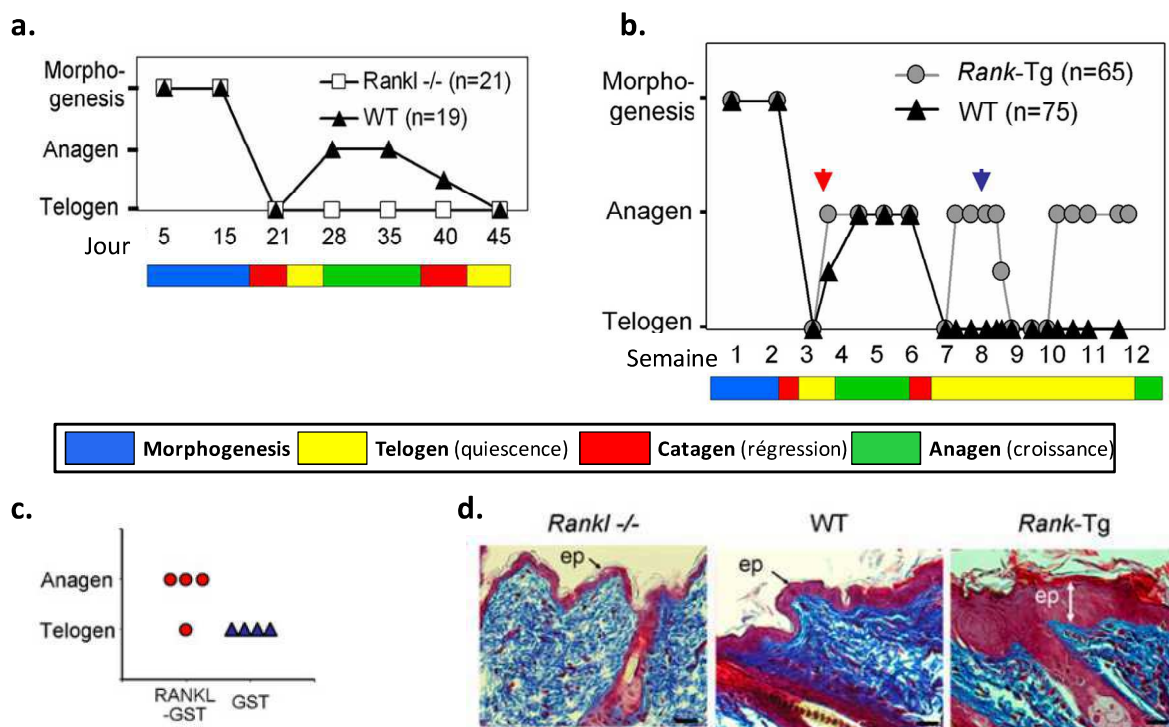
Figure 5 : Rôle de RANK-RANKL-OPG dans le cycle du follicule pileux et dans l'épithélium de l'épiderme. Représentation schématique du cycle du follicule pileux dans des souris *Rankl*^{-/-} (a) et dans les souris *Rank*-Tg (b) à différents âges déterminé sur des coupes de peau incluses en paraffine et colorées par de l'hématoxyline/éosine. Représentation schématique du statut du follicule pileux de souris WT de 8 semaines (en telogen) 6 jours après deux injections sous cutanée de 100µg de RANKL-GST ou GST contrôle. Analyse faite sur des coupe de peau incluses en paraffine et colorées par de l'hématoxyline/éosine (c). Photographie représentative de l'épaisseur de l'épiderme chez les souris *Rankl*^{-/-}, *Rank*-Tg et WT agées de 28 jours. Analyse faite sur des coupe de peau incluses en paraffine et colorées par de l'hématoxyline/éosine (d). (Des informations supplémentaires sur les protocoles utilisés peuvent trouver dans Duhéron et al. Proc Natl Acad Sci USA 2011 Mar 29;108(13):5342-7).

Ainsi, ce travail nous a permis de démontrer pour la première fois l'implication de la triade RANK-RANKL-OPG dans le contrôle du cycle du follicule pileux et dans l'homéostasie de l'épiderme.

2. RANKL induit la croissance organisée du ganglion lymphatique par le biais de la prolifération des cellules stromales

Les souris transgéniques pour RANK présentent une croissance post-natale importante des ganglions lymphatiques drainant la peau (Figure 6a). Dans ces ganglions hyperplasiques, les proportions de cellules hématopoïétiques et de cellules stromales ainsi que leur organisation sont maintenues à l'exception d'une augmentation du nombre de follicules B associée à une diminution de leurs tailles (Figure 6b). Nous avons démontré que les cellules immunes de ces souris ne sont pas activées et répondent correctement aux stimulations faites par des antigènes et des adjuvants, cette hyperplasie n'est donc pas le résultat d'une inflammation. Des expériences de transfert de moelle dans des souris irradiées de manière létale ont montré que l'hyperplasie était due à l'expression du transgène dans des cellules radio-résistantes (Figure 6c). De plus, des expériences de greffe de peau ont montré que le signal nécessaire à l'induction de la croissance ganglionnaire provenait de la peau(Figure 6d).
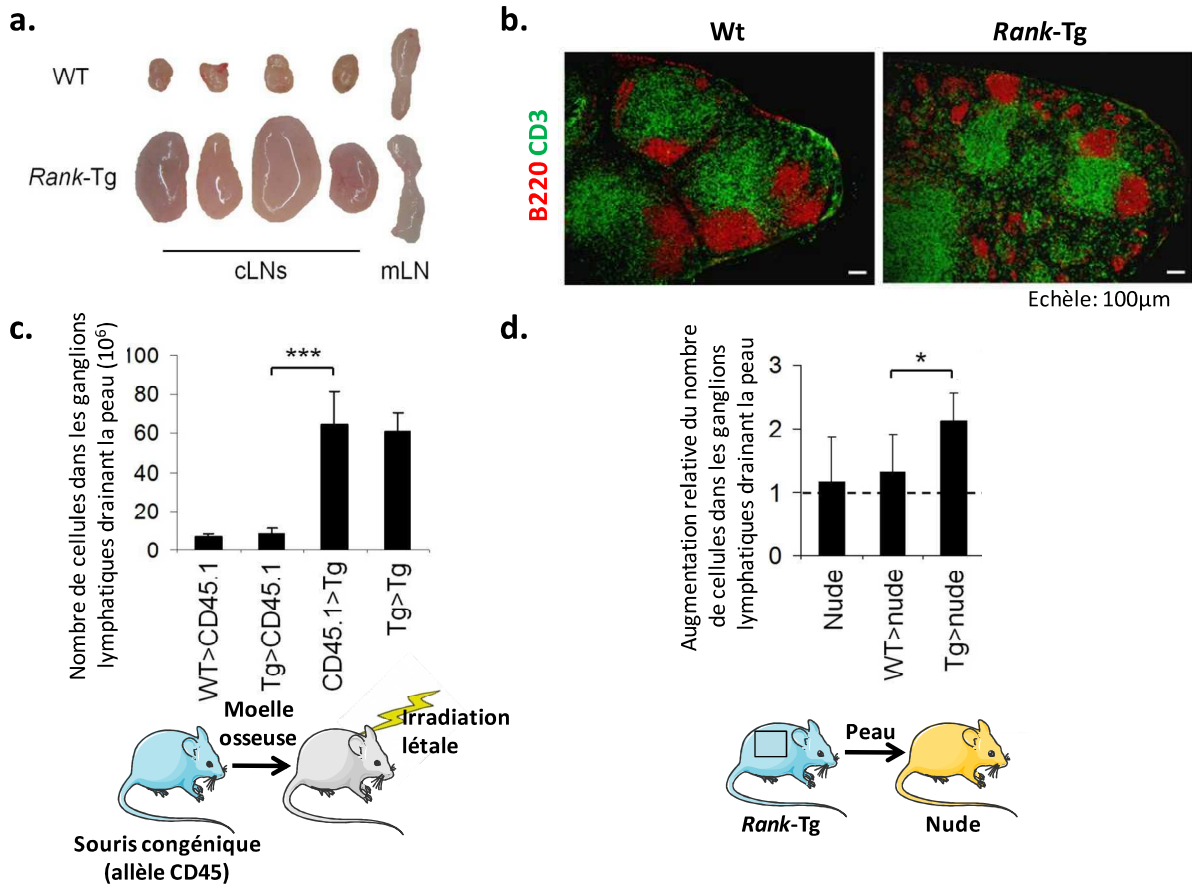
Figure 6 : Hyperplasie des ganglions lymphatiques drainant la peau des souris *Rank*-Tg et son origine cutanée. Photographie représentative des ganglions lymphatiques cutanés (cLNs) et mésentériques (mLNs) de souris *Rank*-Tg et WT de 12 semaines (a). Image représentative de l'organisation des zones B (B220) et T (CD3) déterminé par immunofluorescence sur des coupes congelées de ganglions lymphatiques cutanés de souris *Rank*-Tg et WT de 8 semaines (b). Analyse du nombre de cellules dans les ganglions lymphatiques cutanés suite aux transferts de moelle après irradiation létale (c). Analyse du nombre de cellules dans les ganglions lymphatiques cutanés après une greffe de peau (d). (Des informations supplémentaires sur les protocoles utilisés peuvent trouver dans Hess et al. J Immunol. 2012 Feb 1;188(3):1245-54).

Nous avons montré que RANKL sous une forme soluble est surexprimé dans les follicules pileux des souris transgéniques pour RANK. En neutralisant RANKL grâce à un traitement avec un anticorps anti-RANKL, nous avons restauré une taille normale des ganglions hyperplasiques et un nombre et une taille normale des follicules B (Figure 7a et b). Ces résultats montrent que RANKL sur-produit par la peau est le signal responsable de l'hyperplasie. Les cellules stromales de la zone T (fibroblastic reticular cells) ainsi que les cellules stromales vasculaires (cellules endothéliales sanguines et lymphatiques) ont un rôle critique dans la formation et l'organisation des organes lymphoïdes. Nous avons montré que ces cellules expriment RANK et hyper-prolifèrent et que cette hyper-prolifération est supprimée par le traitement avec l'anticorps bloquant RANKL (Figure 7c). De plus, les cellules stromales des souris transgéniques pour RANK expriment plus de chemokines et plus de molécules d'adhésion, conduisant ainsi à un recrutement soutenu de lymphocytes.
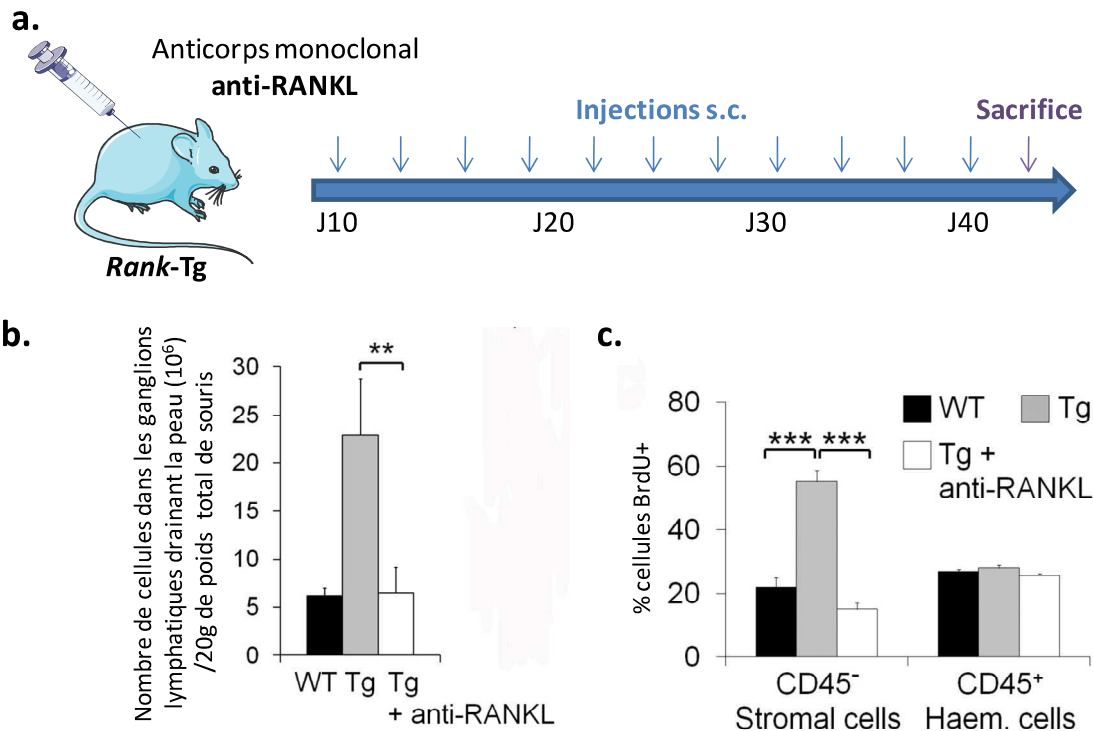
Figure 7 : RANKL induit la prolifération des cellules stromales conduisant à la croissance des ganglions. Représentation du protocole de traitement des souris *Rank*-Tg par un anticorps monoclonal anti-RANKL (a). Représentation du comptage des cellules des ganglions lymphatiques drainant la peau de souris WT, *Rank*-Tg traitées avec un anticorps contrôle ou avec un anti-RANKL (b). Analyse de la prolifération des cellules hématopoïétiques (CD45$^+$) et stromales (CD45$^-$) grâce à la mesure de l'incorporation de BrdU par cytométrie en flux chez des souris WT, *Rank*-Tg traitées avec un anticorps contrôle ou avec un anti-RANKL (c). (Plus d'informations concernant les protocoles utilisés peuvent être trouvé dans Hess et al. J Immunol. 2012 Feb 1;188(3):1245-54).

Ces données ont abouti à une proposition de modèle dans lequel l'activation de RANK induit la croissance ganglionnaire par la prolifération des cellules stromales et leur expression de molécules impliquées dans le recrutement de lymphocytes (Figure 8).
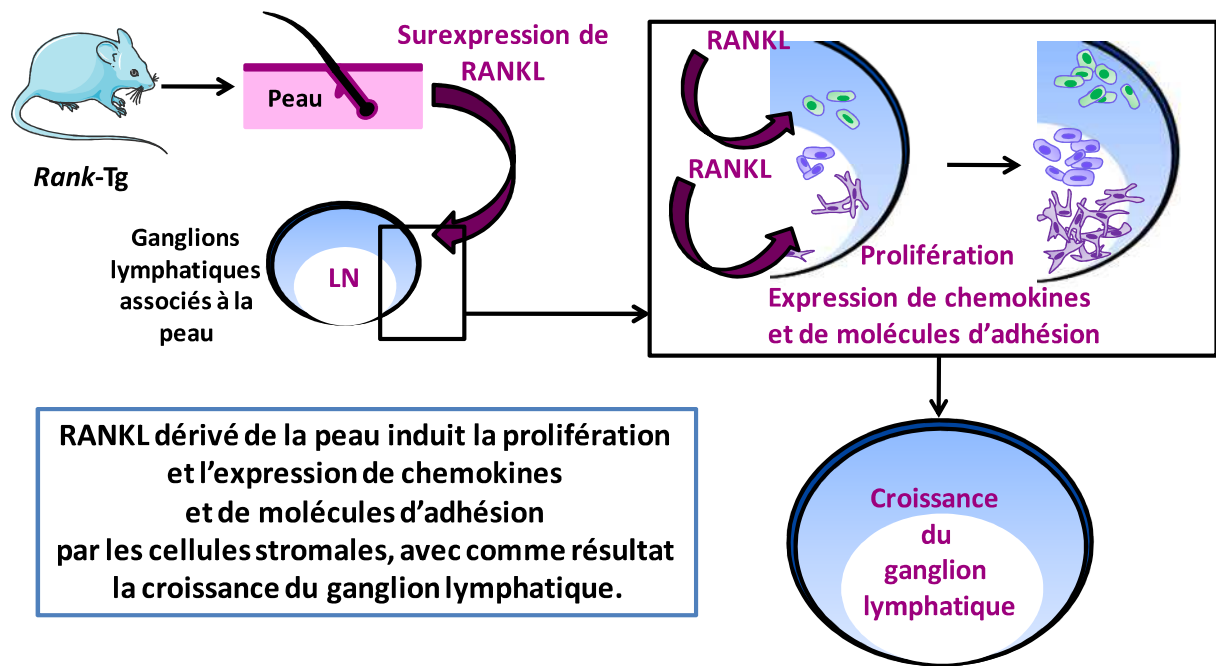
Figure 8 : Modèle du mécanisme responsable de l'hyperplasie des ganglions lymphatiques chez la souris *Rank*-Tg. Les souris *Rank*-Tg sur-expriment RANK dans leurs follicules pileux entrainant une boucle positive de surexpression de RANKL soluble. RANKL soluble dérivé de la peau induit la prolifération et l'expression de chemokines et de molécules d'adhésion par les cellules stromales des ganglions lymphatiques. Ce mécanisme aboutissant à la croissance des ganglions lymphatiques.

Ainsi, ce travail nous a permis de démontrer pour la première fois l'implication de la triade RANK-RANKL-OPG dans la biologie des ganglions lymphatiques après leur développement *in utero* en établissant que RANKL contrôle la plasticité de ces organes chez la souris adulte.

Conclusions et perspectives

Alors que la triade RANK-RANKL-OPG était déjà décrite comme impliquée dans le système osseux et le système immunitaire, les résultats obtenus au cours de cette thèse ont mis en évidence un domaine supplémentaire d'action à ces protéines, à savoir la peau. En effet, RANK régule le renouvellement du follicule pileux et l'homéostasie de l'épiderme. De plus, dans notre modèle murin de surexpression de RANK, RANKL sécrété par le follicule pileux induit la prolifération des cellules stromales et la croissance organisée du ganglion lymphatique drainant la peau. Cette découverte permet de souligner l'importance des signaux dérivés des tissus avoisinant les organes lymphoïdes pour l'organisation de ces derniers et d'identifier RANKL comme une molécule contrôlant la plasticité du ganglion lymphatique (Figure 9).
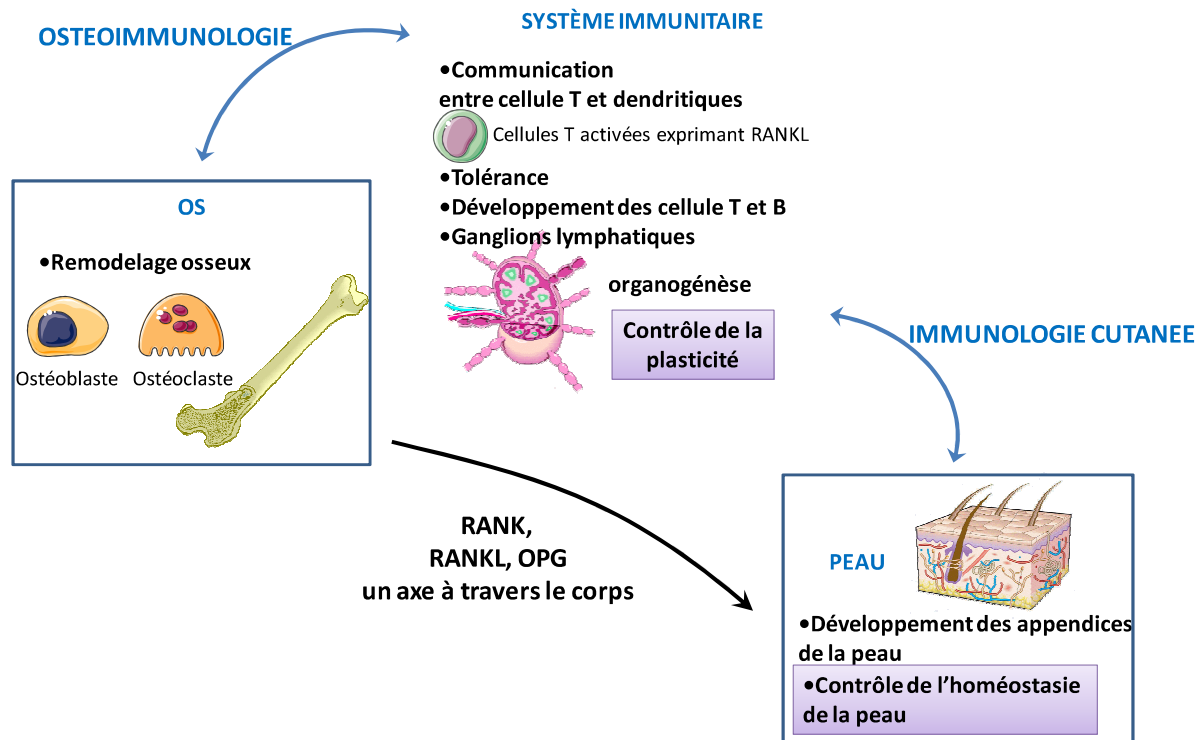
Figure 9 : La triade RANK-RANKL-OPG : un axe à travers le corps. RANK-RANKL et OPG sont des régulateurs clés de l'homéostasie de l'os et RANKL est produit par les cellules T activées. Cette triade moléculaire a permis d'expliquer le dialogue entre ces deux systèmes biologiques créant ainsi le terme d'ostéoimmunologie. De plus nous avons démontré des nouvelles fonctions de RANK à la fois dans les ganglions lymphatiques après leur développement et dans l'homéostasie de la peau. Nous avons mis en évidence un nouveau dialogue médié par RANK entre deux autres système biologique : la peau et les ganglions lymphatiques drainants la peau. Ce dialogue pourrai ainsi s'appeler l'immunologie cutanée.

Ce mécanisme de contrôle de la taille du ganglion par RANKL pourrait suggérer que les cellules T activées exprimant fortement RANKL supporteraient l'expansion des organes lymphoïdes secondaires lors de réponses immunes ou encore contribueraient à la formation de tissus lymphoïdes tertiaires (Figure 10).

a. Tissus non lymphoïdes

Foie

Pancréas

Articulation

Progression d'une inflammation aigue à chronique

TNF-LT constitutif
Chemokines
RANKL constitutif ?

Organes lymphoïdes tertiaires

b.

cellule T

cellule B

cellule dendritique

macrophage

cellule stromale

vaisseau sanguin

vaisseau lymphatique

Infiltration de cellules T RANKL$^+$

Polyarthrite rhumatoïde

L'expression constitutive de RANKL dans la membrane synoviale est-elle un signal pour l'induction / l'expansion d'organes lymphoïdes tertiaires ?

Figure 10 : Une fonction possible pour RANKL dans le développement d'organes lymphoïdes tertiaires. Mécanisme proposé comme impliqué dans le développement d'organes lymphoïdes tertiaires dans des organes non lymphoïdes (a). Fonction possible pour RANKL dans l'induction et/ou l'expansion des organes lymphoïdes tertiaires observés chez les patients atteint de polyarthrite rhumatoïde.

List of abbreviations

Aa: amino acid

ADAM: A disintegrin and metalloproteinase domain

AID: auto-inhibitory domain

AIRE: autoimmune regulator

AP-1: activator protein 1

APC: antigen presenting cell

aPKC: atypical protein kinase C

ARO: autosomal recessive osteopetrosis

BAFF: B cell activating factor

BAFF-R: BAFF receptor

Bcl-3: B cell leukemia lymphoma 3

BCMA: B cell maturation antigen

BCR: B cell receptor

BEC: blood endothelial cell

BMP: bone morphogenic protein

BMU: basic multicellular units

CCL: chemokine (C-C motif) ligand

CCR: chemokine (C-C motif) receptor

CD: cluster of differentiation

cDNA: complementary DNA

CLEVER-1: common lymphatic endothelial and vascular endothelial receptor-1

Cn: calcineurin

CR: cortical ridge

CRAC: calcium release-activated channel

CRD: cysteine-rich domain

cTEC: cortical thymic epithelial cell

CTL: cytotoxic T lymphocyte

CTLA4: cytotoxic T lymphocyte antigen 4

CTS: connective tissue sheath

CXCL: chemokine (C-X-C motif) ligand

CXCR: chemokine (C-X-C motif) receptor

CYLD: cylindromatosis

DAG: diacylglycerol

DAP12: DNAX-activating protein 12

DC: dendritic cell

DcR: decoy receptor

DD: death domain

DDH: death domain homologous

DN: double negative

DNA: deoxyribonucleic acid

DR: death receptor

E8.5: embryonic day 8.5

EDA: ectodermal dysplasia

EDAR: EDA receptor

EDARADD: EDAR associated death domain

EPU: epidermal proliferating unit

ER: endoplasmic reticulum

ERK: Extracellular signalling kinase

ESH: expansile skeletal hyperphosphatasia

FADD: Fas-associated death domain

FcγR: Fc γ receptor

FDC: follicular dendritic cell

FEO: familial expansile osteolysis

FGF: fibroblast growth factor

FRC: fibroblastic reticular cell

GAB2: GRB2-associated binding protein 2

GC: germinal center

GRB2: growth factor receptor-bound protein 2

HEV: high endothelial venule

HF: hair follicle

Hh: hedgehogs

HIF-1α: hypoxia-inducible transcription factor-1α

HIV: human immunodeficiency virus

HSC: hematopoietic stem cell

ICAM-1: intercellular adhesion molecule-1

Id-2: inhibitor of DNA binding 2

iFABP: intestinal fatty acid-binding protein

IFC: interfollicular channel

IFN: interferon

Ig: immunoglobulin

IGF: insulin growth factor

IKK: IκB kinase

IL: interleukin

IRS: inner root sheath

ITAM: immunoreceptor tyrosine-based activation motif

IκB: inhibitor of NF-κB

JAK3: janus kinase 3

JLP: juvenile localized periodontitis

JNK: c-Jun N-terminal kinase

JPD: juvenile PBD

K5: keratin 5

LCMV: lymphocytic choriomeningitis virus

LEC: lymphatic endothelial cell

LFA-1: leukocyte function-associated antigen-1

LN: lymph node

LT: lymphotoxin

LTic: lymphoid tissue inducer cell

LTβR: LTβ receptor

LYVE-1: lymphatic vessel endothelial hyaluronan receptor-1

VEGF: vascular endothelial growth factor

MAdCAM-1: Mucosal addressin cell adhesion molecule-1

MAP3K: MAPKK kinase

MAPK: mitogen activated protein kinase

MAPKK: MAPK kinase

MARCO: macrophage receptor with collagenous structure

MCP-1: monocyte chemoattractant protein-1

M-CSF: macrophage colony-stimulating factor

MEC: mammary epithelial cell

MEK: MAPK/ERK kinase

MHC: major histocompatibility complex

MLR: mixed lymphocyte reaction

MMP: matrix metalloprotease

MRC: marginal reticular cell

mRNA: messenger RNA

mTEC: medullary thymic epithelial cell

NALT: nasal-associated lymphoid tissue

Necl-5: nectin-like molecule

NEMO: NF-κ essential modulator

NFATc: nuclear factor of activated T cells

NF-κB: nuclear factor-κB

NIK: NF-κB inducible kinase

NK: natural killer

NLS: nuclear localization sequence

OCIF: osteoclastogenesis inhibitory factor

ODAR: osteoclast differentiation and activation receptor

ODF: osteoclast differentiation factor

ODFR: ODF receptor

OPG: osteoprotegerin

OPGL: OPG ligand

ORS: outer root sheath

P15: postnatal day 15

PBD: familial Paget's bone disease

PBD2: early onset PBD

PD-1: programmed death 1

PD-L1: PD ligand 1

PECAM-1: platelet-endothelial cell adhesion molecule-1

PH: pleckstrin homology

PI3K: phosphatidylinositol 3-kinase

PIP2: phosphatidylinositol 4,5 biphosphate

PIP3: phosphatidylinositol 1,4,5 biphosphate

PKB: protein kinase B

PKD: 3-phosphatidylinositide-dependant protein kinase

PLAD: pre-ligand-binding assembly domain

PLC: phospholipase C

PNAd: peripheral lymph node addressin

PP: Peyer's Patches

Prox1: prospero homeobox protein 1

PTA: peripheral-tissue-restricted antigen

PTH: parathyroid hormone

PTHrP: parathyroid hormone related-protein

RA: retinoic acid

RA: rheumatoid arthritis

RAG: recombination activating gene

RALDH: retinal deshydrogenase

RANK: Receptor activator of NF-κB

RANKL: RANK ligand

RHD: Rel homology domain

RNA: ribonucleic acid

RORγ: retinoid-related orphan receptor γ

S100A8: S100 calcium-binding protein A8

SCID: severe combined immunodeficiency

SCS: subcapsular sinus

SF: superfamily

SIV: simian immunodeficiency virus

SLO: secondary lymphoid organ

Sox18: Sex determining region Y box 18

STAT-1: signal transducer and activator of transcription 1

T reg cell: T regulatory cell

TAB1: TAK1-binding protein

TACE: TNF-α convertase

TACI: transmembrane activator and calcium-modulator and cyclophilin ligand interactor

TAK1: TGF-β activated kinase

TCR: T cell receptor

TEB: terminal end bud

T_{FH}: follicular helper T cells

TGF-β: transforming growth factor β

T_H cell: T helper cell

THD: TNF homology domain

TLT: tertiary lymphoid tissue

TNF: tumor necrosis factor

TNFR: TNF receptor

TRA: tissue-restricted antigen

TRADD: TNFR-associated death domain

TRAF: TNFR-associated factor

TRAIL: TNF-related apoptosis-inducing ligand

TRAILR1: TRAIL receptor 1

TRANCE: TNF-related activation induced cytokine

TRANCER: TRANCE receptor

TRAP: tartrate-resistant acid phosphatise

VCAM-1: vascular adhesion molecule-1

VEGFR: VEGF receptor

VLA4: very late antigen 4

INTRODUCTION

Chapter 1:
RANK, RANKL and OPG: structures and signal transduction

1.1. *A triad member of the TNF and TNFR superfamilies*

1.1.1. *TNF and TNFR superfamilies*

Four decades ago, lymphotoxin (LT) and tumor necrosis factor (TNF) were identified as products of lymphocytes and macrophages that caused the lysis of certain cell types, especially tumor cells [1, 2]. In 1984, cloning of cDNAs of these two proteins allowed to show strong homologies to one another, suggesting that they were both members of a new gene superfamily (SF) [3, 4]. Large scale sequencing identified many related proteins, collectively referred to as TNFSF proteins. Not surprisingly, the receptors for these proteins also constitute a superfamily of proteins sharing sequence homology, designated as TNF Receptor (TNFR) SF. The first two members of the TNFRSF (TNFR1 and TNFR2) were identified in the early 1990s and since then, the size of the family has steadily grown (Figure 1.01). A hallmark of these ligand-receptor pairs is functional diversity with wide tissue distribution and important roles ranging from regulation of normal biological processes, such as immune responses, hematopoiesis and morphogenesis, to roles in tumorigenesis, septic shock, viral replication, bone resorption and autoimmunity. The functions of TNF/TNFR SFs rely on an obligatory 3-fold symmetry that defines the essential signaling stoichiometry and structure [5]. The oligomeric binding arrangement amplifies the avidity between ligands and receptors. Some TNF/TNFR SFs proteins can bind to more than one partner with high affinity, thereby enhancing regulatory flexibility and complexity (Figure1.01).

TNFSF ligands are type II proteins expressed in a membrane-bound state, with enzymatic cleavage allowing some to be released in soluble forms. The 25%-30% amino acid homology between these ligands is mostly confined to internal aromatic residues responsible for trimeric assembly, this TNF homology domain (THD) is found at the extracellular C terminus (Figure 1.01). The THD folds into an antiparallel β-sandwich that assembles into trimers, each ligand homotrimer having 3 receptor binding sites formed as grooves between adjacent subunits [6]. Individual TNF family cytokines receptor selectivity is provided by differences observed in length and composition of the surface loops connecting the THD β-strands [7].

TNFR are primarily type I transmembrane proteins with characteristic extracellular cysteine-rich domain (CRD) formed of three disulfide bonds surrounding a core motif of CXXCXXC creating an elongated molecule (Figure 1.01). TNFRs were believed to be monomeric units recruited by the trimeric ligand to form a 3:3 complex able to induce subsequent cell signaling. In 2000, it was found

Figure 1.01: Interactions between members of the TNF and TNFR superfamilies. TNFSF and TNFRSF members are shown respectively at the top and the bottom of the figure. Arrows on ligands indicate cleavage site of membrane-bound forms. TNFRSF members are primarily type I transmembrane proteins, but they are exceptions to this rule with some type III transmembrane proteins (lacking a signal peptide), protein anchored by a covalently linked C-terminal glycolipid and soluble proteins. Common names and standard nomenclature are both given, referring to the website www.genenames.org. After www.enzolifesciences.com website.

that several TNFRs can self-assemble in the absence of their ligands, using a conserved domain in the extracellular region named pre-ligand-binding assembly domain (PLAD) [8]. This finding modified the hypothesis of TNFRs trimerization subsequent to the binding with their cognate ligands. Hence, a model of expanding network was additionally proposed where TNFRs would be present in a homodimeric state and engagement with ligand would lead to the creation of a network of TNFRs, resulting in TNFRs activation [9]. The cytoplasmic domains of TNFRs are modest in length and function as docking sites for signaling molecules. Based on their cytoplasmic adaptor proteins, TNFRSF can be separated in two receptor subgroups: activating receptors and death receptors. Death receptors, such as Fas, TNFR1, TRAILR1 (TNF-related apoptosis-inducing ligand receptor 1), signal through a death domain (DD) that can associate with Fas-associated DD proteins (FADD) and TNFR-associated DD proteins (TRADD), inducing caspase-dependent cell death [5]. Activating receptors like TNFR2, CD40 or CD30 contain a TNFR-associated factor (TRAF) binding domain, they outnumber death receptors and many cell signaling pathways can be induced by one of the six known TRAF proteins. Pathways such as mitogen activated protein kinases (MAPKs) and nuclear factor-κB (NF-κB) can be activated by these receptors and can lead to cell growth and survival [5].

1.1.2. Discovery of RANK, RANKL and OPG

In 1997 and 1998 new members of TNF and TNFR SFs were identified by several groups. The american Amgen Inc. group designed a study to identify TNFRSF-related molecules for possible therapeutic utility by generating transgenic mice over-expressing various TNFRs related cDNA, one mouse model developed a remarkable skeletal phenotype. It displayed marked osteopetrosis (increase of bone density) as a result of an absence of natural occurring cells resorbing bones: osteoclasts. The protein encoded by this cDNA was named osteoprotegerin (OPG) as it seemed to protect the skeleton by inhibiting bone resorption by osteoclasts [10]. Independently, the Snow Brand Milk Group in Japan reported the identification of an identical molecule [11]. The authors used another approach to test an hypothesis made in 1981 by Rodan and Martin proposing that the osteoblasts in the bone marrow play a central role in the formation of osteoclasts [12]. To test this hypothesis this group was systematically searching for both osteoclasts stimulatory and inhibitory factors. By purifying a factor from human embryonic fibroblasts that inhibited osteoclastogenesis, they obtained a partial protein sequence they named OCIF for osteoclastogenesis inhibitory factor [13]. Using this partial protein sequence, they isolated cDNA clones encoding OCIF, which turned out to be identical to the protein that had been reported by the Amgen Inc. group [11]. Both groups used expression cloning with OPG as a probe and identified its ligand which was named OPG ligand (OPGL) [14] and osteoclast differentiation factor (ODF) [11]. This ligand turned out to be identical to a member of the TNFSF which had been identified earlier as the receptor activator of NF-κB ligand (RANKL) [15] and as TNF-related activation induced cytokine (TRANCE) [16]. Soon after the identification of OPG ligand, another

cellular receptor was found for this protein, which was identical to the previously identified receptor activator of NF-κB (RANK) discovered while sequencing cDNAs from a human bone marrow-derived dendritic cells (DC) cDNA library [15]. Anderson and co-workers found that RANK had a partial homology with another TNFRSF member, CD40, and that it was involved in T cell activation. They isolated RANKL by direct expression cloning and found that RANK-RANKL interaction increased DC-stimulated naïve T cell proliferation and survival [15]. These discoveries that RANKL has a central role in osteoclastogenesis and in T cell activation have laid the basis for a new field of research, referred to as osteoimmunology.

In two years, a new TNFSF-TNFRSF triad has been discovered with a ligand, RANKL, interacting with two receptors, a cellular receptor, RANK, and a soluble decoy receptor, OPG. The different names that have been given to these proteins and their chromosomal locations in human and mouse are listed in Table 1.01. I will refer to these molecules as RANK, RANKL and OPG.

Standardized names	Other names	Human chromosome	Mouse chromosome
TNFRSF11A	RANK (Receptor activator of NF-κB) ODFR (Osteoclast differentiation factor receptor) TRANCER (TNF-related activation induced cytokine receptor) ODAR (Osteoclast differentiation and activation receptor)	18q22.1	1
TNFRSF11B	OPG (Osteoprotegerin) OCIF (Osteoclastogenesis inhibitory factor)	8q24	15
TNFSF11	RANKL (RANK ligand) OPGL (OPG ligand) TRANCE ODF	13q14	14

Table 1.01: RANK, RANKL and OPG triad known names and chromosomal locations.

In 1998, Emergy and colleagues identified OPG as a receptor for the cytotoxic ligand TRAIL (TNF-related apoptosis-inducing ligand) which is a member of the TNFSF that induces apoptosis upon binding to its death domain containing receptors, DR4 (death receptor 4) and DR5 [17]. In addition to the two receptors lacking functional death domains already known, DcR1 (decoy receptor 1) and DcR2, OPG was identified as the third decoy receptor for TRAIL. A schematic view of RANK, RANKL, OPG and TRAIL interactions is given in Figure 1.02.
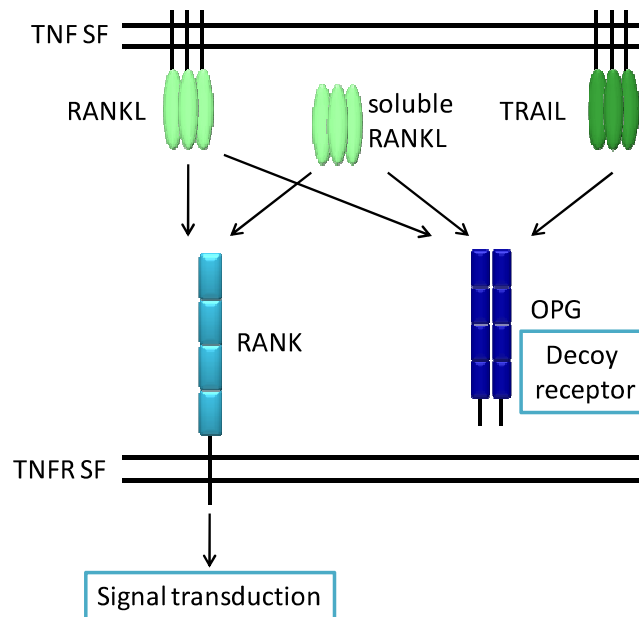
Figure 1.02: Schematic representation of the interactions between RANK, RANKL, OPG and TRAIL. Soluble or membrane-bound RANKL binds to its soluble decoy receptor, OPG or its functional receptor RANK. OPG is also known to interact with TRAIL.

1.2. Structure and expression of OPG, RANKL and RANK

1.2.1. OPG

Human OPG is a 401 amino acid (aa) polypeptide, which is cleaved to 380 aa by a peptidase. This 44 kDa protein is then N-linked glycosylated and secreted as a disulfide linked 110 kDa homodimer. Thus, OPG presents two uncommon features for a TNFRSF member: (i) a covalent dimerization and (ii) a lack of a hydrophobic transmembrane domain [10]. OPG gene has been highly conserved throughout evolution as shown by the 85% and 94% homology between rat and respectively mouse and human proteins [10]. The N-terminal portion of OPG shares a high homology with other members of TNFRSF such as CD40 and TNFR2, and displays four TNFRSF characteristic CRDs (Figure 1.03a) [18]. In addition, OPG comprises two death domain homologous (DDH) regions. These regions were shown to transduce an apoptotic signal when expressed as an OPG/Fas fusion protein in which the transmembrane region of Fas was inserted between CRDs and DDH [18]. Although DDHs are functionally active, it is unlikely that OPG induces cell apoptosis as OPG has only been described as a secreted protein. Finally, the C-terminal region was shown to harbor an aa residue for OPG dimerization (Cys-400) and an heparin binding site. This heparin binding site does not seem to have a direct effect on OPG activity *in vitro* [18] but is implied in OPG binding on Syndecan-1, a transmembrane heparan sulfate proteoglycan implied in several functions like actin cytoskeleton regulation, cell adhesion and migration, and modulation of specific receptor interaction [19].
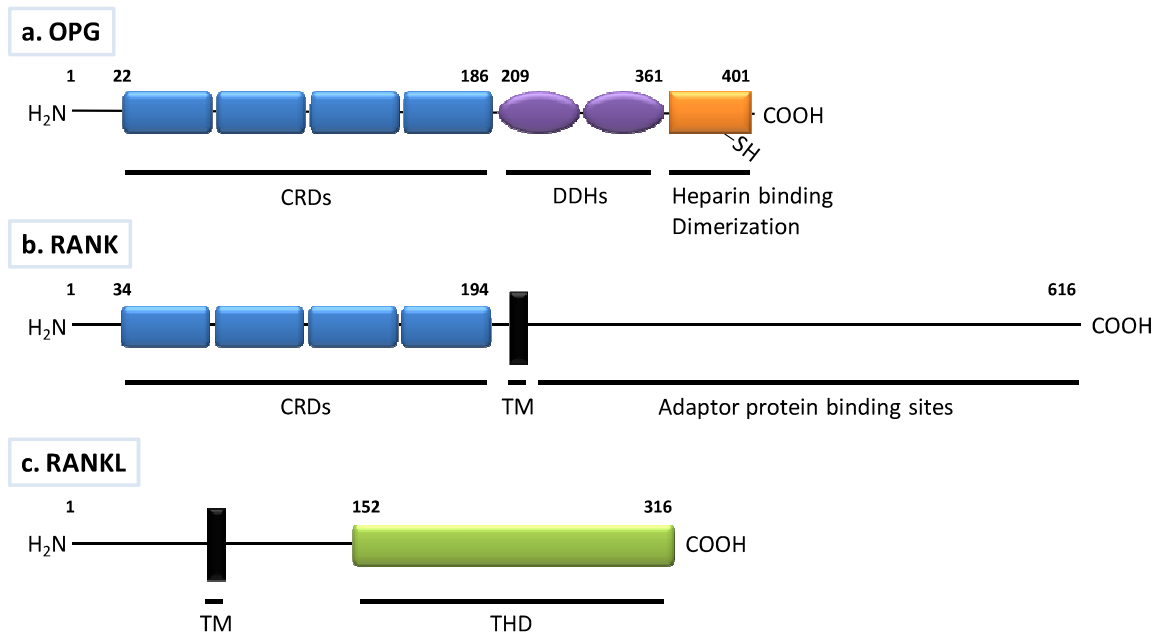
Figure 1.03: Schematic representation of functional domains in OPG, RANK and RANKL. Functional domains found in OPG (a), RANK (b) and RANKL (c) are depicted. Abbreviations: CRD, cysteine-rich domain; DDH, death domain homologous; TM, transmembrane domain; THD, TNF homology domain. After references [5, 18].

OPG is produced by a wide variety of tissues including the cardiovascular system (heart, arteries and veins), lungs, kidneys, intestine, stomach, brain, liver, mammary tissue, placenta, prostate, skin, spleen and bones [20, 21]. The expression of this protein is regulated by various cytokines, peptides, hormones and drugs, which are listed in Table 1.02.

	OPG	RANKL	RANK
Hormones			
Vitamin-D3	↑	↑	↑
Parathyroid hormone	↓	↑	
Estradiol	↑	−	
Testosterone	↑		
Prolactin	↓	↑	
Cytokines			
IL-1β	↑	↑	
IL-6	↑	↑	↓
IL-11	↑	↑	
IL-17		↑	
TNF-α	↑	↑	
IL-4 + αCD3 (T cells)		↑	↑
Oncostatin M		↑	−
Leukemia inhibitory cytokine	↑	↑	−
CD40L (dendritic cells)	↑		↑
Growth factors			
TGF-β	↑	↓	↓
TGF-β + αCD3 (T cells)		↑	↑
BMP-2	↑		
IGF-1	↓		
Immunosuppressive molecules			
Cyclosporine A	↓	↑	
Tacrolimus	↓	↑	
Rapamycin	↓	↑	
Glucocorticoid	↓	↑	

Others	OPG	RANKL	RANK
Prostaglandin E2	↓	↑	↑
Calcium	↑	↑	
LPS	↓	↑	
Ionomycin (T cells)		↑	
PMA (T cells)		−	
Indian Hedgehog	↑	↑	
Vasoactive intestinal peptide		↓	

Table 1.02: Factors modifying OPG, RANKL and RANK expression. Most studies reported here were carried out with osteoclast or osteoblast cell lineages, otherwise the cell type concerned is indicated in parentheses. (↑) increased expression, (↓) decreased expression, (−) unchanged, blank not tested. Abbreviations: IL-1, interleukin-1; TGF-β, transforming growth factor β; BMP-2, bone morphogenic protein-2; IGF-1, insulin growth factor-1; LPS, lipopolysaccharide; PMA, phorbol myristate acetate. After references [22, 23].

1.2.2. RANKL

Human RANKL is a 316 aa type II transmembrane glycoprotein with a cytoplasmic domain of 48 aa and an extracellular domain of 247 aa (Figure 1.03c). It shares 85% sequence homology with murine RANKL [15] and also close homology with other TNFSF members like TRAIL, Fas ligand (FasL) and TNF [16]. In 2001, Lam and colleagues crystallized the ectodomain of murine RANKL and showed that RANKL self-assembles in a homotrimer like other TNFSF from which structures were already published (Figure 1.04) [24].
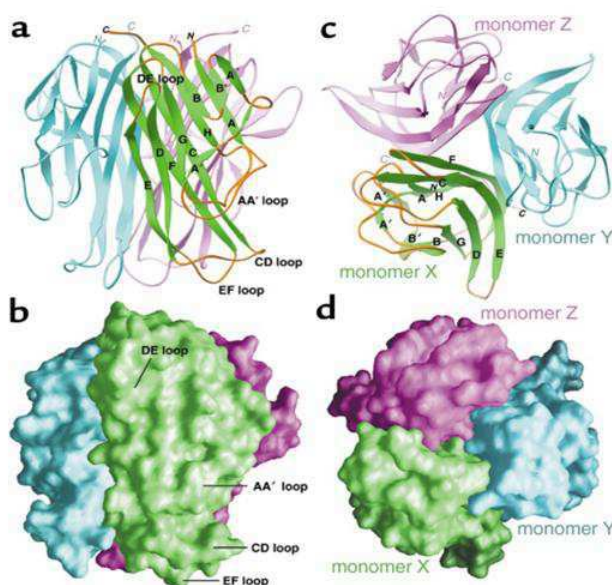
Figure 1.04: Crystal structure of murine RANKL extracytoplasmic domain. (a) Ribbon diagram of a RANKL homotrimer with C terminal at the top and the membrane-distal region at the bottom of the image, showing in green the β-strands and in orange the connecting loops of one RANKL monomer. The two others RANKL monomers are cyan and magenta. (b) Molecular surfaces of a RANKL trimer in the same view as in b. (c) Ribbon diagram of a RANKL trimer with the membrane-distal face forward. (d) Molecular surfaces of a RANKL trimer in the same view as in c. After reference [24].

RANKL has been shown to exist in two biologically active forms: a 45 kDa membrane bound form and a 31 kDa soluble form. RANKL soluble homotrimer is derived from the membrane bound

form, after proteolytic cleavage by the metalloprotease-disintegrin TNF-α convertase (TACE) also referred to as ADAM-17 (A disintegrin and metalloproteinase domain 17) [25]. Matrix metalloproteases (MMPs) 7 and 14 and ADAM-10 were also shown to be implicated in this process [26, 27]. In addition, alternative RNA splicing was reported to give rise to another form of type II transmembrane RANKL with a shorter intracellular domain and to a form of secreted RANKL lacking the transmembrane domain [28].

RANKL was originally characterized as a T lymphocyte specific protein [16], but it was afterwards shown to be widely expressed notably in bone stroma [11, 14]. RANKL expression can also be found in lymph nodes (LNs), spleen, liver, kidneys, thymus, brain, heart, arteries, mammary tissue, placenta, testes, thyroid, skeletal muscles and lungs [21]. Factors known to modulate RANKL expression are listed in Table 1.02, many of them are factors regulating osteoclasts formation and activity.

1.2.3. RANK

Human RANK is a type I transmembrane protein, consisting of 616 aa with around 85% homology with murine RANK. The extracellular region is composed of four CRDs characteristic of TNFRSF and the C terminal 383 residues form one of the largest cytoplasmic domain in this family (Figure 1.03b). However, like other TNFRs this region lacks intrinsic enzymatic activity and transduces signal through recruitment of TRAF adaptor proteins. RANK is known to interact with TRAFs 1, 2, 3 and 5 in a membrane-distal region of the cytoplasmic tail and with TRAF6 at a distinct membrane-proximal binding domain [29]. Among the other members of the TNFRSF, RANK shares the highest sequence homology with CD40, with a score of 40% (Figure 1.05) [15]. In addition to this sequence homology, RANK shares also functional similarities with CD40, which will be discussed in the following chapter.


```
           .  .  .  .10  .  .  .  .20  .  .  .  .30  .  .  .  .40  .  .  .  .50  .  .  .  .60
hurank    24:..........QIAPP..CTSEKHY.EHLG.R.CCNKCEPGKYMSSKCTTTSDSVCLPCGP: 68
hucd40    20:..........PEPPTACR.EKQY.LINS.Q.CCSLCQPGQKLVSDCTEFTETECLPCGE: 64
hutnfr2   23:LPAQVAFTPYAPEPGSTCRLREYY.DQTA.QMCCSKCSPGQHAKVFCTKTSDTVCDSCED: 80

           .  .  .  .70  .  .  .  .80  .  .  .  .90  .  .  .  100 .  .  .  110 .  .  .  120
hurank    69:DEYLDSWNEEDKCLL.HKVCDTGKALVAVVAGNSTTPRRCACTAGYH..WS..QDCECCR:123
hucd40    65:SEFLDTWNRETHCHQ.HKYCDPNLGLRVQQKGTSETDTICTCEEGWHC.TS..EACESCV:120
hutnfr2   81:STYTQLWNWVPECLSCGSRCSSDQ..VETQACTREQNRICTCRPGWYCALSKQEGCRLCA:138

           .  .  .  130 .  .  .  140 .  .  .  150 .  .  .  160 .  .  .  170 .  .  .  180
hurank   124:RNTECAPGLGAQHPLQLNKDTVCKPCLAGYFSDAFSSTDKCRPWTNCTFLGKRVEHHGTE:183
hucd40   121:LHRSCSPGFGVKQIATGVSDTICEPCPVGFFSNVSSAFEKCHPWTSCETKDLVVQQAGTN:180
hutnfr2  139:PLRKCRPGFGVARPGTETSDVVCKPCAPGTFSNTTSSTDICRPHQICN....VVAIPGNA:194

           .  .  .  190 .  .  .  200 .  .  .
hurank   184:KSDAVCGSSLPAR.KPPNEPHVYLP.:207
hucd40   181:KTDVVCGPQDRLR.............:193
hutnfr2  195:SRDAVCTSTSPTRS...........   :254
```

Figure 1.05: Amino acid alignment of human RANK, CD40 and TNFR2 sequences. Amino acid alignment of the cysteine-rich domains of RANK, CD40 and TNFR2 is presented, with identical and similar amino acid residues shown in black and grey, respectively. Modified after reference [30].

Recently it was shown that alternative splicing gives rise to a variant with a new exon between exon 1 and 2, and as this exon contains a stop codon this RNA encodes a truncated protein [31]. This truncated RANK protein is suggested by the authors to be a negative regulator of RANK-RANKL interaction but *in vivo* relevance of such a mechanism still needs to be addressed. After the LTα/TNFR1 complex in 1993 [32] and the TRAIL/DR5 complex in 1999 [33], Liu and co-workers published the RANK-RANKL complex structure in 2010 [34]. They showed that the four CRDs from RANK fold into an elongated shape, and conformational changes occur in both RANK and RANKL after their interaction (Figure 1.06).
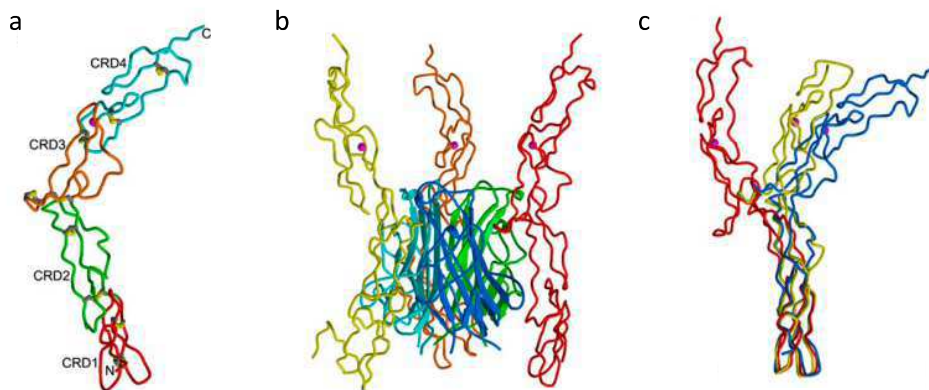
Figure 1.06: Crystal structure of murine RANK and RANK-RANKL complex. (a) Elongated structure of RANK with its four CRDs colored in red, green, orange and cyan, disulfide bounds are shown in yellow. (b) The biological hetero-hexameric complex as viewed perpendicular to the 3-fold axis. (c) Diagram showing structural differences of three copies of RANK, superposition was performed using CRD1 and 2. After reference [34].

RANK has been shown to be widely expressed with messenger RNA found in bones, heart, lungs, brain, skeletal muscles, kidneys, liver, skin, bone marrow, LNs, spleen, mammary glands and cancer cells [20-22]. Factors known to regulate RANK expression are fewer than those affecting RANKL and OPG, nevertheless they are listed in Table 1.02.

1.3. *Signaling induced by RANK*

Homotrimeric RANKL binding to RANK induces receptor trimerization and subsequent intracytoplasmic signaling activation that regulates cell differentiation, function and survival [22]. The mechanism implied in RANK trimerization is as yet unknown and activation could also be achieved by the creation of a receptor network, as hypothesised by Idriss and Naismith [9]. Thus, Kanazawa and Kudo demonstrated that RANK can be found self-assembled at cell surface, and that this is achieved through a cytoplasmic domain differing from the previously described PLAD domain [8, 35]. As described above, RANK belongs to the TNFRSF subgroup of activating receptors like TNFR2 or CD40 and can bind five of the six known TRAFs adaptor proteins. Among these five TRAF proteins, TRAF6 seems to be critical for RANK signaling as TRAF6-deficient mice, similarly to RANK-knockout mice, present severe osteopetrosis and a lack of LNs [36]. TRAF6 differs from other TRAFs

by displaying a distinct Pro-X-Glu-X-X-(aromatic/acidic residue) binding motif which is also found in its upstream activators such as RANK [37]. Another adaptor protein which has been shown to be implied in RANK signal transduction is the molecular scaffold GRB2 (growth factor receptor-bound protein 2)-associated binding protein (GAB2) [38]. RANK recruitment of adaptor molecules results in activation of several signaling pathways, summarized in Figure 1.07.
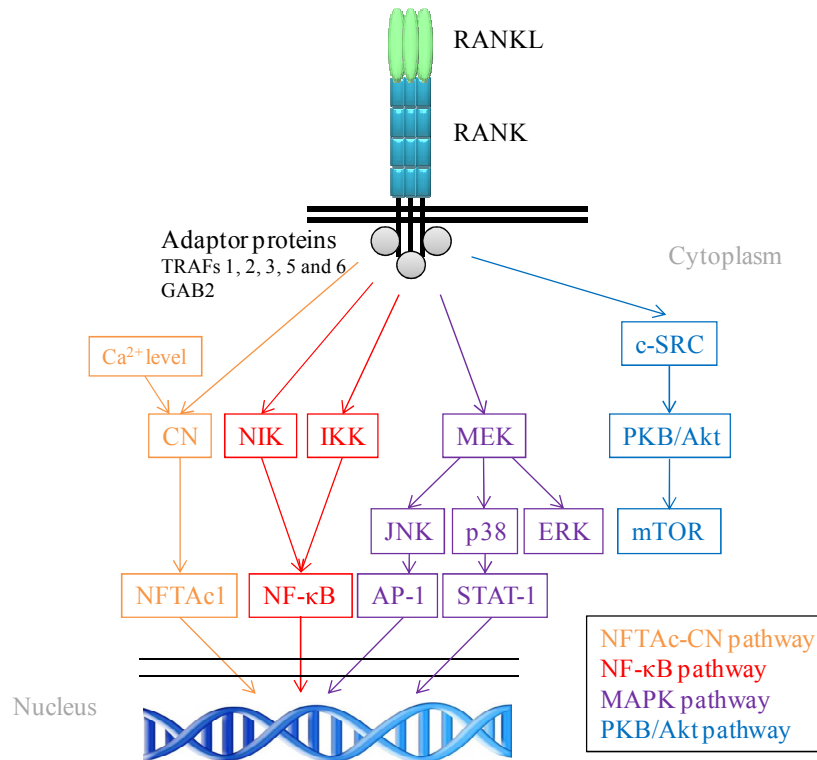
Figure 1.07: Schematic diagram of the known RANKL-RANK-induced signaling cascades. Abbreviations: TRAF, TNFR-associated factors; GAB2, growth factor receptor-bound protein 2-associated binding protein; CN, calcineurin; NFTAc1, nuclear factor of activated T cells 1; NIK, NF-κB inducible kinase; IKK, IκB kinases complex; MAPK, mitogen activated protein kinase; MEK, MAPK/ERK kinase; JNK, c-Jun N-terminal kinase; AP-1, activator protein 1; STAT-1, signal transducer and activator of transcription 1; ERK, extracellular-signal-regulated kinase; c-SRC, cellular-sarcoma; PKB, protein kinase B; mTOR, mammalian target of rapamycin. Modified after reference [39].

RANKL/RANK-induced pathways differ depending on cell type. In the following part, I will describe these pathways and their significance in different RANK/RANKL/OPG biological functions will be addressed in the following chapters.

1.3.1. *NF-κB pathway*

The NF-κB transcription factor family consists of five members: RelA (p65), RelB, c-Rel, p50/p105 (NF-κB1) and p52/p100 (NF-κB2). NF-κB1 and NF-κB2 proteins are first synthesized as precursors before being proteolytically cleaved from p105 and p100 to, respectively, p50 and p52 proteins. These five proteins display a Rel homology domain (RHD) responsible for DNA binding, dimerization and containing a nuclear localization sequence (NLS). However, among the five NF-κB

transcription factors only RelA, RelB and c-Rel contain a transactivating domain through which transcription can be activated, so that p50 and p52 are only able to promote gene transcription when associated in heterodimers with a Rel protein. P50 and p52 homodimers can also be found in cells, they can translocate to nucleus and bind DNA but they will act as gene transcription repressors. In most cell types NF-κB transcription factor dimers are retained in the cytoplasm by specific inhibitors, IκBs proteins, which bind to the RHD and interfere with its NLS function. Five IκB proteins have been identified: IκB-α, IκB-β, IκB-γ, IκB-ε and B cell leukemia lymphoma 3 (Bcl-3). A prototypic NF-κB/IκB complex expressed in a majority of cells is an heterodimer of p50 and RelA associated with IκB-α or β. Bcl-3 differs from other IκBs proteins by containing a gene transactivation domain and by not retaining NF-κB complexes in the cytoplasm. Bcl-3 can stabilize p50 and p52 homodimers binding to NF-κB sites in the nucleus and may transform these repressor dimers in activator heterotrimers. [40]

There are two main pathways that mediate the process of NF-κB activation and translocation to the nucleus: classical (canonical) and alternative (non-canonical) (Figure 1.08). These pathways differ at many levels: from the initiating cytokines/receptors down to NF-κB dimer composition and subsequent biological effects. Most stimuli that activate the classical pathway, such as pro-inflammatory cytokines, do not activate the alternative pathway; however the alternative stimuli can activate both NF-κB pathways leading to specific gene signatures for each signaling pathway [40]. In the classical pathway, engagement of a receptor by its ligand induces the formation of an adaptor protein complex, which facilitates the recruitment and activation of IκB kinases complex (IKK). This activated complex, composed of two kinases subunits IKKα and IKKβ and a regulatory subunit IKKγ/NEMO (NF-κB essential modulator), will in turn phosphorylate IκB proteins leading to their ubiquitinylation and finally proteasomal degradation. IκB degradation reveals the NLS on NF-κB proteins, in the case of a p50/RelA dimer, exposure of p50 NLS allows the dimer to translocate to the nucleus and to regulate target genes transcription. In the alternative pathway, the cytoplasmic retention of p52 is assured by an IκB-homologous region in the C terminus of p100. Activation of this pathway involves the NF-κB inducible kinase (NIK) that phosphorylates and activates the IKKα homodimer, leading to the phosphorylation, ubiquitinylation and cleavage of the p100 precursor to expose the p52 NLS allowing the nuclear translocation of p52-RelB dimers [41]. RANKL binding to RANK is known to induce both classical and non-classical NF-κB pathways resulting in cell responses such as survival or differentiation [42].
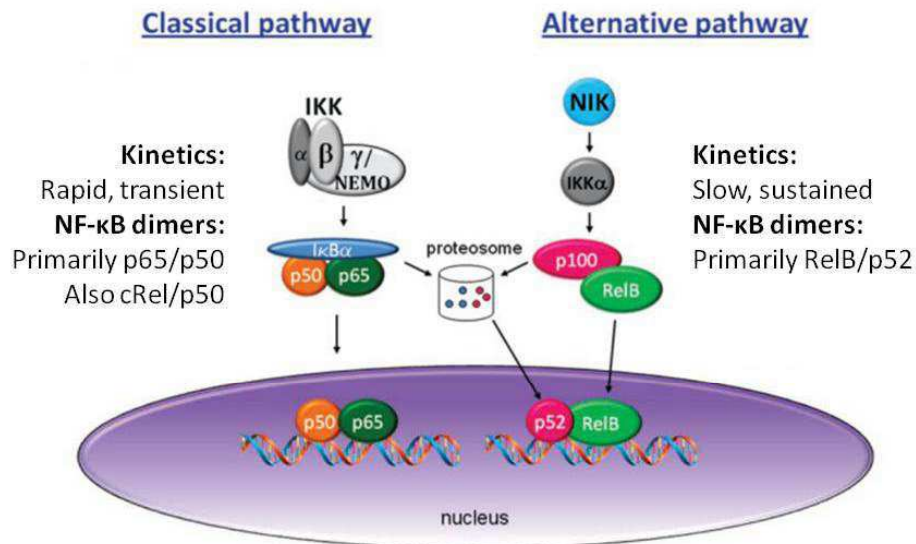
Figure 1.08: Classical and alternative pathways leading to NF-κB activation. The classical pathway is activated by many extracellular signals such as TNF, IL-1β or RANKL, it requires IKKβ and IKKγ/NEMO to phosphorylate IκBα, leading to its degradation by the proteasome. The nuclear translocation of NF-κB has a rapid (minutes) and transient kinetic. In the alternative pathway, the IKKα homodimer activated by NIK induces the phosphorylation, ubiquitinylation and cleavage of the p100 precursor to form p52-RelB dimers. This pathway can be induced by RANKL and $LT\alpha_1\beta_2$, and nuclear translocation of RelB-p52 dimers is known to be slow (hours) and sustained. After reference [43].

Each receptor-inducing NF-κB signaling cascade uses a unique or overlapping combination of adaptor molecules to interact with IKK or NIK. To date, the most prominent model holds that upon engagement of RANK by RANKL, TRAF6 is ubiquitinated on the Lys-63 aa residue. This ubiquitination is mediated by the TRAF6 E3 ubiquitin ligase activity itself and by a dimeric E2 ubiquitin-conjugating enzyme (Ubc13 and Uev1A). Lys-63 ubiquitination differs from the proteasomal-destinated ubiquitination of Lys-48 and induces the recruitment of the adaptor complex TAB2/3-TAB1 (TAK1-binding protein) together with the IKK and MAPKK (Mitogen-activated protein kinase kinase) kinase TAK1 (TGF-β activated kinase 1) [44]. It is believed that TAK1 is then activated via a trans-phosphorylation event made possible by the close proximity generated by the complex formation (Figure 1.09) [44]. Activated TAK1 then phosphorylates downstream factors like IKK but maybe also NIK as it is the case in IL-1-induced NF-κB activation [45]. Recently it was shown that Pim-1, a proto-oncogene kinase, can be a positive modulator for RANKL-induced NF-κB activation through TAK1 [46].

Apart from the TAK1 complex, TRAF6 can also recruit another adaptor molecule, p62, which in turn interacts with atypical protein kinase C (aPKC). aPKC contributes to IKK activation and subsequent NF-κB nuclear translocation. Deubiquitinating enzyme CYLD (Cylindromatosis) targets TRAF6 via its interaction with p62, and thereby negatively regulates TRAF6 ubiquitination and RANK-mediated NF-κB signaling. [47].

RANK can also recruit other TRAFs family member ahead of TRAF6. TRAF2 and TRAF5 can both activate classical and alternative NF-κB pathways, whereas TRAF3 recruitment seems to inhibit activation of alternative pathway [48].

Finally the molecular scaffold protein GAB2 has also been shown to be recruited to RANK and to mediate NF-κB activation [38].
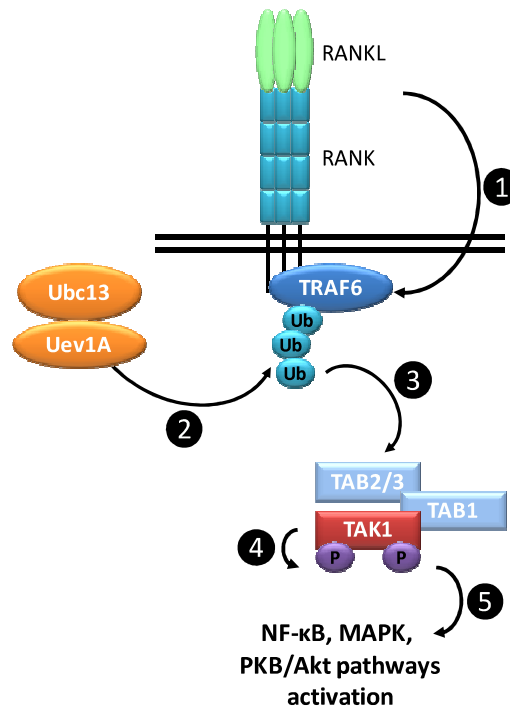
Figure 1.09: Schematic model of signalization cascade possibly induced upon RANK engagement by RANKL. Schematic view of one of the molecular cascade induced upon RANK engagement, chronology of events is given by the numbered black circles. Abbreviations: Ub, Ubiquitin; P, phosphorylation; TAK1, TGF-β activated kinase; TAB, TAK1-binding protein. After reference [44].

1.3.2. *MAPKs pathway*

Mitogen-activated protein kinases (MAPKs) are serine/threonine kinases that transmit signals from extracellular stimuli to multiple substrates involved in cell growth, differentiation and apoptosis. MAPK signal transduction pathways are among the most widespread mechanisms of eukaryotic cells regulation, with all eukaryotic cell possessing multiple MAPK pathways. The MAPK signaling pathway is a phosphorylation cascade starting with activation of MAPK kinase kinase (MAP3K), which phosphorylates and activates a MAPK kinase (MAPKK). This phosphorylated MAPKK finally activates a MAPK that might stay in the cytoplasm to phosphorylate structural proteins or translocates to the nucleus, where it can activate transcription factors involved in DNA synthesis and cell division (Figure 1.10a). Three conventional groups of mammalian MAPKs have been identified: the extracellular signalling kinases (ERK) 1 and 2, the JNK (c-Jun N-terminal kinase) and the p38 MAPKs. MAPKs are activated by the dual phosphorylation of threonine and tyrosine residues within a

TXY activation motif where X is a glutamate, proline and glycine residue in respectively ERK, JNK and p38 MAPKs [49]. RANKL binding to RANK induces these three conventional MAPKs pathways (Figure 1.10b) [50-52].
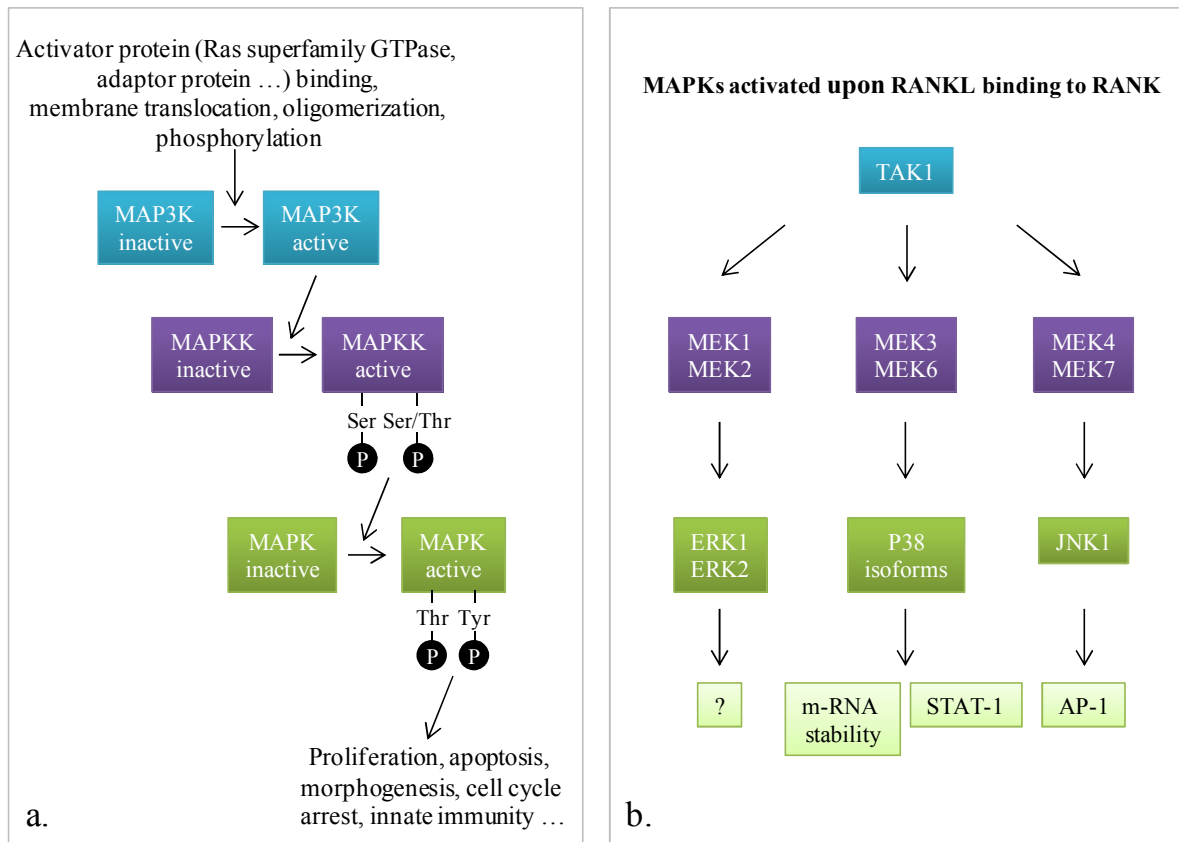
Figure 1.10: MAPKs activated upon RANKL binding to RANK. (a) MAPKs core signaling pathway, after reference [49]. (b) MAPKs pathways by RANK. Abbreviations: MAPK, mitogen-activated protein kinase; MAPKK, MAPK kinase, MAP3K, MAPKK kinase; TAK1, TGF-β-activated kinase; MEK, MAPK/ERK kinase; STAT-1, signal transducer and activator of transcription 1; AP-1, activator protein 1. After references [50-52].

MAP3K represents the entry point of MAPK pathways and is accordingly complex. MAP3K activation is regulated by three processes: (i) recruitment to the membrane, typically mediated by an upstream activating protein, (ii) oligomerization, usually within a multiple complex containing regulatory proteins and finally (iii) activation by phosphorylation [49]. As described for the NF-κB pathway, ubiquitinylated TRAF6 recruits the TAB2/3-TAB1-TAK1 complex, resulting in the MAP3K TAK1 activation. Activated TAK1 leads to the activation of ERK, p38 isoforms and JNK1 by phosphorylating the MAPKK MEK (MAPK/ERK kinase) 1 and 2, MEK3 and 6 and MEK 4 and 7 respectively (Figure 1.10b). Activation of p38 has also been shown to be mediated by TAB1 which binds p38 and recruit it to the TRAF6-TAB2/3-TAB1-TAK1 complex [53]. P38 activation induced by RANK signaling has been shown to induce mRNA stabilization and STAT-1 (signal transducer and activator of transcription 1) phosphorylation, which in turn can translocate in the nucleus and control gene expression [51]. JNK1 activation leads to the phosphorylation of c-Jun which facilitates the formation of the AP-1 (activator protein 1) transcription factor, which is a c-Fos/c-Jun heterodimer

[54]. GAB2 phosphorylation upon RANK stimulation was also shown to mediate JNK activation [38], and CYLD seems to have also a role in regulating AP-1 activation [47]. The role of activated ERK1 and 2 downstream of RANK is less clear, but these proteins are known to be regulators of cell proliferation [49].

1.3.3. Calcineurin/NFATc1 pathway

NFAT (nuclear factor of activated T cells) is a family of transcription factors originally identified in T cells and consisting of five members: NFATc1, c2, c3, c4 and NFAT5. In resting cells, NFATs are located in the cytoplasm in hyperphosphorylated inactive forms. NFAT phophorylation is ensured by the combined action of maintenance kinases that target specific serine aa residues in a conserved NFAT regulatory domain. Signaling through calcineurin/calmodulin results in NFAT dephosphorylation, causing a conformational switch that unmasks their NLS and allows their translocation to the nucleus. In the nucleus NFAT proteins bind to specific DNA response elements to regulate transcription in synergy with a number of other transcriptional regulators, such as AP-1, so that NFAT is coupled to MAPK pathways. Calcineurin is a heterodimer made of a catalytic subunit A (CnA) and a regulatory subunit B (CnB). CnA has three important domains, a binding domain for CnB, a binding domain for the phosphatase calmodulin and an auto-inhibitory domain (AID). When CnA is not active, the catalytic domain interacts with AID. Upstream signals increase intracellular calcium that allows calmodulin to activate calcineurin by removing AID, resulting in subsequent NFAT dephosphorylation (Figure 1.11a) [55].
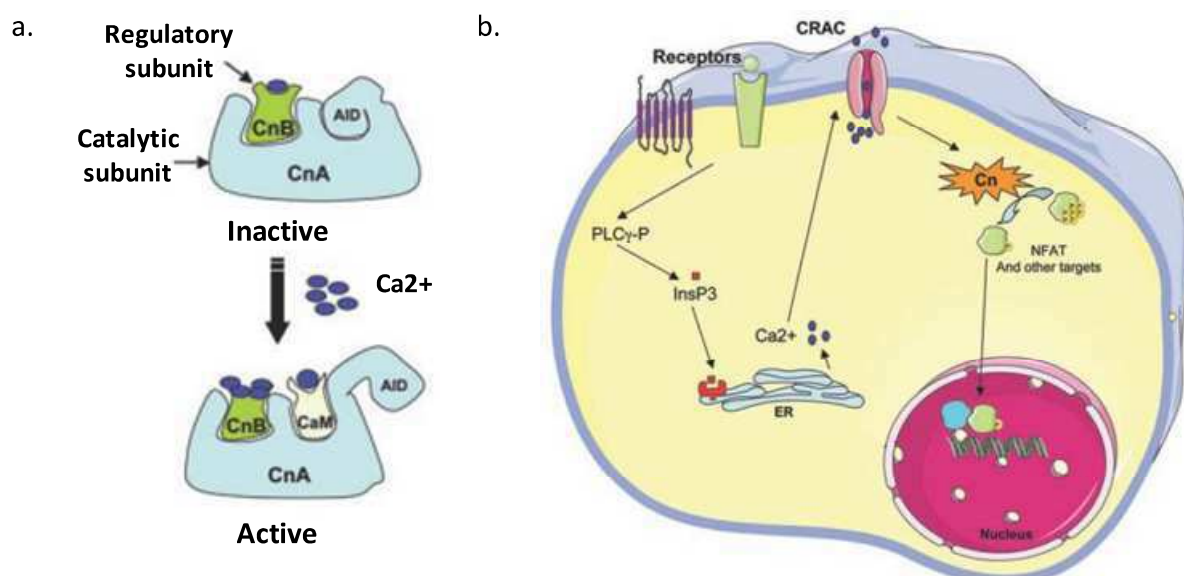
Figure 1.11: Schematic representation of calcineurin/NFAT pathway. (A) Model of calcineurin activation upon intracellular calcium increase. (B) Schematic view of the different steps leading to calcineurin activation and subsequent NFAT nuclear translocation. Abbreviations: AID, auto-inhibitory domain; Cn, calcineurin; CRAC, calcium release-activated channels; PLC, phospholipase C; ER, endoplasmic reticulum; NFAT, nuclear factor of activated T cells; InsP3, phosphatidylinositol 1,4,5 triphosphate. After reference [56].

Increased intracellular calcium can be induced by engagement of cell surface receptors, which then recruit and activate phospholipase C (PLC). Activated PLC catalyses the hydrolysis of phosphatidylinositol 4,5 bisphosphate (PIP2) into diacylglycerol (DAG) and phosphatidylinositol 1,4,5 triphosphate (InsP3 or PIP3). InsP3 binds to a receptor located at the endoplasmic reticulum (ER) to release calcium ions stored in the ER, which induce the opening of calcium release-activated channels (CRAC) at the plasma membrane and results in the import of extracellular calcium (Figure 1.11b) [55].

Even if NFATc1 was shown to be induced after RANKL binding of RANK in osteoclasts [57], how RANK could activate a calcium signal remained unclear as RANK belongs to the TNFRSF which is not directly linked to these pathways. However Koga and co-workers showed that RANK was linked to an ITAM (immunoreceptor tyrosine-based activation motif)–mediated calcium signaling [58]. In their model, RANKL binding to RANK leads to the phosphorylation of ITAM motif in FcγR (Fc γ receptor) and DAP12 (DNAX-activating protein 12) proteins, which in turn recruit Syk kinases that activate PLCγ, explaining the RANKL-induced transient elevation of calcium. PLCγ has been shown to form a complex with a RANK adaptor protein, GAB2; however GAB2 protein does not seem to be implied in NFATc1 activation [59].

NFATc1 has also been shown to be induced by the NF-κB pathway as NF-κB components p50 and p65 are recruited to the NFATc1 promoter upon RANKL stimulation [60].

1.3.4. PKB/Akt pathway

Mammalian cells express three protein kinase B (PKB) isoforms encoded by different genes, but sharing a close structural homology: Akt1/PKBα, Akt2/PKBβ and Akt3/PKBγ. While Akt1 is ubiquitously expressed at high level, Akt2 is restricted in insulin-sensitive tissues (liver, skeletal muscles, adipose tissues) and Akt3 is mostly expressed in brain and testis. All three Akt proteins consist of three conserved domains: a N-terminal regulatory domain including a pleckstrin homology (PH) domain, a central catalytic kinase domain with serine/threonine specificity and a C-terminal region necessary for the induction and maintenance of its kinase activity. Activation of Akt/PKB upon cell stimulation by various growth and survival factors requires activation of phosphatidylinositol 3-kinase (PI3K). PI3K are heterodimeric lipid kinases composed of a regulatory and a catalytic subunit implied in the synthesis of PIP3 from PIP2. The PKB PH domain is recruited to the membrane where it binds to PI3K lipid products, inducing a PKB conformational change so that PKB is sequentially phosphorylated by 3-phosphoinositide-dependent protein kinase 1 (PDK1) and PKD2 on, respectively, a conserved threonine in the kinase domain and a conserved serine in the C-terminal domain. PKB phosphorylation leads to its stabilization, activation and subsequent cellular processes (Figure 1.12) [61].
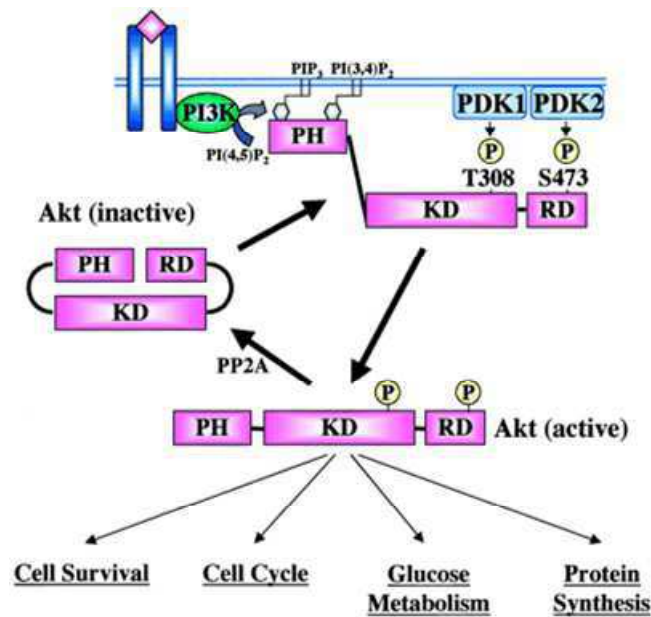
Figure 1.12: Mechanism of Akt activation. Akt is activated in a PI3K-dependent manner, and phosphorylation of two residues by PDK1 (T308) and PDK2 (S473) is required for a complete activation. The downstream cellular processes are indicated. Abbreviations: PI3K, phosphatidylinositol 3-kinase; PH, pleckstrin homology domain; KD, kinase domain; RD, regulating domain. After reference [61].

As described above, upon RANK engagement the adaptor molecule TRAF6 is recruited to the receptor cytoplasmic tail and poly-ubiquitinylated. TRAF6 in turn recruits and activates c-Src, a member of Src family kinases [62]. Members of Cbl family of adaptor molecules such as c-Cbl and Cbl-b, are then recruited to the RANK-TRAF6-c-Src complex. Cbl proteins positively regulate PKB activation via PI3K recruitment to the receptor complex, where it is phosphorylated by c-Src kinase, allowing PIP3 synthesis and subsequent PKB activation [63]. This positive role appears to be short-lived, as Cbl proteins may be responsible for ubiquitinylation of members of the receptor complex and subsequent degradation by the proteasome [63]. Glantschnig and co-workers showed that PKB activation downstream of RANK engagement leads to mTOR (mammalian target of rapamycin) activation, which is a serine/threonine kinase playing a central role in the control of translation [64].

1.4. <u>Conclusions</u>

In a short lapse of time the members of the molecular triad RANK, RANKL and OPG, which belong to the TNF and TNFR SFs, were discovered by four independent groups. Through the interaction with several adaptor molecules, this triad can activate the classical and alternative NF-κB, MAPKs, calcineurin and PKB/Akt pathways. RANK, RANKL and OPG are widely expressed throughout the body, resulting in a complex molecular system. Genetic ablation of RANK and RANKL in mice provided first clues on the essential roles of this system *in vivo*. As expected from *in vitro* results, both RANK- and RANKL-deficient mice showed severe osteopetrosis associated with a lack of tooth eruption but, more surprisingly, a lack of lymph nodes and an impaired development of mammary glands were also observed [65-67]. Thus, this complex system is implicated in several biological processes and even recently new functions for this triad have been identified, like in 2009 when RANK was also found to be implicated in female thermoregulation and in central fever response in inflammation [68]. In my manuscript, I will first focus on the role of RANK, RANKL and OPG in the bone and on the new field of osteoimmunology elicited by these proteins, to then discuss the role of this triad in LNs development. Subsequently, I will treat the new possible roles for this triad in LNs beyond its organogenesis and in skin. Hence, I will follow an axis elicited by these proteins, which starts in the primary lymphoid organ, the bone, through secondary lymphoid organs (LNs) to finally end in the skin (Figure 1.13).
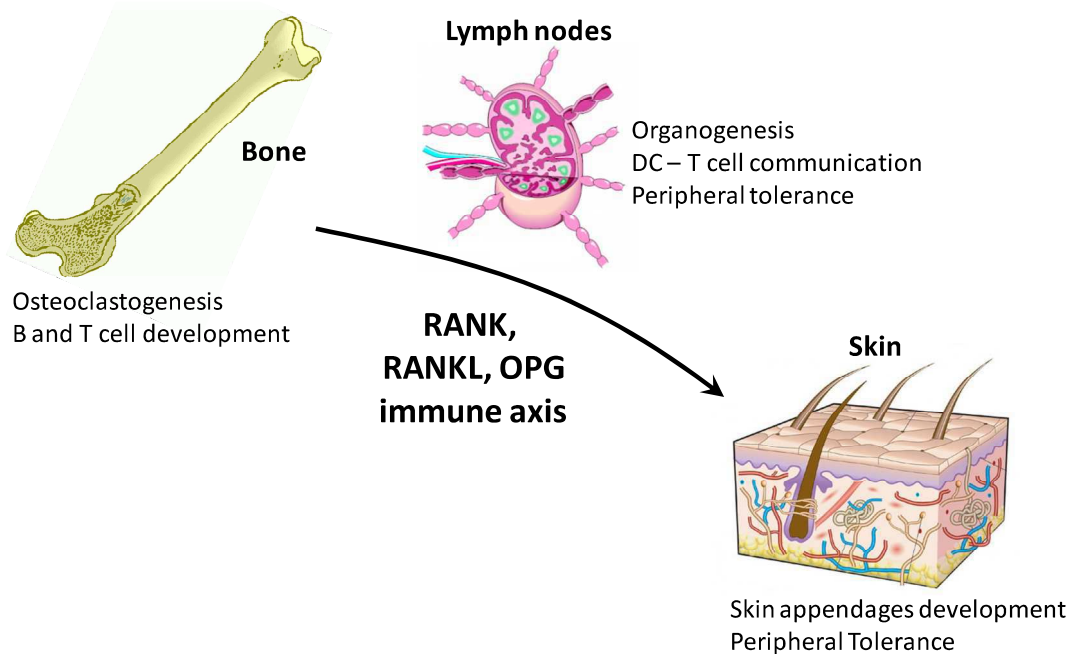
Figure 1.13:The RANK, RANKL and OPG axis across the body: from bone to skin via lymph nodes. Among the multiple roles known for RANK-RANKL-OPG my manuscript will focus on their function in the primary lymphoid organ, the bone marrow, to the secondary lymphoid organs and finally in the skin and in its appendages.

1.5. *Bibliography*

1. Carswell, E.A., et al., *An endotoxin-induced serum factor that causes necrosis of tumors.* Proc Natl Acad Sci U S A, 1975. **72**(9): p. 3666-70.
2. Granger, G.A., et al., *Lymphocyte in vitro cytotoxicity: specific release of lymphotoxin-like materials from tuberculin-sensitive lymphoid cells.* Nature, 1969. **221**(5186): p. 1155-7.
3. Gray, P.W., et al., *Cloning and expression of cDNA for human lymphotoxin, a lymphokine with tumour necrosis activity.* Nature, 1984. **312**(5996): p. 721-4.
4. Pennica, D., et al., *Human tumour necrosis factor: precursor structure, expression and homology to lymphotoxin.* Nature, 1984. **312**(5996): p. 724-9.
5. Locksley, R.M., N. Killeen, and M.J. Lenardo, *The TNF and TNF receptor superfamilies: integrating mammalian biology.* Cell, 2001. **104**(4): p. 487-501.
6. Bodmer, J.L., P. Schneider, and J. Tschopp, *The molecular architecture of the TNF superfamily.* Trends Biochem Sci, 2002. **27**(1): p. 19-26.
7. Zhang, G., *Tumor necrosis factor family ligand-receptor binding.* Curr Opin Struct Biol, 2004. **14**(2): p. 154-60.
8. Chan, F.K., et al., *A domain in TNF receptors that mediates ligand-independent receptor assembly and signaling.* Science, 2000. **288**(5475): p. 2351-4.
9. Idriss, H.T. and J.H. Naismith, *TNF alpha and the TNF receptor superfamily: structure-function relationship(s).* Microsc Res Tech, 2000. **50**(3): p. 184-95.
10. Simonet, W.S., et al., *Osteoprotegerin: a novel secreted protein involved in the regulation of bone density.* Cell, 1997. **89**(2): p. 309-19.
11. Yasuda, H., et al., *Osteoclast differentiation factor is a ligand for osteoprotegerin osteoclastogenesis-inhibitory factor and is identical to TRANCE/RANKL.* Proceedings of the National Academy of Sciences of the United States of America, 1998. **95**(7): p. 3597-3602.
12. Rodan, G.A. and T.J. Martin, *Role of osteoblasts in hormonal control of bone resorption--a hypothesis.* Calcif Tissue Int, 1981. **33**(4): p. 349-51.
13. Tsuda, E., et al., *Isolation of a novel cytokine from human fibroblasts that specifically inhibits osteoclastogenesis.* Biochem Biophys Res Commun, 1997. **234**(1): p. 137-42.
14. Lacey, D.L., et al., *Osteoprotegerin ligand is a cytokine that regulates osteoclast differentiation and activation.* Cell, 1998. **93**(2): p. 165-76.
15. Anderson, D.M., et al., *A homologue of the TNF receptor and its ligand enhance T-cell growth and dendritic-cell function.* Nature, 1997. **390**(6656): p. 175-179.
16. Wong, B.R., et al., *TRANCE (tumor necrosis factor [TNF]-related activation-induced cytokine), a new TNF family member predominantly expressed in T cells, is a dendritic cell-specific survival factor.* J Exp Med, 1997. **186**(12): p. 2075-80.
17. Emery, J.G., et al., *Osteoprotegerin is a receptor for the cytotoxic ligand TRAIL.* J Biol Chem, 1998. **273**(23): p. 14363-7.
18. Yamaguchi, K., et al., *Characterization of structural domains of human osteoclastogenesis inhibitory factor.* J Biol Chem, 1998. **273**(9): p. 5117-23.
19. Mosheimer, B.A., et al., *Syndecan-1 is involved in osteoprotegerin-induced chemotaxis in human peripheral blood monocytes.* J Clin Endocrinol Metab, 2005. **90**(5): p. 2964-71.
20. Schoppet, M., K.T. Preissner, and L.C. Hofbauer, *RANK ligand and osteoprotegerin - Paracrine regulators of bone metabolism and vascular function.* Arteriosclerosis Thrombosis and Vascular Biology, 2002. **22**(4): p. 549-553.
21. Theoleyre, S., et al., *The molecular triad OPG/RANK/RANKL: involvement in the orchestration of pathophysiological bone remodeling.* Cytokine Growth Factor Rev, 2004. **15**(6): p. 457-75.
22. Walsh, M.C. and Y. Choi, *Biology of the TRANCE axis.* Cytokine Growth Factor Rev, 2003. **14**(3-4): p. 251-63.
23. Hanada, R., et al., *RANKL/RANK-beyond bones.* J Mol Med, 2011. **29**: p. 29.

24.   Lam, J., et al., *Crystal structure of the TRANCE/RANKL cytokine reveals determinants of receptor-ligand specificity.* J Clin Invest, 2001. **108**(7): p. 971-9.

25.   Lum, L., et al., *Evidence for a role of a tumor necrosis factor-alpha (TNF-alpha)-converting enzyme-like protease in shedding of TRANCE, a TNF family member involved in osteoclastogenesis and dendritic cell survival.* J Biol Chem, 1999. **274**(19): p. 13613-8.

26.   Hikita, A., et al., *Negative regulation of osteoclastogenesis by ectodomain shedding of receptor activator of NF-kappaB ligand.* J Biol Chem, 2006. **281**(48): p. 36846-55.

27.   Lynch, C.C., et al., *MMP-7 promotes prostate cancer-induced osteolysis via the solubilization of RANKL.* Cancer Cell, 2005. **7**(5): p. 485-96.

28.   Ikeda, T., et al., *Determination of three isoforms of the receptor activator of nuclear factor-kappa B ligand and their differential expression in bone and thymus.* Endocrinology, 2001. **142**(4): p. 1419-1426.

29.   Galibert, L., et al., *The involvement of multiple tumor necrosis factor receptor (TNFR)-associated factors in the signaling mechanisms of receptor activator of NF-kappa B, a member of the TNFR superfamily.* Journal of Biological Chemistry, 1998. **273**(51): p. 34120-34127.

30.   Yun, T.J., et al., *OPG/FDCR-1, a TNF receptor family member, is expressed in lymphoid cells and is up-regulated by ligating CD40.* Journal of Immunology, 1998. **161**(11): p. 6113-6121.

31.   Mukai, S., et al., *Identification and analysis of function of a novel splicing variant of mouse receptor activator of NF-kappaB.* Mol Cell Biochem, 2011. **350**(1-2): p. 29-38.

32.   Banner, D.W., et al., *Crystal structure of the soluble human 55 kd TNF receptor-human TNF beta complex: implications for TNF receptor activation.* Cell, 1993. **73**(3): p. 431-45.

33.   Mongkolsapaya, J., et al., *Structure of the TRAIL-DR5 complex reveals mechanisms conferring specificity in apoptotic initiation.* Nat Struct Biol, 1999. **6**(11): p. 1048-53.

34.   Liu, C., et al., *Structural and functional insights of RANKL-RANK interaction and signaling.* J Immunol, 2010. **184**(12): p. 6910-9.

35.   Kanazawa, K. and A. Kudo, *Self-assembled RANK induces osteoclastogenesis ligand-independently.* J Bone Miner Res, 2005. **20**(11): p. 2053-60.

36.   Naito, A., et al., *Severe osteopetrosis, defective interleukin-1 signalling and lymph node organogenesis in TRAF6-deficient mice.* Genes Cells, 1999. **4**(6): p. 353-62.

37.   Ye, H., et al., *Distinct molecular mechanism for initiating TRAF6 signalling.* Nature, 2002. **418**(6896): p. 443-7.

38.   Wada, T., et al., *The molecular scaffold Gab2 is a crucial component of RANK signaling and osteoclastogenesis.* Nat Med, 2005. **11**(4): p. 394-9.

39.   Baud'huin, M., et al., *RANKL, RANK, osteoprotegerin: key partners of osteoimmunology and vascular diseases.* Cell Mol Life Sci, 2007. **64**(18): p. 2334-50.

40.   Bonizzi, G. and M. Karin, *The two NF-kappaB activation pathways and their role in innate and adaptive immunity.* Trends Immunol, 2004. **25**(6): p. 280-8.

41.   Xu, J., et al., *NF-kappaB modulators in osteolytic bone diseases.* Cytokine Growth Factor Rev, 2009. **20**(1): p. 7-17.

42.   Novack, D.V., et al., *The IkappaB function of NF-kappaB2 p100 controls stimulated osteoclastogenesis.* J Exp Med, 2003. **198**(5): p. 771-81.

43.   Novack, D.V., *Role of NF-kappaB in the skeleton.* Cell Res, 2011. **21**(1): p. 169-82.

44.   Mizukami, J., et al., *Receptor activator of NF-kappaB ligand (RANKL) activates TAK1 mitogen-activated protein kinase kinase kinase through a signaling complex containing RANK, TAB2, and TRAF6.* Mol Cell Biol, 2002. **22**(4): p. 992-1000.

45.   Ninomiya-Tsuji, J., et al., *The kinase TAK1 can activate the NIK-I kappaB as well as the MAP kinase cascade in the IL-1 signalling pathway.* Nature, 1999. **398**(6724): p. 252-6.

46.   Kim, K., et al., *Pim-1 regulates RANKL-induced osteoclastogenesis via NF-kappaB activation and NFATc1 induction.* J Immunol, 2010. **185**(12): p. 7460-6.

47.   Jin, W., et al., *Deubiquitinating enzyme CYLD negatively regulates RANK signaling and osteoclastogenesis in mice.* J Clin Invest, 2008. **118**(5): p. 1858-66.

48.   Hauer, J., et al., *TNF receptor (TNFR)-associated factor (TRAF) 3 serves as an inhibitor of TRAF2/5-mediated activation of the noncanonical NF-kappaB pathway by TRAF-binding TNFRs.* Proc Natl Acad Sci U S A, 2005. **102**(8): p. 2874-9.

49.   Kyriakis, J.M. and J. Avruch, *Mammalian mitogen-activated protein kinase signal transduction pathways activated by stress and inflammation.* Physiol Rev, 2001. **81**(2): p. 807-69.

50.   Miyazaki, T., et al., *Reciprocal role of ERK and NF-kappaB pathways in survival and activation of osteoclasts.* J Cell Biol, 2000. **148**(2): p. 333-42.

51.   Lee, S.E., et al., *The phosphatidylinositol 3-kinase, p38, and extracellular signal-regulated kinase pathways are involved in osteoclast differentiation.* Bone, 2002. **30**(1): p. 71-77.

52.   David, J.P., et al., *JNK1 modulates osteoclastogenesis through both c-Jun phosphorylation-dependent and -independent mechanisms.* J Cell Sci, 2002. **115**(Pt 22): p. 4317-25.

53.   Ge, B., et al., *MAPKK-independent activation of p38alpha mediated by TAB1-dependent autophosphorylation of p38alpha.* Science, 2002. **295**(5558): p. 1291-4.

54.   Lee, S.W., et al., *TAK1-dependent activation of AP-1 and c-Jun N-terminal kinase by receptor activator of NF-kappaB.* J Biochem Mol Biol, 2002. **35**(4): p. 371-6.

55.   Hogan, P.G., et al., *Transcriptional regulation by calcium, calcineurin, and NFAT.* Genes Dev, 2003. **17**(18): p. 2205-32.

56.   Medyouf, H. and J. Ghysdael, *The calcineurin/NFAT signaling pathway: a novel therapeutic target in leukemia and solid tumors.* Cell Cycle, 2008. **7**(3): p. 297-303.

57.   Takayanagi, H., et al., *Induction and activation of the transcription factor NFATc1 (NFAT2) integrate RANKL signaling in terminal differentiation of osteoclasts.* Developmental Cell, 2002. **3**(6): p. 889-901.

58.   Koga, T., et al., *Costimulatory signals mediated by the ITAM motif cooperate with RANKL for bone homeostasis.* Nature, 2004. **428**(6984): p. 758-763.

59.   Mao, D., et al., *PLCgamma2 regulates osteoclastogenesis via its interaction with ITAM proteins and GAB2.* J Clin Invest, 2006. **116**(11): p. 2869-79.

60.   Asagiri, M., et al., *Autoamplification of NFATc1 expression determines its essential role in bone homeostasis.* J Exp Med, 2005. **202**(9): p. 1261-9.

61.   Shiojima, I. and K. Walsh, *Role of Akt signaling in vascular homeostasis and angiogenesis.* Circ Res, 2002. **90**(12): p. 1243-50.

62.   Wong, B.R., et al., *TRANCE, a TNF family member, activates Akt/PKB through a signaling complex involving TRAF6 and c-Src.* Mol Cell, 1999. **4**(6): p. 1041-9.

63.   Arron, J.R., et al., *A positive regulatory role for Cbl family proteins in tumor necrosis factor-related activation-induced cytokine (trance) and CD40L-mediated Akt activation.* J Biol Chem, 2001. **276**(32): p. 30011-7.

64.   Glantschnig, H., et al., *M-CSF, TNF alpha and RANK ligand promote osteoclast survival by signaling through mTOR/S6 kinase.* Cell Death and Differentiation, 2003. **10**(10): p. 1165-1177.

65.   Dougall, W.C., et al., *RANK is essential for osteoclast and lymph node development.* Genes & Development, 1999. **13**(18): p. 2412-2424.

66.   Fata, J.E., et al., *The osteoclast differentiation factor osteoprotegerin-ligand is essential for mammary gland development.* Cell, 2000. **103**(1): p. 41-50.

67.   Kong, Y.Y., et al., *OPGL is a key regulator of osteoclastogenesis, lymphocyte development and lymph-node organogenesis.* Nature, 1999. **397**(6717): p. 315-323.

68.   Hanada, R., et al., *Central control of fever and female body temperature by RANKL/RANK.* Nature, 2009. **462**(7272): p. 505-509.

Chapter 2:
RANK, RANKL and OPG in the field of osteoimmunology

2.1. RANK, RANKL and OPG in bone biology

2.1.1. A dynamic system

Bone is a multifunctional organ enabling locomotive activity, calcium storage and harboring of hematopoietic stem cells (HSCs) from which immune cells are derived. Bones are characterized by calcified hard tissue composed of type I collagen and highly organized deposits of calcium referred to as hydroxyapatite. Even if this organ seems relatively inert, it undergoes a constant remodeling with around 10% of bone mass being replaced per year [1]. Bone remodeling involves a controlled cross-talk between two cell populations: the osteoblasts and the osteoclasts. Osteoblasts originate from bone marrow mesenchymal stem cells and are responsible for new bone formation, whereas osteoclasts differentiate from hematopoietic cells and are specialized in bone resorption [2, 3]. Bone remodeling occurs through temporary anatomic structures: the basic multicellular units (BMUs). The BMUs are cylindrical canal progressing inside the bones, with osteoclasts in the front and osteoblasts in the back, supported by blood vessels, nerves and connective tissue [2, 3]. The remodeling cycle consists of three consecutive phases: resorption, reversal and formation (Figure 2.01). Partially differentiated mononuclear preosteoclasts migrate to the bone surface where they form multinucleated osteoclasts. Multinucleated osteoclast attach to the bone surface via their podosomes and create a sealing zone, in which bone is resorbed by acidification and proteolysis of its matrix. A reversal phase then takes place, with mononuclear cells preparing the bone surface for osteoblasts and providing signals for osteoblast differentiation and migration. The formation phase follows with osteoblasts laying down bone until the resorbed bone is completely replaced by new, the surface is then covered with flattened lining cells, and some osteoblasts are entrapped in bone matrix. These entrapped osteoblasts are referred to as osteocytes. Osteocytes form a network permeating the entire matrix and, once this matrix is calcified, their metabolic activity is decreased but they still produce matrix proteins [2, 3]. Changes in either osteoblast or osteoclast activities can lead to skeletal abnormalities known as osteoporosis (decrease of bone mass) and osteopetrosis (increase of bone mass) so that bone remodelling must be finely tuned. Imbalances can arise from a wide variety of hormonal changes, inflammatory or growth factors [2, 3].
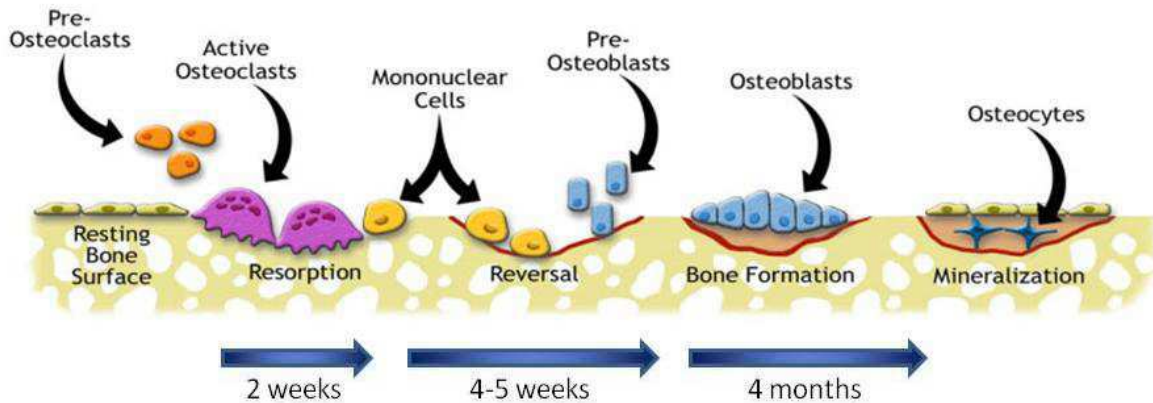
Figure 2.01: Bone remodeling cycle. Schematic representation of the three consecutive phases of bone remodeling. Resorption is thought to last around 2 weeks, the reversal phase may last 4 to 5 weeks and bone formation can last for up to 4 months. After reference [4].

2.1.2. RANK, RANKL and OPG, key factors in bone biology

In 1981, Rodan and Martin proposed a novel hypothesis in which osteoblasts may play a central role in the regulation of osteoclasts formation and subsequent bone resorption [5]. In the early 1990s, studies showed that M-CSF (macrophage colony-stimulating factor) expression by osteoblasts and cell to cell interactions were required for progenitor cells to differentiate into osteoclasts [2]. This requirement for M-CSF was mainly based on the observation that op/op mice, which do not express functional M-CSF, display osteopetrosis, as a result of a lack of osteoclasts [6]. However, *in vitro* studies showed that M-CSF was necessary for progenitor maturation but not sufficient [2]. Many investigators have attempted to identify the osteoclast-activating factor by completing differentiation of precursors induced by M-CSF, but it was only in the late 1990s that the missing pieces of the puzzle were found when OPG, RANKL and RANK were characterized by four different groups. Indeed, the discovery of the TNF and TNFR SFs molecular triad was a major event of the past decade in bone biology. When OPG was first identified, it was demonstrated to act as a soluble decoy-like factor able to inhibit osteoclastogenesis *in vitro* and to induce osteopetrosis when transgenically overexpressed in mice [7]. In contrast, abolition of OPG expression in mice leads to the development of osteoporosis and massive production of osteoclasts [8]. When the link between OPG and RANKL was established, more information about osteoclastogenesis was obtained from mice with modified expression of RANKL. In fact, *Rankl*$^{-/-}$ mice were found to be osteopetrotic and had no tooth eruption because of a defect in osteoclasts development [9], while *Rankl*-transgenic mice exhibit marked osteoporosis [10]. Finally, RANKL was detected on osteoblasts and bone marrow stromal cells, and as RANK is expressed by osteoclasts progenitors, it allowed the conception of the model for osteoclastogenesis described in figure 2.02.
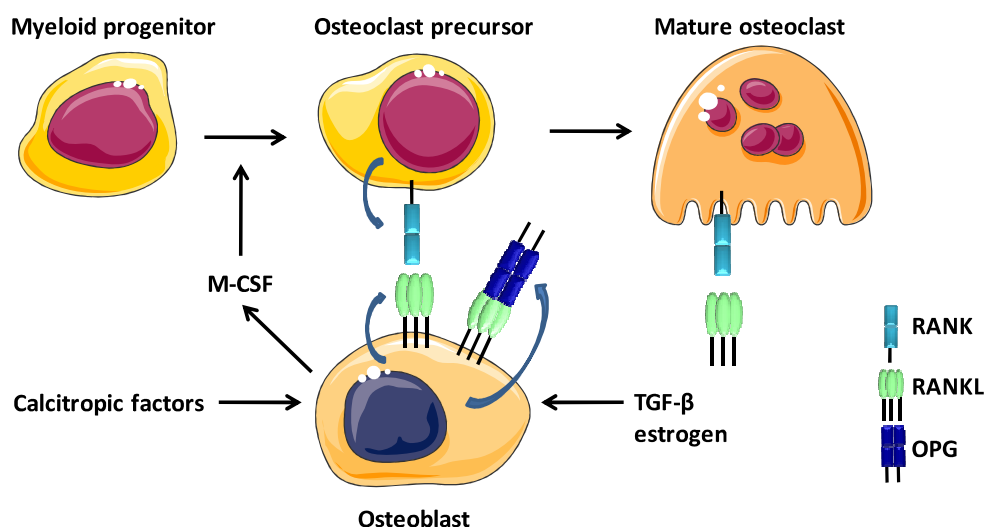
Figure 2.02: Regulation of osteoclastogenesis in bone tissues. Calcitropic factors (vitamin-D3, prostaglandin E, IL-1β, TNF,…) induce osteoblasts to express RANKL and M-CSF. M-CSF promotes the differentiation of myeloid progenitors toward RANK-expressing osteoclasts precursors. RANKL binding to RANK induces signaling cascades leading to the formation of mature plurinucleated osteoclasts. RANKL is also necessary for bone resorbing activity in mature osteoclasts as it induces MMP9 secretion. TGF-β released during bone resorption induces OPG secretion by osteoblasts, thus it is a negative regulator of osteoclastogenesis. Estrogen does also have a regulator action by the same mechanism as TGF-β. After reference [11].

A systemic regulation of bone remodeling is achieved by various factors, such as parathyroid hormone (PTH), vitamin-D3, prostaglandin E2, IL-1β, TNF or estrogen. These factors have been shown to positively or negatively influence osteoclastogenesis by directly affecting RANKL, RANK and OPG expression levels (Chapter 1, Table 1.01) and/or by regulating RANK signal transduction [3]. All the described signaling pathways in Chapter 1 are activated upon RANK engagement by RANKL in osteoclast precursors. Still, TRAF6 seems to be the main adaptor molecule required in osteoclast maturation as TRAF6-deficient mice, like RANK-deficient mice, develop severe osteoporosis [12]. This phenotype is not observed in such a severe form in murine models deficient for other adaptor molecules known to interact with RANK. NF-κB and MAPKs JNK1 and p38 signaling pathways contribute to osteoclast differentiation; MAPK ERK 1 and 2, and PKB/Akt are implied in survival, cytoskeletal reorganization and motility [13]. NFATc1, induced by PKB/Akt and by the NF-κB pathway [14] is a key transcription factor in osteoclast final maturation, as shown by the fact that osteoclast precursors from NFATc1-deficient mice are unable to differentiate into osteoclasts *in vitro* in response to RANKL and M-CSF [15]. NFATc1 promotes expression of osteoclast-specific genes such as tartrate-resistant acid phosphatase (TRAP) [15].

2.1.3. *RANK-, RANKL- and OPG-associated bone pathologies*

- *Genetic inheritance of RANK, RANKL, and OPG*

Implication of the RANK-RANKL-OPG molecular triad in bone biology was also demonstrated in man, as several mutations in genes encoding these proteins were reported in

association with rare severe bone pathologies. The known mutations in these genes and the associated pathologies and symptoms are listed in Table 2.01. In case of autosomal recessive osteopetrosis associated with mutations in *Rankl* sequence, HSC transplantation has been shown to rescue bone phenotype in patients. Accordingly to the proposed mechanism of osteoclastogenesis shown in Figure 2.02 this treatment was less efficient in ARO associated with mutations in *RANK* sequence [16]. In case of osteolysis syndromes, therapies to reduce osteoclastogenesis can be considered. For instance, a human monoclonal blocking antibody against RANKL from Amgen Inc. (Denosumab), is approved since 2010 by the American Food and Drug Administration and by the European Committee for Medicinal Products for human use.

Gene	Allelic variant	Type of mutation	Associated pathology
RANKL		1-3 Loss of function	**ARO** Severe osteopetrosis Lack of osteoclasts
RANK		1-7 Loss of function	**ARO** Severe osteopetrosis Hypogammaglobulinemia
		8,9 Gain of function	**FEO** Osteolytic lesions Hearing loss Tooth loss
		10 Gain of function	**PDB2** Osteolytic lesions Hypercalcemia
		11 Gain of function	**ESH** Osteolytic lesions Hypercalcemia Hearing loss Tooth loss
OPG		1-6 Loss of function	**JPD** Osteolytic lesions Hyperphosphatasia Hearing loss Tooth loss
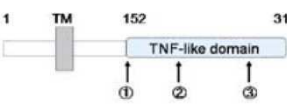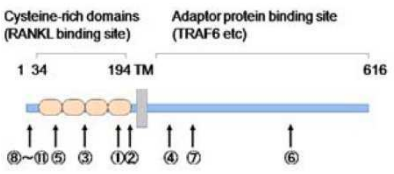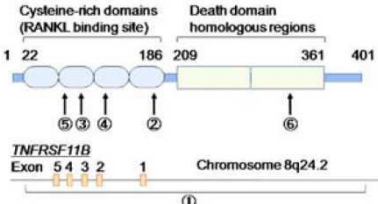
Table 2.01: Genetic inheritance of RANK, RANKL and OPG. Known human mutations in *RANK*, *RANKL* and *OPG* sequences. Abbreviations: ARO, autosomal recessive osteopetrosis; FEO, familial expansile osteolysis; PDB2, early onset Paget's bone disease; ESH, expansile skeletal hyperphosphatasia; JPD, juvenile Paget's bone disease. Modified after reference [16].

- ***Osteoporosis in postmenopausal women***

Postmenopausal women, in whom estrogen levels naturally decline, are at the highest risk for developing osteoporosis. Morphological studies and measurements of biochemical markers indicated that bone remodeling is accelerated at menopause, as both markers of resorption and formation are increased [17, 18]. Thus, an increase in bone resorption but not an impaired bone formation appears to be the mechanism responsible for bone loss in postmenopausal women. The rapid and continuous bone

loss that occurs for several years after the menopause must indicate an impaired bone formation response, since in younger individuals going through the pubertal growth spurt, even faster rates of bone resorption can be associated with an increase in bone mass [19]. It was shown that estradiol attenuates RANK signaling by strongly inducing OPG expression in osteoblasts [20]. In addition, compared to premenopausal women or women on estrogen therapy, postmenopausal women have increased RANKL expression in pre-osteoblasts [18]. Inhibition of osteoclastogenesis by estrogen was also attributed to reduced expression of proinflammatory cytokines, including IL-1, IL-6, TNF and prostaglandin E2 which are known to influence expression of both RANKL and OPG (Chapter 1, Table 1.02) [21]. All these data provide evidence of the role of RANKL-RANK-OPG triad in osteoporosis associated with a diminished estrogen level. Reinforcing this role, RANKL-blocking Denosumab was shown to act as an anti-resorptive agent [22]. Nevertheless, another study about efficiency and safety of Denosumab in over 10000 postmenopausal women with osteoporosis had shown that despite its effectiveness as an anti-resorptive agent, Denosumab had not yet proved its efficacy on fracture risk reduction while increased infection risks question its safety [22].

- *Bone metastasis and tumor-associated osteolysis*

Certain tumor types, such as breast cancer, prostate cancer and myeloma, frequently metastasize to the bones. Approximately 75% of patients with advanced breast or prostate cancers develop bone metastasis, which are associated with severe pain, pathological fractures, nerve compression syndromes and hypercalcemia [23]. Propensity of these cancers to metastasize specifically to the bone can be explained by RANK expression by most of the cancer cells found in the bone metastasis, so that RANKL produced in the bone marrow has an important role in cell migration and tissue-specific behavior of cancer cells [24]. RANK activation was also shown to inhibit expression of Maspin protein in prostate cancer cells, which is implicated in inhibition of invasion and motility of cancer cells [25]. Bone metastasis induce dysregulation of the normal bone remodeling process, resulting most frequently in osteolytic lesions (bone destruction) but osteoblastic lesions (new bone formation) are also found associated with prostate cancer bony metastasis. Osteoclastic bone resorption growth factors, such as TGF-β, insulin like growth factor (IGF) or bone morphogenic proteins (BMPs) are released from bone matrix in active forms. These factors provide a fertile ground in which tumor cells can proliferate. In turn, tumor cells secrete factors such as PTH, activating osteoblasts to secrete RANKL, or pre-osteoclasts to differentiate, resulting in a vicious circle of bone osteolysis (Figure 2.03) [24, 26]. Three phase III clinical trials were conducted to test Denosumab efficacy in preventing bone metastasis osteolysis in over 5000 patients with breast, prostate cancers or myelomas [27-29]. Compared with zoledronic acid, a bisphosphonate currently used to prevent osteolysis in cancer patients, Denosumab showed significant effects in delaying apparition of osteolysis symptoms, but there was no difference in cancer progression. Two phase III clinical trials are currently under progress to test bone metastasis prevention efficacy of Denosumab in patient with

breast and prostate cancer without metastasis [30]. It should be noted that all of the studies with Denosumab were funded by Amgen Inc.
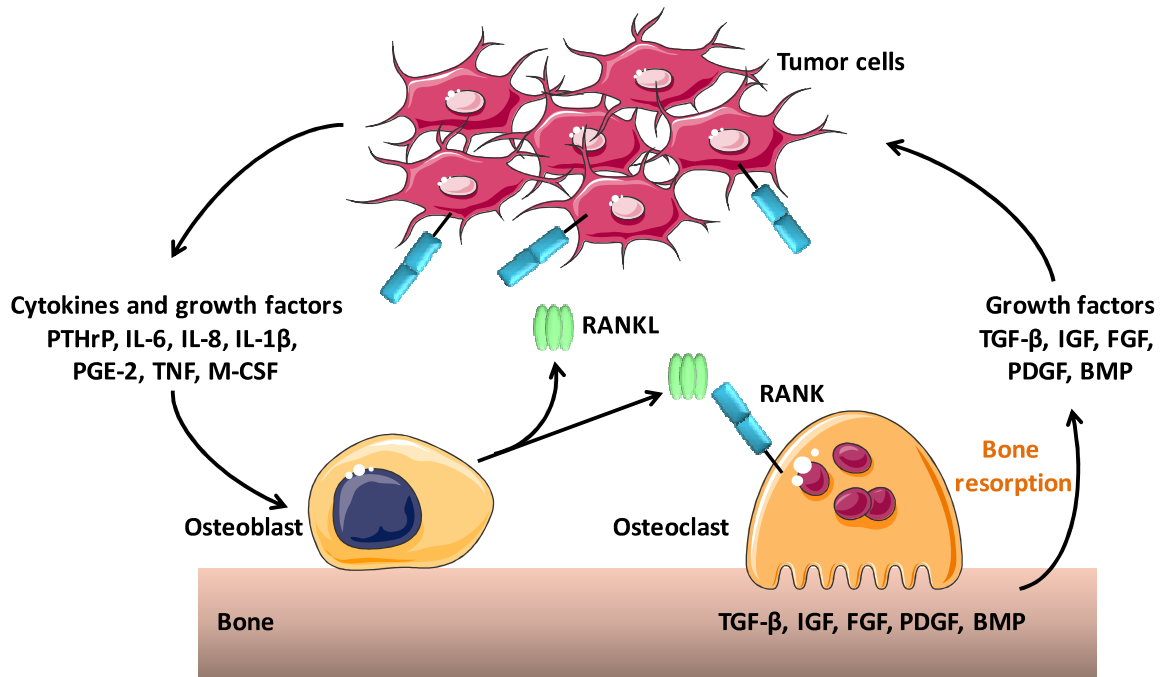
Figure 2.03: RANKL, the key mediator in the vicious cycle of bone destruction. Interactions between tumor cells and bone micoenvironment is showed, highlighting the central role of RANKL in this deleterious process. In this vicious cycle, tumor-induced osteoclastic bone resorption causes the release of growth factors, which provide a fertile ground for tumor cells proliferation. Abbreviations: BMP, bone morphogenic protein; M-CSF, macrophage colony-stimulated factor; FGF, fibroblast growth factor; IGF, insulin-like growth factor; IL, interleukin; PDGF, platelet-derived growth factor; PTHrP, parathyroid hormone-related protein; TGF, transforming growth factor; TNF, tumor necrosis factor. After reference [31].

2.2. *RANK, RANKL and OPG in the immune system*

It was unexpected that the long-sought osteoclast-differentiation factor expressed by osteoblasts would be the same molecule expressed by T cells to stimulate dendritic cells (DCs), as described by Anderson and co-workers [32]. A role of RANK-stimulation in DC biology has since then been confirmed and additionally other crucial roles in the immune system have also been attributed to RANK and RANKL. In fact, RANK- and RANKL-deficient mice completely lack lymph nodes (LNs) [9, 33], and transfer of wild-type bone marrow cells into newborn RANKL-knockout mice did not rescue LNs formation suggesting that impaired homing of lymphocytes is not the cause leading to defective LNs formation [9]. RANK and RANKL are key factors directly affecting LN organogenesis and this function will be fully described in Chapter 3. In addition to these roles, RANK and RANKL are also implicated in T and B cell development, as well as in immune tolerance.

2.2.1. Role in dendritic cell biology

DCs are short-lived professional antigen-presenting cells and are effective in initiating T-cell-mediated immunity *in vivo*. RANK surface expression can be detected on DCs from various sources, such as mature bone marrow-derived DCs, freshly isolated LN and splenic DCs and mucosal DCs [34, 35], whereas RANKL is only expressed on activated CD4^{+} and CD8^{+} T cells [36]. Interaction between RANKL expressed by activated T cells and RANK on DCs induces DCs survival by upregulating the anti-apoptotic protein Bcl-xL [35] through activation of the classical NF-κB pathway [37]. RANK also induces the anti-apoptotic PKB/Akt pathway through recruitment of PI3K by TRAF6, Cbl-b and c-Src [38, 39]. *In vivo* relevance of this anti-apoptotic effect has been shown by Zhong and co-workers as DC "vectors" intended for use in immunotherapy persist longer when they are pre-treated with RANKL [40]. This survival function of RANK has also been shown on Langerhans cells, which are the resident DCs in the epidermis [41]. In addition to this pro-survival activity, RANKL also stimulates DC to produce pro-inflammatory cytokines (IL-6, IL-1β) and T cells differentiation factors (IL-12, IL-15) [42]. At the same time, it has also been shown that mucosal DCs, isolated from Peyer's patches preferentially secrete the anti-inflammatory cytokine IL-10 [34]. Unlike CD40L, expressed on T cells, which binds CD40 on DCs and induces also DCs survival and activation, RANK engagement does not lead to an increase in MHC (major histocompatibility complex) class II or the costimulatory molecules CD80 and CD86 [35]. Moreover, mice deficient for RANK, RANKL or OPG present no overt defect in DCs, with intact basic subsets and an intact *in vitro* mediation of T cell mixed lymphocyte reaction (MLR) and cytokines secretion [9, 33, 43]. DCs from two patients presenting autosomal recessive osteopetrosis pathology linked to a mutation in *Rank* showed no maturation defect and displayed a normal MLR activity [44]. An explanation to this could be the degree of overlapping functions between RANK-RANKL and CD40-CD40L. Thus, blockade of RANK signaling *in vivo* results in a slightly reduced CD4^{+} T cell response to lymphocytic choriomeningitis virus (LCMV) but the anti-viral response is more severely inhibited when both RANK and CD40 signaling are absent [45]. Differences between CD40 and RANK requirement for an effective immune response may be explained by differential expression patterns and kinetics. RANK expression within the immune system is mainly restricted to DCs, whereas CD40 can be found highly expressed on DCs, macrophages and B cells. The kinetics of RANKL and CD40L expression after T cell activation are also different, with a maximal level of CD40L expression reached after 6 to 8h, and down-regulated to resting level after 24 to 48h, whereas RANKL maximal expression is achieved around 48h and last until 96h. Thus, CD40-CD40L interactions might primarily control initiation and effector phases, and RANK-RANKL signaling could be more important in waning phases (Figure 2.04a) [46]. It was also shown that RANKL can cooperate with CD40L to maximise the ability of DCs to expand virus-specific cytotoxic T lymphocyte response, mainly by enhancing survival of CD40L-activated DCs [47]. It can be noted that CD40 signaling in DCs leads to OPG expression [48] and, since activated T

cells express both RANKL and TRAIL, one could speculate that the balance between these factors regulates the fate of DCs. Nevertheless, OPG affinity for TRAIL is around 10,000 times weaker than its affinity for RANKL, and the *in vivo* relevance of such a mechanism needs to be clarified (Figure 2.04b) [46].
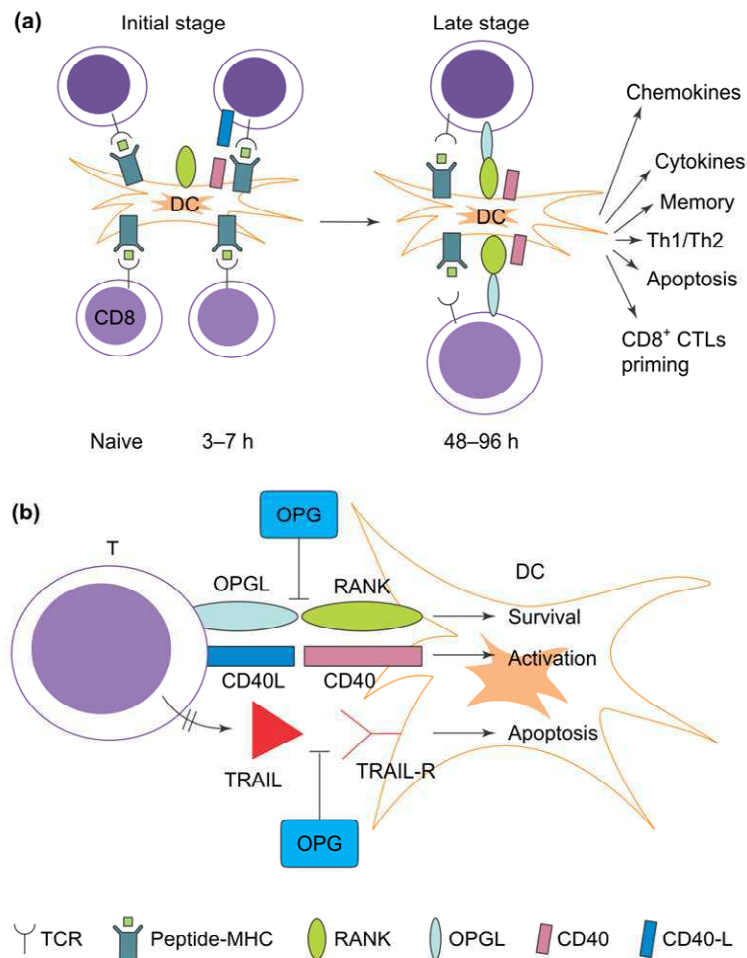
Figure 2.04: Proposed RANK, RANKL and OPG interactions during an immune response. (a) Proposed kinetic in DC activation by T cells expressing CD40L and RANKL. (b) Different functions for RANK and CD40 signaling in DCs and proposed OPG regulation role. After reference [49].

2.2.2. *T cell and B cell development*

RANKL-deficient mice described by Kong and colleagues present a block in the progression of CD4$^-$CD8$^-$CD44$^-$CD25$^+$ (DN3) precursors to CD4$^-$CD8$^-$CD44$^-$CD25$^-$ (DN4) thymocytes due to an intrinsic defect, that only become apparent at around two weeks of age [9]. This defect occurs just before the first principal checkpoint in T lymphocyte development, where the expression of a pre-TCR (T cell receptor) on CD4$^-$CD8$^-$ is required for further expansion (Figure 2.05). RANKL expression has been detected on CD4$^-$CD8$^-$ early thymocytes precursors [32], however, although RANK was shown to be expressed in RANKL-deficient mice thymus [9], RANK-deficient mice do not present any

thymocytes impaired development [33]. This difference in thymocyte development is the only distinction between RANK- and RANKL-deficient mice, suggesting that RANKL might act on another unidentified receptor or that this phenotype was the result of other *in vivo* phenotypes in RANKL-knockout mice, an explanation proposed recently by authors who described this murine model [46].
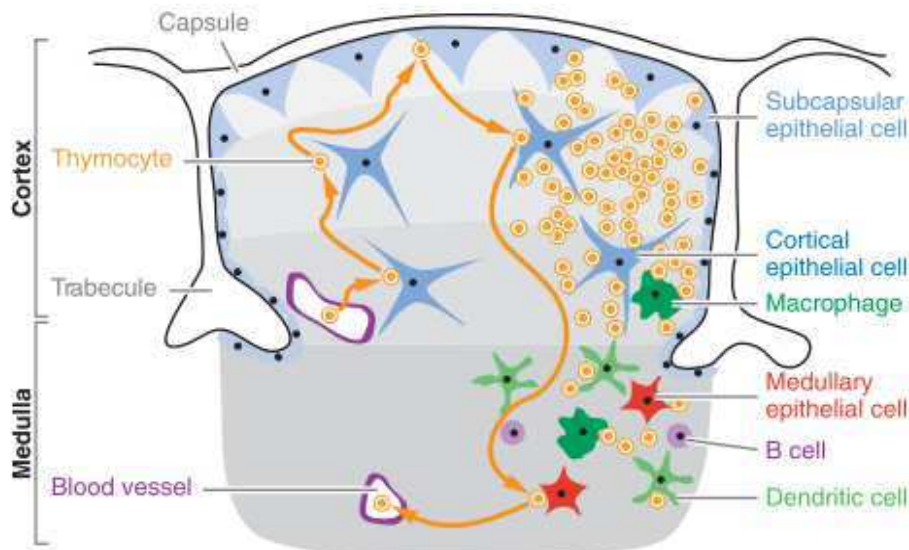
Figure 2.05: Thymic T cells selection. Thymocytes double negative (DN) CD44$^+$CD25$^-$ progenitors (DN1) enter the thymus via blood vessels near the cortico-medullary junction. Cells then migrate toward the subcapsular epithelium, upregulate CD25 (DN2) and down-regulate CD44 (DN3). At this point TCRβ rearrangement occurs, if pairing with pre-TCRα is successful, cells downregulate CD25 (DN4) proliferate and start expressing CD4 and CD8 (DP). Afterwards, rearrangement of TCRα occurs and cortical thymocytes are subjected to positive and negative selection. Single positive cells finally migrate through the medulla before exiting the thymus. After reference [50].

In addition to T cells, RANKL and RANK have a role in B cells development, which was confirmed in human, as most *Rank* mutations are associated with hypogammaglobulinemia [44, 51]. RANK- and RANKL-deficient mice display a reduced number of mature B220$^+$IgD$^+$ and B220$^+$IgM$^+$ B cells in spleen and LNs and slightly disorganized B cells areas in splenic follicles [9, 33, 52]. The reduced cellularity is best explained by osteopetrosis-associated diminished bone marrow cavities but Kong and co-workers have found that RANKL regulates the progression of the B220$^+$CD43$^+$CD25$^-$ pro-B cell to the B220$^+$CD43$^-$CD25$^+$ pre-B cell stage [9]. Hence, when RANKL-deficient bone marrow was transferred into RAG (recombination activating gene)-knockout mice which provide a RANKL proficient environment, the defect of RANKL-deficient cells progression from the pro-B to the pre-B stage was maintained [9]. Moreover, B cells were shown to express OPG and, upon CD40 stimulation, its expression was up-regulated [48]. In OPG-knockout mice, type 1 transitional B cells accumulate in the spleen and pro-B cells have a greater *in vitro* proliferative response to IL-7 than wild-type pro-B cells [43]. The expansion of transitional B cells in OPG-deficient mice and the arrest of progression between pro- and pre-B cells stage in RANK- and RANKL-knockout mice may suggest

that this molecular triad regulates the proliferative expansion of pro-B cells. RANKL and RANK were shown to be expressed by B cells [53].

2.2.3. *Immune Tolerance*

- #### *DCs and T regulatory cells in peripheral tolerance*

RANK signaling has been implicated in the induction of oral tolerance in mice. In mice fed with low-dose of ovalbumin concomitant with intravenous RANKL injections, T cells were refractory to re-challenge compared to T cells from non RANKL-treated mice [34]. The authors did not attribute this effect to an enhanced survival effect mediated by RANKL, as this was not observed *in vitro* for mucosal DCs, but rather to IL-10, based on their result of an *in vitro* production of IL-10 by RANKL treated mucosal DCs [34].

RANK signaling has been found to prevent the onset of autoimmune disease in a TNF-inducible murine diabetes model [54]. In this CD8^{+} T cell-mediated autoimmune disease model, RANKL and RANK are required for CD4^{+}CD25^{+} T regulatory (reg) cells elicitation. Ablation of this pathway leads to a decrease in T reg cells in LNs and pancreatic-associated tissues coupled with rapid diabetes progress, as T reg cells were shown to prevent differentiation of CD8^{+} T cells into cytotoxic T cells in islets of Langerhans [54]. It remains unclear whether RANKL directly triggers T lymphocytes suppression or if this effect is mediated by DCs. Loser and co-worker showed that RANKL is expressed in keratinocytes of inflamed skin and that this expression leads to functional alterations of resident epidermal DCs (Langerhans cells) resulting in an increase of CD4^{+}CD25^{+} T reg cells [55]. The same authors have also shown that epidermal RANKL expression induced by ultraviolet leads to immunosuppression and that overexpression of epidermal RANKL suppressed allergic contact hypersensitivity responses and the development of systemic autoimmunity [55]. UV irradiation locally generates active vitamin D3 in the skin, which functions as a potent enhancer of RANKL (Chapter 1, Table1.02). RANKL appears to enhance the migration of RANK-expressing Langerhans cells to skin draining LNs and thus induces expansion of peripheral CD4^{+}CD25^{+} T reg cells [56] .

- #### *AIRE mediated central tolerance*

In addition to peripheral tolerance-mediated by T reg cells, RANK, RANKL and OPG have also been implicated in central tolerance. RANK controls the development of AIRE[+] (autoimmune regulator) thymic medullary epithelial cells (mTECs) [57]. mTECs play a crucial role in preventing autoimmunity by expressing tissue-restricted antigens (TRAs). After having undergone positive and negative selection mainly mediated by cortical TECs (cTECs), thymocyte precursors migrate from the thymic cortex to the medulla, where they encounter mTECs, which function to help purge the emerging T-cell receptor repertoires from self-reactive specifities by TRAs expression (Figure 2.05).

TRAs expression in mTECs mirrors virtually all tissues of the body, irrespective of the developmental expression patterns and is partially mediated by the transcription factor AIRE [50]. In 2007, Rossi and co-workers have shown that the previously described $CD4^+CD3^-$ lymphoid tissue inducer cells (LTic), linked to secondary lymphoid organ development, are important mediators of functional regulation of TRAs expression by mTECs [57]. RANKL-expressing LTic are closely associated with thymic mTECs and promote the maturation of $RANK^+CD80^-AIRE^-$ mTECs progenitors into $CD80^+AIRE^+$ TRAs-expressing mTECs [57]. One year later, another study proposed that RANKL produced by positively-selected thymocytes regulates mTECs cellularity and thereby provides the thymic medulla integrity and associated central tolerance [58]. In this study, Id-2-deficient mice which do not display Id-2-dependent LTics present no impaired mTECs numbers and mTECs AIRE expression [58]. Nevertheless, both studies agree that RANK signaling has a key role in regulation of mTECs development [57, 58]. Of note, OPG-knockout thymi present medullary hypertrophy and increased number of mTECs [58]. Transplantation of thymic tissue from RANK-deficient mice under the kidney capsule of nude mice induces inflammatory liver infiltrates and autoantibodies deposit in several tissues, confirming the crucial role of RANK signaling in central tolerance [57]. It can be noted that mTECs are also involved in T reg cell induction, indicating another plausible link between RANKL and T reg cells [59].

2.3. *Interactions between systems: the osteoimmunology field*

2.3.1. *T cells and bone loss: emergence of osteoimmunology*

The role that bone plays in the immune system seems obvious as immune cells arise from the bone marrow. Moreover, it is known that HSCs need to interact with specialized microenvironments, known as stem-cell niches to maintain their ability of self-renewal and pluripotency, so that bone microenvironment is crucial for the maintenance of HSCs functions. Hence, osteoblast lineage support HSCs and B cells differentiation in these niches [60]. Although inflammatory autoimmunity can be associated with bone destruction, a role of immune cells in affecting bone long remained uncertain and the molecular link between the two was unclear. The discovery of the molecular triad RANK-RANKL-OPG implied in both bone biology and DC-T cell interactions was a perfect candidate to be the missing piece between chronic inflammation and bone lysis. Thus, as described above, activated T cells express RANKL which is the crucial mediator of osteoclast differentiation and it was tempting to speculate that T cells may play an important role in triggering pathological osteoclastogenesis. Soon after the RANKL discovery, Kong and colleagues confirmed that activated T cells affect bone physiology *in vivo* [61]. In their study, mice lacking CTLA4 (Cytotoxic T-Lymphocyte Antigen 4), in which T cells are spontaneously activated, exhibit severe osteoporosis which can be prevented with OPG treatment [61]. In a complementary study, it was shown that transgenic overexpression of

RANKL in B and T lymphocytes of RANKL-deficient mice partially rescue the osteopetrotic phenotype observed in these mice [62]. These two studies established the ability of lymphocytes to regulate bone homeostasis *in vivo* and raise the question of why no extensive bone loss is observed while there is permanently a proportion of activated T cells in our body. One possible mechanism counteracting RANKL-mediated bone resorption of activated T cells is the upregulation of interferon-γ (IFN-γ) in certain T cells subsets (mainly CD4$^+$ T helper 1, T$_H$1). INF-γ activates the ubiquitin proteasome pathway in osteoclasts, leading to the rapid degradation of TRAF6 and therefore RANK signaling arrest [63]. Other T cell-derived molecules such as IL-12 or IL-4 can inhibit osteoclastogenesis, thus T cell-derived cytokines can counteract osteoclastogenesis [46]. This regulating mechanism seem to be bypassed in inflammatory pathologies associated with bone destruction such as rheumatoid arthritis and periodontitis, and subsequently particular efforts were made to reveal immunologic bases for bone destruction in inflammatory conditions.

2.3.2. RANK, RANKL and OPG in arthritis

Rheumatoid arthritis (RA) is a human autoimmune disease affecting 1% of the world's population and is characterized by chronic inflammation of synovial joints, progressive destruction of bone and cartilage, associated with severe joint pain and ultimately crippling. In a model of adjuvant-induced RA in rat, OPG treatment prevented bone loss and cartilage destruction, but had no effect on inflammation [61]. A subsequent study, using a serum transfer model that bypasses the requirement for T cell activation in RA onset, showed that arthritic RANKL-deficient mice were protected from bone erosion but not from cartilage destruction [64]. These results showed that RANKL is implied in bone lysis but is not essential for cartilage destruction. To establish a clinical relevance of RANKL implications in RA, cellular components from synovial fluids from RA patients were examined for RANKL and OPG expression and in all cases RANKL but not OPG was detected [61]. Studies then characterized an osteoclastogenic T$_H$ subset present in RA synovial fluids which turned out to be T$_H$17 cells. IL-17 is a potent inducer of RANKL expression and can be found in synovial fluid from RA patients, moreover T$_H$17 cells are the only T subsets that can trigger osteoclastogenesis *in vitro* [46, 65]. These T$_H$17 cells fulfilled the three criteria observed in T cells infiltrating synovial fluid: (i) they do not produce large amounts of IFN-γ, (ii) they trigger local inflammation and produce inflammatory cytokines such as TNF and (iii) they express RANKL [66]. Thus, the T$_H$17 cells reduced production of IFN-γ does not suppress RANK signaling in osteoclasts, IL-17 secretion induce an increased RANKL expression on synovial fibroblasts and RANKL expression by T$_H$17 cells themselves induces osteoclastogenesis. These observations lead to the model explaining RA bone loss depicted in Figure 2.06. A role of T cells in non-inflammatory bone diseases such as post-menopausal osteoporosis has also been proposed but is not yet fully recognized [67].
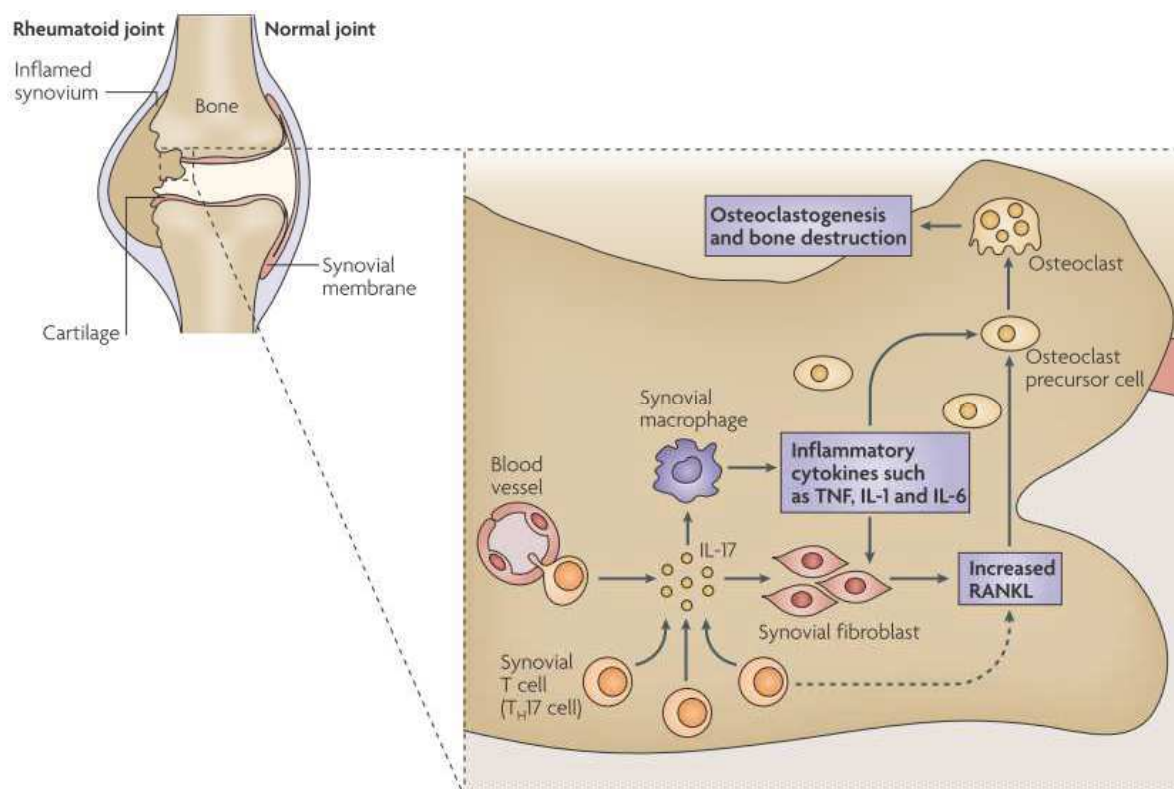
Figure 2.06: Schematic representation of osteoclastogenesis induction by T cells in RA. Infiltrating T_H17 cells in inflamed synovium induce osteoclastogenesis by different mechanisms: (i) direct RANKL expression, (ii) IL-17-induced RANKL expression on synovial fibroblast and (iii) IL-17-induced macrophages activation. After reference [68].

In addition to T_H17 T cells, $CD4^+CD25^+$ T reg cells have also been proposed to have a role in RA, as suppression of T reg function exacerbates arthritis and an increase of their numbers results in amelioration of inflammation and bone destruction [69]. Explanation for this protective role for T reg cells in RA could arise from their ability to inhibit *in vitro* osteoclasts formation induced by M-CSF and RANKL [70]. However, transferred T reg cells appear to be unable to counteract established acute or chronic inflammation [69]

The efficiency of the RANKL-specific antibody, Denosumab, has been tested in clinical trials implying 227 RA patients and a significant decrease in bone and cartilage turnover markers was observed, making a future RA therapy based on RANKL inhibition likely [71].

2.3.3. *RANK, RANKL and OPG in periodontitis*

Periodontitis is another chronic inflammation inducing bone loss in which RANKL-expressing T cells are implicated. Periodontitis is induced by infection with various subgingival bacteria and is a major cause of tooth loss. In order to examine disease etiology, peripheral blood leucocytes from patients with a juvenile localized periodontitis (JLP) were transferred in immunodeficient RAG2-knockout mice, which were then inoculated with a bacteria known to induce periodontitis in man (*Actinobacillus actinomycetemcomitans*) [72]. JLP was reproduced in recipient animals and was

accompanied by an accumulation of osteoclasts in jaw alveolar bones. The authors also demonstrated that treatment with OPG inhibited the osteoclast infiltration, and that deletion of RANKL^{+}CD4^{+} activated T cells specific for *A. actinomycetemcomitans* resulted in disease attenuation [72]. This study demonstrated the importance of RANKL-expressing CD4^{+} T cells in bone destruction associated with periodontitis, and was confirmed by work showing an up-regulation of RANKL vs OPG mRNA in both inflammatory cells and in epithelium from periodontitis patients [73].

2.4. Conclusions

Bone is a dynamic system in which two main protagonists are implied: osteoblasts and osteoclasts. Constant bone remodeling needs to be finely tuned to avoid skeletal abnormalities. The long-sought key osteoclast differentiation factor turned out to be RANKL and it was surprising for both bone biologists and immunologists that this bone resorbing factor was also found to be expressed by activated T cells. Hence, in addition to its functions in bone remodeling, RANKL with its receptor RANK and its decoy receptor OPG were found to be implicated in numerous immune processes such as T cell-DC interactions, B and T cell development, peripheral and central immune tolerance. Synthesis of the crucial mediator of osteoclastogenesis by activated-T cells triggered the discovery of the underlying mechanism for bone loss during chronic inflammation and the emergence of the field of osteoimmunology. Thus, T cell-mediated osteoclastogenesis was found related to bone loss in many human diseases, such as rheumatoid arthritis or periondotitis. In addition, this mechanism was found involved in other pathologies, such as adult and childhood leukemia, chronic infections such as hepatitis C or HIV (human immunodeficiency virus), autoimmune disorders such as diabetes mellitus and lupus erythematous and allergic diseases, such as asthma [46]. T cell-mediated osteoclastogenesis may even play a role in lytic bone metastases associated with multiple cancers, as tumor infiltrating T cells could also directly activate osteoclasts [74]. In the following chapter, I will discuss another important immunological function for RANK, RANKL and OPG, which is their function in lymph node development.
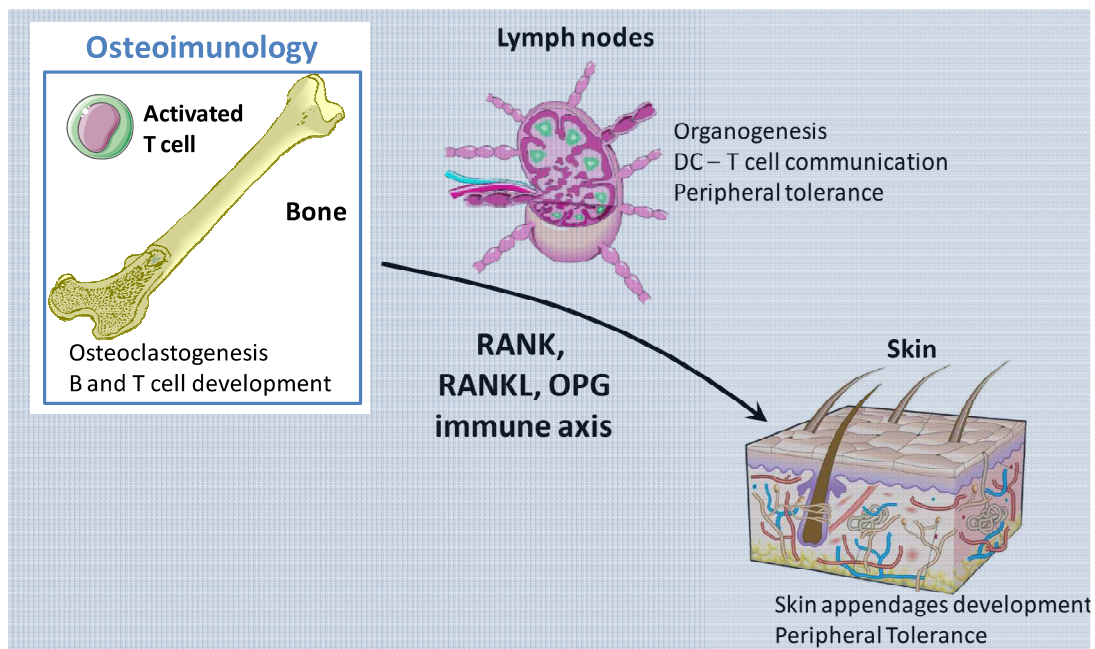
Figure 2.07: The RANK, RANKL and OPG axis: the osteoimmunology field. RANK, RANKL and OPG play crucial role in bone remodeling, and are involved in several immune functions, thereby creating a new field referred to as osteoimmunology. Expression of RANKL by activated T cells provided an explanation for bone lysis often associated with chronic inflammation.

2.5. *Bibliography*

1.   Alliston, T. and R. Derynck, *Medicine: interfering with bone remodelling.* Nature, 2002. **416**(6882): p. 686-7.
2.   Hadjidakis, D.J. and Androulakis, II, *Bone remodeling.* Ann N Y Acad Sci, 2006. **1092**: p. 385-96.
3.   Karsenty, G. and E.F. Wagner, *Reaching a genetic and molecular understanding of skeletal development.* Dev Cell, 2002. **2**(4): p. 389-406.
4.   http://ns.umich.edu/index.html?Releases/2005/Feb05/r022005.
5.   Rodan, G.A. and T.J. Martin, *Role of osteoblasts in hormonal control of bone resorption--a hypothesis.* Calcif Tissue Int, 1981. **33**(4): p. 349-51.
6.   Kodama, H., et al., *Essential role of macrophage colony-stimulating factor in the osteoclast differentiation supported by stromal cells.* J Exp Med, 1991. **173**(5): p. 1291-4.
7.   Simonet, W.S., et al., *Osteoprotegerin: a novel secreted protein involved in the regulation of bone density.* Cell, 1997. **89**(2): p. 309-19.
8.   Bucay, N., et al., *osteoprotegerin-deficient mice develop early onset osteoporosis and arterial calcification.* Genes Dev, 1998. **12**(9): p. 1260-8.
9.   Kong, Y.Y., et al., *OPGL is a key regulator of osteoclastogenesis, lymphocyte development and lymph-node organogenesis.* Nature, 1999. **397**(6717): p. 315-323.
10.   Lacey, D.L., et al., *Osteoprotegerin ligand is a cytokine that regulates osteoclast differentiation and activation.* Cell, 1998. **93**(2): p. 165-76.
11.   Theill, L.E., W.J. Boyle, and J.M. Penninger, *RANK-L and RANK: T cells, bone loss, and mammalian evolution.* Annu Rev Immunol, 2002. **20**: p. 795-823.
12.   Lomaga, M.A., et al., *TRAF6 deficiency results in osteopetrosis and defective interleukin-1, CD40, and LPS signaling.* Genes Dev, 1999. **13**(8): p. 1015-24.
13.   Theoleyre, S., et al., *The molecular triad OPG/RANK/RANKL: involvement in the orchestration of pathophysiological bone remodeling.* Cytokine Growth Factor Rev, 2004. **15**(6): p. 457-75.
14.   Asagiri, M., et al., *Autoamplification of NFATc1 expression determines its essential role in bone homeostasis.* J Exp Med, 2005. **202**(9): p. 1261-9.
15.   Takayanagi, H., *The role of NFAT in osteoclast formation.* Ann N Y Acad Sci, 2007. **1116**: p. 227-37.
16.   Nakashima, T. and H. Takayanagi, *Osteoimmunology: crosstalk between the immune and bone systems.* J Clin Immunol, 2009. **29**(5): p. 555-67.
17.   Ebeling, P.R., et al., *Bone turnover markers and bone density across the menopausal transition.* J Clin Endocrinol Metab, 1996. **81**(9): p. 3366-71.
18.   Eghbali-Fatourechi, G., et al., *Role of RANK ligand in mediating increased bone resorption in early postmenopausal women.* J Clin Invest, 2003. **111**(8): p. 1221-30.
19.   Harada, S. and G.A. Rodan, *Control of osteoblast function and regulation of bone mass.* Nature, 2003. **423**(6937): p. 349-55.
20.   Hofbauer, L.C., et al., *Stimulation of osteoprotegerin ligand and inhibition of osteoprotegerin production by glucocorticoids in human osteoblastic lineage cells: potential paracrine mechanisms of glucocorticoid-induced osteoporosis.* Endocrinology, 1999. **140**(10): p. 4382-9.
21.   Pacifici, R., *Estrogen, cytokines, and pathogenesis of postmenopausal osteoporosis.* J Bone Miner Res, 1996. **11**(8): p. 1043-51.
22.   Anastasilakis, A.D., et al., *Efficacy and Safety of Denosumab in Postmenopausal Women with Osteopenia or Osteoporosis: A Systematic Review and a Meta-analysis.* Hormone and Metabolic Research, 2009. **41**(10): p. 721-729.
23.   Dougall, W.C. and M. Chaisson, *The RANK/RANKL/OPG triad in cancer-induced bone diseases.* Cancer Metastasis Rev, 2006. **25**(4): p. 541-9.
24.   Jones, D.H., et al., *Regulation of cancer cell migration and bone metastasis by RANKL.* Nature, 2006. **440**(7084): p. 692-696.

25.   Luo, J.L., et al., *Nuclear cytokine-activated IKK alpha controls prostate cancer metastasis by repressing Maspin.* Nature, 2007. **446**(7136): p. 690-694.

26.   Akhtari, M., et al., *Biology of breast cancer bone metastasis.* Cancer Biol Ther, 2008. **7**(1): p. 3-9.

27.   Fizazi, K., et al., *Randomized phase II trial of denosumab in patients with bone metastases from prostate cancer, breast cancer, or other neoplasms after intravenous bisphosphonates.* J Clin Oncol, 2009. **27**(10): p. 1564-71.

28.   Henry, D.H., et al., *Randomized, double-blind study of denosumab versus zoledronic Acid in the treatment of bone metastases in patients with advanced cancer (excluding breast and prostate cancer) or multiple myeloma.* J Clin Oncol, 2011. **29**(9): p. 1125-32.

29.   Stopeck, A.T., et al., *Denosumab compared with zoledronic acid for the treatment of bone metastases in patients with advanced breast cancer: a randomized, double-blind study.* J Clin Oncol, 2010. **28**(35): p. 5132-9.

30.   Lipton, A. and C. Goessl, *Clinical development of anti-RANKL therapies for treatment and prevention of bone metastasis.* Bone, 2011. **48**(1): p. 96-9.

31.   Castellano, D., et al., *The role of RANK-ligand inhibition in cancer: the story of denosumab.* Oncologist, 2011. **16**(2): p. 136-45.

32.   Anderson, D.M., et al., *A homologue of the TNF receptor and its ligand enhance T-cell growth and dendritic-cell function.* Nature, 1997. **390**(6656): p. 175-179.

33.   Dougall, W.C., et al., *RANK is essential for osteoclast and lymph node development.* Genes & Development, 1999. **13**(18): p. 2412-2424.

34.   Williamson, E., J.M. Bilsborough, and J.L. Viney, *Regulation of mucosal dendritic cell function by receptor activator of NF-kappa B (RANK)/RANK ligand interactions: impact on tolerance induction.* J Immunol, 2002. **169**(7): p. 3606-12.

35.   Wong, B.R., et al., *TRANCE (tumor necrosis factor [TNF]-related activation-induced cytokine), a new TNF family member predominantly expressed in T cells, is a dendritic cell-specific survival factor.* J Exp Med, 1997. **186**(12): p. 2075-80.

36.   Wong, B.R., et al., *TRANCE is a novel ligand of the tumor necrosis factor receptor family that activates c-Jun N-terminal kinase in T cells.* J Biol Chem, 1997. **272**(40): p. 25190-4.

37.   Ouaaz, F., et al., *Dendritic cell development and survival require distinct NF-kappaB subunits.* Immunity, 2002. **16**(2): p. 257-70.

38.   Arron, J.R., et al., *A positive regulatory role for Cbl family proteins in tumor necrosis factor-related activation-induced cytokine (trance) and CD40L-mediated Akt activation.* J Biol Chem, 2001. **276**(32): p. 30011-7.

39.   Wong, B.R., et al., *TRANCE, a TNF family member, activates Akt/PKB through a signaling complex involving TRAF6 and c-Src.* Mol Cell, 1999. **4**(6): p. 1041-9.

40.   Zhong, L., et al., *Recombinant adenovirus is an efficient and non-perturbing genetic vector for human dendritic cells.* Eur J Immunol, 1999. **29**(3): p. 964-72.

41.   Barbaroux, J.B., et al., *Epidermal receptor activator of NF-kappaB ligand controls Langerhans cells numbers and proliferation.* J Immunol, 2008. **181**(2): p. 1103-8.

42.   Josien, R., et al., *TRANCE, a TNF family member, is differentially expressed on T cell subsets and induces cytokine production in dendritic cells.* J Immunol, 1999. **162**(5): p. 2562-8.

43.   Yun, T.J., et al., *Osteoprotegerin, a crucial regulator of bone metabolism, also regulates B cell development and function.* J Immunol, 2001. **166**(3): p. 1482-91.

44.   Guerrini, M.M., et al., *Human osteoclast-poor osteopetrosis with hypogammaglobulinemia due to TNFRSF11A (RANK) mutations.* Am J Hum Genet, 2008. **83**(1): p. 64-76.

45.   Bachmann, M.F., et al., *TRANCE, a tumor necrosis factor family member critical for CD40 ligand-independent T helper cell activation.* J Exp Med, 1999. **189**(7): p. 1025-31.

46.   Leibbrandt, A. and J.M. Penninger, *Novel Functions of RANK(L) Signaling in the Immune System.* Adv Exp Med Biol, 2010. **658**: p. 77-94.

47.   Yu, Q., et al., *Cooperation of TNF family members CD40 ligand, receptor activator of NF-kappa B ligand, and TNF-alpha in the activation of dendritic cells and the expansion of viral*

        specific CD8+ T cell memory responses in HIV-1-infected and HIV-1-uninfected individuals. J
        Immunol, 2003. **170**(4): p. 1797-805.

48.   Yun, T.J., et al., *OPG/FDCR-1, a TNF receptor family member, is expressed in lymphoid cells
        and is up-regulated by ligating CD40.* Journal of Immunology, 1998. **161**(11): p. 6113-6121.

49.   Kong, Y.Y., W.J. Boyle, and J.M. Penninger, *Osteoprotegerin ligand: a regulator of immune
        responses and bone physiology.* Immunol Today, 2000. **21**(10): p. 495-502.

50.   Kyewski, B. and L. Klein, *A central role for central tolerance.* Annu Rev Immunol, 2006. **24**: p.
        571-606.

51.   Crockett, J.C., et al., *New knowledge on critical osteoclast formation and activation pathways
        from study of rare genetic diseases of osteoclasts: focus on the RANK/RANKL axis.* Osteoporos
        Int, 2011. **22**(1): p. 1-20.

52.   Hsu, H., et al., *Tumor necrosis factor receptor family member RANK mediates osteoclast
        differentiation and activation induced by osteoprotegerin ligand.* Proc Natl Acad Sci U S A,
        1999. **96**(7): p. 3540-5.

53.   Senftleben, U., et al., *Activation by IKKalpha of a second, evolutionary conserved, NF-kappa B
        signaling pathway.* Science, 2001. **293**(5534): p. 1495-9.

54.   Green, E.A., Y. Choi, and R.A. Flavell, *Pancreatic lymph node-derived CD4(+)CD25(+) Treg
        cells: highly potent regulators of diabetes that require TRANCE-RANK signals.* Immunity,
        2002. **16**(2): p. 183-91.

55.   Loser, K., et al., *Epidermal RANKL controls regulatory T-cell numbers via activation of
        dendritic cells.* Nature Medicine, 2006. **12**(12): p. 1372-1379.

56.   Loser, K. and S. Beissert, *Regulation of cutaneous immunity by the environment: an important
        role for UV irradiation and vitamin D.* Int Immunopharmacol, 2009. **9**(5): p. 587-9.

57.   Rossi, S.W., et al., *RANK signals from CD4(+)3(-) inducer cells regulate development of Aire-
        expressing epithelial cells in the thymic medulla.* J Exp Med, 2007. **204**(6): p. 1267-72.

58.   Hikosaka, Y., et al., *The cytokine RANKL produced by positively selected thymocytes fosters
        medullary thymic epithelial cells that express autoimmune regulator.* Immunity, 2008. **29**(3):
        p. 438-50.

59.   Hinterberger, M., et al., *Autonomous role of medullary thymic epithelial cells in central
        CD4(+) T cell tolerance.* Nat Immunol, 2010. **11**(6): p. 512-9.

60.   Horowitz, M.C., J.A. Fretz, and J.A. Lorenzo, *How B cells influence bone biology in health and
        disease.* Bone, 2010. **47**(3): p. 472-9.

61.   Kong, Y.Y., et al., *Activated T cells regulate bone loss and joint destruction in adjuvant
        arthritis through osteoprotegerin ligand.* Nature, 1999. **402**(6759): p. 304-9.

62.   Kim, N., et al., *Diverse roles of the tumor necrosis factor family member TRANCE in skeletal
        physiology revealed by TRANCE deficiency and partial rescue by a lymphocyte-expressed
        TRANCE transgene.* Proc Natl Acad Sci U S A, 2000. **97**(20): p. 10905-10.

63.   Takayanagi, H., et al., *T-cell-mediated regulation of osteoclastogenesis by signalling cross-talk
        between RANKL and IFN-gamma.* Nature, 2000. **408**(6812): p. 600-605.

64.   Pettit, A.R., et al., *TRANCE/RANKL knockout mice are protected from bone erosion in a serum
        transfer model of arthritis.* Am J Pathol, 2001. **159**(5): p. 1689-99.

65.   Kotake, S., et al., *IL-17 in synovial fluids from patients with rheumatoid arthritis is a potent
        stimulator of osteoclastogenesis.* J Clin Invest, 1999. **103**(9): p. 1345-52.

66.   Sato, K., et al., *Th17 functions as an osteoclastogenic helper T cell subset that links T cell
        activation and bone destruction.* J Exp Med, 2006. **203**(12): p. 2673-82.

67.   Cenci, S., et al., *Estrogen deficiency induces bone loss by increasing T cell proliferation and
        lifespan through IFN-gamma-induced class II transactivator.* Proc Natl Acad Sci U S A, 2003.
        100(18): p. 10405-10.

68.   Takayanagi, H., *Osteoimmunology: shared mechanisms and crosstalk between the immune
        and bone systems.* Nat Rev Immunol, 2007. **7**(4): p. 292-304.

69.   Frey, O., et al., *The role of regulatory T cells in antigen-induced arthritis: aggravation of arthritis after depletion and amelioration after transfer of CD4+CD25+ T cells.* Arthritis Res Ther, 2005. **7**(2): p. R291-301.

70.   Zaiss, M.M., et al., *Treg cells suppress osteoclast formation: a new link between the immune system and bone.* Arthritis Rheum, 2007. **56**(12): p. 4104-12.

71.   Sharp, J.T., et al., *Denosumab prevents metacarpal shaft cortical bone loss in patients with erosive rheumatoid arthritis.* Arthritis Care Res (Hoboken), 2010. **62**(4): p. 537-44.

72.   Teng, Y.T., et al., *Functional human T-cell immunity and osteoprotegerin ligand control alveolar bone destruction in periodontal infection.* J Clin Invest, 2000. **106**(6): p. R59-67.

73.   Liu, D., et al., *Expression of RANKL and OPG mRNA in periodontal disease: possible involvement in bone destruction.* Int J Mol Med, 2003. **11**(1): p. 17-21.

74.   Colucci, S., et al., *T cells support osteoclastogenesis in an in vitro model derived from human multiple myeloma bone disease: the role of the OPG/TRAIL interaction.* Blood, 2004. **104**(12): p. 3722-30.

Chapter 3:
Lymph node development: the function of RANK, RANKL and OPG

3.1. *The lymphatic system: lymph, lymphatic vessels and lymph nodes*

The lymphatic system is the system of lymphoid channels and tissues that drains extracellular fluid from the periphery to the blood. It is composed of a vascular network and secondary lymphoid organs (SLOs) such as lymph nodes (LNs), Peyer's Patches (PPs), tonsils or, in rodents, nasal-associated lymphoid tissue (NALT), spleen and thymus. After a description of the lymphatic vasculature, in the following part I will mainly focus on the development of one of these SLOs: the LN.

3.1.1. *Lymph and cell entry into the lymphatic vessels*

The primary role of the lymphatic vascular system is the maintenance of tissue fluid homeostasis by draining excess interstitial fluid (lymph leaking from blood capillaries) and returning it into the blood flow. In a healthy adult, around 20 liters of protein-poor lymph fluid leaks into the extravascular space in a day, around 90% of it being resorbed locally and the 2 remaining liters are returned to the circulation through the lymph vessels [1]. This vascular system is associated with absorption of lipids from the intestinal tract and initiation of immune response by the transport of migrating cells and soluble antigens to SLOs [2, 3]. The lymphatic capillaries form wide-meshed plexuses in the extracellular matrices of most tissues and run in parallel to blood vasculature. They begin as dilated, blind-ended tubes larger than blood capillaries. In contrast to blood capillaries, they lack continuous basal membrane and associated pericytes but are composed of a continuous single layer of overlapping endothelial cells (lymphatic endothelial cells, LECs) forming loose intercellular junctions (Figure 3.01a) [3, 4]. Instead of the adherens junctions found in blood vessels, LECs form discontinuous junctions composed of platelet-endothelial cell adhesion molecule-1 (PECAM-1 or CD31) and vascular endothelial cadherin, with a spacing between them in the range of 3μm. Thus, lymphatic capillaries openly communicate with the interstitium. They are prevented from collapsing by anchoring filaments which attach their walls to the surrounding connective tissue structures and are thought to pull lymph capillaries open when interstitial pressure increases (Figure 3.01b) [3, 4].
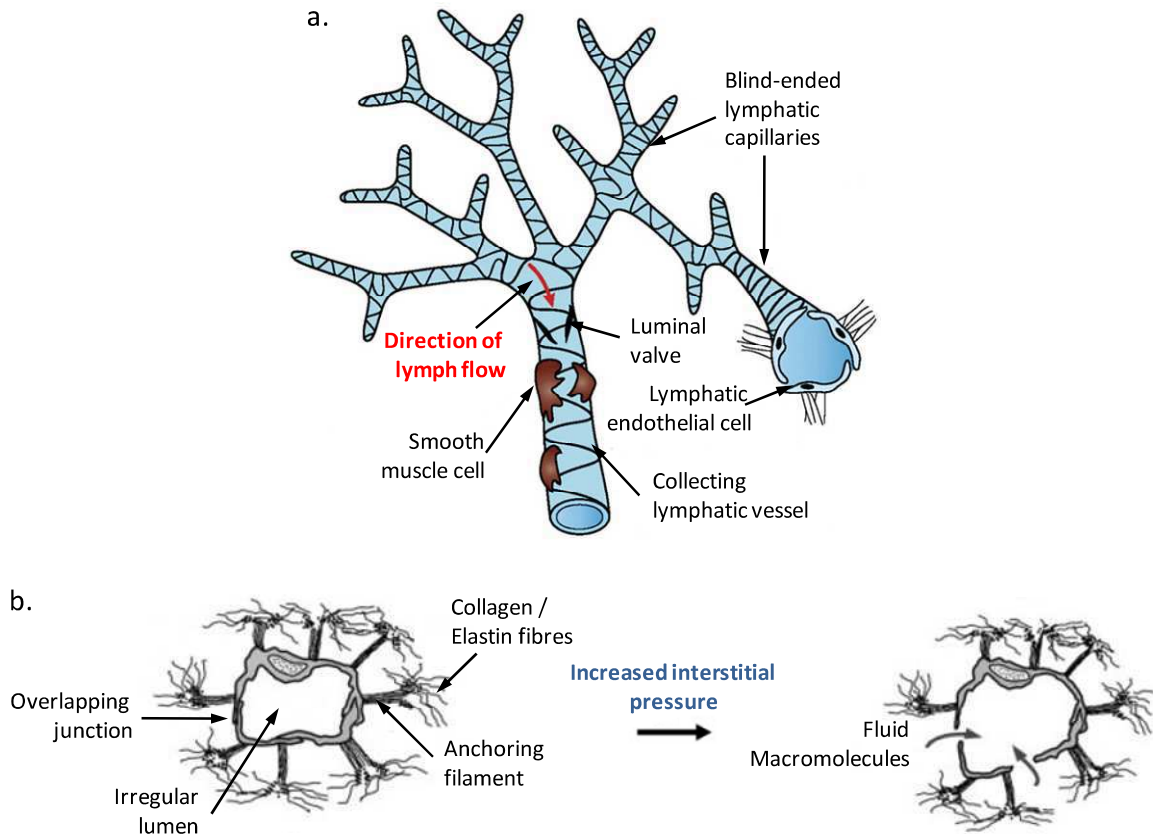
Figure 3.01: Schematic representation of the structure of lymphatic vessels. (a) General organization of lymphatic capillaries and collecting vessels. Modified after reference [5]. (b) Model of a lymphatic capillary opening by an increased interstitial pressure. Modified after reference [4].

These characteristics make lymphatic capillaries highly permeable to interstitial fluid but also to large macromolecules, pathogens and migrating cells. Based on *in vitro* assays and pharmacological inhibition tests, several adhesion molecules have been found to be implicated in cell entry. These molecules include the leukocyte function-associated antigen-1 (LFA1) and very late antigen 4 (VLA4) on DCs and their respective encounter ligands, vascular cell adhesion molecule-1 (VCAM-1) and intercellular adhesion molecule-1 (ICAM-1) on LECs [6]. Other molecules implied in this process have been described, such as mannose receptor and common lymphatic endothelial and vascular endothelial receptor-1 (CLEVER-1) expressed by some peri-tumoral vessels. These molecules seem to be involved in the binding of cancer cells [7]. A second model of cell entry in lymphatic capillaries is emerging. In this model, the gaps between the junctions of LECs would be sufficient for cells to squeeze through the endothelium without using specialized mechanisms of intravasion. In such a model, leukocytes [8] and DCs [9] could follow a gradient of CCL21 (chemokine C-C motif ligand 21) expressed by LECs to enter the lymph capillaries. However, the continuous interstitial flow would counteract a diffuse distribution of chemokines by rather sucking CCL21 into the vessels. An alternative model for chemotactic migration was referred to as the autologous chemotaxis. As many cells, which express the receptor CCR7 (chemokine C-C motif receptor 7), also express its ligand

CCL19, convection of interstitial fluid was proposed to create a gradient of this chemokine toward lymph capillaries that can be followed by the same cell. This mechanism was shown to be relevant in the migration of cancer cells into lymph vessels [10].

3.1.2. *Transport within the lymphatic vessels*

Transport within the lymphatic capillaries of molecules and cells is a passive unidirectional flow towards larger collecting vessels, such as the thoracic duct which is a major collecting duct. The forces that move lymph through the vessels include periodic contractions of lymphatic vessels which unlike capillaries display a muscular layer (Figure 3.01a). Respiratory movements and skeletal muscles action are also implied in this process. The unidirectional flow of lymph is maintained by the presence of valves in the larger collecting vessels (Figure 3.02) [2].
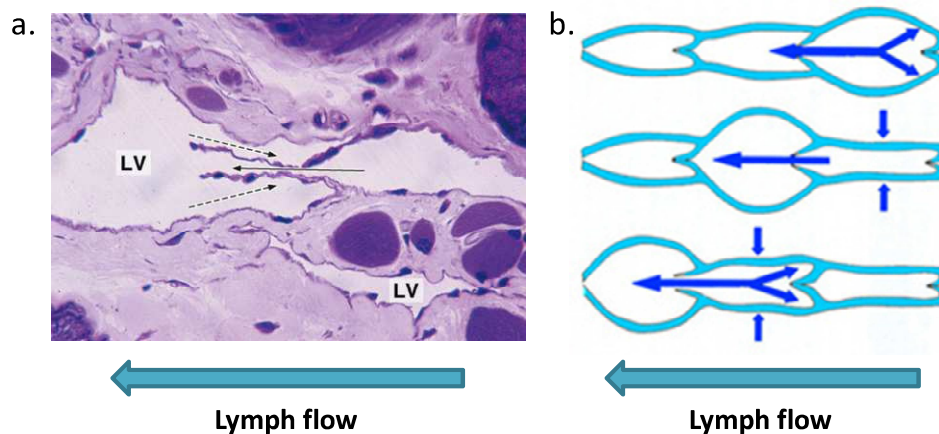
Figure 3.02: The lymph flow through collecting lymphatic vessels. (a) A lymphatic vessel (LV) with its valve in a longitudinal section. Solid arrows show the lymph flow and dotted arrows indicate how the lymph reflux is prevented by the valve (pararosaniline-toluidine staining). (b) Schematic representation of a collecting lymphatic vessel depicting the valve function in lymph flow. Modified after reference [11].

The collecting lymph vessels join to form lymph trunks, which drain lymph into one of the two lymph ducts: the right lymph duct and the thoracic duct. The thoracic duct, which is structurally similar to a medium-sized vein in man, collects most of the lymph in the body. Exceptions are made with lymph arising from the right arm and the right side of the chest, the neck and the head and the lower left lobe of the lung, which is collected by the right lymphatic duct. The thoracic duct drains lymph back into blood circulation by dumping into the left subclavian vein, while the right lymphatic duct opens into the right subclavian vein (Figure 3.03) [12].
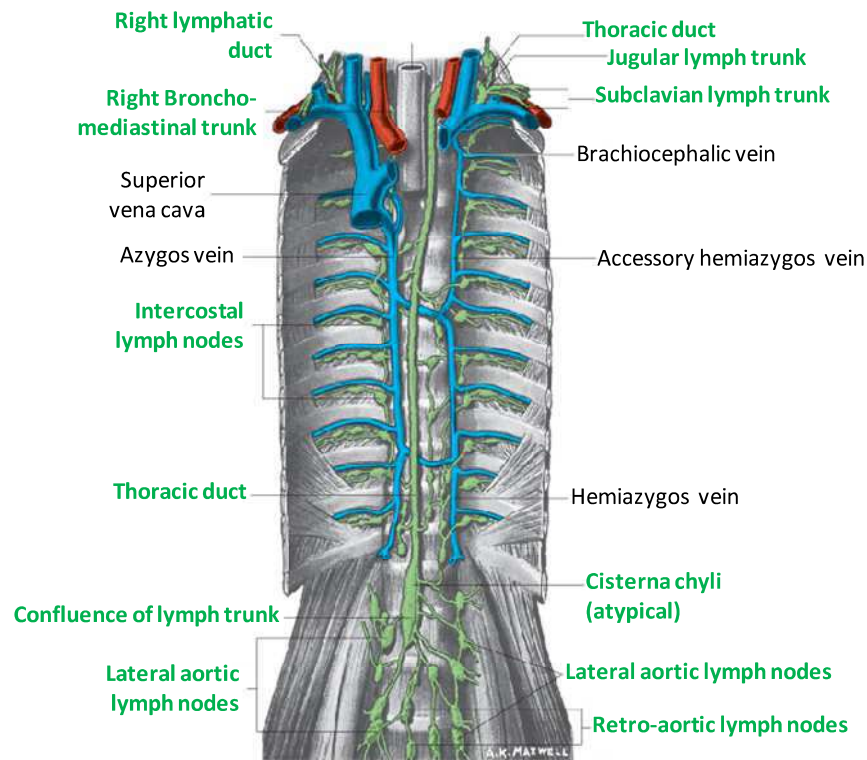
Figure 3.03: Representation of the thoracic and right lymphatic ducts. Anatomical drawing of the human thorax and abdomen, showing several lymph nodes, lymph vessels, lymph trunks and the two lymph ducts. After reference [12].

3.1.3. Lymph filtration by the lymph nodes

Before the lymph reaches one of the two lymph ducts, it flows through LNs which can be viewed as organs bathing within the lumen of lymphatic vessels (Figure 3.03). Like other SLOs, LNs are specialized sites where B and T lymphocytes and antigen presenting cells (APCs) come together to initiate immune responses to foreign antigens. Thus, LNs filter particles from the lymph by the action of numerous phagocytic macrophages and generate mature, antigen-primed B and T cells. A normal human young adult contains up to 450 LNs, 60 to 70 of which are found in the head and neck, around 100 in the thorax and approximately 250 in the abdomen and pelvis [12]. By far the greatest number of LNs lies close to the viscera, especially in the mesenteries. In contrast to humans, mice have only 22 identifiable LNs [13] but the LNs structure is similar in the different mammalian species. In large vertebrates, lymph passes through a series of nodes before reaching its collecting duct (Figure 3.03). As a consequence, different filtration steps take place so that interstitial fluid, afferent and efferent lymph have quantitatively different molecular compositions, although they are in continuous exchange [8]. There are exceptions such as the lymph vessels of the thyroid gland and esophagus, and of the coronary and triangular ligaments of the liver, which all directly drain into the thoracic duct without passing through LNs [12].

Different anatomically compartments are distinguished in the LNs: the sinuses, the superficial cortex, the paracortex and the medulla (Figure 3.04).
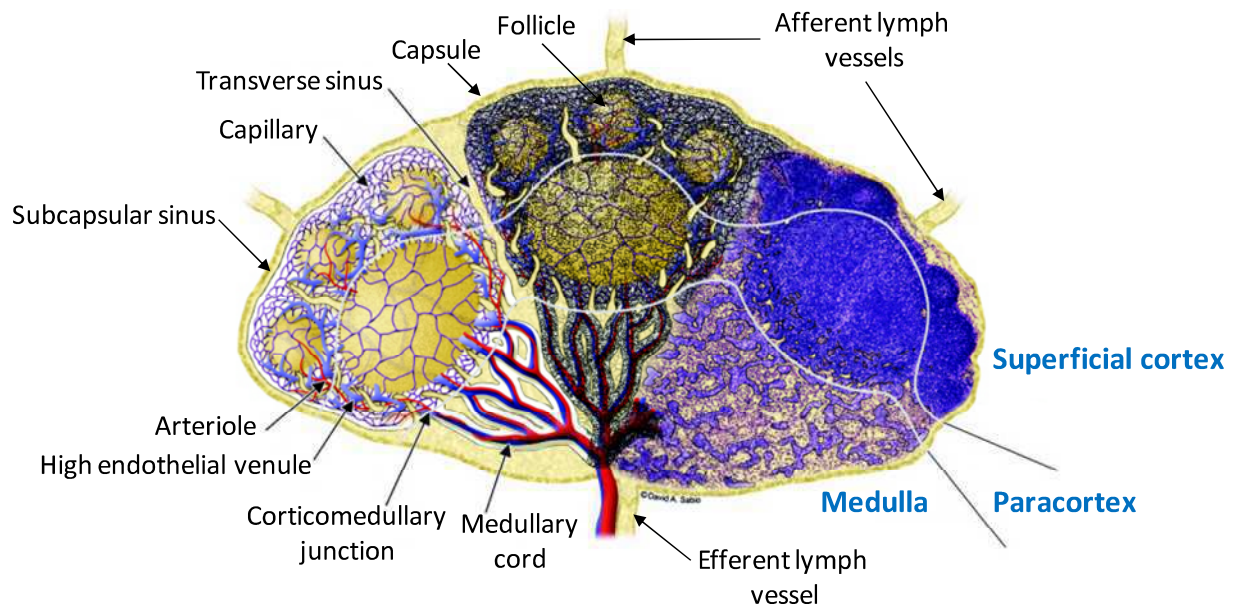
Figure 3.04: General organization of a LN. Schematic section of a LN depicting its general organization into lobular structural units. Each lobule is centered under an afferent lymphatic vessel, but only one efferent lymph vessel leaves the organ. The left lobule shows the LN blood supply, the center represents in addition the reticular meshwork, and finally the right lobule depicts a histological section of a rat mesenteric LN. After reference [14].

LNs are subdivided into structural units referred to as lobules (Figure 3.04). Although mouse LNs typically consist of a single lobule, in larger animals 10 or more lobules can be found in a single LN [15]. In small animals, such as rats, lobules are separated by open communicating sinuses, whereas in larger animals lobules are separated by fibrous radial bands referred to as trabeculae [15]. LNs mark sites where lymph vessels coming from different drainage areas meet, therefore generally every LN has several afferent but only one efferent lymph vessel. These kidney-shaped organs have a convex surface, which is the entrance site of lymphatic vessels and a concave depression, the hilum, through which arteries and nerves enter and veins and lymphatic vessel leave the organ. Beneath the capsule surrounding the organ, lies the subcapsular sinus (SCS) in which lymph from afferent vessels pours. The transverse sinus connects the SCS directly to the medulla and its medullary sinuses. The sinuses represent the remaining lumen of the vessel. Beneath the SCS lays the superficial cortex, which consists largely of lymphoid follicles, containing mainly B lymphocytes but also the stromal subsets of follicular dendritic cells (FDCs) and a small number of T cells and macrophages. In the outer follicular region, just underneath the SCS, are found the marginal reticular cells (MRCs). The paracortex is the lymphoid tissue between the follicles and the medulla, it represents the T cell zone of LNs, so that more than 95% of its cellular mass are T cells. The remaining space is occupied by DCs and by stromal cells, the fibroblastic reticular cells (FRCs). Under the paracortex lies the medulla which is composed of the medullary cords separated by medullary sinuses, and is mainly populated by plasma B cells. Medullary cords consist of a pair of arterioles and venules running along a central sheath of reticular meshwork and surrounded by a dense network of capillaries. The different immunological

functions fulfilled by LNs will be described in detail in the following Chapter, but first I will describe the organogenesis of LNs and the role of RANK and RANKL in this process [12].

3.2. *First step in lymphatic system organogenesis: development of lymph sacs*

3.2.1. *Two opposing historical models*

The foundation of the cooperation of LN and lymphatic vasculature lays on the embryonic development of these two structures, as both arise from the same embryonic tissue. Over the last few years many steps of this developmental cascade process have been characterized in mice. The earliest event during lymphatic system development is the formation of lymph sacs during embryogenesis. Historically, there have been two opposing models describing the development of the lymphatic system. In 1902, Sabin proposed a model based on results obtained by ink injecting experiments in pig embryos [16]. Florence Sabin proposed that endothelial cells bud from veins to form primary lymphatic sacs. From these sacs, budding cells then centrifugally sprout towards the periphery, forming capillaries that surround tissues and organs (Figure 3.05).
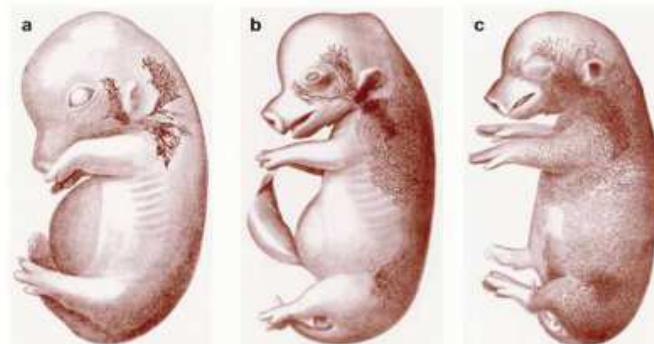
Figure 3.05: Growth of lymphatic vessels in pig embryos visualized by the ink injection method of Sabin. **(**a) Embryo (3.0 cm in length) showing the lymphatic vessels in the side of the neck growing in three directions: the back of the head behind the ear, the scapular region and the region of the jaw. (b) Embryo (4.3 cm in length) showing the ducts of the primary plexus, which have grown to the median line in the back and anastomosed with those on the other side. (c) Embryo (5.5 cm in length) in which the lymphatic vessels have now covered most of the body. After reference [3].

In 1909, Huntington and McClure proposed an alternative model in which lymphatic vessels developed from mesenchymal precursors and connections with veins were only established later on during development [17]. This theory was supported by recent studies in avian species, in which the lymphatic vessels of the wing were found not to exclusively develop from sprouts of the lymph sacs, but also by recruitment of local lymphangioblasts [18]. Nevertheless, later studies using molecular markers for LECs in the mouse such as the lymphatic vessel endothelial hyaluronan receptor 1

(LYVE-1), Prox1 (Prospero homeobox protein 1) and vascular endothelial growth factor receptor 3 (VEGFR-3) supported Sabin's model of embryonic lymphatic development [19].

3.2.2. A three-step model of development

The different studies conducted to elucidate the lymphatic system development led to the emergence of a three-step model with first the acquisition of a lymphatic endothelial competence, followed by a lymphatic commitment, and finally a budding of cells, which subsequently form the lymph sacs (Figure 3.06).

- ### *Lymphatic endothelial cell competence*

In mice, the autonomous endothelial cells of the anterior cardinal vein start to express LYVE-1 and VEGFR-3 at around embryonic day 8.5 (E8.5). The molecular factors that regulate this initial stage of lymphatic competence remain unknown, but the expression of LYVE-1 could be considered as the first morphological indication that venous endothelial cells are already competent to respond to a lymphatic-inducing signal. Mice with a targeted deletion of LYVE-1 do not present any obvious alteration of their lymphatic system [20], indicating that venous endothelial cells do not require this gene activity to acquire lymphatic competence. Instead, another unidentified molecule must initiate lymphatic competence in venous endothelial cells. It was recently shown that retinoic acid induces LYVE-1 expression *in vitro* and, as retinoic acid receptor-α is expressed by the embryonic endothelial cells of the cardinal vein, it was proposed that retinoic acid could mediate the earliest step of lymphatic vasculature development [21].

- ### *Lymphatic commitment*

Around E9.5, cells on one side of the vein follow the lymphatic commitment and start to express the transcription factor Prox1, which is essential for establishment of LEC identity [3]. The signal triggering the expression of Prox1 is still unknown but its expression is controlled by the transcription factor Sox18 (SRY (sex determining region Y) box 18) [22]. Over-expression of Prox1 in cultured vascular endothelial cells leads to a lymphatic reprogramming of these cells with upregulation of LEC markers and suppression of some blood endothelial cell (BEC) markers [23]. Prox1 also increases endothelial cell motility and migration [24].

- ### *Lymphatic specification, budding and migration*

At E10.5-11.5, in response to VEGF-C, the cells expressing Prox1 bud from the vein and migrate into the surrounding tissue where they form a lymph sac. By this time LECs start to express additional lymphatic lineage markers, like the mucin-type transmembrane glycoprotein podoplanin

[25]. Around E11.5–12.5 the lymphatic and the blood vascular system are separated, and the subsequent lymphatic vessel development and LN development will take place [3, 4].
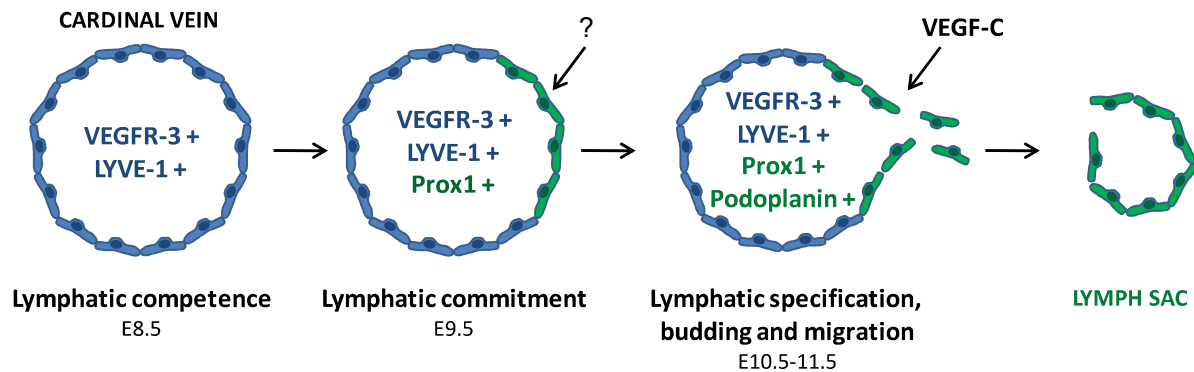
Figure 3.06: Development of the lymphatic endothelium. Schematic representation of the key steps in lymphatic specification of blood endothelial cells from the cardinal vein in mouse embryos. Abbreviations: VEGF, vascular endothelial growth factor; VEGFR, vascular endothelial growth factor receptor; LYVE-1, lymphatic vessel endothelial hyaluronan receptor 1; Prox1, prospero homeobox protein 1. Modified after reference [2].

3.3. Lymph node development

3.3.1. Lymph node organogenesis

- *A five stage process*

Based on histological observations made in the past, five different stages in LN development can be distinguished [26, 27]. The **first stage** of LN development is achieved when lymph sacs are formed, although it was recently found that these structures are not required for initiation of LN formation [28]. In their study, Vondenhoff and co-workers showed that LN formation is initiated normally in E14.5 Prox1-deficient mice which are devoid of lymph sacs, however subsequent stages of LN development were less efficient [28]. The **second stage** of LN formation is the development of the lymphatic vessels through budding and sprouting from lymph sac endothelial cells, a process which is completed at around E14.5-15.5 [3]. The **third stage** then takes place and mesenchymal connective tissue protrudes into the lymph sacs forming the earliest LN anlagen (Figure 3.07) [26, 27, 29]. These primordial LNs contain stromal cells, some leukocytes, capillaries and vascular loops [30]. LN morphogenesis will be completed during embryogenesis at around E17.5-E18. It was shown that the different LNs do not develop simultaneously but sequentially in mice, with mesenteric LNs developing the earliest (E11) and popliteal LNs the latest (E16) [31]. During the **fourth stage**, LN organogenesis will require the recruitment of the first hematopoietic precursors into the anlagen, the lymphoid tissue inducer cells (LTics) and the interaction of these cells with the stromal organizer cells

already present in the LN anlagen (Table 3.01) [29, 32]. Finally, a **fifth stage** will take place, in which the LN anlagen will expand with incoming B and T cells.
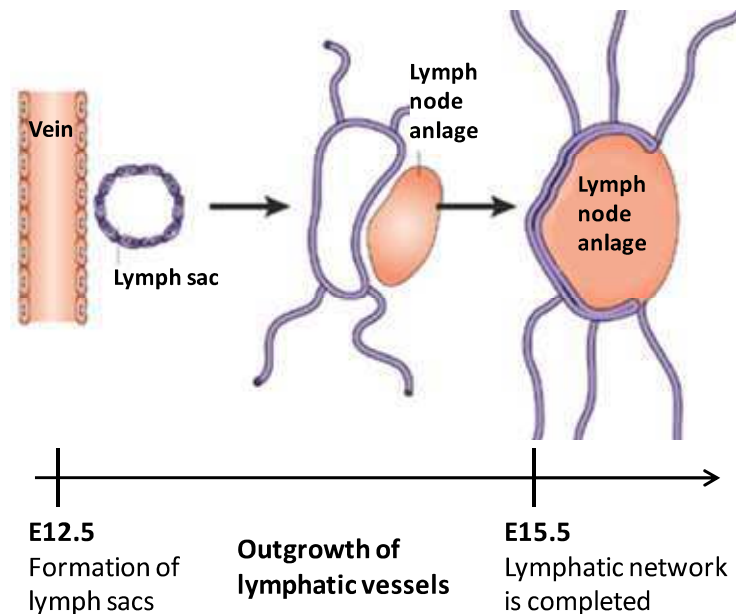
Figure 3.07: Development of a LN anlage. After the formation of the lymph sacs, mesenchyme tissue protrudes into the lymph sac forming the lymph node anlage. Modified after reference [29].

- *LTics and their recruitment to the lymph node anlagen*

At around E12.5-13.5, the LN anlagen can already be detected in mouse as a cluster of IL-7 receptor-α (IL-7Rα or CD127) expressing cells [33]. These hematopoietic cells are the first cells to colonize the lymph sacs and were first described in 1992 as a cell population negative for lymphoid, myeloid and erythroid lineage markers (apart from CD4) [34]. They are now known to belong to the family of innate lymphoid cells, like natural killer (NK) cells [35]. The function of this cell population remained unknown for several years, and the relation between them and lymphoid tissues organogenesis was only demonstrated later by adoptive transfer studies and by targeted deletion of genes required for their generation [36-39]. Thus, this $CD45^+CD3^-CD4^+$ cell population is required for LN, PP and NALT organogenesis and is now referred to as LTics. LTics were shown to originate from fetal liver precursors and to express CD25 (IL-2Rα), CD132 (IL-2Rγ), CD44, CD90, CD117 (c-kit), MHC class II, integrins α4β7 and α4β1, RANK, RANKL and $LT\alpha_1\beta_2$ (Table 3.01) [33].

	Surface antigens	TNFSF and TNFRSF members	Chemokines and chemokines receptors	Adhesion molecules
LTic	CD45, CD4 CD16/CD32 CD25 (IL-2Rα, ±75%) CD32, CD44 CD90 (Thy1) CD127 (IL-7Rα) CD132 (IL-2Rγ) MHC class II (±50%) CD117 (c-kit, low)	LTα$_1$β$_2$ RANK RANKL	CXCR4 CXCR5 CCR7	Integrin α4β7 Integrin α4β1 ICAM-1
Stromal organizer		RANKL LTβR	CXCL13 CCL19 CCL21	VCAM-1 ICAM-1 MAdCAM-1

Table 3.01 Principal molecules expressed by murine LTics and stromal organizer cells. Abbreviations: LT, lymphotoxin; LTβR, LTβ receptor; CCR, chemokine C-C motif ligand; CCL, chemokine C-C motif ligand; CXCR, chemokine C-X-C motif receptor; CXCL, chemokine C-X-C motif ligand; VCAM-1, vascular cell adhesion molecule 1; ICAM-1, intercellular adhesion molecule 1; MAdCAM-1, mucosal vascular addressin cell adhesion molecule 1. After references [29, 33].

As LNs always develop at the same location, e.g. along large veins and often at sites of blood vessel branching, it is tempting to speculate that these sites deliver specific signals for developing LNs [40]. Initial clustering of LTics at sites of future LNs does not occur in the absence of CXCL13 (chemokine C-X-C motif ligand 13) or its receptor CXCR5 (chemokine C-X-C motif receptor 5), suggesting that local CXCL13 production could attract CXCR5-expressing LTics [41]. In addition to CXCL13, another chemokine seems also to be implicated in LTic recruitment: CCL21 derived from lymphatic endothelium. Although mice deficient for CCL21 receptor (CCR7) do not present defect in LN formation [42], comparison of the phenotype of mice deficient for both CXCR5 and CCR7 with mice lacking CXCL13 and CCL21 Ser could show the importance of CCL21 in this process [43, 44]. CCL21 Ser is a CCL21 isoform expressed by LN stromal cells and high endothelial venules (HEVs) [45]. Thus, mice deficient for the CCL21 Ser isoform still express the CCL21 Leu isoform, which is produced by the lymphatic endothelium [45]. No LNs developed in mice lacking both CXCR5 and CCR7 [44] whereas cervical LNs were observed in mice lacking CXCL13 but expressing the CCL21 Leu isoform [43]. Hence, lymphatic endothelium-derived CCL21 seems to function in the initial attraction of LTics to the site of future LNs. In 2010, van de Pavert and co-workers showed *in vitro* that CXCL13 and CCL21 could mediate LTic migration and that these two chemokines could be found in LN anlagen [41]. In addition, retinoic acid (RA), derived from vitamin A, induced CXCL13 expression by mesenchymal cells and RA was found to be indispensable for LN development [41].

Moreover, the enzymes responsible for vitamin A conversion into RA, retinal dehydrogenases (RALDHs), are expressed in LN anlagen adjacent nerve fibers and vagal nerve stimulation led to CXCL13 expression [41]. All together, these data support the idea that the signal mediating the location of LN formation could derive from neurons (Figure 3.08) [41].
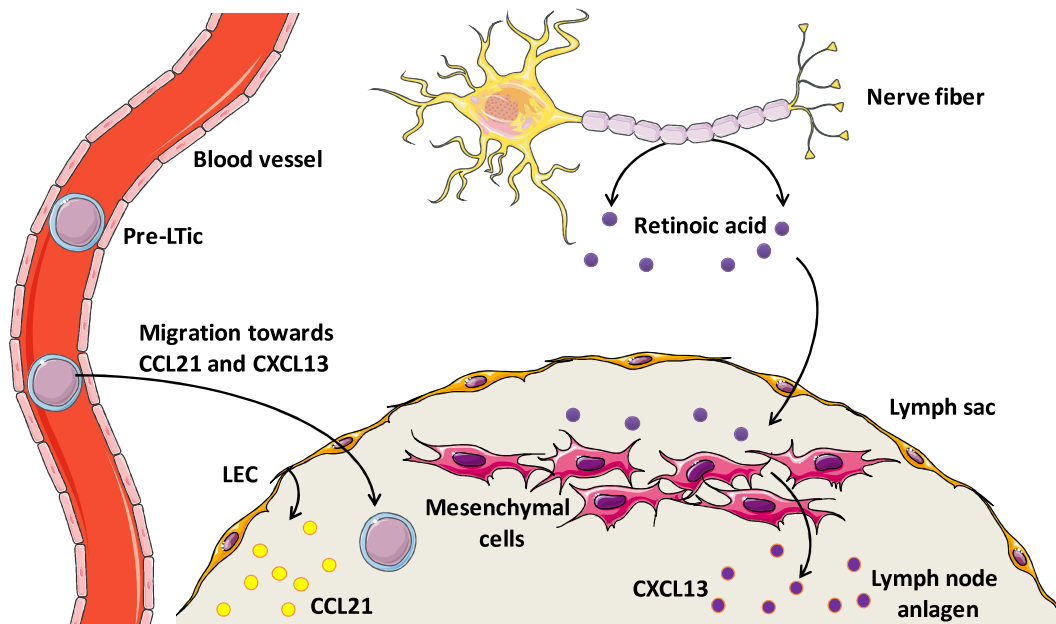
Figure 3.08: Model of LN developing site induction by retinoic acid. Retinoic acid, possibly produced by nerve fibers, induces the expression of CXCL13 by mesenchymal cells of the LN anlage. Together with CXCL13, CCL21 produced by LECs from the lymph sacs attract LTic precursors from the blood to form the first cell cluster in LN anlage. Modified after reference [46].

- *Stromal organizer cells development in the lymph node anlagen*

Clusters of LTics were shown to co-localize with VCAM-1-expressing cells, now referred to as stromal organizer cells [40]. Interactions between these two cell subpopulations is required for the induction of LN organogenesis [46]. In 2004, Cupedo and colleagues showed that these LN stromal organizer cells were ICAM-1, VCAM-1 and MAdCAM-1 (mucosal addressin cell adhesion molecule 1) positive (Table 3.01) [47]. In addition, these cells form two discrete populations, expressing either intermediate or high level of these adhesion molecules, the former was shown to be specifically reduced in peripheral LNs compared to mesenteric LNs [47]. A recent study showed that lymphoid tissue organizer stromal cells undergo a gradual maturation, which renders them the crucial stromal organizer cells [48]. Bénézech and colleagues showed that LN anlagen developed from mesenchymal cells surrounding the lymph sacs and that these cells subsequently underwent a two-step maturation process. First these ICAM-1$^-$VCAM-1$^-$ precursors become ICAM-1^{int}VCAM-1^{int} cells, and this independently of LTics and LTβR (Lymphotoxin β receptor) signaling. Then, these cells mature into ICAM1^{high}VCAM1^{high}MAdCAM1$^+$ organizer cells, a process depending on both LTics and LTβR, and subsequently coordinate the process of LN organogenesis with the LTics [48].

- ***Interactions between these two main protagonists***

Following accumulation of LTics in the lymphoid tissue anlagen, RANKL stimulates LTics to express $LT\alpha_1\beta_2$, which activates the surrounding $LT\beta R$ stromal organizer cells to express adhesion molecules (VCAM1, ICAM1, MAdCAM1), chemokines (CXCL13, CCL19, CCL21) and cytokines implicated in the subsequent process of cell attraction to the developing organ (Figure 3.09) [49]. In response to $LT\beta R$ signaling, stromal cells express RANKL and IL-7, which together further induce the expression of $LT\alpha_1\beta_2$ by the newly arriving LTics [50]. In turn, $LT\alpha_1\beta_2$ fosters $LT\beta R$ triggering generating a positive feedback loop [50]. Furthermore, $LT\beta R$ induces the stromal organizer to express the lymphangiogenic factor VEGF-C (vascular endothelial growth factor C) which will promote the connection of the developing LN to the lymphatic vasculature [50]. During the fifth stage of LN development the LN anlagen continues to expand through incoming B and T lymphocytes. Subsequently, when a large enough cluster develops, blood vessels start to differentiate into HEVs, allowing cells to enter from the bloodstream [29]. B and T cells begin to take over the role of LTics by expressing $LT\alpha_1\beta_2$ to maintain the differentiation and survival of the $LT\beta R^+$ stromal cells [29, 46].
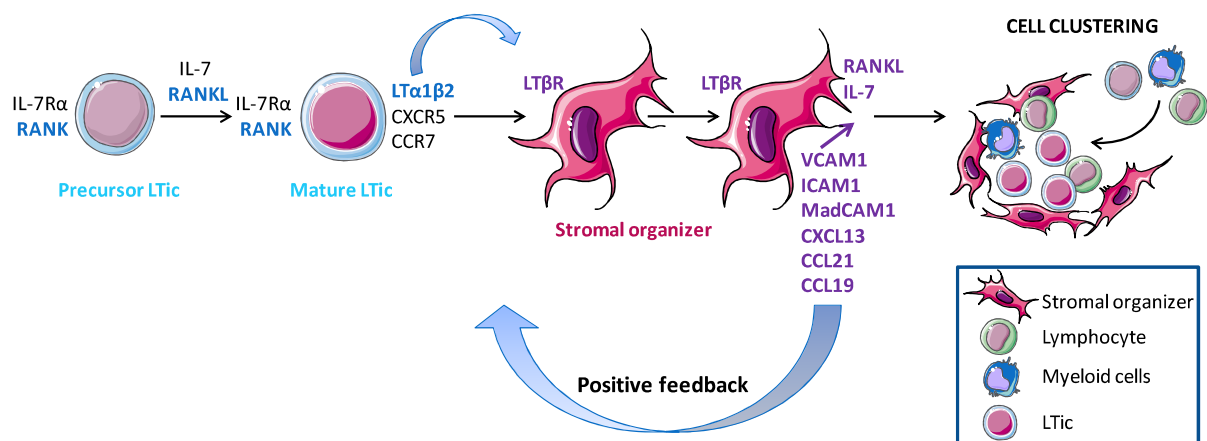
Figure 3.09: Schematic interactions between LTic and stromal organizer during LN organogenesis. Precursor LTic matures under the action of IL-7 and RANKL, and expresses $LT\alpha_1\beta_2$ which will interact with $LT\beta R$ on stromal organizer. The stromal organizer then expresses adhesion molecules and chemokines, leading to a positive feedback, in which chemokines and adhesion molecules attract and retain more LTics, increasing $LT\alpha_1\beta_2$ expression in LN anlagen, further increasing RANKL expression by stromal organizers and differentiation of LTics. After references [29, 51].

3.3.2. Importance of TNFSF members during lymph node organogenesis

Concerning the molecular players implied in LN development, much was learned from genetic studies in mice. Hence, the dissection at the cellular and molecular levels of LN organogenesis began with the characterization of the $LT\alpha$-deficient mice in 1994 [52]. Since then, other mutations impairing

LN development were reported (Table 3.02), and the crucial roles of RANKL and $LT\alpha_1\beta_2$ were also discovered through the study of knockout mice.

Mutation	Signaling pathway	Cells affected	LNs	PPs	NALT
$Lt\alpha^{-/-}$, $Lt\beta r^{-/-}$, $Nik^{-/-}$, Aly/aly, Rela x $Tnfr^{-/-}$	LTβR	stroma	-	-	-
$Nf\kappa b2^{-/-}$, $Relb^{-/-}$	LTβR	stroma	±°	-	ND
$Lt\beta^{-/-}$	LTβR	stroma	CLN, MLN	-	+
$Light^{-/-}$	LTβR	stroma	+	+	+
$Light/Lt\beta^{-/-}$	LTβR	stroma	<MLN than LTβ^{-/-}	-	ND
$Ikk\alpha^{-/-}$	LTβR	stroma	-	-	+
$Tnfr1^{-/-}$	TNFR1	stroma	+	reduced in number	+
$Tnf^{-/-}$	TNFR1 and 2	stroma	+	reduced in number	+
$Il7ra^{-/-}$, $Jak3^{-/-}$, $\gamma c^{-/-}$	IL-7R	LTic	BLN, ALN, MLN	-	+
$IL-7^{-/-}$	IL-7R	LTic	MLN?	-	-
$Rank^{-/-}$, $Rankl^{-/-}$, $Traf6^{-/-}$	RANK	LTic	-	smaller	+
$Rorc^{-/-}$		LTic	-	-	+
$Id2^{-/-}$		LTic	-	-	-
$Ikaros^{-/-}$		LTic	-	-	ND
$Cxcl13^{-/-}$, $Cxcr5^{-/-}$	CXCR5	LTic/B	CLN, FLN, MLN	reduced number	-
Plt/plt, $Ccr7^{-/-}$	CCR7	LTic/B/T	+	+	+
Cxcr5 x $Ccr7^{-/-}$	CXCR5/CCR7	LTic/B/T	+	-	ND
Plt/plt/$Cxcl13^{-/-}$	CXCR5/CXCR7	LTic/B/T	-	-	-

Table 3.02: Mutant mice with defective lymphoid organogenesis. Abbreviations and symbols: + indicates that the lymphoid organ can develop; - stands for an impaired development; ND, not determined; °, LN development was reported to be normal one day after birth, but at P10 lymphoid depletion was observed; ALN, axillary LN; BLN, brachial LN; CLN, cervical LN; FLN, facial LN; MLN, mesenteric LN; NALT, nasal-associated lymphoid tissue; PPs, Peyer's Patches; aly, alymphoplasia; γc, common cytokine receptor γ-chain; CCR7, chemokine receptor for CCL19 and CCL21; CXCL13, chemokine (C-X-C motif) ligand 13; CXCR5, receptor for CXCL13; IKK, inhibitor of κB kinase; IL-7, interleukin-7; Jak3, Janus kinase 3; LT, lymphotoxin; NIK, nuclear-factor-κB-inducing kinase; Plt, paucity of lymph node T cells; RORγ, retinoid-related orphan receptor γ; TNF, tumor-necrosis factor; Traf6, TNF-receptor-associated factor 6. After references [29, 42-44].

- *LTα₁β₂ pathway in lymph node organogenesis*

Lymphotoxin signaling is a key event in LN development, as it promotes the expression of many cytokines, chemokines and adhesion molecules by the mesenchymal stromal organizer (Figure 3.09). LTα-deficient mice were shown to lack PPs and LNs but abnormal mesenteric LN-like structures occasionally appear in some mice (<5%) [52, 53]. Given the structural and functional

similarities between LTα and TNF, and the ability of LTα to bind to the same receptors as TNF, e.g. TNFR1 and TNFR2, it was speculated that TNF and its receptors could have a comparable role as LTα in LN organogenesis [54]. However, mutations in *Tnf*, *Tnfr1* or *Tnfr*2 were not associated with impaired LNs or PPs development, although structural alterations in B cells follicles were observed [55-57]. This difference in function was explained by the possible interaction of LTα with LTβ to form a heterotrimer $LT\alpha_1\beta_2$ known to interact with a distinct receptor: LTβR (Figure 3.10) [58, 59].
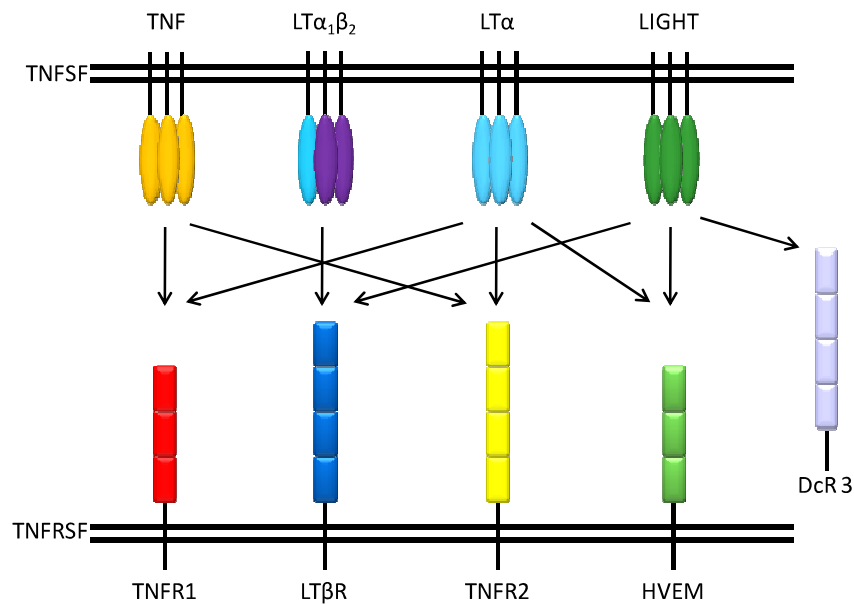
Figure 3.10: Interactions between the family members of the TNF, LT and LIGHT system. Schematic representation of the interactions between TNF, LTα and β and LIGHT and their respective receptors. Abbreviations: TNF, tumor necrosis factor; LT, lymphotoxin; TNFR, TNF receptor; LTβR, LTβ receptor; HVEM, herpes virus entry mediator; DcR3, decoy receptor 3. After reference [60].

Indeed, it was shown that organogenesis of secondary lymphoid organs is disrupted in LTβ- and LTβR-knockout mice, demonstrating that the surface heterotrimer $LT\alpha_1\beta_2$ has a key role in lymphoid organ development [61, 62]. Nevertheless, TNF also participates in secondary lymphoid organs development to some degree. It was shown that mice treated *in utero* with soluble LTβR-Ig (coupled to the Fc portion of an immunoglobulin) retain mesenteric and cervical LNs, but mice treated with both LTβR-Ig and TNF-Ig do not develop these organs [63]. In addition, it has been shown that, although *Light*^{-/-} and *Ltβ*^{-/-} mice display mesenteric LNs, mice deficient for both LIGHT and LTβ display a marked reduction in the presence of these LNs [64]. Thus, although $LT\alpha_1\beta_2$ signaling through LTβR is the major pathway through which LNs organogenesis is achieved, TNF and LIGHT also contribute to LN development. While it was shown that the *in utero* administration of an agonistic anti-LTβR antibody promoted LN formation in LTα-deficient mice, the administration of this antibody in mice lacking LTics (RORγ-deficient mice) did not rescue LN, emphasizing the crucial role for LTics in delivering an additional signal to mesenchymal cells [63].

Like RANK, LTβR is known to activate both NF-κB classical and alternative pathways, and each of these two pathways is implied in the expression of different genes (Figure 3.11) [65].
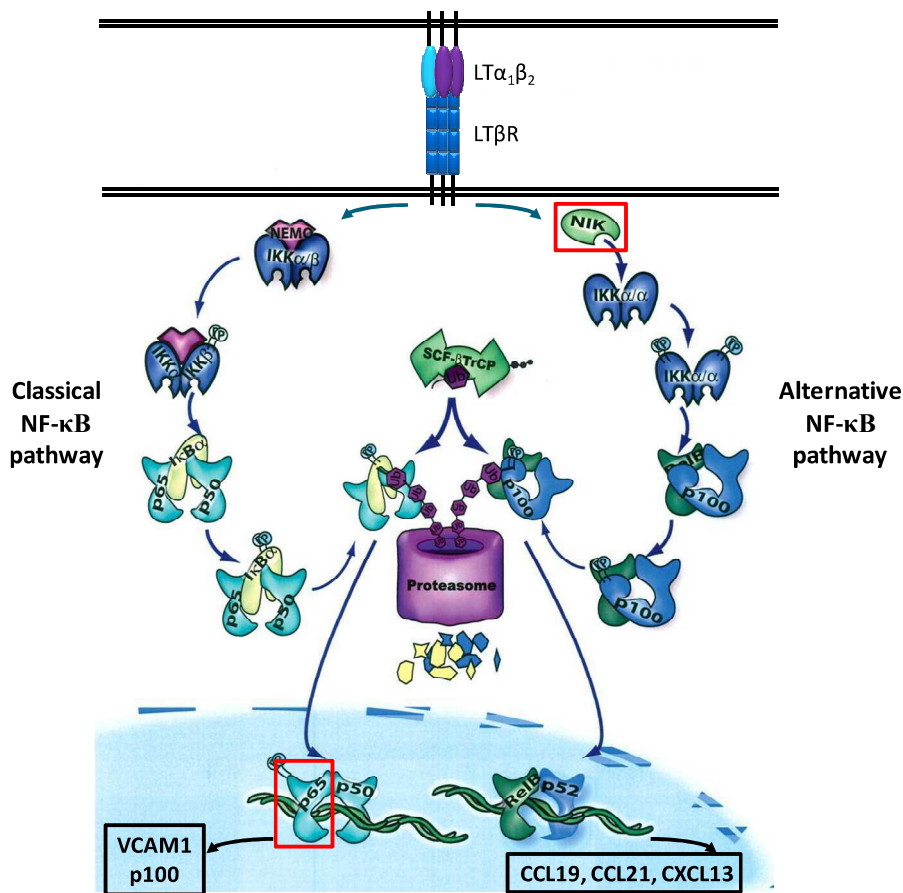
Figure 3.11: NF-κB pathway activation upon LTβR engagement by LTα₁β₂. Schematic representation of NF-κB activation by LTβR, genes expression induced by classical and alternative pathways are shown in black boxes, proteins that were shown to be essential for LNs development are highlighted by red boxes. Abbreviations: LT, lymphotoxin; LTβR, LTβ receptor; NIK, NF-κB inducing kinase; IKK, inhibitory-κB kinase; NEMO, NF-κB essential modulator; SCF-βTrCP, Skp1/Cul1/F-box protein beta-transducin repeat-containing protein; VCAM-1, vascular adhesion molecule 1. Modified after references [65-69].

Activation of the classical NF-κB pathway upon LTβR engagement was shown to induce the expression of inflammatory proteins such as VCAM-1, CCL4 and CXCL1, and to increase the production of the NF-κB precursor p100 [65]. Upon alternative pathway activation, molecules involved in secondary lymphoid development and homeostasis, such as CCL19, CCL21 and CXCL13, are expressed [65]. Genetic studies show that both pathways are important for lymphoid organ formation. Thus, Aly/aly mice, which are deficient for the alternative pathway protein NIK (NF-κB inducing kinase) do not develop LNs nor PPs [68, 69]. In addition RelA of the classical pathway was also shown to be crucial. As deficiency for RelA is lethal for mice during embryogenesis, mice knockout for RelA are bred onto a TNFR1-null background, protecting the mice from uncontrolled TNFR1 induced apoptosis. These mice deficient for both TNFR1 and RelA do not display LNs and PPs [66].

In addition, it was shown that LTα$_1$β$_2$ also functions in the expression of adhesion molecules of HEV cells for lymphocyte transmigration into LN [70]. Moreover, LTβR is of importance for the micro-architecture of B cell follicles. Thus, even if *in utero* LTβR engagement by a monoclonal agonist antibody can rescue LNs in LTα-deficient mice, this gestational signaling is not sufficient for the establishment and maintenance of normal LN cellular organization [63].

- ### *RANK pathway in lymph node organogenesis*

The importance of the RANK signaling pathway for the development of LNs arose in 1999 with the analysis of RANKL-deficient mice by Kong and co-workers. They unexpectedly observed a complete absence of LNs but normal splenic structure and smaller but otherwise normal PPs and NALTs [71], providing the first evidence that LN and PP development can be genetically uncoupled. A similar phenotype was observed in RANK- [72] and TRAF6-deficient mice [73]. Patients with osteoclast-poor form of autosomal recessive osteopetrosis (ARO) were reported to present no palpable LNs, suggesting that RANK-RANKL signaling also controls LNs formation in humans [74]. Transfer of fetal liver cells from RANKL-deficient mice into RAG1-knockout mice showed that RANKL-deficient B and T cells can populate LNs, indicating that the lack of LNs was not the result of a defective cellular homing [71]. In addition, transfer of normal bone-marrow cells into newborn RANKL-deficient mice did not restore LNs formation [71]. Moreover, RANK and RANKL are also expressed in the spleen and in PPs, so that restricted RANK-RANKL expression cannot account for the selective lack of LNs. Thus, the absence of LNs in RANKL-deficient mice was explained by a different mechanism: the proportion of LTics in LN anlagen from these mice was greatly decreased and the few cells present failed to form clusters and to interact with the stromal organizer cells [75]. Molecules such as Ikaros, Id-2 (inhibitor of DNA binding 2) and RORγt (retinoic acid related orphan receptor), were shown to be crucial for LTics development [39, 76, 77]. Although LTics number is reduced, they are still present in RANKL-deficient mice and TRAF6-knockout mice, indicating that the RANK pathway is not required for the generation of these cells [75, 78]. Transgenic over-expression of RANKL in B and T cells in RANKL-deficient mice rescued the number of LTics and the development of certain LNs [75], leading to a model in which a critical number of LTics is required for LNs development and RANKL would be a crucial factor for the proliferation and/or survival of these cells (Figure3.12).
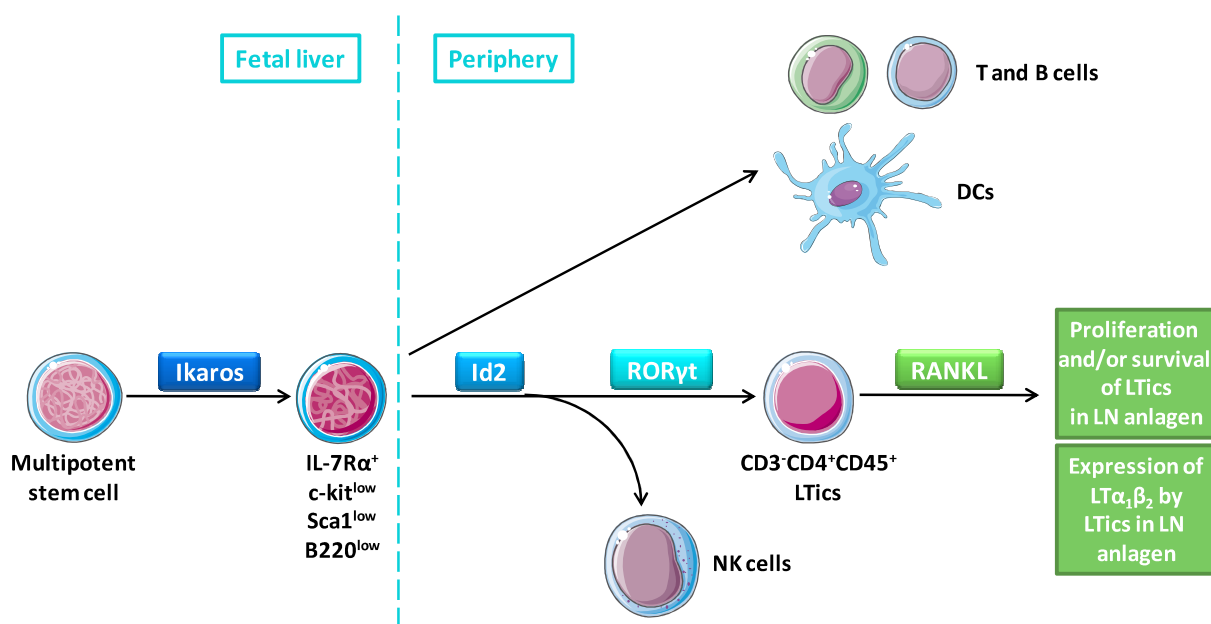
Figure 3.12: Generation of CD3$^-$CD4$^+$CD45$^+$ LTics. Precursors of LTics can be found in the fetal liver and are known to express IL-7Rα and low levels of c-kit and Sca-1. These cells arose from multipotent stem cells under the influence of the transcription factor Ikaros. IL-7Rα$^+$ fetal liver cells were shown to be precursors for B, T and NK cells and DCs. Id2 and RORγt are required for subsequent differentiation towards LTic phenotype. Finally RANKL is implicated as a growth factor for LTics in developing LNs, and also induces LTα$_1$β$_2$ expression by LTics. Abbreviations: Il-7Rα, interleukin-7 receptor α, NK, natural killer, DC, dendritic cell, LTic, lymphoid tissue inducer cell, LT, lymphotoxin; Id2, inhibitor of DNA binding 2; RORγt, retinoic acid related orphan receptor. Modified after references [29, 51].

In addition to this potential role as a "growth factor" for LTics, RANKL was also shown to induce the expression of LTα$_1$β$_2$ on LTics (Figure 3.12) [40]. As LTics express both RANK and RANKL, LTics clustering in LN anlagen could lead to activation in *trans* of these cells, resulting in LTα$_1$β$_2$ expression [50]. LTα$_1$β$_2$ can subsequently mediate LTβR signaling on stromal organizer cells, which was shown to be essential for the expression of RANKL by these stromal cells [50]. In addition to RANKL, IL-7 also acts as a local growth-factor regulating LTic numbers and their expression of LTα$_1$β$_2$ but IL-7 is preferentially required for organogenesis of PPs and not of LNs [43, 79-81]. Nevertheless, ectopic application of IL-7 to developing TRAF6-deficient embryos, in which RANK signaling cascade is impaired, could rescue early phases of LN development and discrete mesenteric LNs were recovered [40]. IL-7-deficient mice do develop LNs, suggesting that the role of IL-7 in the development of these organs is minimal, but mice lacking both CXCL13 and IL-7Rα completely fail to form LNs, including mesenteric LNs, normally present in CXCL13-deficient mice [43]. In addition, IL-7 overexpression promotes the development of extra-LNs as a result of increased numbers of LTics [82]. Thus, even if the role of RANKL is predominant in LN organogenesis, IL-7 also contributes to this process.

3.3.3. *Cellular organization in the developing lymph node*

Once sufficient cell clustering has taken place in the fetal LN anlagen, differentiation of endothelial cells into HEVs occurs [29]. HEVs are known to be specialized PNAd (peripheral LN addressin)-expressing endothelium for lymphocyte migration into lymphoid organs. It remains a plastic structure in the adult as it can be reverted to an endothelial surface lacking PNAd expression upon ligation of the afferent lymphatic vessels of the LNs [83]. Subsequently, after the recruitment of lymphocytes, segregation of B and T cell areas and formation of mature B cells follicles take place. These last steps in LN development were shown to take place soon after birth in mice. Hence, a switch of the addressin expressed by HEVs was found to occur soon after birth [84]. From fetal life through the first day of life, MAdCAM-1 is the predominant adhesion molecule found on HEVs, attracting α4β7 expressing cells, e.g. LTics. Soon after birth HEVs start to express PNAd, enabling the recruitment of L-selectin (CD62L)-positive leukocytes [84]. LTβR signaling seems to be crucial for this expression of addressin by HEVs. Thus, cellularity of LNs in adult mice was reduced by blocking its signaling with a soluble decoy receptor concomitant with lower levels of PNAd and MAdCAM-1 on HEV [70]. A sequence of different molecular steps must be successfully achieved for leukocytes to transmigrate through the HEVs, explaining the specific homing of some subsets of leukocytes to LNs (Figure 3.13) [1]. Hence, expression of L-selectin is not sufficient for leukocytes to enter HEVs; CCR7 or CXCR4 expression is also subsequently required to induce Gαi-signaling and LFA1-mediated arrest on endothelial ICAM-1. As a result, naïve B cells, naïve and central memory T cells preferentially enter LNs through HEVs [1]. For B cell entry, it was also reported that CXCL13 is another arrest chemokine on HEVs, and is expressed by a substantial proportion of HEV cells [85].

	Step 1 *Rolling*	Step 2 *Activation*	Step 3 *Adhesion*	Step 4 *Transmigration*
	L-selection: PNAD	B cells CCL21: CCR7 CXL12: CXCR4 T cells CCL21: CCR7 (CXC12: CXCR4)	LFA1: ICAM1	HEV
Naïve B cells	Yes	Yes	Yes	Yes
Naive or central memory T cells	Yes	Yes	Yes	Yes
Monocytes/Neutrophils	Yes	No	No	No
Effector memory or effector T cells	No	No	No	No
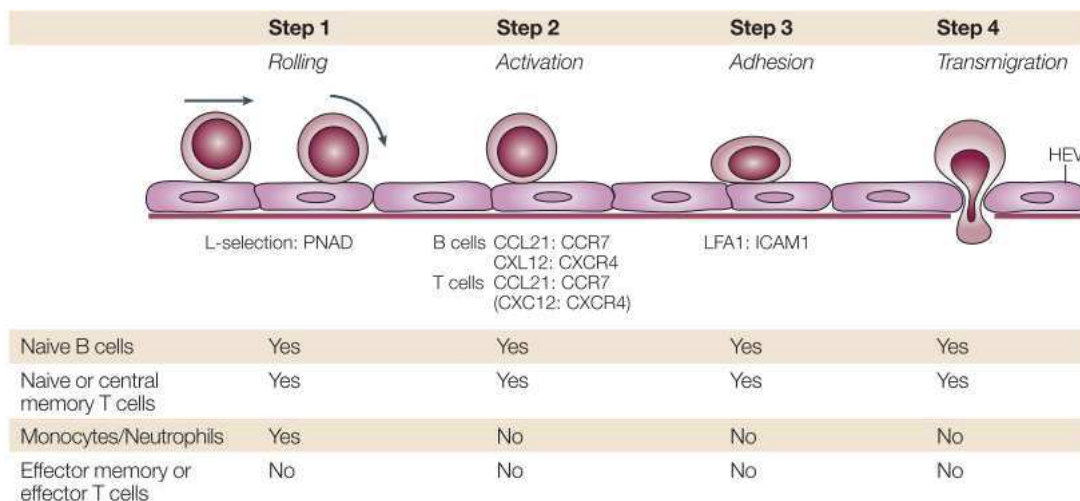
Figure 3.13: Homing specificity determined by leukocytes adhesion on HEVs. Naïve B and T cells, memory T cells and monocytes/neutrophils, initiate rolling on HEV through L-selectin binding to PNAd. HEV express CCL21 and to a lesser extend CCL19 and CXCL12, inducing rapid Gαi-signaling and LFA1-mediated arrest on ICAM1, leading to cell transmigration across the HEVs. After reference [1].

It can be noted that MAdCAM1 expression is still found in adult HEV associated with mucosal LNs, such as mesenteric LNs, and has a relevant biological function. Hence, β7 integrin deficiency has no effect on peripheral LNs homing but causes reduced homing into mesenteric LNs [86]. In addition to L-selectin, P-selectin, vascular adhesion protein A (VAP1), CD43 and CD44 also modulate LN leukocytes homing [1].

During recruitment of lymphocytes, organization into distinct B- and T-cell areas starts. This process was shown to mainly rely on the chemokines CCL19, CCL21, CXCL12 and CXCL13 which attract T and B cells (Figure 3.14) [87]. Impaired expression of these chemokines or their receptors leads to an altered compartmentalization in lymphoid organs [87]. Mice deficient for CXCR5, expressed by re-circulating B cells [88], or CXCL13, expressed by the stromal subsets of FDCs, fail to form B cell follicles [89]. Similarly, CCL19 and CCL21, expressed by stromal cells in T zone, and their receptor CCR7, expressed by resting T cells and DCs, were found critical for the integrity of the T cell areas [42]. $LT\alpha_1\beta_2$ and TNF are both required for stromal cell expression of these homing chemokines [90]. When B cells colonize the developing LN, they do not respond to CXCL13 and lack $LT\alpha_1\beta_2$ surface expression, nevertheless segregation of B cells in a ring-like pattern localized in the outer cortex occurs at P4 [91]. Although CXCL13 is expressed at this time in a $LT\alpha_1\beta_2$-dependent manner, B cells are unable to respond to this chemokine until P4. Thus, at this time LTics are the main source of $LT\alpha_1\beta_2$ and are the only cells able to respond to CXCL13, owing to their CXCR5 receptor [91]. After P4, B cells become responsive to CXCL13 and start to express $LT\alpha_1\beta_2$. Further organization of B cells into follicles becomes CXCL13-dependent and B cells progressively replace LTic in the maintenance of LN architecture (Figure 3.14) [91]. Consistent with the idea that $LT\alpha_1\beta_2$ expressing B cells take over the role of LTics, mice lacking NK, B and T cells develop the initial LN anlage but this structure dissipates after birth [92].
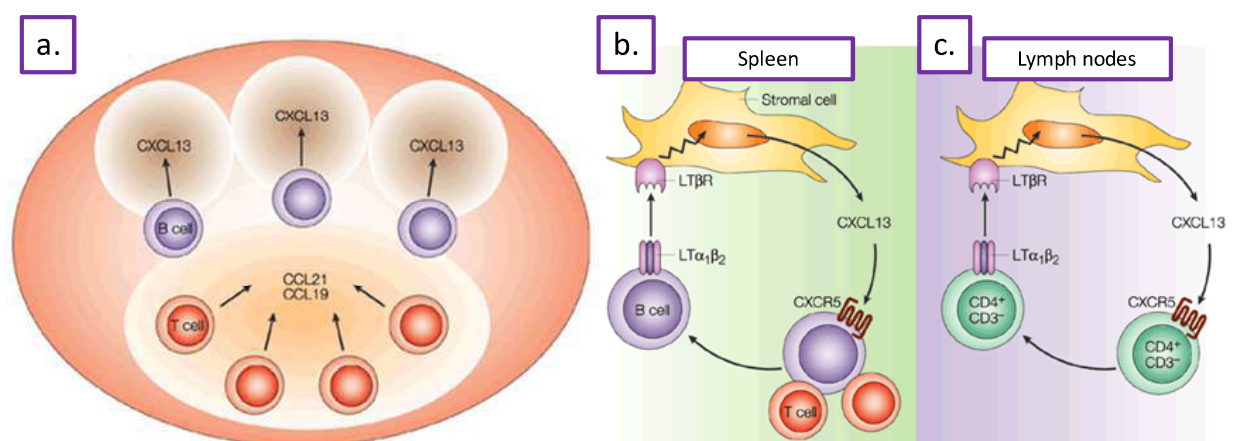
Figure 3.14: Chemokines mediate lymphoid organ organization. (a) Chemokines involved in B and T cell zone segregation. CXCL13 attracts CXCR5-expressing B cells, establishing B-cell follicles, and CCL19 and CCL21 attract T cells and DCs expressing the cognate receptor CCR7. (b and c) Formation of splenic (b) and LN (c) follicles is depicted. B cells replace LTics in LNs in a similar way to the process taking place in spleen follicle development. After reference [29].

3.3.4. Lymph node development in the human

The mechanism of LN development described in this Chapter derived from genetic studies in mice, leading to the question of whether this information can be transferred to man. Most of the knowledge about this point comes from studies performed in 1970s and 1980s, mainly based on analyses by microscopy techniques. The first stages of LN development in humans parallels those observed in mice: a lymph sac is formed by budding from the jugular and cardinal veins and a LN anlage subsequently develops (8–11 weeks gestation) [26, 93, 94]. Like in mice, LNs in humans develop in a temporally-regulated manner, whether this developmental process also relies on LTβR still remains unknown and the existence of a human counterpart for murine LTics is still not demonstrated [93, 95]. After the 12th week of gestation, lymphocytes start to colonize LN anlagen, and at 14 weeks B and T cells start to segregate [96]. Clearly defined B cell follicles will not be detected before 17 to 22 weeks of gestation [96]. Concerning HEVs, they can be identified at 15 weeks of gestation, and in contrast to mice, HEVs in both peripheral and mesenteric nodes express PNAd and MAdCAM-1 throughout fetal development [97]. During the following years MAdCAM-1 expressing HEVs progressively disappear from peripheral LNs [97]. In comparison with data obtained in knockout mice, only few genetic defects in humans have so far been associated with a lack of LNs [98]. Thus, three patients suffering SCID (severe combined immunodeficiency) disorders linked to mutation in gene encoding IL-7Rα protein, lack palpable LNs [99]. Defects of molecules of the IL-7Rα signaling cascade, such as JAK3 (janus kinase 3) and the common γ chain (γc), also result in hypoplasia or lack of LNs [100, 101]. In addition, patients with autosomal recessive osteopetrosis (ARO) linked to mutation in the RANK-RANKL axis, presented no palpable LNs [74, 102]. Nevertheless, additional work is still needed before making a full parallel between mouse and human for the molecular mechanisms of LN development.

3.4. Conclusions

The interstitial fluid leaking from blood capillaries is drained by lymphatic vessels toward collecting ducts, before being drained back to the systemic blood circulation. During this process, lymph percolates through LNs and is thereby filtered. In a simplified view, LNs can be seen as organs bathing within the lumen of lymphatic vessels. Development of these organs started to be described more than one hundred years ago, with Sabin's model of lymph sac development through the sprouting of blood endothelial cells. Subsequent LN development requires close interactions between LTics and stromal organizer cells. Genetic studies in mice enabled researchers to unravel the molecular players functioning in these interactions. Since the characterization of LTα-deficient mice in 1994, other TNFSF members have been found to be crucial for this process. $LT\alpha_1\beta_2$-LTβR is essential for the maturation of stromal organizers and for chemokine expression. RANK and RANKL were found to be required for sufficient LTics number and their clustering, and also for their $LT\alpha_1\beta_2$ expression. LNs are crucial for the encounter between immune cells and antigens or APCs arising from the periphery, and are therefore strategic sites throughout the body for the triggering of immune responses. In the following Chapter, I will discuss the functions of LNs in regard to their architecture and the role played by TNFSF members in these organs.
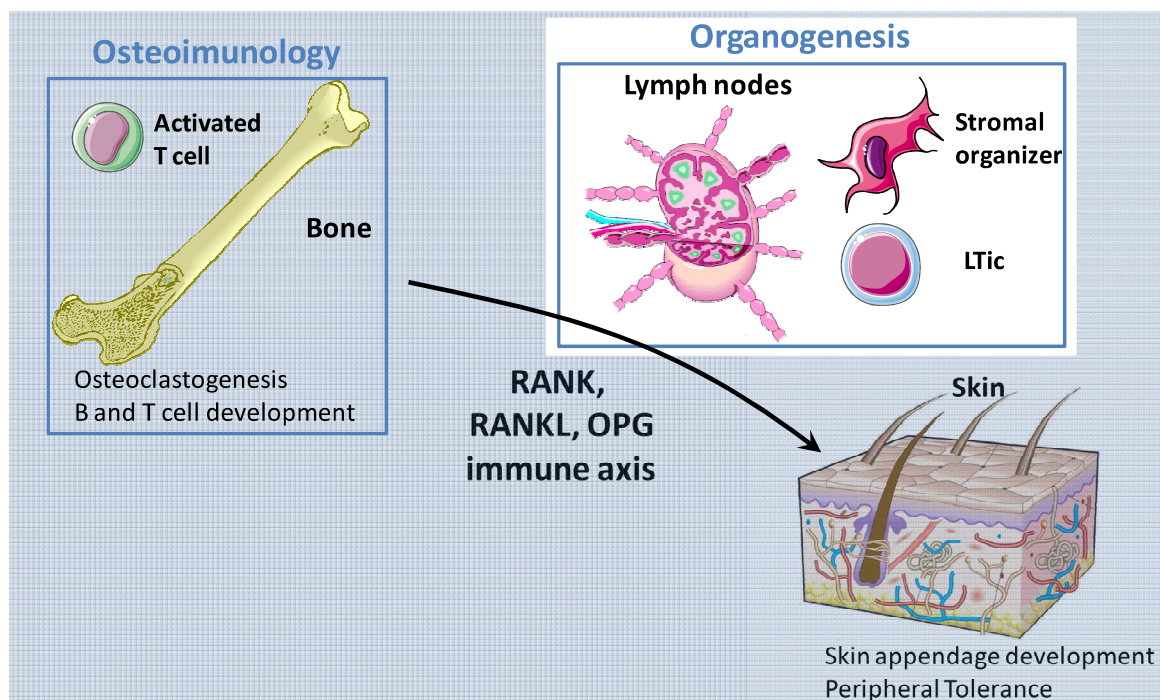
Figure 3.15: The RANK, RANKL and OPG axis: LN organogenesis. This molecular triad was found to be crucial for the interactions between stromal organizers and LTics during LN organogenesis. RANKL is expressed both by LTics and stromal organizer cells whereas RANK is only fond on LTics. RANKL is needed for the survival and/or proliferation of LTics, and for their expression of $LT\alpha_1\beta_2$.

3.5. *Bibliography*

1. von Andrian, U.H. and T.R. Mempel, *Homing and cellular traffic in lymph nodes.* Nat Rev Immunol, 2003. **3**(11): p. 867-78.
2. Jurisic, G. and M. Detmar, *Lymphatic endothelium in health and disease.* Cell Tissue Res, 2009. **335**(1): p. 97-108.
3. Oliver, G., *Lymphatic vasculature development.* Nat Rev Immunol, 2004. **4**(1): p. 35-45.
4. Hong, Y.K., J.W. Shin, and M. Detmar, *Development of the lymphatic vascular system: a mystery unravels.* Dev Dyn, 2004. **231**(3): p. 462-73.
5. Wang, Y. and G. Oliver, *Current views on the function of the lymphatic vasculature in health and disease.* Genes Dev, 2010. **24**(19): p. 2115-26.
6. Johnson, L.A. and D.G. Jackson, *Cell traffic and the lymphatic endothelium.* Ann N Y Acad Sci, 2008. **1131**: p. 119-33.
7. Irjala, H., et al., *Mannose receptor (MR) and common lymphatic endothelial and vascular endothelial receptor (CLEVER)-1 direct the binding of cancer cells to the lymph vessel endothelium.* Cancer Res, 2003. **63**(15): p. 4671-6.
8. Lammermann, T. and M. Sixt, *The microanatomy of T-cell responses.* Immunol Rev, 2008. **221**: p. 26-43.
9. Johnson, L.A. and D.G. Jackson, *Inflammation-induced secretion of CCL21 in lymphatic endothelium is a key regulator of integrin-mediated dendritic cell transmigration.* Int Immunol, 2010. **22**(10): p. 839-49.
10. Shields, J.D., et al., *Autologous chemotaxis as a mechanism of tumor cell homing to lymphatics via interstitial flow and autocrine CCR7 signaling.* Cancer Cell, 2007. **11**(6): p. 526-38.
11. Junqueira, L.C. and J. Carneiro, eds. *Basic Histology: Text & Atlas*. 11 ed. 2005, McGraw-Hill Medical. 544.
12. Standring, S., ed. *Gray's Anatomy: The Anatomical Basis of Clinical Practice*. 40 ed. 2008, Churchill-Livingstone, Elsevier. 1576.
13. Van den Broeck, W., A. Derore, and P. Simoens, *Anatomy and nomenclature of murine lymph nodes: Descriptive study and nomenclatory standardization in BALB/cAnNCrl mice.* J Immunol Methods, 2006. **312**(1-2): p. 12-9.
14. Willard-Mack, C.L., *Normal structure, function, and histology of lymph nodes.* Toxicol Pathol, 2006. **34**(5): p. 409-24.
15. Gretz, J.E., A.O. Anderson, and S. Shaw, *Cords, channels, corridors and conduits: critical architectural elements facilitating cell interactions in the lymph node cortex.* Immunol Rev, 1997. **156**: p. 11-24.
16. Sabin, F.R., *On the origin of the lymphatic system from the veins and the development of the lymph hearts and thoracic duct in the pig.* Am J of Anat, 1902. **1**(3): p. 367-89.
17. Huntington, G.S. and C.F.W. McClure, *The anatomy and development of the jugular lymph sac in the domestic cat.* Am J of Anat, 1910. **10**: p. 177-311.
18. Schneider, M., et al., *Lymphangioblasts in the avian wing bud.* Dev Dyn, 1999. **216**(4-5): p. 311-9.
19. Srinivasan, R.S., et al., *Lineage tracing demonstrates the venous origin of the mammalian lymphatic vasculature.* Genes Dev, 2007. **21**(19): p. 2422-32.
20. Gale, N.W., et al., *Normal lymphatic development and function in mice deficient for the lymphatic hyaluronan receptor LYVE-1.* Mol Cell Biol, 2007. **27**(2): p. 595-604.
21. Marino, D., et al., *A role for all-trans-retinoic Acid in the early steps of lymphatic vasculature development.* J Vasc Res, 2011. **48**(3): p. 236-51.
22. Francois, M., et al., *Sox18 induces development of the lymphatic vasculature in mice.* Nature, 2008. **456**(7222): p. 643-7.

23.   Petrova, T.V., et al., *Lymphatic endothelial reprogramming of vascular endothelial cells by the Prox-1 homeobox transcription factor.* Embo J, 2002. **21**(17): p. 4593-9.

24.   Mishima, K., et al., *Prox1 induces lymphatic endothelial differentiation via integrin alpha9 and other signaling cascades.* Mol Biol Cell, 2007. **18**(4): p. 1421-9.

25.   Schacht, V., et al., *T1alpha/podoplanin deficiency disrupts normal lymphatic vasculature formation and causes lymphedema.* Embo J, 2003. **22**(14): p. 3546-56.

26.   Bailey, R.P. and L. Weiss, *Ontogeny of human fetal lymph nodes.* Am J Anat, 1975. **142**(1): p. 15-27.

27.   Eikelenboom, P., et al., *The histogenesis of lymph nodes in rat and rabbit.* Anat Rec, 1978. **190**(2): p. 201-15.

28.   Vondenhoff, M.F., et al., *Lymph sacs are not required for the initiation of lymph node formation.* Development, 2009. **136**(1): p. 29-34.

29.   Mebius, R.E., *Organogenesis of lymphoid tissues.* Nat Rev Immunol, 2003. **3**(4): p. 292-303.

30.   Cupedo, T., G. Kraal, and R.E. Mebius, *The role of CD45+CD4+CD3- cells in lymphoid organ development.* Immunol Rev, 2002. **189**: p. 41-50.

31.   Rennert, P.D., et al., *Surface lymphotoxin alpha/beta complex is required for the development of peripheral lymphoid organs.* J Exp Med, 1996. **184**(5): p. 1999-2006.

32.   Randall, T.D., D.M. Carragher, and J. Rangel-Moreno, *Development of secondary lymphoid organs.* Annu Rev Immunol, 2008. **26**: p. 627-50.

33.   Mebius, R.E., P. Rennert, and I.L. Weissman, *Developing lymph nodes collect CD4+CD3-LTbeta+ cells that can differentiate to APC, NK cells, and follicular cells but not T or B cells.* Immunity, 1997. **7**(4): p. 493-504.

34.   Kelly, K.A. and R. Scollay, *Seeding of neonatal lymph nodes by T cells and identification of a novel population of CD3-CD4+ cells.* Eur J Immunol, 1992. **22**(2): p. 329-34.

35.   Spits, H. and J.P. Di Santo, *The expanding family of innate lymphoid cells: regulators and effectors of immunity and tissue remodeling.* Nat Immunol, 2011. **12**(1): p. 21-7.

36.   Finke, D., et al., *CD4+CD3- cells induce Peyer's patch development: role of alpha4beta1 integrin activation by CXCR5.* Immunity, 2002. **17**(3): p. 363-73.

37.   Fukuyama, S., et al., *Initiation of NALT organogenesis is independent of the IL-7R, LTbetaR, and NIK signaling pathways but requires the Id2 gene and CD3(-)CD4(+)CD45(+) cells.* Immunity, 2002. **17**(1): p. 31-40.

38.   Sun, Z., et al., *Requirement for RORgamma in thymocyte survival and lymphoid organ development.* Science, 2000. **288**(5475): p. 2369-73.

39.   Yokota, Y., et al., *Development of peripheral lymphoid organs and natural killer cells depends on the helix-loop-helix inhibitor Id2.* Nature, 1999. **397**(6721): p. 702-6.

40.   Yoshida, H., et al., *Different cytokines induce surface lymphotoxin-alphabeta on IL-7 receptor-alpha cells that differentially engender lymph nodes and Peyer's patches.* Immunity, 2002. **17**(6): p. 823-33.

41.   van de Pavert, S.A., et al., *Chemokine CXCL13 is essential for lymph node initiation and is induced by retinoic acid and neuronal stimulation.* Nat Immunol, 2009. **10**(11): p. 1193-9.

42.   Forster, R., et al., *CCR7 coordinates the primary immune response by establishing functional microenvironments in secondary lymphoid organs.* Cell, 1999. **99**(1): p. 23-33.

43.   Luther, S.A., K.M. Ansel, and J.G. Cyster, *Overlapping roles of CXCL13, interleukin 7 receptor alpha, and CCR7 ligands in lymph node development.* J Exp Med, 2003. **197**(9): p. 1191-8.

44.   Ohl, L., et al., *Cooperating mechanisms of CXCR5 and CCR7 in development and organization of secondary lymphoid organs.* J Exp Med, 2003. **197**(9): p. 1199-204.

45.   Nakano, H. and M.D. Gunn, *Gene duplications at the chemokine locus on mouse chromosome 4: multiple strain-specific haplotypes and the deletion of secondary lymphoid-organ chemokine and EBI-1 ligand chemokine genes in the plt mutation.* J Immunol, 2001. **166**(1): p. 361-9.

46.   van de Pavert, S.A. and R.E. Mebius, *New insights into the development of lymphoid tissues.* Nat Rev Immunol, 2010. **10**(9): p. 664-74.

47.   Cupedo, T., et al., *Presumptive lymph node organizers are differentially represented in developing mesenteric and peripheral nodes.* J Immunol, 2004. **173**(5): p. 2968-75.

48.   Benezech, C., et al., *Ontogeny of stromal organizer cells during lymph node development.* J Immunol, 2010. **184**(8): p. 4521-30.

49.   Honda, K., et al., *Molecular basis for hematopoietic/mesenchymal interaction during initiation of Peyer's patch organogenesis.* J Exp Med, 2001. **193**(5): p. 621-30.

50.   Vondenhoff, M.F., et al., *LTbetaR signaling induces cytokine expression and up-regulates lymphangiogenic factors in lymph node anlagen.* J Immunol, 2009. **182**(9): p. 5439-45.

51.   Blum, K.S. and R. Pabst, *Keystones in lymph node development.* J Anat, 2006. **209**(5): p. 585-95.

52.   De Togni, P., et al., *Abnormal development of peripheral lymphoid organs in mice deficient in lymphotoxin.* Science, 1994. **264**(5159): p. 703-7.

53.   Banks, T.A., et al., *Lymphotoxin-alpha-deficient mice. Effects on secondary lymphoid organ development and humoral immune responsiveness.* J Immunol, 1995. **155**(4): p. 1685-93.

54.   Aggarwal, B.B., T.E. Eessalu, and P.E. Hass, *Characterization of receptors for human tumour necrosis factor and their regulation by gamma-interferon.* Nature, 1985. **318**(6047): p. 665-7.

55.   Erickson, S.L., et al., *Decreased sensitivity to tumour-necrosis factor but normal T-cell development in TNF receptor-2-deficient mice.* Nature, 1994. **372**(6506): p. 560-3.

56.   Pasparakis, M., et al., *Immune and inflammatory responses in TNF alpha-deficient mice: a critical requirement for TNF alpha in the formation of primary B cell follicles, follicular dendritic cell networks and germinal centers, and in the maturation of the humoral immune response.* J Exp Med, 1996. **184**(4): p. 1397-411.

57.   Pasparakis, M., et al., *Peyer's patch organogenesis is intact yet formation of B lymphocyte follicles is defective in peripheral lymphoid organs of mice deficient for tumor necrosis factor and its 55-kDa receptor.* Proc Natl Acad Sci U S A, 1997. **94**(12): p. 6319-23.

58.   Browning, J.L., et al., *Lymphotoxin beta, a novel member of the TNF family that forms a heteromeric complex with lymphotoxin on the cell surface.* Cell, 1993. **72**(6): p. 847-56.

59.   Crowe, P.D., et al., *A lymphotoxin-beta-specific receptor.* Science, 1994. **264**(5159): p. 707-10.

60.   Locksley, R.M., N. Killeen, and M.J. Lenardo, *The TNF and TNF receptor superfamilies: integrating mammalian biology.* Cell, 2001. **104**(4): p. 487-501.

61.   Futterer, A., et al., *The lymphotoxin beta receptor controls organogenesis and affinity maturation in peripheral lymphoid tissues.* Immunity, 1998. **9**(1): p. 59-70.

62.   Koni, P.A., et al., *Distinct roles in lymphoid organogenesis for lymphotoxins alpha and beta revealed in lymphotoxin beta-deficient mice.* Immunity, 1997. **6**(4): p. 491-500.

63.   Rennert, P.D., et al., *Lymph node genesis is induced by signaling through the lymphotoxin beta receptor.* Immunity, 1998. **9**(1): p. 71-9.

64.   Scheu, S., et al., *Targeted disruption of LIGHT causes defects in costimulatory T cell activation and reveals cooperation with lymphotoxin beta in mesenteric lymph node genesis.* J Exp Med, 2002. **195**(12): p. 1613-24.

65.   Dejardin, E., et al., *The lymphotoxin-beta receptor induces different patterns of gene expression via two NF-kappaB pathways.* Immunity, 2002. **17**(4): p. 525-35.

66.   Alcamo, E., et al., *Requirement for the NF-kappaB family member RelA in the development of secondary lymphoid organs.* J Exp Med, 2002. **195**(2): p. 233-44.

67.   Hayden, M.S. and S. Ghosh, *Signaling to NF-kappaB.* Genes Dev, 2004. **18**(18): p. 2195-224.

68.   Miyawaki, S., et al., *A new mutation, aly, that induces a generalized lack of lymph nodes accompanied by immunodeficiency in mice.* Eur J Immunol, 1994. **24**(2): p. 429-34.

69.   Shinkura, R., et al., *Alymphoplasia is caused by a point mutation in the mouse gene encoding Nf-kappa b-inducing kinase.* Nat Genet, 1999. **22**(1): p. 74-7.

70.   Browning, J.L., et al., *Lymphotoxin-beta receptor signaling is required for the homeostatic control of HEV differentiation and function.* Immunity, 2005. **23**(5): p. 539-50.

71.   Kong, Y.Y., et al., *OPGL is a key regulator of osteoclastogenesis, lymphocyte development and lymph-node organogenesis.* Nature, 1999. **397**(6717): p. 315-323.

72.   Dougall, W.C., et al., *RANK is essential for osteoclast and lymph node development.* Genes & Development, 1999. **13**(18): p. 2412-2424.

73.   Naito, A., et al., *Severe osteopetrosis, defective interleukin-1 signalling and lymph node organogenesis in TRAF6-deficient mice.* Genes Cells, 1999. **4**(6): p. 353-62.

74.   Sobacchi, C., et al., *Osteoclast-poor human osteopetrosis due to mutations in the gene encoding RANKL.* Nat Genet, 2007. **39**(8): p. 960-2.

75.   Kim, D., et al., *Regulation of peripheral lymph node genesis by the tumor necrosis factor family member TRANCE.* J Exp Med, 2000. **192**(10): p. 1467-78.

76.   Georgopoulos, K., et al., *The Ikaros gene is required for the development of all lymphoid lineages.* Cell, 1994. **79**(1): p. 143-56.

77.   Kurebayashi, S., et al., *Retinoid-related orphan receptor gamma (RORgamma) is essential for lymphoid organogenesis and controls apoptosis during thymopoiesis.* Proc Natl Acad Sci U S A, 2000. **97**(18): p. 10132-7.

78.   Finke, D., *Fate and function of lymphoid tissue inducer cells.* Curr Opin Immunol, 2005. **17**(2): p. 144-50.

79.   Adachi, S., et al., *Essential role of IL-7 receptor alpha in the formation of Peyer's patch anlage.* Int Immunol, 1998. **10**(1): p. 1-6.

80.   Chappaz, S. and D. Finke, *The IL-7 signaling pathway regulates lymph node development independent of peripheral lymphocytes.* J Immunol, 2010. **184**(7): p. 3562-9.

81.   Chappaz, S., et al., *Kit ligand and Il7 differentially regulate Peyer's patch and lymph node development.* J Immunol, 2010. **185**(6): p. 3514-9.

82.   Meier, D., et al., *Ectopic lymphoid-organ development occurs through interleukin 7-mediated enhanced survival of lymphoid-tissue-inducer cells.* Immunity, 2007. **26**(5): p. 643-54.

83.   Mebius, R.E., et al., *The influence of afferent lymphatic vessel interruption on vascular addressin expression.* J Cell Biol, 1991. **115**(1): p. 85-95.

84.   Mebius, R.E., et al., *A developmental switch in lymphocyte homing receptor and endothelial vascular addressin expression regulates lymphocyte homing and permits CD4+ CD3- cells to colonize lymph nodes.* Proc Natl Acad Sci U S A, 1996. **93**(20): p. 11019-24.

85.   Kanemitsu, N., et al., *CXCL13 is an arrest chemokine for B cells in high endothelial venules.* Blood, 2005. **106**(8): p. 2613-8.

86.   Wagner, N., et al., *Critical role for beta7 integrins in formation of the gut-associated lymphoid tissue.* Nature, 1996. **382**(6589): p. 366-70.

87.   Cyster, J.G., *Chemokines and cell migration in secondary lymphoid organs.* Science, 1999. **286**(5447): p. 2098-102.

88.   Forster, R., et al., *A putative chemokine receptor, BLR1, directs B cell migration to defined lymphoid organs and specific anatomic compartments of the spleen.* Cell, 1996. **87**(6): p. 1037-47.

89.   Legler, D.F., et al., *B cell-attracting chemokine 1, a human CXC chemokine expressed in lymphoid tissues, selectively attracts B lymphocytes via BLR1/CXCR5.* J Exp Med, 1998. **187**(4): p. 655-60.

90.   Ngo, V.N., et al., *Lymphotoxin alpha/beta and tumor necrosis factor are required for stromal cell expression of homing chemokines in B and T cell areas of the spleen.* J Exp Med, 1999. **189**(2): p. 403-12.

91.   Cupedo, T., et al., *Initiation of cellular organization in lymph nodes is regulated by non-B cell-derived signals and is not dependent on CXC chemokine ligand 13.* J Immunol, 2004. **173**(8): p. 4889-96.

92.   Coles, M.C., et al., *Role of T and NK cells and IL7/IL7r interactions during neonatal maturation of lymph nodes.* Proc Natl Acad Sci U S A, 2006. **103**(36): p. 13457-62.

93.   Hoorweg, K. and T. Cupedo, *Development of human lymph nodes and Peyer's patches.* Semin Immunol, 2008. **20**(3): p. 164-70.

94.   Markgraf, R., B. von Gaudecker, and H.K. Muller-Hermelink, *The development of the human lymph node.* Cell Tissue Res, 1982. **225**(2): p. 387-413.

95.   Kyriazis, A.A. and J.R. Esterly, *Development of lymphoid tissues in the human embryo and early fetus.* Arch Pathol, 1970. **90**(4): p. 348-53.

96.   Asano, S., et al., *Immunohistologic detection of the primary follicle (PF) in human fetal and newborn lymph node anlages.* Pathol Res Pract, 1993. **189**(8): p. 921-7.

97.   Salmi, M., et al., *Immune cell trafficking in uterus and early life is dominated by the mucosal addressin MAdCAM-1 in humans.* Gastroenterology, 2001. **121**(4): p. 853-64.

98.   Cunningham-Rundles, C. and P.P. Ponda, *Molecular defects in T- and B-cell primary immunodeficiency diseases.* Nat Rev Immunol, 2005. **5**(11): p. 880-92.

99.   Roifman, C.M., et al., *A partial deficiency of interleukin-7R alpha is sufficient to abrogate T-cell development and cause severe combined immunodeficiency.* Blood, 2000. **96**(8): p. 2803-7.

100.   Buckley, R.H., *Molecular defects in human severe combined immunodeficiency and approaches to immune reconstitution.* Annu Rev Immunol, 2004. **22**: p. 625-55.

101.   Russell, S.M., et al., *Mutation of Jak3 in a patient with SCID: essential role of Jak3 in lymphoid development.* Science, 1995. **270**(5237): p. 797-800.

102.   Leibbrandt, A. and J.M. Penninger, *Novel Functions of RANK(L) Signaling in the Immune System.* Adv Exp Med Biol, 2010. **658**: p. 77-94.

Chapter 4:
RANK, RANKL and OPG in lymph node:
from development to homeostasis ?

4.1. Structure/function in lymph nodes: importance of stromal cells

4.1.1. Different subtypes of stromal cells

Stromal cells have long been ignored by immunologists, nevertheless the importance of these cells for immune responses is now arising. LNs are strategically positioned to collect antigens and to organize cellular encounter needed to initiate immune responses. It is the LN stromal cells which establish the microanatomy necessary for these processes by providing distinct areas and migratory tracks that create dynamic but ordered movement patterns of immune cells. LN microanatomy provides a sophisticated filtration system in which relevant antigens are loaded onto APCs while inert substances return into the blood circulation. During immune responses, stromal cells support LN expansion and a massive increase in lymphocytes numbers [1]. Hence, there is a dependency between LN organization and immune response [2]. Nevertheless, stromal cells from LNs and in general from lymphoid organs do not respond to a clear definition. An explanation to this can be that the term of stromal cells does not refer to a specific cell type but rather to a heterogeneous functional group of non-hematopoietic cells. These CD45$^-$ cells consist of various cell types including obviously stromal cells but also lymphatic and blood endothelial cells [3]. The different stromal cells subsets found in LNs are listed in Table 4.01. Given their importance during B cell responses, most early studies on stromal cells focused on follicular dendritic cells (FDCs) [4]. The T cell zones fibroblastic reticular cells (FRCs) are now known to play an important role during T cell immune responses [5]. The importance of lymph and blood endothelial cells has already been partly discussed in the previous Chapter, these cells are important for lymph, antigen and cell entry in LNs. Less is known about the marginal reticular cells (MRCs) or about LN medullary fibroblasts [6]. The origin of stromal subsets is still poorly understood and controversial, as for instance FDCs have been proposed to derive either from bone marrow stromal cells, myeloid cells or local mesenchymal precursors [7-9]. The fibroblastic-like cells are thought to be mainly of mesenchymal origin [10] and some authors hypothesized that stromal cells could derive from stromal organizers found in LNs during organogenesis. Hence, Cupedo and co-workers showed that fetal mesenchymal cells from LN anlagen could give rise to two different stromal subsets present in LNs: FDCs and FRCs [11]. Moreover, MRCs lying under the subcapsular sinus (SCS) are thought to be the adult counterpart of the stromal organizer cells as they share molecular expression patterns. Similarly to stromal organizers, MRCs show LTβR-dependent expression of VCAM-1, ICAM-1, MAdCAM-1 and CXCL13 [12]. Further investigations are needed to clarify the origin of stromal cell subsets in adult LNs.

Stromal cell subset	LN location	Markers	Functions
Fibroblastic reticular cells (FRCs)	T cell zone	ER-TR7 antigen, podoplanin, laminin, desmin, fibrilin, fibronectin, vimentin,α-SMA, LTβR, TNFR1, TNFR2, ICAM-1, VCAM-1, collagen I, II and IV, integrins α1, α4 and β1, MHC class I and II, VEGF, PDGFR, CXCR6, CCL21, CCL19, CXCL16, IL-7 and IL-6	Structural support, production of reticular fibres, formation of conduit network, chemokine prodution and presentation, substrate for lymphocyte migration, APC adhesion, T cell homeostasis, antigen presentation
Follicular dendritic cells (FDCs)	B cell zone	CD16, CD21, CD23 (FcξRIIb), CD32 (FcγRIIb), CD35, C4, ICAM-1, VCAM-1, MAdCAM-1, laminin, desmin, CXCL12, CXCL13 and BAFF	Antigen capture, presentation of immune complexes, chemokine production and presentation, B cell homeostasis, germinal center response
Marginal reticular cells (MRCs)	Subcapsular sinus	ER-TR7 antigen, ICAM-1, VCAM-1, MAdCAM-1, RANKL, laminin, desmin, 1BL-11 antigen and CXCL13	Structural support, chemokine production, conduit function
Lymphatic endothelial cells (LECs)	All LN	CD31, LYVE-1, ICAM-1, ICAM-2, VCAM-1, ER-TR7 antigen, podoplanin, laminin, VE-cadherin, claudin 5, JAM-A, PROX1, TLRs, CCL21 and S1P	Transport of lymph, antigen and cells, chemokine production and presentation
Blood endothelial cells (BECs)	All LN	PNAd, CD31, CD34, VD-cadherin, laminin, JAM-A, JAM-B, JAM-C, ZO1, ZO2, ESAM1, claudin 5 and CCL21	Transport of blood, entry of cells from the blood into tissues
LN medullary fibroblasts	Medulla	ER-TR7 antigen, desmin, laminin and collagen III (CXCL12?)	Macrophage and plasma cell attraction

Table 4.01: Stromal cell subsets in LNs. Stromal cell subsets found in LNs are listed, along with their location in the organ, known markers and functions. Abbreviations: α-SMA, α-smooth muscle actin; BAFF, B cell activating factor; C4, complement component 4; CCL, CC-chemokine ligand; CXCL, CXC-chemokine ligand; ESAM1, endothelial cell-specific adhesion molecule 1; ICAM-1, intercellular adhesion molecule 1; IL, interleukin; JAM, junctional adhesion molecule; LTβR, lymphotoxin-β receptor; LYVE1, lymphatic vessel endothelial hyaluronan receptor 1; MADCAM-1, mucosal vascular addressin cell adhesion molecule 1; PDGFR, platelet-derived growth factor receptor; PNAd, peripheral node addressin; PROX1, Prospero homeobox protein 1; RANKL, receptor activator of NF-κB ligand; S1P, sphingosine 1-phosphate; TLR, Toll-like receptor; TNFR, tumour necrosis factor receptor; VCAM-1, vascular cell adhesion molecule 1; VEGF, vascular endothelial growth factor; Zo, zonula occludens protein. After references [1, 6].

4.1.2. Lymph node infrastructure: the reticular network

The reticular network observed in LNs for more than 100 years can be considered as the LN infrastructure as it supports the whole tissue architecture (Figure 4.01) [1]. This reticular network extends from the capsule throughout the node and forms specific structures, such as the interfollicular channel (IFC) running between B follicles, the cortical ridge (CR) lying between B and T cell zones and the paracortical cord forming the repeating unit of the cortex [13, 14]. It is only in the 1960s that cellular components of this network began to be characterized [15-17]. This intricate sponge-like structure is composed of reticular fibers, extracellular matrix and FRCs [13].
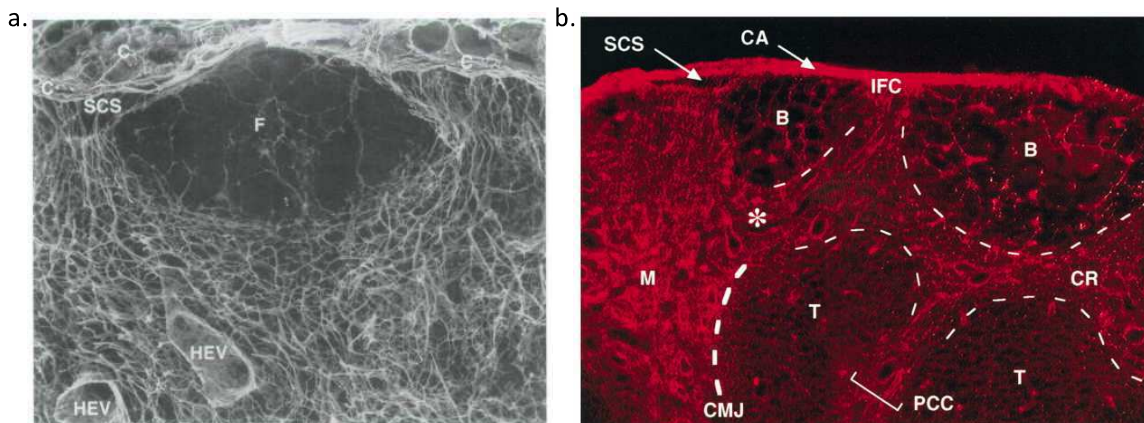
Figure 4.01: The LN infrastructure. (a) Scanning electron microscope visualization of a rat LN after cell removal by alkali maceration. (b) Fluorescence section on mouse LN sections stained with an ET-R7 antibody. Abbreviations: B or F, B cell follicle; C or CA, capsule; CMJ, cortico-medullary junction; CR, cortical ridge; HEV, high endothelial venule; IFC, interfollicular channel; M, medulla; PCC, paracortical cord; SCS, subcapsular sinus; T, T cell zone. After references [14, 18].

FRCs produce and surround collagen-rich fibres, thereby forming an enclosed conduit structure that is separate from the parenchyma of the LN. Hence, FRCs contrast with most of the fibroblasts in the connective tissues which are embedded in the extracellular matrix [1, 5]. These conduits have a diameter ranging from 200 nm to 3 µm and contain parallel bundles of fibrillar collagen I and III. In the larger conduits these bundles are found associated with crosslinking and stabilizing molecules, such as fibromodulin, decorin and lumican [5]. In addition, an unordered meshwork of microfibrils of fibrillins fills the space between the collagen fibres (Figure 4.02c) [19]. FRCs were found to almost continuously enwrap the conduits by connecting one to each other through intercellular junctions. Hence, more than 95% of the conduits are covered with FRCs and the gaps are enclosed by DCs which extend processes into the lumen of the conduit (Figure 4.02b) [20]. Thus, FRCs display features of endothelial or epithelial cells, such as an apical-basal polarity, cell-cell junctions and a basal membrane but they also display characteristics of fibroblasts as they produce interstitial matrix, smooth muscle actin and express desmin and vimentin [5, 6]. The conduit system belongs to the functional unit of the cortex: the paracortical cords. These paracortical cords consist of concentric spaces: HEV lumen, perivenular channels, corridors and cortical sinuses [13]. When lymphocytes enter the LNs through the HEVs, they emerge in a narrow compartment referred to as the perivenular channel. This compartment is delineated by HEV endothelial cells and by the surrounding FRCs. At least two layers of FRCs are found around the abluminal surface of HEVs. Subsequently, lymphocytes migrate out of this channel into a more open space constituting most of the cortex parenchyma: the corridor. The corridor is filled with lymphocytes and its walls are provided by the FRC network depicted just above. Thus, the corridors present an irregular geometrical arrangement allowing lymphocytes to migrate without encountering physical barriers [13]. The notion of paracortical cords was first introduced in 1975 by Kelly *et al.*, since then these structures were

reported in different studies but for some authors the existence of these cords remains unsubstantiated [21].
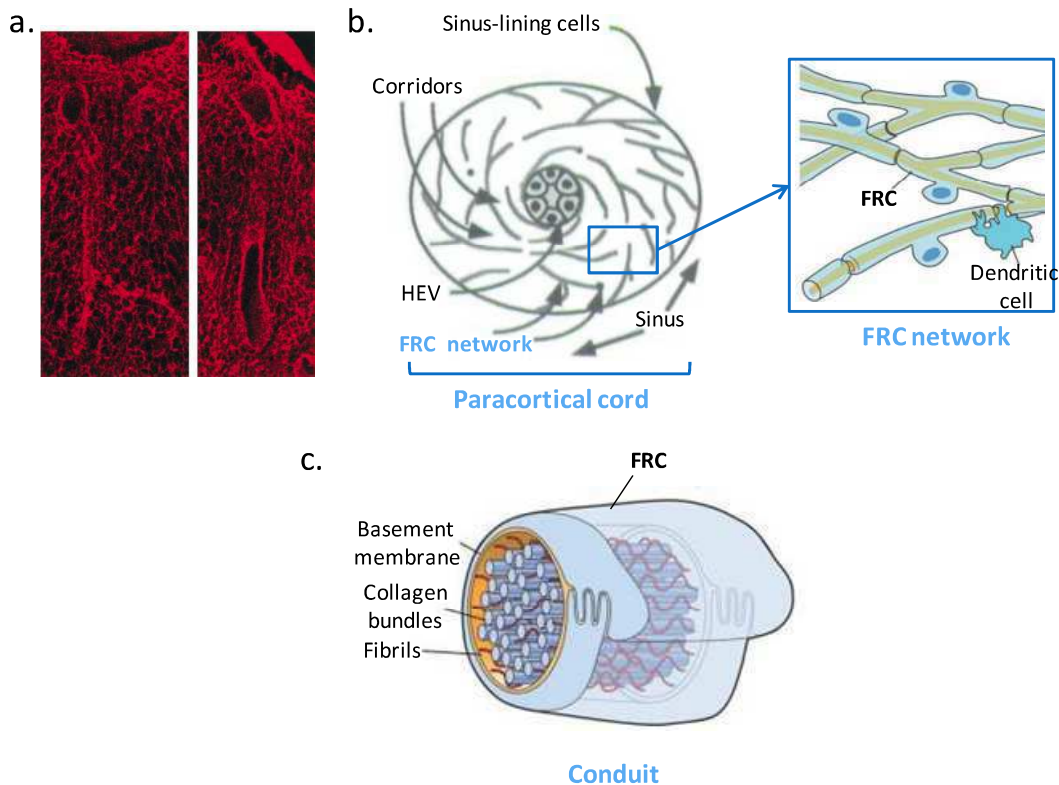
Figure 4.02: Structure of the paracortical cords in the LN. (a) Paracortical cord as seen on a section from mouse LN stained with an ET-R7 antibody. After reference [14]. (b) Representation of an idealized cross-section through a paracortical cord depicting different structures composing this functional unit. After reference [13, 22]. (c) Representation of a cross-section through a LN conduit showing the fibroblastic cells enwrapping the collagen and fibrils. After reference [22]. Abbreviations: HEV, high endothelial venule, FRC, fibroblastic reticular cells.

4.1.3. The reticular network and the lymph traffic

- ### *T cell zone*

Lymph enters the LNs by the SCS where it is filtered by specialized macrophages and DCs, turning this anatomical part of the LNs into an antigen-sampling zone. Different types of macrophages are located in the SCS and in close proximity to other sinuses, they express specific C-type lectins (CD169 or SIGNR1) or type I scavenger receptor (MARCO, macrophage receptor with collagenous structure) [2]. These cells fulfill the important function of pathogen filtering and antigen presentation to lymphocytes, but are also important for innate immune-mediator delivering upon infections [23]. Their specific depletion can lead to the systemic dissemination of pathogen throughout the body [24]. Studies in the 1930s have suggested that lymph, after entering the SCS, percolates throughout the LN by diffusion in the parenchyma to finally reach the HEVs [25]. Since then, additional studies were performed to understand the rules governing the lymph flow within the LN but it was only in 2000 that

Gretz and colleagues depicted more precisely the mechanism implied [26]. The authors found that the larger molecules that they had injected in mice (≥70 kDa) were visible in the subcapsular and medullary sinuses but were largely excluded from the cortical parenchyma. At the same time, lower molecular mass molecules (≤40 kDa), such as chemokines, enter the cortex in a defined manner. Hence, the low molecular mass molecules labeled with fluorophores stained the SCS, the reticular fibers and the abluminal and luminal surfaces of HEVs. These small molecules were found inside the reticular network formed by FRCs. Thus, lymph-borne molecules travel rapidly from the SCS to the HEVs by using the FRCs conduits [26]. This exclusion was preserved during the acute LN enlargement observed upon viral infections and could thereby prevent the lymph-blood shunt within the LNs of being exploited by infectious agents [26]. The lymph-borne molecule-transport within the conduits allows resident DCs in the cortex to sense rapidly the incoming signals from the periphery through their extended processes into the conduits. It was found that chemokines produced in the periphery are rapidly (within seconds) channeled by the interstitial flux towards the conduit system [27]. This process leads to a rapid recruitment of circulating immune cells to the LNs, such as monocytes, as depicted in Figure 4.03.
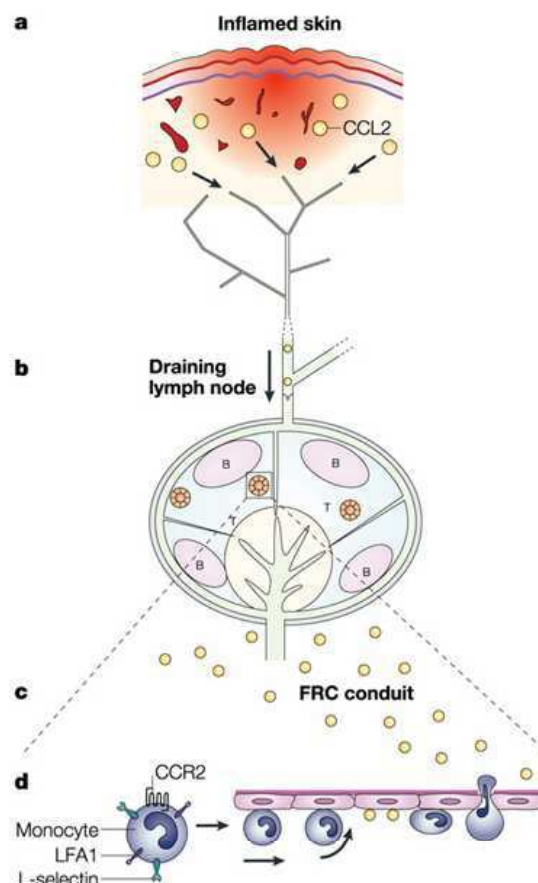
Figure 4.03: Role of FRC conduits in monocyte recruitment to LNs during inflammation. (a) Inflammation induces production of chemokines, for instance CCL2, and increases the microvascular permeability. (b) CCL2 and other lymph-borne molecules are transported to the subcapsular sinus and reach the conduit system. (c) Molecules further progress in the conduits and reach the perivenular channels around the HEV. (d) Transendothelial vesicular-transported CCL2 is presented on HEV lumen. CCL2 induces CCR2-dependent integrin activation of the rolling monocytes. After reference [28].

Soluble antigens presented by resident DCs can elicit T cell responses that were however not sustained and needed to be consolidated by later incoming DCs [29]. During *Leishmania major* infection, T-cell responses mainly rely on resident DCs and thus on soluble antigens arising from the periphery through the lymph [30]. In addition, conduits may also have a role in fluid homeostasis because high amounts of fluids are resorbed through the LNs back into blood circulation. Thus, in the absence of conduits, lymph would mainly recirculate in the efferent lymph vessels or could even form oedema [5].

- ### *B cell zone*

The conduit network formed by FRCs is dense in T cell zone but is only sparse in B cell follicles. In 2009, Roozendaal and co-workers found that, like in the T cell zone, transport of small protein antigens from the SCS into the B cell follicular region was mediated by the sparse reticular network [31]. Additionally, it was recently found that FRCs form the conduits of the B cell area during ontogeny, as B cell follicles develop at the periphery of the T cell zone, in regions where the conduit network is already formed and functional [32]. When new T and B cells enter the developing LNs, the density of the conduit system is preserved in T cell zone but not in B cell follicles, resulting in a sparse network in this compartment that nevertheless retains its connectivity [32]. Subsequently, FRCs disappear from the follicular region and are replaced by FDCs, which is generated with the accumulation of B cells. The positioning of FDCs around the follicular conduits correlates with their capacity to capture soluble antigen draining from the periphery, even in the absence of antigen-specific antibodies [32]. These discoveries provided an alternative to the previously described model of soluble antigen distribution through the floor of the SCS, which was presumed to be porous and to allow free diffusion of antigens into the B cell follicle [32]. Although FDCs appear insignificant in the formation of the extracellular matrix structure ensuring LN architecture, their dense network provides an important B cell niche.

4.2. FRCs in T cell responses

Different subsets of FRCs are defined according to their topographic and phenotypic features. FRCs characteristic of the T cell zone express both podoplanine and IBL-11 marker, whereas FRCs from the marginal zone (MRCs) additionally express MAdCAM-1 [33]. MRCs are mainly described for their structural support function and possibly for being the adult counterpart of the fetal stromal organizer cells [12]. Although it was initially assumed that the role of FRCs in LNs was mainly structural, these cells are now known to be key players in many processes, among which lymphocytes homing, migration and survival, endothelial cell proliferation and peripheral tolerance. These functions are resumed in Figure 4.04 and are now going to be reviewed in more detail.
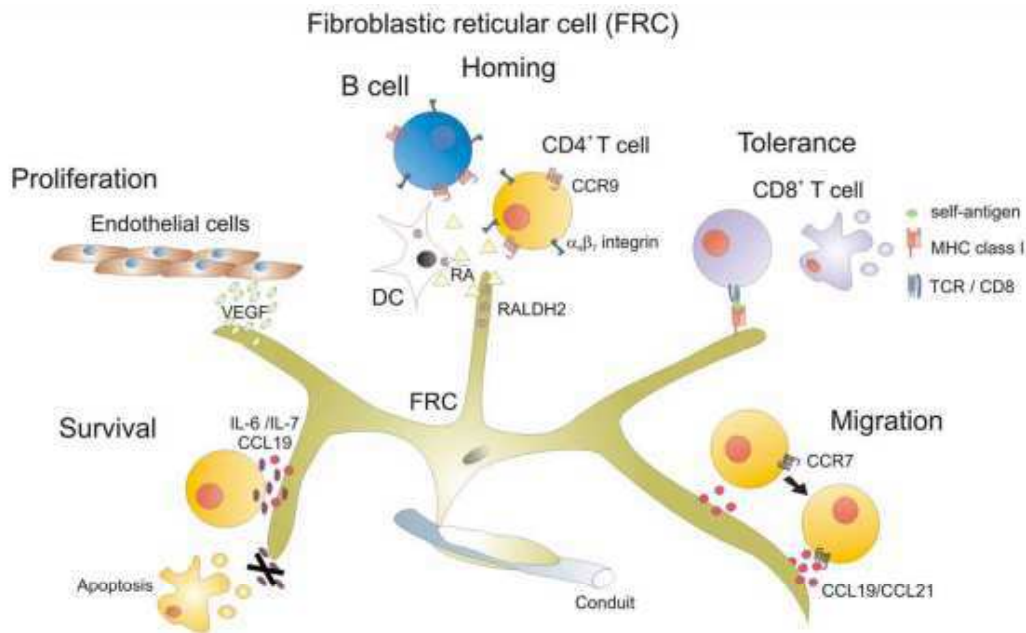
Figure 4.04. Immunological functions of FRCs. FRCs mediate the motility of lymphocytes through the expression of CCL19 and CCL21 chemokines. FRCs possibly express genes encoding for peripheral-tissue antigens, leading to peripheral tolerance by the deletion of autoreactive T cells. Through their expression of the RA-producing enzyme RALDH2, FRCs induce the expression of gut-homing molecules (CCR9, α4β7 integrin) by activated T cells. FRCs are also implicated in endothelial cell proliferation as they produce VEGF. Finally, FRCs are implied in naïve T cells homeostasis by secreting CCL19 and IL-7. Abbreviations: MHC, major histocompatibility complex; RA, retinoic acid; RALDH2, retinaldehyde dehydrogenase 2; DC, dendritic cell; VEGF, vascular endothelial growth factor. After reference [6].

4.2.1. FRCs in lymphocyte homing and migration

Lymphocytes specific for a particular antigen are rare, in the case of a naïve T cell, it is estimated that 1 out of 10^5 to 1 out of 10^6 cells will be reactive to a given peptide-MHC complex [34]. Thus, the immune system faces the challenge to promote the encounter between the rare lymphocytes specific for an antigen and APCs. As described above, the lymphatic system provides a solution to this problem by concentrating tissue-derived antigen and APCs in lymphoid organs. Lymphocytes "simply" need to patrol all the LNs in search of their specific antigen and a generally held view was that accumulation of cells within LNs was enough to induce a sufficient frequency of cell-cell contacts. Nevertheless, how precisely a naïve T cells could encounter a DC, bearing its cognate antigen was elusive, as the volume of a resting LN is roughly 10 million times the volume of a naïve T cell [35]. It was only during the last decade that studies gave a more precise view of cell behaviour within the parenchyma, mainly thanks to technical advances such as the two-photon microscopy enabling fluorescence imaging of living tissue with relatively high depth [36]. These initial studies, which mainly focused on hematopoietic cells, showed that B and T cells migration was more dynamic than anticipated and apparently random in direction [36]. As a result of this migration pattern, it has been estimated that 500 to 5000 T cells may contact individual DCs per hour [37]. Nevertheless, this

erratic movement of migration incited the question of how lymphocytes specifically migrate into T and B cell zones. Although it is well known that chemokines are essential for LN compartmentalization, this apparently random migration negates a simple role for diffusible chemoattractant exerting long-distance directional control. In 2006, Bajénof and co-workers confirmed the hypothesis proposed almost 10 years earlier by Gretz and colleagues that FRC network supports T cell motility in the paracortical area of LNs [13, 38]. Thus, by simultaneously visualizing FRCs and T cells *in vivo*, the authors demonstrated that T cell migration was not erratic but rather deterministic as they moved preferentially along the FRCs network [38]. The work of Bajénof and colleagues explained the previously described T cell behavior, since the frequent shift in migration direction was correlated with network branching. In addition, the authors showed that the acute turns of naïve T cells at the border of B cell follicles back into the paracortex was a result of the presence of the dense reticular network in the T cell cortex compared to its paucity in the B cell zone. Migration of T cells on the network was random and most probably mediated by CCL19 and CCL21 immobilized to the FRCs network that generate a chemokinetic surface [5, 39]. Another proposed mechanism for T cell motility is the presence of extra-cellular matrix proteins produced by FRCs not only in the conduits but also on the outer surface of FRCs [40]. These proteins were proposed by the authors to act like ligands for cell adhesion receptors expressed by lymphocytes but the physiological relevance of this proposed mechanism still needs to be addressed. As far as B cells are concerned, Bajénof reported that initial B cell migration in the cortex was also governed by the FRCs network before these cells reach the follicles. Hence, almost 90% of B cells present in the cortex were found associated with the FRC network [38].

Another important concept about lymphocyte migration within the cortex aroused in 2006 from the work of Castellino and co-workers [41]. In their study, the authors found using *in vivo* single cell tracking that CD8$^+$ T cells are able to respond quickly to locally-released chemokines upon successful interaction between DC and T$_H$ cells [41]. Thus, locally released chemokines can overcome the principle of swarming and attract cells in a specific direction.

FRCs also seem to be implied in the generation of gut-homing T cells *in vivo*. It has been found that retinoic acid (RA) led to the induction of CCR9 and integrin α4β7 upon activation of T cells, enabling them to migrate to the small intestine [42]. Although *in vitro* activation by intestinal DCs is sufficient to instruct expression of these gut-homing molecules by T cells, it was found that *in vivo* stromal cells are essential for the generation of gut-homing T cells [43]. Furthermore, only stromal cells from mesenteric LNs and not from peripheral LNs were able to support induction of CCR9 and express high level of RA producing enzymes (RALDH), so that the authors suggested that the RALDH-positive stromal were FRCs [44].

4.2.2. *FRCs in T cell and lymph node homeostasis*

In 2007, Link and co-workers found that FRCs were crucial for naïve T cells homeostasis, notably by producing CCL19 and IL-7 [45]. The authors identified the FRCs as the main producers of IL-7, a crucial factor for naïve T cells survival. In addition, they also found a non-redundant role for CCL19 in survival of naïve T cells. Hence, FRCs are key players in naïve T cells survival by secreting survival factors and access to LN is critical for T cells homeostasis [45]. Moreover, FRCs also play an important role in global LN homeostasis. FRCs were found to upregulate expression of transglutaminase during LN expansion, thereby forming a collagen-rich reticular network important for the increase of LN size [46]. Additionally, FRCs also play an important role in the regulation of LN vasculature, a crucial process upon infection [47]. In their study, Chyou and co-workers showed that FRCs are the principal VEGF (vascular endothelial growth factor)-expressing cells. VEGF is an important mediator of endothelial cell proliferation in stimulated LNs and FRCs were found to upregulate expression of VEGF during immune responses, probably upon LTβR triggering [47]. Thus, modulation of VEGF expression level by FRCs would be a means to regulate LN vascularity, turning FRCs into paracrine regulators of endothelial cells proliferation. In addition to FRCs, DCs and, during inflammation, B cells and macrophages are also known to secrete endothelial growth factor. Recently T cells were shown to negatively regulate lymphatic vessel formation, leading to the model of regulation of lymphangiogenesis depicted in Figure 4.05 [48].
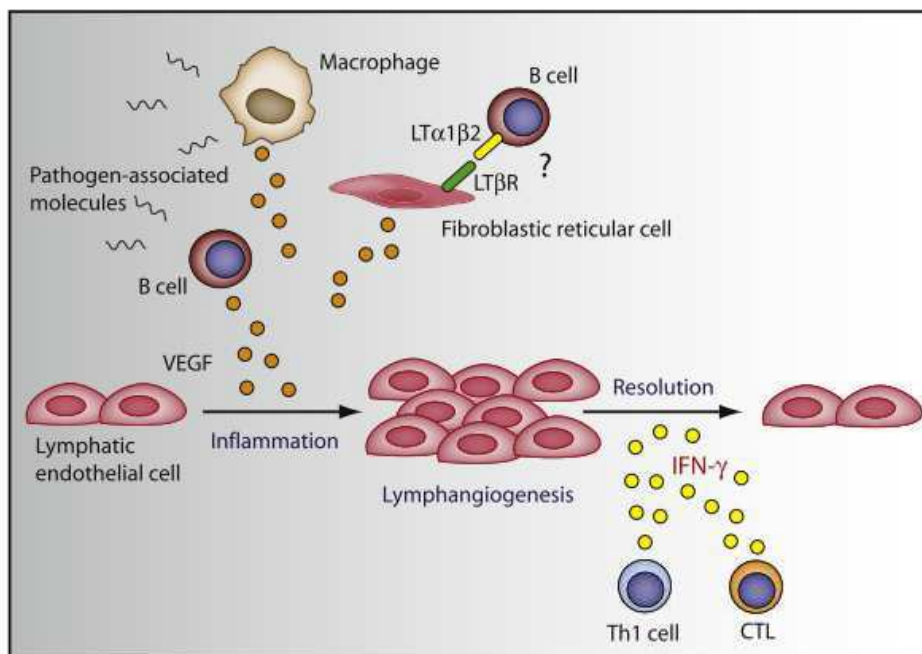
Figure 4.05: Regulation of lymphatic vessel formation by FRCs and other cell types. Upon inflammation B cells, macrophages and FRCs are triggered to secrete VEGF. B cells are thought to activate FRCs through LTβR activation. Subsequent to the VEGF-induced lymphangiogenesis, T cells regulate the homeostatic balance of lymphatic vessels density through a negative paracrine action of IFN-γ. Abbreviations: VEGF, vascular endothelial growth factor; IFN-γ, interferon-γ; Th1, T helper 1 cells; CTL, cytotoxic T lymphocyte. After reference [49].

Finally, it has been shown *in vitro* that fluid flow regulates FRC morphology, organization and CCL21 secretion [50]. Thus, lymph flow could be considered as a homeostatic regulator of FRCs activity and increased lymph flow under inflammatory condition could be an early mechanism enhancing CCL21 expression by FRCs and thereby inducing efficient cell trafficking within the LNs.

4.2.3. FRCs in peripheral tolerance

Most T cells expressing TCR with a strong affinity for self-antigen are being depleted in the thymus. Yet, this process is incomplete and peripheral tolerance mechanisms are needed. Thus, suppression of autoreactive T cells implies T reg cells and resident and incoming DCs in LNs which cross-present self-antigens [1]. Until recently, the prevailing peripheral tolerance model heavily relied on DCs. However, profiling of medullary thymic epithelial cell (mTEC)-mediated peripheral tissue-restricted antigen (PTA) expression has demonstrated that resident non-hematopoietic cells could be potent tolerance inducers which led to the hypothesis that such cells are present in the periphery [51]. In 2007, Lee and colleagues found that LN stromal cells contribute to peripheral tolerance through the expression of PTA [52]. The authors used a transgenic model of expression of truncated ovalbumin under the control of the intestinal fatty acid-binding protein (iFABP) promoter. Upon transfer of ovalbumin-specific CD8$^+$ T cells in these mice, transferred cells were activated in LNs even when hematopoietic cells, including DCs, were prevented from presenting antigen. These T cells were subsequently lost from the peripheral T cell pool resulting in tolerance [52]. Gardner and co-workers also reported PTA expression by LN stromal cells and found, like Lee and colleagues, that autoreactive CD8$^+$ T cells interacting with the self-antigen expressing stromal cells were subsequently deleted [52, 53]. In their model, mice expressed the autoimmune regulator (AIRE) transcription factor together with green fluorescent protein which enabled the authors to identify non-bone-marrow-derived-AIRE-expressing cells in the periphery [53]. Additionally, LN stromal cells were shown to induce tolerance in a non-transgenic model by Nichols and colleagues further underlining the biological relevance of this finding [54]. In this study, tolerance to tyrosinase, which is a melanocyte-specific self-antigen, required LN stromal cells. Although the tyrosinase transcript was detected in the thymus, it was insufficient to delete all autoreactive T cell clones as shown by the transplantation of tyrosinase-sufficient thymi into albino mice lacking tyrosinase expression. In these mice, T cells were not entirely deleted. The authors found that in a wild-type background tyrosinase-specific CD8$^+$ T cells trafficked to LNs where they were activated and tolerized directly by stromal cells [54]. Still, the exact stromal subset expressing PTA remain elusive. In 2010, FRCs were shown to directly present PTAs both under steady-state and inflammatory conditions [55]. Hence, FRCs were the only stromal cells in the LN expressing truncated-ovalbumin in the iFABP-truncated ovalbumin model [55]. However, tolerance induction was not restricted to a single subset of stromal cells and LECs were found to be responsible for tyrosinase expression in LNs and for tolerance to this antigen [56]. In

Chapter 4

RANK, RANKL and OPG in lymph node: from development to homeostasis ?

79

addition, each stromal subset expresses characteristic PTAs, and blood endothelial cells (BEC) and the double negative cells (podoplanine-CD31-) also express a specific pattern of PTAs [55, 56]. Nevertheless, tolerance induction has not been directly demonstrated for these two subsets. In light of its role in the thymus discussed in Chapter 2, it was proposed that AIRE would also regulate expression of PTAs by LN stromal cells. Hence, *Aire* transcript was detected in stromal cells-enriched fraction of LNs [52]. Although AIRE regulates the transcription of some PTAs expressed in LNs, it does not regulate the expression of all of them [53, 55]. For instance, expression of tyrosinase by LN stromal cells was found to be AIRE independent as LECs from AIRE-deficient mice express this PTA [56]. In addition, *Aire* transcript was mainly found in the double negative stromal subset, whereas another PTA regulating transcription factor, DEAF1, was found equally expressed between FRCs, LECs, BECs and double negative stromal subsets [55]. The precise mechanism implied in this suppression of CD8$^+$ T cells is unknown but at least in the model of iFABBP-truncated-ovalbumin, the PD-1 (programmed cell death) /PD-L1 (PD-ligand 1) pathway is suggested as anti-PD-L1 treatment led to an acute inflammation of the gastrointestinal tract [57]. A possible role for RANKL, similar to its role in the thymus for the induction of AIRE-expressing mTECs, has yet not been addressed in the LNs.

4.2.4. *Pathogen interaction with FRCs*

Lymphoid stromal cells are targeted by several intracellular pathogens. In 2003, chronic infection of non-human primates with the simian immunodeficiency virus (SIV) was found to lead to a progressive decrease in the expression of CCL21 and CCL19 by stromal cells, suggesting an alteration in FRCs network [58]. In 2011, lymphoid tissue fibrosis associated with HIV-1 infection (human immunodeficiency virus 1) was found to be the result of increased TGF-β1 expression by activated T reg cells along with an increased expression of its receptor on FRCs. In addition, FRCs can be directly targeted by virus, as it has been found by Mueller and co-workers in a model of murine infection by the lymphocytic choriomeningitis virus (LCMV) [59]. In their study the LCMV clone 13, which is associated with a chronic infection, infected a high number of FRCs, whereas the Armstrong LCMV acute strain infected only few FRCs. As a result of LCMV clone 13 infection, FRCs network was altered by the action of CD8$^+$ T cells, although protected from complete destruction by FRCs upregulation of programmed death ligand 1 (PD-L1) after infection. The PD-1 pathway prevents excessive immunopathology but contributes to viral persistence in FRC [59]. In 2008, Scandella and colleagues also reported infection of FRCs by the LCMV WE strain which displays intermediate replication kinetics [60]. Again, FRCs were shown to be eliminated by CD8$^+$ T cells but additionally the authors showed that upon loss of FRCs, a transcriptional reorganization program was initiated. Thus, transcription of molecules implicated in the development of lymphoid tissues and the crosstalk between stromal organizers and LTics was found to be induced. This process was associated with the

proliferation of LTics which were found to be required for re-establishment of the FRC network after virus clearance, possibly through LTβR engagement on FRCs [60]. In addition, Ebola, Marburg and Lassa viruses were found to infect FRCs and endothelial cells in non-human primates [61]. These highly pathogenic viruses induce considerable apoptosis of the stromal compartment of secondary lymphoid organs [61]. Moreover, *Leishmania major* was shown to infect FRCs and 40% of the persisting parasites were associated with LN FRCs [62].

4.3. *FDCs in B cell responses*

The FDCs are the major subset of stromal cells in B cell follicles, but in contrast to FRCs, FDCs were mainly studied in connection to their immunological function rather than for their contribution to the LNs architecture [6]. Hence, FDCs were found to be implicated in B cells homing, migration, survival and proliferation. They are also involved in antigen presentation and in T cell dependent antibody response. These functions are summarized in Figure 4.06.
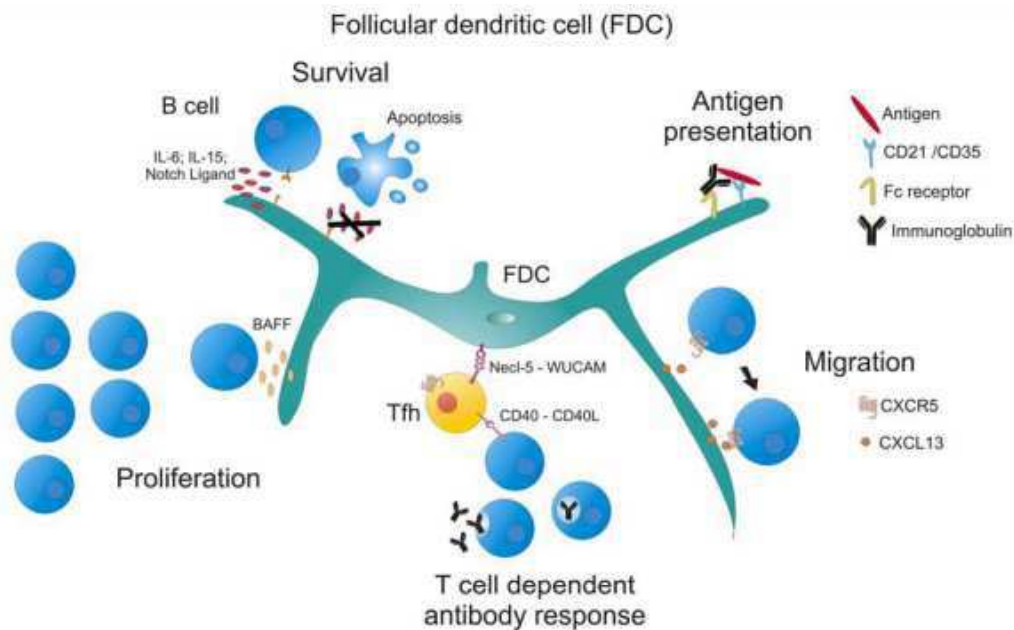
Figure 4.06: Immunological functions of FDCs. FDCs mediate the organization of B cell follicles through the expression of CXCL13. They have influence on the proliferation and survival of B cells by producing BAFF, IL-6, IL-15 and Notch ligand. FDCs are antigen presenting cells and are able to mediate T cell-dependent antibody responses by interacting with follicular helper T cells (T_{FH}) via Necl-5. After reference [6].

4.3.1. *FDCs in B cells homing and migration*

- *Homing and migration in primary follicles*

FDCs actively contribute to the segregation of B and T cell zones. FDCs, DCs, MRCs and follicular helper T cells (T_{FH}) express CXCL13, a critical chemokine for B cell follicle formation [63]. However, bone-marrow chimera experiments established that the majority of splenic CXCL13

expression was of radio-resistant origin, suggesting that FDCs would be the major source of CXCL13 [63, 64]. CXCL13 receptor CXCR5 is expressed by all mature B cells: *in vitro*, all these cells can respond to CXCL13 although, *in vivo*, other factors can override CXCL13 responsiveness as not all mature B cells respond to a CXCL13 gradient [63]. As mentioned in the previous Chapter, B cells like T cells, enter LNs through the HEVs. CXCL13 expressed by some HEV cells is an arrest cytokine for B cells [65]. As they exit the HEV, B cells migrate along the FRC network towards the B cell follicles where they crawl in close association with the dense network of FDCs [38]. As the conduits in B cell zones are structurally similar to those in the T cell zone, it has been suggested that they play a similar role in B cell homing as it is recognized for T cells [31]. CXCL13 expression by FDCs was found to be dependent on $LT\alpha_1\beta_2$ and to a lesser extent on TNF. CXCL13 induces expression of $LT\alpha_1\beta_2$ by naïve B cells, thereby creating a positive feedback loop [66]. B cells migrate extensively within B cell follicles and this migration is thought to be important for B cells to survey the surfaces of APCs, whether FDCs, DCs or sinus associated macrophages (Figure 4.07).
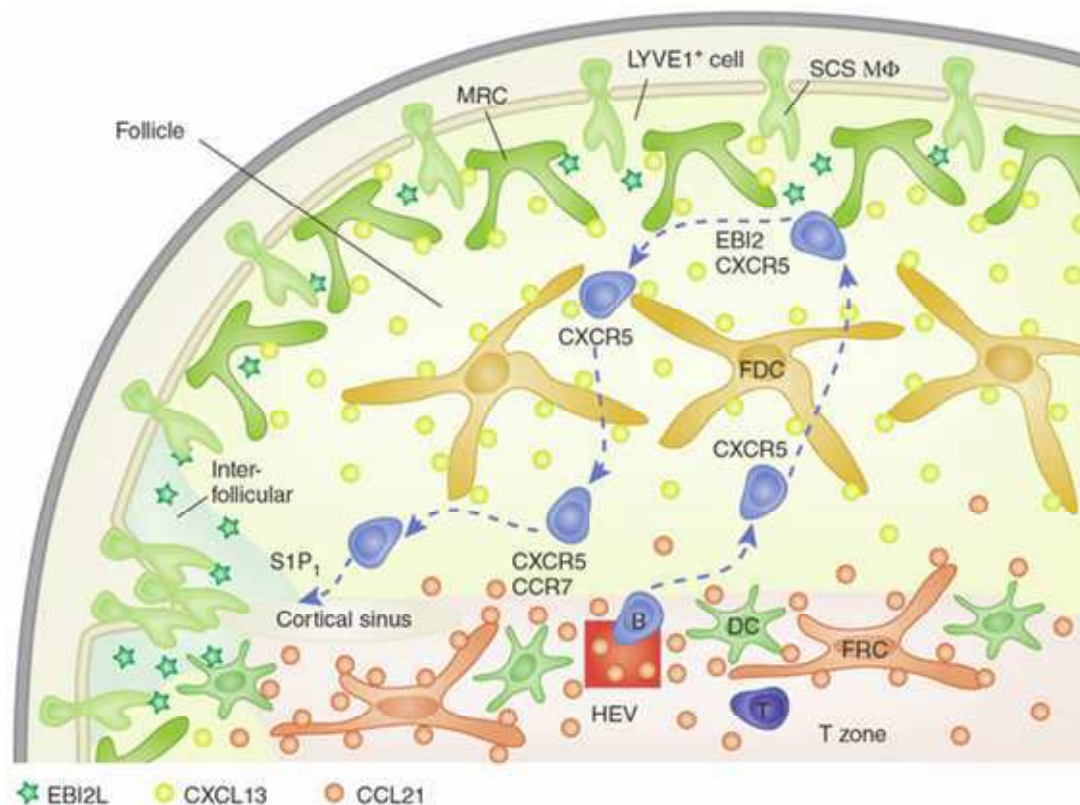
Figure 4.07: B cell trafficking in LNs. Multiple cues direct B cell migration within the LN. B cells entering the LN through the HEV, migrate in the follicle through a CXCR5-CXCL13 dependent manner. B cells are attracted to the outer follicle cortex by CXCL13 and also EBI2L (Epstein Barr virus induced molecule 2 ligand) which is secreted by a yet unknown source, thereby enhancing possible encounter with antigens presented by subcapsular sinus macrophages. B cells travel back through the FDCs network and reach the T cell zone-proximal follicle through CCR7 expression. Finally, B cells exit the LN through a cortical sinus. Abbreviations: SCS, subcapsular sinus, MΦ, macrophages, B, B cell, T, T cell, EBI2, Epstein Barr virus induced molecule 2, EBI2-L, EIB2-ligand. After reference [67].

- *Homing and migration in secondary follicles*

B cell follicles in lymphoid organs can exist in two different states, either a quiescent state referred to as primary follicles (described above) and composed largely of naïve B cells, or an activated state, so called secondary follicles. Activated follicles contain a central germinal centre (GC) composed of B cell blasts (Figure 4.08a) [1, 68]. About a week is required for GC formation which will then remain during weeks [68]. The major events known to occur in GCs include Ig (immunoglobulin) class switching, somatic hypermutation and selection of somatically mutated B cells with high affinity BCRs (B cell receptors) [1, 68]. GCs are compartmentalized in two defined histological zones: the dark and the light zones. In the dark zone, which is localized close to the T cell area, are found large, proliferating B cells with down-regulated surface Ig expression referred to as centroblasts. In the light zone, B cells density is lower than in the dark zone and B cells are small, non-mitotic and expressing surface Ig [63, 68]. In primary follicles, FDCs are localized in the central region, whereas a polarized distribution is observed in GCs [63]. FDCs network is dense in the dark zone and rather sparse in the light zone. Different patterns of surface molecule expression are observed between primary FDCs and FDCs in GC light and dark zones and it is not known if dark zone FDCs are a subset of FDCs or a distinct type of stromal cells (Figure 4.08b) [1, 63].

Primary follicle FDCs	Germinal center light zone FDCs	Germinal center dark zone FDCs
BP-3^{++}	BP-3^{+++}	BP-3^{++}
IC-trapping^{+}	IC-trapping^{+++}	IC-trapping$^{+¤}$
CD21/35^{++}	CD21/35^{+++}	CD21/35^{++}
FcεRIIb^{-}	FcεRIIb^{+++}	FcεRIIb^{-}
FcγRIIb$^{+/-¤}$	FcγRIIb^{+++}	FcγRIIb^{-}
FDC-M1$^{+/-}$	FDC-M1^{+++}	FDC-M1$^{+/-}$
FDC-M2^{+}	FDC-M2^{+++}	FDC-M2^{-}
CXCL13^{++}	CXCL13^{++}	CXCL13^{-}
ICAM1^{+}	CXCL12^{-}	CXCL12^{+}
VCAM1$^{+/-}$	ICAM1^{++}	ICAM1^{+}
	MAdCAM1^{+++}	VCAM1^{+}
	VCAM1^{+++}	Fibrinogen$^{++¤}$
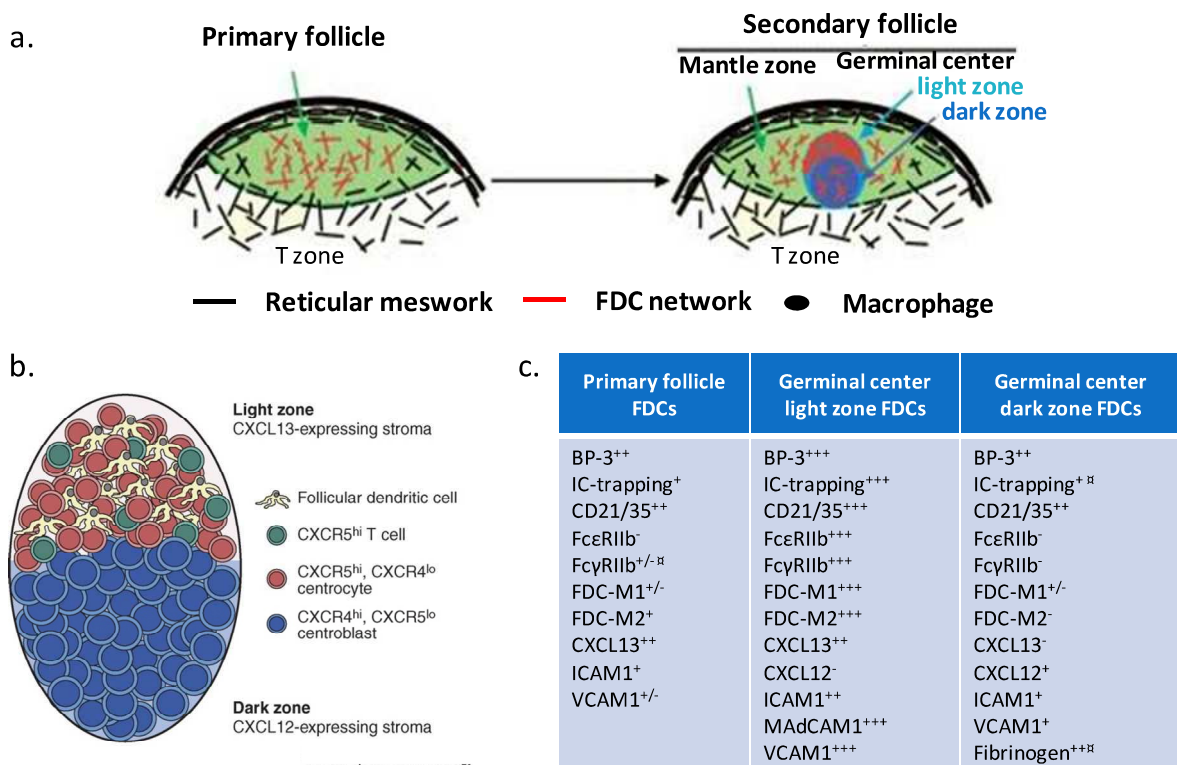
Figure 4.08: Schematic representation of the relationship of stromal cells between primary and secondary follicles. (a) Primary follicles are essentially constituted of naïve B cells (green shading) and FDCs (red). Secondary follicles contain a germinal center (GC), and a mantle of non reactive B cells surrounds them. (b) Antigen-specific B cell blasts (centroblasts) predominate in the GC dark zone and give rise to the centrocytes of

the light zone. FDCs from the primary follicle are thought to mature in response to LT, TNF, immune complexes and maybe other signals to form FDCs from the dark and light zones. After references [69, 70]. (c) Surface markers expressed by primary follicles FDCs, GC light and dark zone associated FDCs. +/- refer to variable report in the literature; ¤ stands for variable notes: FcγRIIb+/- indicates functional evidence only; FcεRIIb is only present in certain GCs; IC (immune complex)-trapping only after *in vitro* incubation. After reference [63].

Only dark zone FDCs express CXCL12, possibly explaining the B cell compartmentalization observed in GCs, as centroblasts express a high level of CXCL12 receptor (CXCR4). ICAM-1, VCAM-1 and MAdCAM-1 were found to be abundantly expressed on light zone FDCs processes and *in vitro* studies suggested that these molecules could promote B cell attachment [63]. Nevertheless, two-photon microscopy observations showed that B cells were highly motile in the light zone, suggesting that integrin ligands do not statically fix B cells to FDCs [71]. In a recently published study on B cells migration, Beltman and co-workers showed that the random walk of B cells within the GC had a small preference for the light zone which is consistent with classical views of dark to light zone movement of the GC reaction [72]. B cells present in the GC express higher level of $LT\alpha_1\beta_2$ than naïve B cells, and addition of $LT\alpha_1\beta_2$ and TNF to FDCs *in vitro* leads to the expression of molecules associated with the light zone FDCs [66, 73]. Hence, light zone FDCs seem to have acquired additional and specific properties which could suggest that a differentiation program takes place during the GC formation.

4.3.2. FDCs in B cells survival and proliferation

Beside their function in guiding B cells into the follicles, FDCs play a key role in both naïve and activated B cells survival and proliferation. In 2003, Gorelik and colleagues found that the TNFSF member B cell activating factor (BAFF) expressed by radio-resistant cells was required for BAFF-R[+] (BAFF receptor) B cells homeostasis [74]. However, this study did not clearly address whether these cells corresponded to FDCs. Indeed, in the spleen of mice deficient for TNF, LTα, LTβ or B cells, thereby lacking FDCs, BAFF transcripts were still found, suggesting other stromal sources of BAFF [63]. Mice deficient for BAFF or BAFF-R present a GC that decays prematurely and presents impaired maturation and function, suggesting that BAFF has a role in sustaining the GC [75]. However, not only is BAFF expression in GC FDCs conflictual but also GC B cells appear to lack BAFF-R [76]. This conflict may be partly resolved by B cells expressing BCMA (B cell maturation antigen) and TACI (transmembrane activator and calcium-modulator and cyclophilin ligand interactor), two other receptors for BAFF [77]. CD320 was discovered in human tonsil FDCs and in the FDC-like HK cell line and was found to stimulate GC B cells proliferation and plasma cells differentiation [78, 79]. The basis of this functional effect is yet not defined. Interestingly, CD320 may be implicated in B cell lymphomas and treatment with a CD320-directed antibody blocked lymphoma cells proliferation in a HK-cell dependent mouse lymphoma model [80]. Notch ligands Delta-like 1

(Dll1) and Jagged 1 (Jg1) were found to be expressed by FDCs and to support the survival of GC B cells which express Notch1 and Notch2 [81]. In addition, FDCs produce IL-15 which supports GC B cells proliferation [82]. Some studies using *in situ* hybridization, immunohistochemical staining and analysis of FDC-like cell lines provided evidence that FDCs produce IL-6 [63]. Mice deficient for IL-6 develop a reduced GC response [83]. Hence, FDCs provide different trophic factors to support B cell survival and proliferation.

4.3.3. FDCs are antigen presenting cells

More than 40 years ago, opsonized antigen was found to become distributed inside lymphoid follicles in a "reticular fashion" leading to further studies which identified FDCs as specialized antigen-trapping cells [84]. FDCs efficiently trap immune complexes by their Fc and complement receptors. Complement receptors CD21/35 are found on all FDCs subtypes and $Fc\gamma RIIb$ (CD32) and $Fc\varepsilon RIIb$ (CD23) are mainly expressed by light zone FDCs [63]. FDCs not only capture and display immune complexes but also have the unique property to retain them on their surface for long periods, which raises the possibility that they function in memory B cell maintenance [63]. Mice deficient in CD21/35 have a compromised antibody response to several antigens [67, 85]. FDCs carry only few pattern-recognition receptors suggesting inefficient capture of non-opsonized antigens [67]. In primary follicles, FDCs are positioned in the center of the follicle and do not extend to the SCS nor to the T cell zone which may protect opsonized antigens from being scavenged by macrophages and DCs [67]. However, their location within the center of the follicle raises the question of how immune complexes reach the FDC network in the first case. Different mechanisms are possible: (i) the non-cognate B cells could capture immune complexes from SCS macrophages before migrating into the follicle and delivering the antigen to FDCs [86], (ii) migrating DCs could deliver antigens to B cells at the junction of the cortex-proximal follicle [67] and (iii) the conduit system could be implied in antigen delivery as it is fully functional in B cell follicles [32]. In 2009, using two-photon microscopy, B cells were shown to capture cognate antigens from FDCs during brief periods but occasionally longer than 30 minutes [87]. Within GCs, immune complexes displayed by FDCs were long suggested to promote antibody affinity maturation by providing a depot of antigens for which newly mutated B cells compete [68]. A study, showed that FDCs could possibly induce apoptosis of B cells in the GC by expressing Fas-ligand [88]. Another way through which FDCs can mediate production of high-affinity antibodies to T-dependent antigens is through the recruitment and interaction with T_{FH}. During an immune response to T-dependent antigen, interaction between B cells and T_{FH} cells expressing receptors specific for the same antigen is required. Migration of T_{FH} was found to rely on expression of CXCR5, promoting their migration towards CXCL13-secreting FDCs [89]. Human FDCs express the nectin-like molecule-5 (Necl-5 or poliovirus receptor PVR) which mediates their interaction with human follicular B cells, carrying its cognate receptor WUCAM (Washington university cell adhesion

molecule) [90]. In addition to its survival function, BAFF is implied in the induction of CD21 and CD23 on B cells [91, 92]. FDCs were found to present periodically arranged immune complexes on their membrane allowing BCR cross-linking (Figure 4.09a) [93]. Along with the expression of the complement receptors C3 and C4 (FDC-M2), CD137 and CD21L, it provides a mechanism of activation of B cells by FDCs to T cell-independent antigen (Figure 4.09b) [93, 94]. Additionally this mechanism is involved in antibody response to T cell-dependent antigen [95]. Recently, CXCL13, mainly produced by FDCs, was found to enhance BCR-mediated B cell activation by promoting membrane ruffling and LFA-1-supported adhesion of B cells [96].
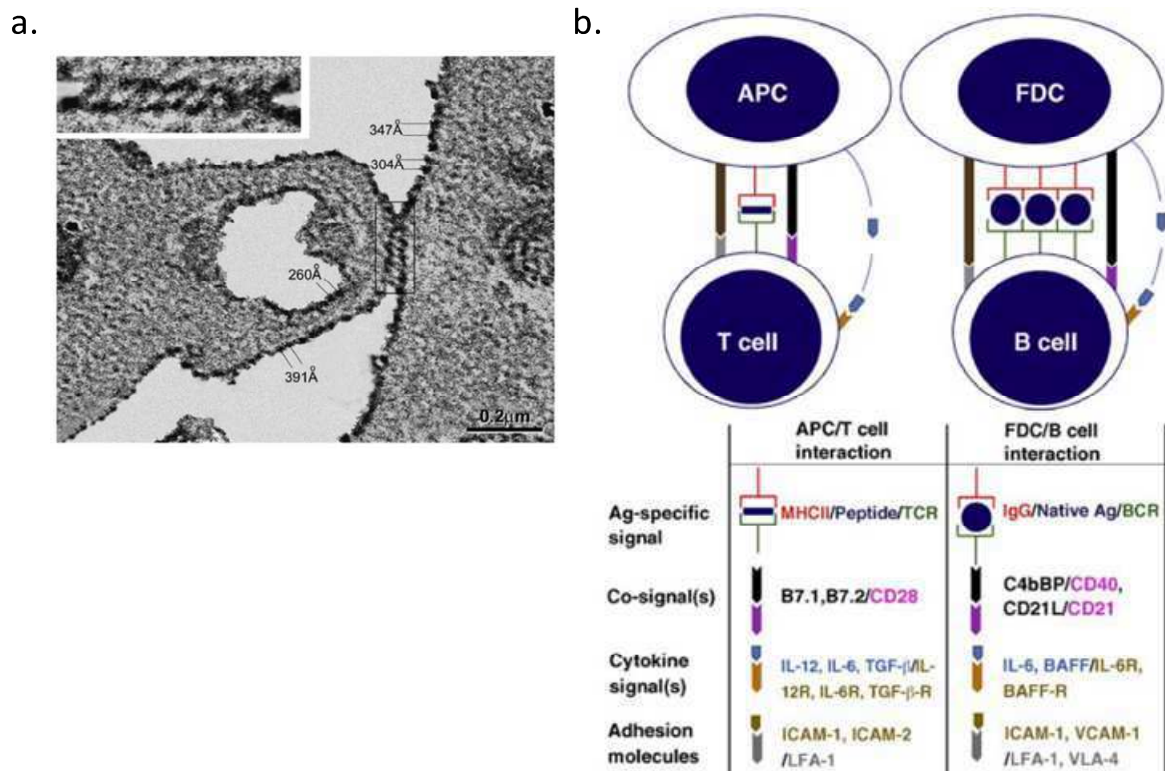
Figure 4.09: Antigen presentation and costimulatory signals delivered by FDCs. (a) EM picture of periodicity of antigen display on purified FDCs incubated with horseradish peroxidase immune complexes. (b) Comparison of antigen-presentation to T and B cells highlighting similarities between them. After reference [97].

4.4. *TNFSF and TNFRSF members in LNs beyond organogenesis*

In addition to their function in LNs development, described in the previous Chapter, TNFSF members play key roles in numerous processes in lymphoid organs of adult animals, including maintenance of the stromal cell types and control of homeostatic chemokines expression.

4.4.1. LTβR and TNFR

Due to the multiple functions of LTβR during embryogenesis and subsequent development defect in knockout models, functions of LTβR in the adult were mainly elicited by using a soluble decoy LTβR (LTβR-Ig) to inhibit both LT- and LIGHT-mediated activation of this receptor. As described in the previous Chapter, gene deletion experiments in mice have shown that signaling through TNF and LT was required for FDC development during embryogenesis. LT expression by multiple cell types in the adult LNs (B, T cells, NK) led to the hypothesis that LTβR was implied in the maintenance of LN architecture. In 1998, Mackay and Browning showed that adult wild-type mice treatment with LTβR-Ig led to the disappearance of multiple markers (FDC-M1, FDC-M2, MAdCAM-1 and CR35) on FDCs within one day [98]. LTβR-Ig treatment prevented the trapping of newly formed immune complexes and also eliminated previously trapped complexes. Accordingly, LTβR-Ig treatment was found to down-regulate CXCL13 expression in LNs [99]. Inhibition of the TNF pathway using a TNFR1-Ig molecule was also found to be efficient but only in the absence of a strong immune response. Hence, TNFR1-Ig treatment associated with sheep red blood cells was inefficient to alter FDC network [98]. FDCs network disruption induced by LTβR-Ig was also reported in non-human primates LNs [100]. Thus, LT and TNF are required for the maintenance of FDC function in the adult. The formation of the FRCs network was also found to rely on contact with lymphocytes and TNF/LT signaling [101]. In targeted knockout mice, it was found that TNF expressed by both B and T cells was necessary for the maintenance of the LN microarchitecture [102]. By treating adult mice with LTβR-Ig, Browning and co-workers also found that cellularity of LNs was reduced as a result of an impaired lymphocyte entry into LNs. LTβR was required to maintain homeostatic levels of PNAd and MAdCAM-1 expression on HEV, ensuring a proper recruitment of lymphocytes into the LNs [99]. In the same study, the authors showed that neither treatment with LTβR-Ig nor TNFR-Ig, modified CCL21 expression in resting or activated LNs. Thus, LN CCL21 does not seem to be under the control of LTβR although it controls expression of this chemokine in the spleen [99]. CCL19 was found to be slightly decreased (<2 fold) upon treatment with LTβR-Ig or TNFR-Ig [99]. LTβ was found to be an important mediator of LNs growth during viral infection [103]. It was reported that in conditional or complete LTβ-deficient mice, which present an altered B cell follicle organization, anti-viral B cell response was not altered. However, impaired response against non-replicating antigens was reported in these models in correlation with the loss of organization of the SLOs [104]. Impaired maturation of antibodies, CD4^{+} T cell responses as well as CD8^{+} T cells responses were reported upon mice treatment with LTβR-Ig [105].

4.4.2. Toward a novel function for RANKL in lymph node ?

- #### RANK in B cell follicle architecture: similarity with LTβR

A striking feature shared by RANK and LTβR, in addition to their requirement for LNs formation, is their importance for proper B cell follicles formation. Many studies showed that LTβR engagement is required for both embryogenic development of B cell follicles and for the maintenance of their architecture in the adult state. Although the importance of RANK in B cell follicles establishment was less studied, some clues let presume a similar role in this process. In the murine model described in 2000 by Kim and co-workers, the authors reported that even if B and T cells segregate into discrete zones in the spleen, the integrity of the B cell follicle is altered in almost 75% of RANKL-knockout mice [106]. Nevertheless, upon immunization of mice with a T cell dependent antigen, normal splenic germinal centers form in RANKL-null mice suggesting that RANKL contributes to but is not essential for the proper formation of B cells follicles in the spleen [106]. In the same study, it was also reported that the occasionally developing cervical LNs in RANKL-deficient mice are small, poorly populated and that B cells fail to form proper follicles in those LNs [106]. In addition, in TRAF-6-knockout embryos, in which RANK signaling is impaired, ectopic application of IL-7 can rescue the development of LNs but the discrete mesenteric LNs recovered present altered B cell follicles [107]. In RANKL-deficient mice, transgenic expression of RANKL by T and B cells is able to restore LNs formation but, again, LNs are poorly populated and B cell follicles architecture defects were observed [106]. Together these data suggest a possible function of RANKL in the formation of B cell follicles. Interestingly, RANKL is known to be expressed in the adult LNs by the MRCs, lining the SCS at B follicle junction [12]. Functional relevance of RANKL expression in this stromal subset is not yet addressed.

- #### RANK in endothelial cell biology

Endothelial cells, whether blood or lymphatic, also belong to the LN stromal cells compartment and play an important role for LN homeostasis under steady state by being implied in cell entry and egress. In addition, these cells are crucial during inflammation. Upon infection, an increase in the blood and lymphatic vasculatures is observed along with a shutdown of lymphocytes egress and an increased recruitment of lymphocytes and DCs leading to the LN hypertrophy [108, 109]. The mechanisms underlying LN hypertrophy remain only poorly defined but TNFSF members are implicated in this process. LTβR is required for HEV homeostasis and function, and lymphangiogenesis [47, 99]. LT was thought to be the ligand required for these functions elicited by LTβR but recently LIGHT was also found to be required for LN hypertrophy during inflammation [110].

88

Chapter 4
RANK, RANKL and OPG in lymph node: from development to homeostasis ?

In 2002, RANKL was shown to induce blood vessels angiogenesis both *in vitro* and *in vivo* through the activation of Src and phospholipase C (PLC) [111]. One year later, another study found that RANK was also expressed by endothelial cells of those vessels [112]. RANKL was found to protect endothelial cells from TNF- and LPS-induced apoptosis *in vitro* and this survival was mediated by the PI3K/Akt pathway activation [112]. Smooth muscle cells, which surround blood vessels, except capillaries and venules, express RANKL in a soluble form, leading to a model in which these cells would deliver the paracrine signal to protect RANK-expressing endothelial cells from apoptosis (Figure 4.10) [112]. OPG was also found to mediate endothelial cells survival through the neutralization of pro-apoptotic TRAIL [113]. OPG is upregulated in endothelial cells through αvβ3 integrin by its ligand osteopontin and by the subsequent NF-κB activation [113, 114]. In addition to their expression of RANK, endothelial cells were found to express OPG and RANKL and smooth vascular muscle cells to express OPG (Figure 4.10) [115]. RANKL induces expression of adhesion molecules, such as ICAM-1 and VCAM-1, on endothelial cells in a NF-κB, PLC, PI3K and PKC dependent mechanism [116]. Thus, RANKL enhances leukocytes adhesiveness to endothelial cells and can function as an inflammatory mediator [116]. Possible functions of RANK and RANKL in lymphatic endothelial cells are unknown but mediators of lymphangiogenesis are released by osteoclasts upon RANKL stimulation. Hence, VEGF-C is expressed by RANK-activated osteoclasts [117]. In addition, VEGF-A is triggered by RANKL by an indirect mechanism implicating HIF-1α (hypoxia-inducible transcription-factor 1α) [118].
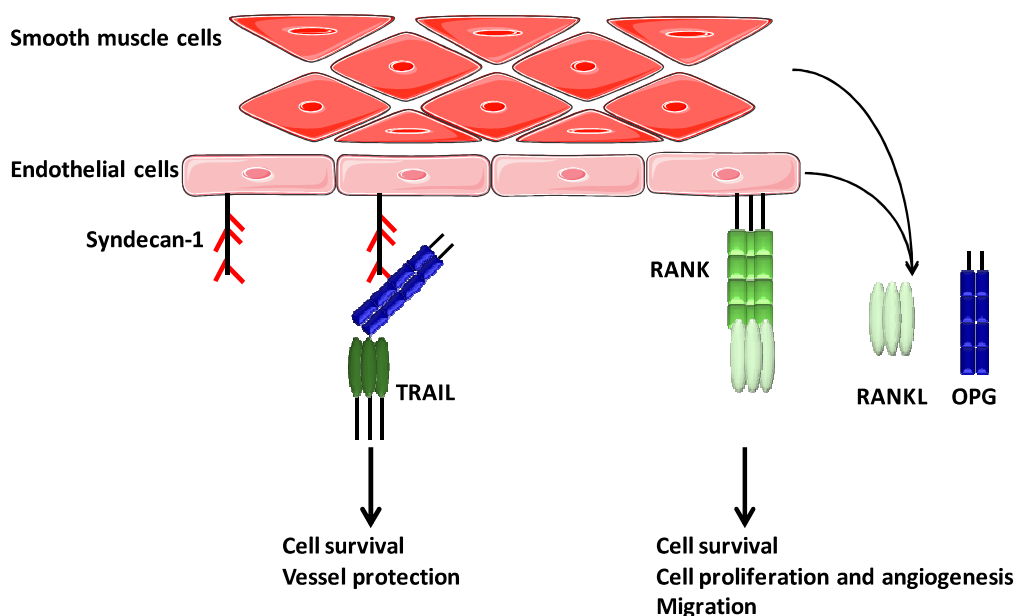
Figure 4.10: RANK, RANKL and OPG in endothelial cell biology. Endothelial cells and smooth muscle cells express and secrete RANKL and OPG. OPG binds syndecan-1 on the surface of endothelial cells and protects cells from TRAIL-induced apoptosis. RANKL binding to RANK induces endothelial cell survival, proliferation and angiogenesis. Modified after reference [119].

Given the similarity between RANK and LTβR during development and possibly in B cell follicles organization, along with the function of RANK in endothelial cell survival and proliferation we addressed the question whether RANK is implied in adult LN organization and homeostasis. To this end we used a murine model over-expressing murine RANK under the control of the human S100A8 (S100 calcium-binding protein A8) promoter active both in the granulo-myeloid lineage and in hair follicle stem cells. This model was developed by Yongwong Choi and displays a massive hyperplasia of skin-draining LNs.

4.5. *Conclusions*

Stromal cells are essential to provide the LN microarchitecture required for this organ to fulfill its function of being an efficient platform for the encounter between lymphocytes and antigens and APCs. After having long been ignored by immunologists, their importance is now arising. The reticular meshwork formed by FRCs can be considered as the LN infrastructure and additionally provide an efficient system for lymph to circulate from the SCS to the HEVs through the conduit system. By the secretion of respectively CCL19 and CCL21, and CXCL13, FRCs and FDCs are crucial for lymphocyte homing and compartmentalization in the LNs. In addition to their contribution to the LN structure and organization, stromal cells fulfill other crucial immunological functions such as survival, proliferation and activation of lymphocytes but also immune peripheral tolerance maintenance. TNFRSF members LTβR and, under some conditions, TNFR1 were found to be required for the maintenance of the microarchitecture of B cells follicles. Evidence of a similar role for RANK has been described but, unlike LTβR, RANK function in the architecture of adult LNs has not been clearly addressed. In the light of the similarities between RANK and LTβR, and the functions of RANK in endothelial cells survival and proliferation, we address the question of a role for RANK in the homeostasis of adult LNs.
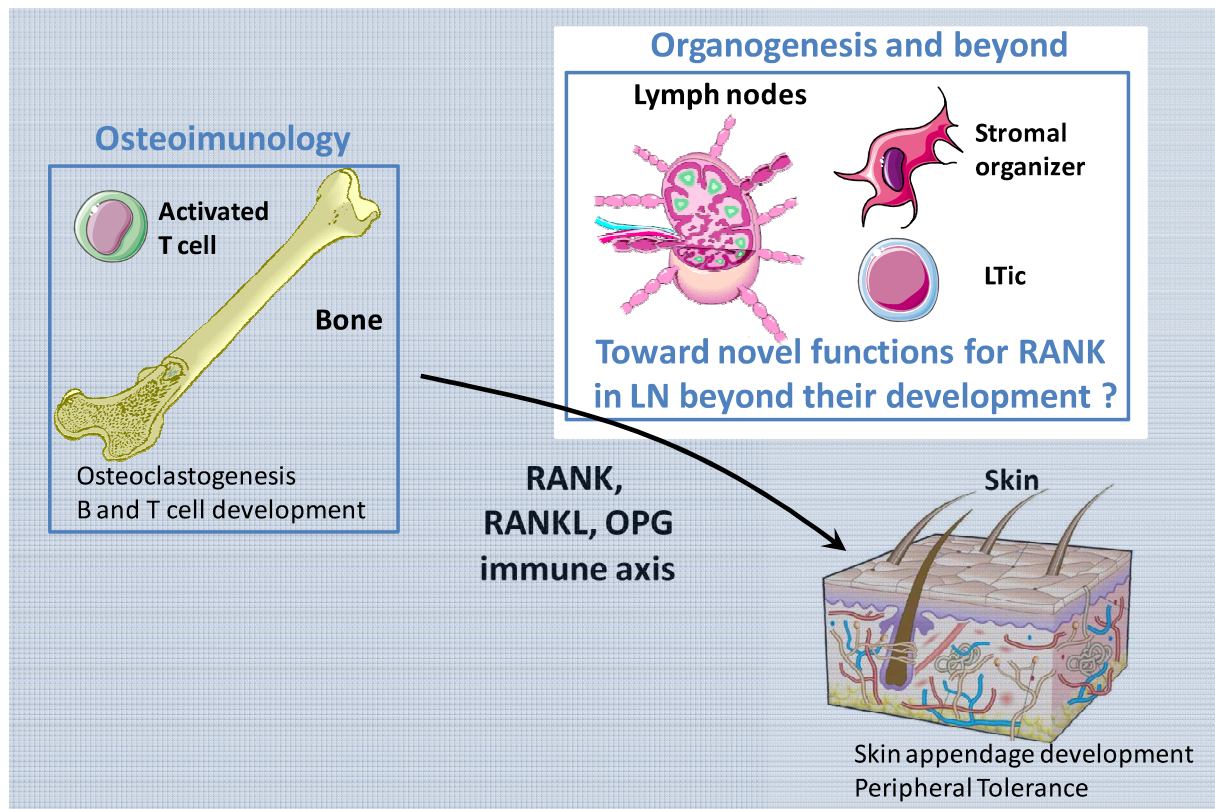
Figure 4.11: The RANK, RANKL and OPG axis: a function beyond LN organogenesis ? RANK, RANKL and OPG are crucial for the organogenesis of LNs, during my thesis we addressed the possible role of RANK in LNs beyond their development.

4.6. *Bibliography*

1.   Mueller, S.N. and R.N. Germain, *Stromal cell contributions to the homeostasis and functionality of the immune system.* Nat Rev Immunol, 2009. **9**(9): p. 618-29.

2.   Junt, T., E. Scandella, and B. Ludewig, *Form follows function: lymphoid tissue microarchitecture in antimicrobial immune defence.* Nat Rev Immunol, 2008. **8**(10): p. 764-75.

3.   Collier, A.Y., J.W. Lee, and S.J. Turley, *Self-encounters of the third kind: lymph node stroma promotes tolerance to peripheral tissue antigens.* Mucosal Immunol, 2008. **1**(4): p. 248-51.

4.   Phan, T.G., E.E. Gray, and J.G. Cyster, *The microanatomy of B cell activation.* Curr Opin Immunol, 2009. **21**(3): p. 258-65.

5.   Lammermann, T. and M. Sixt, *The microanatomy of T-cell responses.* Immunol Rev, 2008. **221**: p. 26-43.

6.   Buettner, M., R. Pabst, and U. Bode, *Stromal cell heterogeneity in lymphoid organs.* Trends Immunol, 2010. **31**(2): p. 80-6.

7.   Munoz-Fernandez, R., et al., *Follicular dendritic cells are related to bone marrow stromal cell progenitors and to myofibroblasts.* J Immunol, 2006. **177**(1): p. 280-9.

8.   van Nierop, K. and C. de Groot, *Human follicular dendritic cells: function, origin and development.* Semin Immunol, 2002. **14**(4): p. 251-7.

9.   Mabbott, N.A., et al., *Expression of mesenchyme-specific gene signatures by follicular dendritic cells: insights from the meta-analysis of microarray data from multiple mouse cell populations.* Immunology, 2011. **3**(10): p. 1365-2567.

10.   Luther, S.A., T.K. Vogt, and S. Siegert, *Guiding blind T cells and dendritic cells: A closer look at fibroblastic reticular cells found within lymph node T zones.* Immunol Lett, 2011. **17**: p. 17.

11.   Cupedo, T., et al., *Induction of secondary and tertiary lymphoid structures in the skin.* Immunity, 2004. **21**(5): p. 655-67.

12.   Katakai, T., et al., *Organizer-like reticular stromal cell layer common to adult secondary lymphoid organs.* J Immunol, 2008. **181**(9): p. 6189-200.

13.   Gretz, J.E., A.O. Anderson, and S. Shaw, *Cords, channels, corridors and conduits: critical architectural elements facilitating cell interactions in the lymph node cortex.* Immunol Rev, 1997. **156**: p. 11-24.

14.   Katakai, T., et al., *A novel reticular stromal structure in lymph node cortex: an immuno-platform for interactions among dendritic cells, T cells and B cells.* Int Immunol, 2004. **16**(8): p. 1133-42.

15.   Glegg, R.E., D. Eidinger, and C.P. Leblond, *Some carbohydrate components of reticular fibers.* Science, 1953. **118**(3073): p. 614-6.

16.   Clark, S.L., Jr., *The reticulum of lymph nodes in mice studied with the electron microscope.* Am J Anat, 1962. **110**: p. 217-57.

17.   Moe, R.E., *Fine structure of the reticulum and sinuses of lymph nodes.* American Journal of Anatomy, 1963. **112**(3): p. 311-335.

18.   Ushiki, T., O. Ohtani, and K. Abe, *Scanning electron microscopic studies of reticular framework in the rat mesenteric lymph node.* Anat Rec, 1995. **241**(1): p. 113-22.

19.   Sixt, M., et al., *The conduit system transports soluble antigens from the afferent lymph to resident dendritic cells in the T cell area of the lymph node.* Immunity, 2005. **22**(1): p. 19-29.

20.   Hayakawa, M., M. Kobayashi, and T. Hoshino, *Direct contact between reticular fibers and migratory cells in the paracortex of mouse lymph nodes: a morphological and quantitative study.* Arch Histol Cytol, 1988. **51**(3): p. 233-40.

21.   Sainte-Marie, G., *The lymph node revisited: development, morphology, functioning, and role in triggering primary immune responses.* Anat Rec (Hoboken), 2010. **293**(2): p. 320-37.

22.   Roozendaal, R., R.E. Mebius, and G. Kraal, *The conduit system of the lymph node.* Int Immunol, 2008. **20**(12): p. 1483-7.

23.   Cervantes-Barragan, L., et al., *Type I IFN-mediated protection of macrophages and dendritic cells secures control of murine coronavirus infection.* J Immunol, 2009. **182**(2): p. 1099-106.

24.   Junt, T., et al., *Subcapsular sinus macrophages in lymph nodes clear lymph-borne viruses and present them to antiviral B cells.* Nature, 2007. **450**(7166): p. 110-4.

25.   Nordmann, M., *Studien an lymphknoten bei akuten und chronischen allgemeininfektionen.* . Virchows Arch. Pathol. Anat., 1928. **267**: p. 158-207.

26.   Gretz, J.E., et al., *Lymph-borne chemokines and other low molecular weight molecules reach high endothelial venules via specialized conduits while a functional barrier limits access to the lymphocyte microenvironments in lymph node cortex.* J Exp Med, 2000. **192**(10): p. 1425-40.

27.   Palframan, R.T., et al., *Inflammatory chemokine transport and presentation in HEV: a remote control mechanism for monocyte recruitment to lymph nodes in inflamed tissues.* J Exp Med, 2001. **194**(9): p. 1361-73.

28.   von Andrian, U.H. and T.R. Mempel, *Homing and cellular traffic in lymph nodes.* Nat Rev Immunol, 2003. **3**(11): p. 867-78.

29.   Itano, A.A., et al., *Distinct dendritic cell populations sequentially present antigen to CD4 T cells and stimulate different aspects of cell-mediated immunity.* Immunity, 2003. **19**(1): p. 47-57.

30.   Iezzi, G., et al., *Lymph node resident rather than skin-derived dendritic cells initiate specific T cell responses after Leishmania major infection.* J Immunol, 2006. **177**(2): p. 1250-6.

31.   Roozendaal, R., et al., *Conduits mediate transport of low-molecular-weight antigen to lymph node follicles.* Immunity, 2009. **30**(2): p. 264-76.

32.   Bajenoff, M. and R.N. Germain, *B-cell follicle development remodels the conduit system and allows soluble antigen delivery to follicular dendritic cells.* Blood, 2009. **114**(24): p. 4989-97.

33.   Balogh, P., V. Fisi, and A.K. Szakal, *Fibroblastic reticular cells of the peripheral lymphoid organs: unique features of a ubiquitous cell type.* Mol Immunol, 2008. **46**(1): p. 1-7.

34.   Blattman, J.N., et al., *Estimating the precursor frequency of naive antigen-specific CD8 T cells.* J Exp Med, 2002. **195**(5): p. 657-64.

35.   Bajenoff, M., et al., *Highways, byways and breadcrumbs: directing lymphocyte traffic in the lymph node.* Trends Immunol, 2007. **28**(8): p. 346-52.

36.   Germain, R.N., et al., *An extended vision for dynamic high-resolution intravital immune imaging.* Semin Immunol, 2005. **17**(6): p. 431-41.

37.   Breart, B. and P. Bousso, *Cellular orchestration of T cell priming in lymph nodes.* Curr Opin Immunol, 2006. **18**(4): p. 483-90.

38.   Bajenoff, M., et al., *Stromal cell networks regulate lymphocyte entry, migration, and territoriality in lymph nodes.* Immunity, 2006. **25**(6): p. 989-1001.

39.   Asperti-Boursin, F., et al., *CCR7 ligands control basal T cell motility within lymph node slices in a phosphoinositide 3-kinase-independent manner.* J Exp Med, 2007. **204**(5): p. 1167-79.

40.   Sobocinski, G.P., et al., *Ultrastructural localization of extracellular matrix proteins of the lymph node cortex: evidence supporting the reticular network as a pathway for lymphocyte migration.* BMC Immunol, 2010. **11**: p. 42.

41.   Castellino, F., et al., *Chemokines enhance immunity by guiding naive CD8+ T cells to sites of CD4+ T cell-dendritic cell interaction.* Nature, 2006. **440**(7086): p. 890-5.

42.   Iwata, M., et al., *Retinoic acid imprints gut-homing specificity on T cells.* Immunity, 2004. **21**(4): p. 527-38.

43.   Hammerschmidt, S.I., et al., *Stromal mesenteric lymph node cells are essential for the generation of gut-homing T cells in vivo.* J Exp Med, 2008. **205**(11): p. 2483-90.

44.   Molenaar, R., et al. *Lymph node stromal cells support dendritic cell-induced gut-homing of T cells.* J Immunol, 2009. **183**(10): p. 6395-402.

45.   Link, A., et al., *Fibroblastic reticular cells in lymph nodes regulate the homeostasis of naive T cells.* Nat Immunol, 2007. **8**(11): p. 1255-65.

Chapter 4

RANK, RANKL and OPG in lymph node: from development to homeostasis ?

93

46.   Thomazy, V.A., et al., *Phenotypic modulation of the stromal reticular network in normal and neoplastic lymph nodes: tissue transglutaminase reveals coordinate regulation of multiple cell types.* Am J Pathol, 2003. **163**(1): p. 165-74.

47.   Chyou, S., et al., *Fibroblast-type reticular stromal cells regulate the lymph node vasculature.* J Immunol, 2008. **181**(6): p. 3887-96.

48.   Kataru, R.P., et al., *T lymphocytes negatively regulate lymph node lymphatic vessel formation.* Immunity, 2011. **34**(1): p. 96-107.

49.   Zhu, M. and Y.X. Fu, *Deflating the lymph node.* Immunity, 2011. **34**(1): p. 8-10.

50.   Tomei, A.A., et al., *Fluid flow regulates stromal cell organization and CCL21 expression in a tissue-engineered lymph node microenvironment.* J Immunol, 2009. **183**(7): p. 4273-83.

51.   Derbinski, J., et al., *Promiscuous gene expression in medullary thymic epithelial cells mirrors the peripheral self.* Nat Immunol, 2001. **2**(11): p. 1032-9.

52.   Lee, J.W., et al., *Peripheral antigen display by lymph node stroma promotes T cell tolerance to intestinal self.* Nat Immunol, 2007. **8**(2): p. 181-90.

53.   Gardner, J.M., et al., *Deletional tolerance mediated by extrathymic Aire-expressing cells.* Science, 2008. **321**(5890): p. 843-7.

54.   Nichols, L.A., et al., *Deletional self-tolerance to a melanocyte/melanoma antigen derived from tyrosinase is mediated by a radio-resistant cell in peripheral and mesenteric lymph nodes.* J Immunol, 2007. **179**(2): p. 993-1003.

55.   Fletcher, A.L., et al., *Lymph node fibroblastic reticular cells directly present peripheral tissue antigen under steady-state and inflammatory conditions.* J Exp Med, 2010. **207**(4): p. 689-97.

56.   Cohen, J.N., et al., *Lymph node-resident lymphatic endothelial cells mediate peripheral tolerance via Aire-independent direct antigen presentation.* J Exp Med, 2010. **207**(4): p. 681-8.

57.   Reynoso, E.D., et al., *Intestinal tolerance is converted to autoimmune enteritis upon PD-1 ligand blockade.* J Immunol, 2009. **182**(4): p. 2102-12.

58.   Choi, Y.K., et al., *Simian immunodeficiency virus dramatically alters expression of homeostatic chemokines and dendritic cell markers during infection in vivo.* Blood, 2003. **101**(5): p. 1684-91.

59.   Mueller, S.N., et al., *Viral targeting of fibroblastic reticular cells contributes to immunosuppression and persistence during chronic infection.* Proc Natl Acad Sci U S A, 2007. **104**(39): p. 15430-5.

60.   Scandella, E., et al., *Restoration of lymphoid organ integrity through the interaction of lymphoid tissue-inducer cells with stroma of the T cell zone.* Nat Immunol, 2008. **9**(6): p. 667-75.

61.   Steele, K.E., A.O. Anderson, and M. Mohamadzadeh, *Fibroblastic reticular cell infection by hemorrhagic fever viruses.* Immunotherapy, 2009. **1**(2): p. 187-97.

62.   Bogdan, C., et al., *Fibroblasts as host cells in latent leishmaniosis.* J Exp Med, 2000. **191**(12): p. 2121-30.

63.   Allen, C.D. and J.G. Cyster, *Follicular dendritic cell networks of primary follicles and germinal centers: phenotype and function.* Semin Immunol, 2008. **20**(1): p. 14-25.

64.   Ansel, K.M., R.B. Harris, and J.G. Cyster, *CXCL13 is required for B1 cell homing, natural antibody production, and body cavity immunity.* Immunity, 2002. **16**(1): p. 67-76.

65.   Kanemitsu, N., et al., *CXCL13 is an arrest chemokine for B cells in high endothelial venules.* Blood, 2005. **106**(8): p. 2613-8.

66.   Ansel, K.M., et al., *A chemokine-driven positive feedback loop organizes lymphoid follicles.* Nature, 2000. **406**(6793): p. 309-14.

67.   Cyster, J.G., *B cell follicles and antigen encounters of the third kind.* Nat Immunol, 2010. **11**(11): p. 989-96.

68.   MacLennan, I.C., *Germinal centers.* Annu Rev Immunol, 1994. **12**: p. 117-39.

69.   Cozine, C.L., K.L. Wolniak, and T.J. Waldschmidt, *The primary germinal center response in mice.* Curr Opin Immunol, 2005. **17**(3): p. 298-302.

70.   Cyster, J.G., et al., *Follicular stromal cells and lymphocyte homing to follicles.* Immunol Rev, 2000. **176**: p. 181-93.

71.   Schwickert, T.A., et al., *In vivo imaging of germinal centres reveals a dynamic open structure.* Nature, 2007. **446**(7131): p. 83-7.

72.   Beltman, J.B., et al., *B cells within germinal centers migrate preferentially from dark to light zone.* Proc Natl Acad Sci U S A, 2011. **108**(21): p. 8755-60.

73.   Husson, H., et al., *Functional effects of TNF and lymphotoxin alpha1beta2 on FDC-like cells.* Cell Immunol, 2000. **203**(2): p. 134-43.

74.   Gorelik, L., et al., *Normal B cell homeostasis requires B cell activation factor production by radiation-resistant cells.* J Exp Med, 2003. **198**(6): p. 937-45.

75.   Rahman, Z.S., et al., *Normal induction but attenuated progression of germinal center responses in BAFF and BAFF-R signaling-deficient mice.* J Exp Med, 2003. **198**(8): p. 1157-69.

76.   Darce, J.R., et al., *Divergent effects of BAFF on human memory B cell differentiation into Ig-secreting cells.* J Immunol, 2007. **178**(9): p. 5612-22.

77.   Park, C.S. and Y.S. Choi, *How do follicular dendritic cells interact intimately with B cells in the germinal centre?* Immunology, 2005. **114**(1): p. 2-10.

78.   Li, L., et al., *Identification of a human follicular dendritic cell molecule that stimulates germinal center B cell growth.* J Exp Med, 2000. **191**(6): p. 1077-84.

79.   Zhang, X., et al., *The distinct roles of T cell-derived cytokines and a novel follicular dendritic cell-signaling molecule 8D6 in germinal center-B cell differentiation.* J Immunol, 2001. **167**(1): p. 49-56.

80.   Li, L., et al., *Novel follicular dendritic cell molecule, 8D6, collaborates with CD44 in supporting lymphomagenesis by a Burkitt lymphoma cell line, L3055.* Blood, 2004. **104**(3): p. 815-21.

81.   Yoon, S.O., et al., *Notch ligands expressed by follicular dendritic cells protect germinal center B cells from apoptosis.* J Immunol, 2009. **183**(1): p. 352-8.

82.   Park, C.S., et al., *Follicular dendritic cells produce IL-15 that enhances germinal center B cell proliferation in membrane-bound form.* J Immunol, 2004. **173**(11): p. 6676-83.

83.   Kopf, M., et al., *Interleukin 6 influences germinal center development and antibody production via a contribution of C3 complement component.* J Exp Med, 1998. **188**(10): p. 1895-906.

84.   Nossal, G.J., G.L. Ada, and C.M. Austin, *Antigens in Immunity. Iv. Cellular Localization of 125-I- and 131-I-Labelled Flagella in Lymph Nodes.* Aust J Exp Biol Med Sci, 1964. **42**: p. 311-30.

85.   Carroll, M.C., *The role of complement and complement receptors in induction and regulation of immunity.* Annu Rev Immunol, 1998. **16**: p. 545-68.

86.   Phan, T.G., et al., *Subcapsular encounter and complement-dependent transport of immune complexes by lymph node B cells.* Nat Immunol, 2007. **8**(9): p. 992-1000.

87.   Suzuki, K., et al., *Visualizing B cell capture of cognate antigen from follicular dendritic cells.* J Exp Med, 2009. **206**(7): p. 1485-93.

88.   Hur, D.Y., et al., *Role of follicular dendritic cells in the apoptosis of germinal center B cells.* Immunol Lett, 2000. **72**(2): p. 107-11.

89.   Hardtke, S., L. Ohl, and R. Forster, *Balanced expression of CXCR5 and CCR7 on follicular T helper cells determines their transient positioning to lymph node follicles and is essential for efficient B-cell help.* Blood, 2005. **106**(6): p. 1924-31.

90.   Boles, K.S., et al., *A novel molecular interaction for the adhesion of follicular CD4 T cells to follicular DC.* Eur J Immunol, 2009. **39**(3): p. 695-703.

91.   Gorelik, L., et al., *Cutting edge: BAFF regulates CD21/35 and CD23 expression independent of its B cell survival function.* J Immunol, 2004. **172**(2): p. 762-6.

92.   Hase, H., et al., *BAFF/BLyS can potentiate B-cell selection with the B-cell coreceptor complex.* Blood, 2004. **103**(6): p. 2257-65.

93.   Aydar, Y., et al., *The influence of immune complex-bearing follicular dendritic cells on the IgM response, Ig class switching, and production of high affinity IgG.* J Immunol, 2005. **174**(9): p. 5358-66.

94.   Pauly, S., et al., *CD137 is expressed by follicular dendritic cells and costimulates B lymphocyte activation in germinal centers.* J Leukoc Biol, 2002. **72**(1): p. 35-42.

95.   El Shikh, M.E., et al., *T-independent antibody responses to T-dependent antigens: a novel follicular dendritic cell-dependent activity.* J Immunol, 2009. **182**(6): p. 3482-91.

96.   Saez de Guinoa, J., et al., *CXCL13/CXCR5 signaling enhances B-cell receptor-triggered B-cell activation by shaping cell dynamics.* Blood, 2011. **9**: p. 9.

97.   El Shikh, M.E., et al., *Activation of B cells by antigens on follicular dendritic cells.* Trends Immunol, 2010. **31**(6): p. 205-11.

98.   Mackay, F. and J.L. Browning, *Turning off follicular dendritic cells.* Nature, 1998. **395**(6697): p. 26-7.

99.   Browning, J.L., et al., *Lymphotoxin-beta receptor signaling is required for the homeostatic control of HEV differentiation and function.* Immunity, 2005. **23**(5): p. 539-50.

100.   Gommerman, J.L., et al., *Manipulation of lymphoid microenvironments in nonhuman primates by an inhibitor of the lymphotoxin pathway.* J Clin Invest, 2002. **110**(9): p. 1359-69.

101.   Katakai, T., et al., *Lymph node fibroblastic reticular cells construct the stromal reticulum via contact with lymphocytes.* J Exp Med, 2004. **200**(6): p. 783-95.

102.   Tumanov, A.V., et al., *Cellular source and molecular form of TNF specify its distinct functions in organization of secondary lymphoid organs.* Blood, 2010. **116**(18): p. 3456-64.

103.   Kumar, V., et al., *Global lymphoid tissue remodeling during a viral infection is orchestrated by a B cell-lymphotoxin-dependent pathway.* Blood, 2010. **115**(23): p. 4725-33.

104.   Junt, T., et al., *Expression of lymphotoxin beta governs immunity at two distinct levels.* Eur J Immunol, 2006. **36**(8): p. 2061-75.

105.   McCarthy, D.D., et al., *The lymphotoxin pathway: beyond lymph node development.* Immunol Res, 2006. **35**(1-2): p. 41-54.

106.   Kim, D., et al., *Regulation of peripheral lymph node genesis by the tumor necrosis factor family member TRANCE.* J Exp Med, 2000. **192**(10): p. 1467-78.

107.   Yoshida, H., et al., *Different cytokines induce surface lymphotoxin-alphabeta on IL-7 receptor-alpha cells that differentially engender lymph nodes and Peyer's patches.* Immunity, 2002. **17**(6): p. 823-33.

108.   Soderberg, K.A., et al., *Innate control of adaptive immunity via remodeling of lymph node feed arteriole.* Proc Natl Acad Sci U S A, 2005. **102**(45): p. 16315-20.

109.   Schwab, S.R. and J.G. Cyster, *Finding a way out: lymphocyte egress from lymphoid organs.* Nat Immunol, 2007. **8**(12): p. 1295-301.

110.   Zhu, M., et al., *LIGHT Regulates Inflamed Draining Lymph Node Hypertrophy.* J Immunol, 2011. **186**(12): p. 7156-63.

111.   Kim, Y.M., et al., *TNF-related activation-induced cytokine (TRANCE) induces angiogenesis through the activation of Src and phospholipase C (PLC) in human endothelial cells.* J Biol Chem, 2002. **277**(9): p. 6799-805.

112.   Kim, H.H., et al., *RANKL regulates endothelial cell survival through the phosphatidylinositol 3'-kinase/Akt signal transduction pathway.* Faseb J, 2003. **17**(14): p. 2163-5.

113.   Pritzker, L.B., M. Scatena, and C.M. Giachelli, *The role of osteoprotegerin and tumor necrosis factor-related apoptosis-inducing ligand in human microvascular endothelial cell survival.* Mol Biol Cell, 2004. **15**(6): p. 2834-41.

114.   Malyankar, U.M., et al., *Osteoprotegerin is an alpha vbeta 3-induced, NF-kappa B-dependent survival factor for endothelial cells.* J Biol Chem, 2000. **275**(28): p. 20959-62.

115.   Collin-Osdoby, P., *Regulation of vascular calcification by osteoclast regulatory factors RANKL and osteoprotegerin.* Circulation Research, 2004. **95**(11): p. 1046-1057.

116.   Min, J.K., et al., *TNF-related activation-induced cytokine enhances leukocyte adhesiveness: induction of ICAM-1 and VCAM-1 via TNF receptor-associated factor and protein kinase C-dependent NF-kappaB activation in endothelial cells.* J Immunol, 2005. **175**(1): p. 531-40.

117. Zhang, Q., et al., *VEGF-C, a lymphatic growth factor, is a RANKL target gene in osteoclasts that enhances osteoclastic bone resorption through an autocrine mechanism.* J Biol Chem, 2008. **283**(19): p. 13491-9.

118. Trebec-Reynolds, D.P., et al., *VEGF-A expression in osteoclasts is regulated by NF-kappaB induction of HIF-1alpha.* J Cell Biochem, 2010. **110**(2): p. 343-51.

119. Baud'huin, M., et al., *RANKL, RANK, osteoprotegerin: key partners of osteoimmunology and vascular diseases.* Cell Mol Life Sci, 2007. **64**(18): p. 2334-50.

Chapter 5:
RANK, RANKL and OPG: new possible functions in the skin and in its appendages

5.1. *Skin and skin appendages*

5.1.1. *Skin structure*

The skin is implicated in numerous functions: (i) it is a protection against external physical, chemical and biological aggressions, (ii) it ensures a sensor activity due to the presence of numerous nervous fibers, (iii) it regulates the body temperature with its sweat gland and (iv) it has a metabolical role with triglycerides storage. The skin is a highly vascularized tissue composed of three morphologically distinct layers: the epidermis, the dermis and the hypodermis (Figure 5.01a).
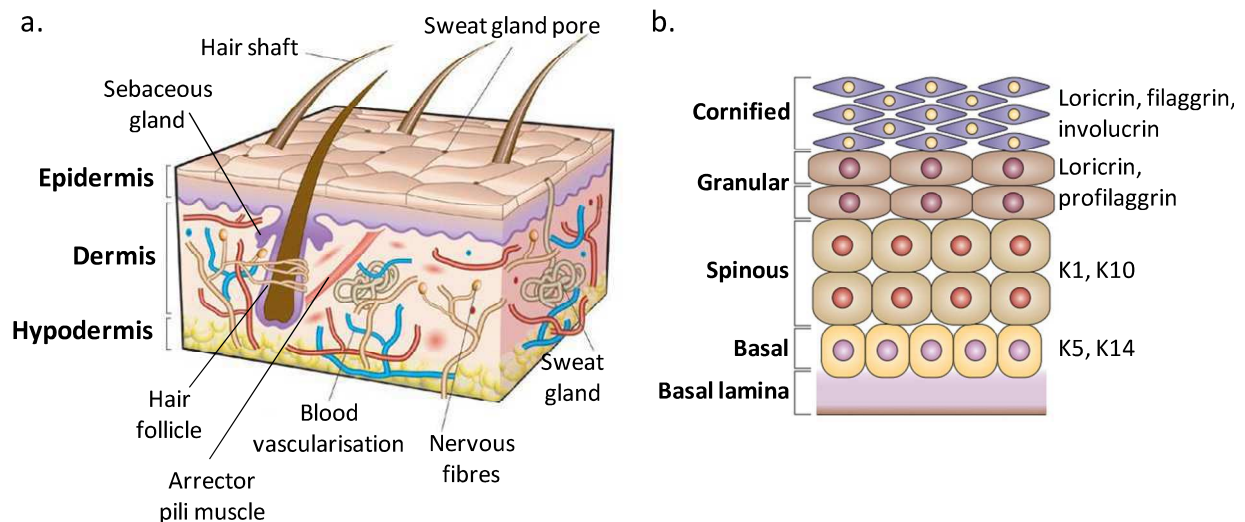
Figure 5.01: Schematic representation of skin and epidermal organizations. (a) General organization of the skin into three layers: epidermis, dermis and hypodermis. (b) Schematic organization of keratinocyte layers in the epidermis, specific proteins expressed as a function of the cell differentiation are depicted at the right (K stands for keratin). Modified after reference [1].

- *Epidermis*

The epidermis is a continually renewing, stratified, squamous epithelium, mostly composed of keratinocytes. According to their differentiation stage, epidermal keratinocytes are arranged into four different layers: basal, spinous, granular and cornified layers (Figure 5.01b). Epidermal proliferation needs to be strictly regulated both temporally and spatially to avoid loss of epidermal integrity or uncontrolled growth leading to a hyperproliferative state and tumorigenesis. In the epidermis, keratinocytes of the basal layer are the most undifferentiated cells, with the highest capacity to proliferate. More than 30 years ago has emerged the concept of an epidermal proliferating unit (EPU), which is composed of a central stem cell in the epidermal basal layer that gives rise to surrounding

transient amplifying cells. Transient amplifying cells undergo a limited number of divisions in the basal layer before they differentiate [2]. According to this concept, the epidermal basal layer could be schematically represented as a mosaic of clonal units consisting of around 20 cells [2]. In addition to these EPUs, lineage analysis has provided evidence for the existence of much larger clonal epidermal units, consisting of hundreds to thousands of cells derived from multiple classes of epidermal progenitors [3]. Thus, stem cells in the epidermis have a crucial role in maintaining tissue homeostasis by providing new cells to replace those that are constantly lost during tissue turnover or following injury. During normal epidermal homeostasis, the stem cells pool present in the skin remains constant as a result of asymmetrical division, during which a stem cell gives rise to two daughter cells, one remaining a stem cell and the other one becoming committed to differentiation [4].

After leaving the basal layer, keratinocytes start an uninterrupted differentiation process of morphological and biochemical changes, culminating in the production of dead, flattened, enucleated squames [5]. During these differentiation stages keratinocytes can be identified by specific markers (Figure 5.01b). Intracytoplasmic filaments of keratin 5 (K5) and K14 expressed by keratinocytes of the basal layer, are replaced by K1 and K10 in the spinous layer. Subsequently, keratinocytes further progress into the epidermis and join the granular layer. This migration is associated with the expression of loricrin and profilaggrin, proteins implicated in the aggregation of the keratin filaments, thus cell collapse with destruction of organelles and cell flattening. At the interface between granular and cornified layers, terminal differentiation occurs, during which the viable cells are transformed into dead keratin-filled cells, the corneocytes. In corneocytes, profilaggrin is conversed into filaggrin by proteolysis and together with the expression of another structural protein, involucrin, it further reinforces the cornified envelope. Corneocytes are embedded in lipids and form a structure often compared to a brick wall, turning the layer into an impenetrable barrier against pathogens, water loss and ultraviolet irradiation [1, 5].

Langerhans cells are located in the spinous layer and thus form a surveillance network covering the body (Figure 5.02). In addition to these resident DCs, γδ-T cells are another immune cell type found in the epidermis, mostly in the basal layer [6, 7]. Melanocytes localize to the basal layer, where they synthesize melanin which is subsequently transferred through melanosomes to adjacent keratinocytes to protect them from ultraviolet light [6]. In the basal layer reside also the Merkel cells, which are associated with nervous fibers and required for tactile discrimination of shape and textures [8]. Although the general organization of the mouse epidermis closely resembles that of humans, it should be noted that no melanocytes are found in the basal layer and that the epidermis is thinner [9].
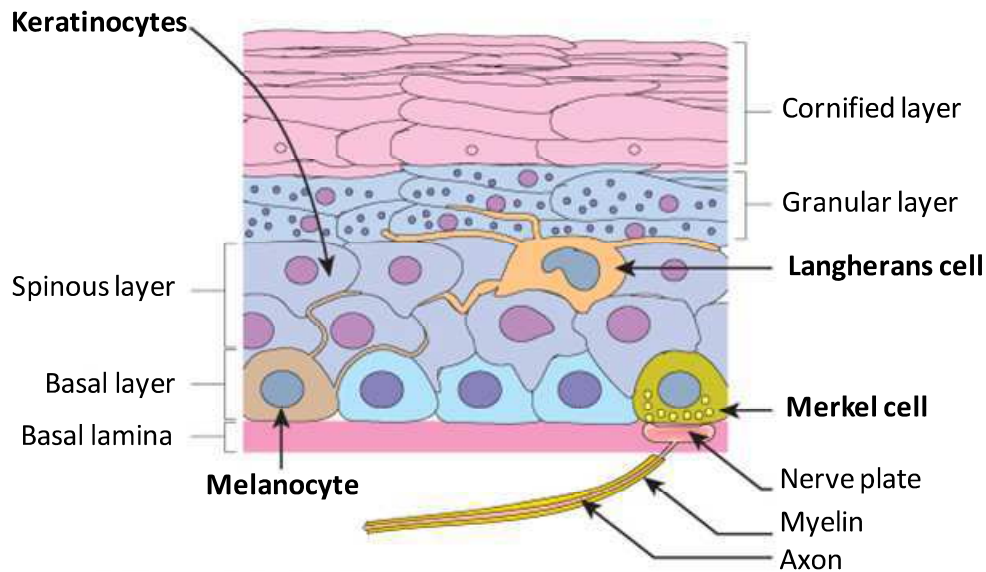
Figure 5.02: Cell type distribution in the epidermis. Schematic representation of cell type organization in the human epithelium. After reference [10].

- *Dermis*

The dermis is organized in two different layers: the superficial or papillary dermis and the deep or reticular dermis (Figure 5.03). The superficial dermis lies just beneath the epidermis and is rich in fibroblasts, vessels, nerve endings and contains collagen fibers and thin elastic fibers. The reticular dermis comprises fewer cells but thicker collagen and elastic fibers. Space between fibers and dermal cells is filled with macromolecules named ground substance consisting of glycoproteins and proteoglycans [6]. The fibroblasts are the main cells of the dermis, they synthesize all types of fibers, the ground substance and release soluble factors such as cytokines or growth factors.

The epidermis is connected to the dermis by the dermal-epidermal junction, which is a complex basement membrane synthesized by basal keratinocytes and dermal fibroblasts. It plays a fundamental role as mechanical support for adhesion of the epidermis to the dermis and regulates exchanges of metabolic products between these two compartments [6].

Dermal immune cells are mostly composed of DCs, macrophages, mastocytes and memory T cells. Dermal DCs are present around vessels of the reticular dermis, in the subcutaneous fat, around sweat glands and in the papillary dermis. They lack the Birbeck granules and exhibit monocyte-macrophage markers, thus they are thought to be involved more in phagocytosis than in antigen presentation. Mast cells are specialized secretory cells releasing mediators, growth factors and other soluble molecules. They modulate skin inflammation, particularly in the context of allergy. They are localized near the dermal-epidermal junction and alongside hair follicles. In addition, it was recently found that γδ-T cells are also present in the dermis [11]. Moreover, as the dermis is highly vascularized, other immune cells like leukocytes can rapidly infiltrate the skin during inflammation [5, 6].

In addition to immune cells, specialized structures like hair follicles and sweat glands are found mainly located in the dermis and connected to the epidermal surface. These structures are referred to as skin appendages (Figure 5.01a) [6].
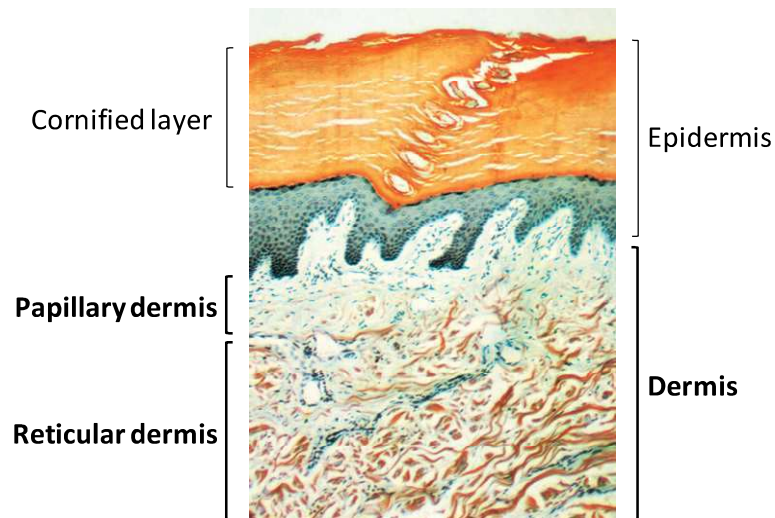
Figure 5.03: Histomorphology of the dermis of the thick skin on the sole of the foot. The pale staining papillary layer of the dermis contains fin collagen fibril bundles, compared to the thick bundles of collagen (light orange) in the underneath reticular dermis. Note in the thick orange cornified layer the profile of a sweat duct spiraling towards the surface (vertical section, trichrome-stained). After reference [10].

- *Hypodermis*

The hypodermis, also called subcutis, is a highly vascularized fatty tissue lying beneath the reticular dermis and containing adipocytes. It plays an important role in thermoregulation, as a provision of energy and for protection from mechanical injuries [5, 6].

5.1.2. The hair follicle: a skin appendage

- *Hair follicle structure*

The hair follicle (HF) is a complex miniorgan of the skin, which constitutes the pilosebaceous unit together with its associated structures, the sebaceous gland, the apocrine gland and the arrector pili muscle (Figure 5.01a). The sebaceous glands are made of a cluster of sebocytes associated with a sebaceous duct opening in the HF. Sebocytes produce lipid droplet, which are released upon cell disintegration, providing a hydrophobic protection against over-wetting and heat insulation. The apocrine gland is a sweat gland, which like the sebaceous gland, is associated with a duct opening in the HF. Sweat gland are usually described as dermal "balls" of spiraling tubular element (Figure 5.03), and are implied in the regulation of body temperature and toxins excretion.

HF morphogenesis occurs during embryonic life, so that mammals are born with a fixed number of HFs. The structure of a newly formed HF is depicted in Figure 5.04.
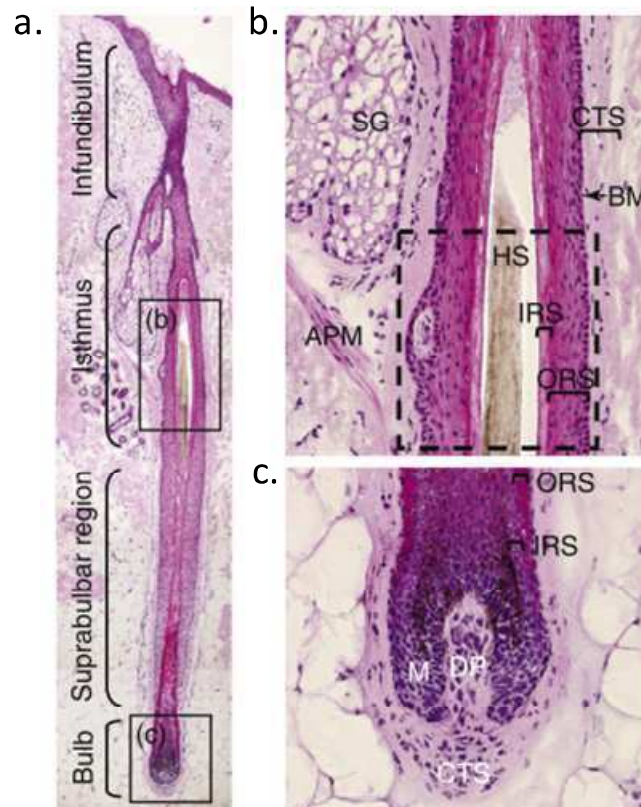
Figure 5.04: Histomorphology of the HF. (a) Sagittal section through a human scalp HF in anagen showing the different parts of the HF. (b) Higher magnification of the isthmus with the approximative localization of the bulge indicated by the dashed square. (c) Higher magnification of the bulb. Abbreviations: APM, arrector pili muscle; BM, basal membrane; CTS, connective tissue sheath; DP, dermal papilla; HS, hair shaft; IRS, inner root sheath; M, matrix; ORS, outer root sheath; SG, sebaceous gland. After reference [12].

The upper part of the HF is composed of the infundibulum and the isthmus. The infundibulum is the opening of the hair canal to the skin surface and is marked by the insertion of the sebaceous gland duct. At the end of the isthmus can be found the arrector pili muscle and a small region harbouring epithelial and melanocytic HF stem cells referred as the bulge. A full length HF can be viewed as a multicylindric structure composed of several layers, such as the inner and the outer root sheath (IRS and ORS) and the connective tissue sheath (CTS), that surround the hair shaft in its centre (Figure 5.04b). The lower part of the HF, just beneath the bulge, comprises the bulb and the suprabulbar region. The bulb contains the proliferating matrix keratinocytes, the melanocytes and the dermal papilla, which consists of a small cluster of densely packed fibroblasts (Figure 5.04c) [12].

- *Hair follicle cycle*

While the infundibulum and the isthmus will remain as permanent structures, the lower part of the HF will be continuously remodeled throughout life (Figure 5.05) [9].
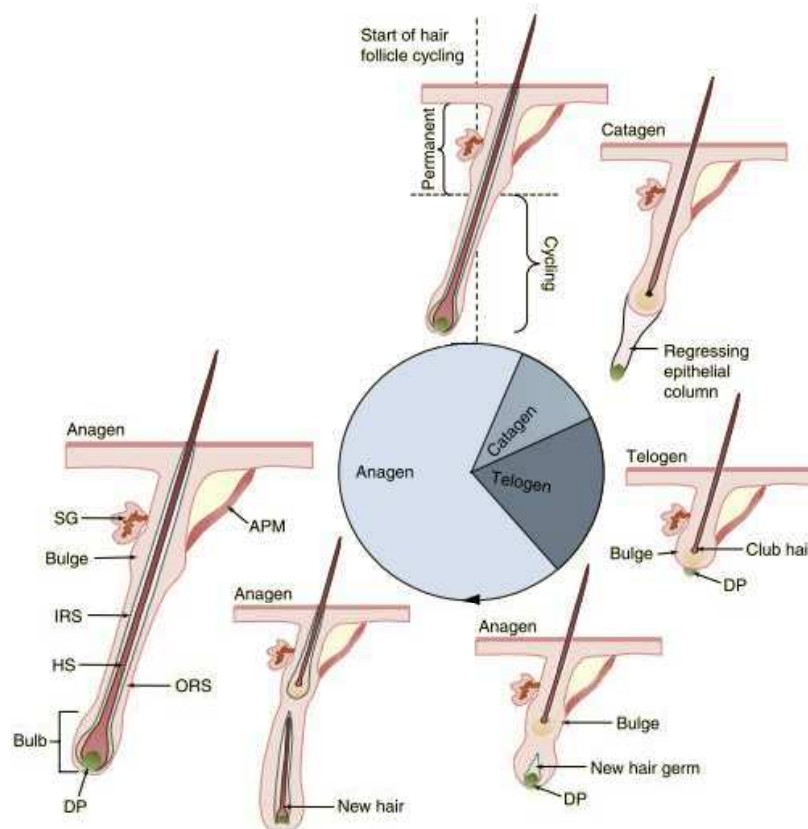
Figure 5.05: Key stages of the hair follicle cycle. Schematic representation of the three stages of follicular cycling: catagen (regressing), telogen (resting) and anagen (growing). Abbreviations: DP, dermal papilla; ORS, outer root sheath; IRS, inner root sheath; HS, hair shaft; SG, sebaceous gland; APM, arrector pili muscle. Modified after reference [12].

This remodeling occurs through a cycle of phases of rapid growth (anagen), followed by relative quiescence (telogen) and apoptosis-driven regression (catagen) [9]. In mice, at around postnatal day 15 (P15), HF morphogenesis is completed and HF cycling is initiated. At this time, HF enters catagen, a phase of rapid organ involution, which lasts two to three days. During this phase the lower two-thirds of the HF regress as a result of apoptosis of the majority of the follicular keratinocytes, without affecting the bulge and the dermal papilla. The few other cells that survive this apoptotic process form a structure referred to as the secondary hair germ [13]. In mice, the old hair shaft (club hair) remains in its canal during several cycles, thereby contributing to the density of the coat. Towards the end of catagen, the dermal papilla condenses and moves upward to rest underneath the bulge. The molecular interaction between dermal papilla and stem cells is essential to form a new hair follicle. After catagen, a resting phase takes place, in which the HF entirely resides in the upper dermis and no more in the hypodermis. The first real growth phase of the HF cycle occurs around four weeks after birth, when a critical concentration of hair growth signals is reached. Although the bulge and the β-catenin protein are known to be important for anagen induction, the complete mechanism is far from being understood. The earliest changes during anagen are observed in the dermal papilla and the secondary hair germ. Then, hair matrix keratinocytes, which represent transient amplifying cells

derived from epithelial hair follicle stem cells in the bulge, proliferate intensively, thereby enclosing the dermal papilla to form an anagen bulb and then differentiate into the distinct epithelial hair lineages. The anagen bulb moves downwards through the dermis and reaches the hypodermis. In contrast with the continuous melanogenesis of the epidermis, hair bulb melanocyte activity is coupled to the anagen phase, thus anagen development is associated with characteristic changes in skin pigmentation. While the first HF cycle is fully synchronized in mice, asynchrony occurs for the second cycle due to different telogen duration, and will become more and more pronounced with accumulation of renewal cycles [9, 12, 14-16].

5.1.3. *Mammary gland and tooth: other skin appendages*

In addition to the HFs described above, other skin appendages exist such as feathers or nails, or more surprisingly teeth and mammary glands. Although fully formed skin appendages vary considerably in form and function, their early stages of development are notably similar both morphologically and molecularly (Figure 5.06) [17]. This developmental link is exemplified in human syndromes known as ectodermal dysplasias, which are a large group of congenital disorders characterized by lack or dysfunctions of at least two skin appendages. Frequent symptoms associated with this pathology are sparse hair, presence of only few conical teeth, absent or reduced sweating, and an altered lactation for females [18].
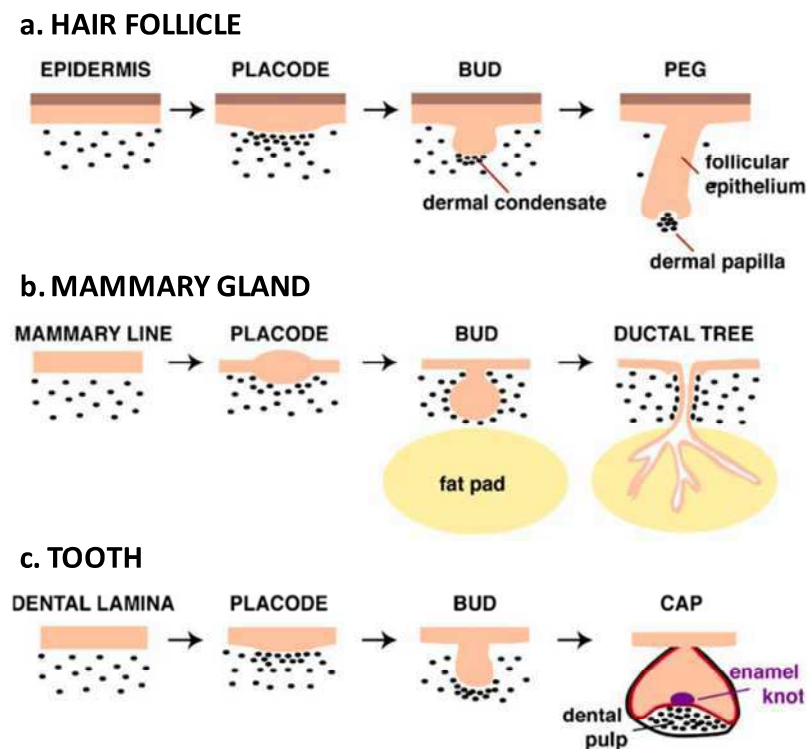
Figure 5.06: Schematic representation of embryonic development of skin appendages. Key stages of hair follicle (a), mammary gland (b) and tooth (c) embryonic development are depicted. Black ovals represent mesenchymal cells, pink and brown structures represent epithelial cells. After reference [17].

During embryogenesis skin appendage development is induced by close interaction between ectodermal epithelium and mesenchyme, originating either from the mesoderm (mammary gland and HF formation) or from the neural crest (teeth formation). The first common step of development is a local epithelial thickening referred to as placode, associated with condensation of the underlying mesenchyme. Restricted to the newly formed placode, is found the expression of different growth factor families, such as Wnts, fibroblasts growth factors (FGFs), bone morphogenetic proteins (BMPs), transforming growth factor-β (TGF-β), and Hedgehogs (Hh) proteins [17]. Hence the different skin appendages share the same factors for their development. The next common step is invagination of the placode into the mesenchyme, thereby forming a bud. It is only in the following stages of morphogenesis and differentiation that anatomical differences between the organs will appear. In the case of HFs, a cluster of mesenchymal cells, referred to as dermal condensate, is formed beneath the bud (Figure 5.06a). Reciprocal signaling from the dermal condensate to the epithelium results in the proliferation of epithelial cells into the dermis, thereby forming a hair germ. This hair germ elongates and surrounds the dermal condensate, which will then form the dermal papilla. The follicular epithelium subsequently differentiates to form the concentric layers of the HF [9, 14, 17]. After bud formation of the developing mammary gland, epithelial cells begin to proliferate and each bud extends through the mesenchyme forming a small ductal tree emanating from the nipple. In male embryos, the mammary buds become separated from the ectodermal surface under the influence of fetal androgens and eventually degenerate. In female embryos, this mammary epithelium invades a pad of fatty tissue called the mammary fat pad, and forms a small, branched ductal network in the proximal corner of the fat pad (Figure 5.06b) [17, 19]. The last skin appendage discussed here, e.g. the teeth, undergoes more complex morphogenesis stages. After placode invagination, cells at the tip of the bud form the primary enamel knot, an aggregate of cells that control the shape of the tooth crown (Figure 5.06c) [20]. The dental epithelium surrounding the enamel knot proliferates into a cap-shaped structure, that envelopes mesenchymal cells forming the dental papilla that will later give rise to dentin-secreting odontoblasts and tooth pulp [20-22]. Subsequently, the enamel knot dies by apoptosis and epithelial cells differentiate into tooth-specific structures: outer enamel epithelium, stellate reticulum, stratum intermedium, and inner enamel epithelium. Secondary enamel knots form, marking the future teeth cusps, thereby patterning the tooth crown [20-22].

5.2. *TNF family members in skin appendage development*

As mentioned above, several important growth factor families are necessary for skin appendages development, among which are Wnts, FGFs, BMPs, TGF-β and Hedgehog proteins. In addition to these proteins, an increasing attention is now given to members of the TNF family.

5.2.1. *The Eda pathway*

Only one year before OPG was cloned, Kere and co-workers reported the identification of the gene mutated in human X-linked anhidrotic ectodermal dysplasia (EDA), which is the most common form of ectodermal dysplasia [18, 23]. This X-linked EDA gene is mutated in 90% of cases. Investigations into the rarer recessive and dominant autosomal inheritance led to the discovery of a new TNF ligand/receptor/adaptor family: EDA, EDAR (EDA receptor) and EDARADD (EDAR associated death domain) [23-26]. The EDA transcripts undergo alternative splicing and only the two longest isoforms, EDA-A1 and EDA-A2 are functional [27]. Although these two isoforms differ only by insertion of two amino acids in their TNF domain, they engage two different receptors: EDAR is specific for EDA-A1 whereas XEDAR (X-linked EDA-A2 receptor) binds EDA-A2 [27]. Signalling through XEDAR seems dispensable for skin appendage development as XEDAR-knockout mice show no phenotype similar to that displayed by the Tabby mice, deficient for *EDA* [27]. EDAR activation upon engagement by soluble trimeric EDA leads to the recruitment of its specific adaptor, EDARADD (Figure 5.07). Interaction between these two proteins is mediated by DD (death domain) present in both proteins, nevertheless apoptosis induction by this motif has not yet been demonstrated [28].
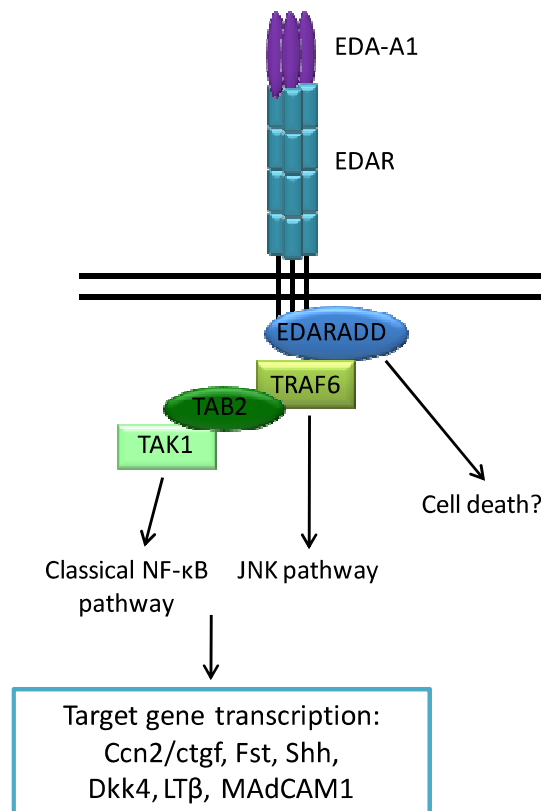
Figure 5.07: Schematic representation of the EDA-A1/EDAR signal transduction pathways. Molecular cascades leading to NF-κB and JNK pathway activation is depicted. EDA signaling positively activates Shh and LTβ, but exerts a negative feedback on Wnt through pathway specific antagonists (Ccn2/ctgf, Fst, Dkk4). Abbreviations: Ccn2/ctgf, connective tissue growth factor, Fst, follistatin, Shh, sonic hedgehog homolog, Dkk4, Dickkopf-4, LTβ, lymphotoxin β, MAdCAM1, Mucosal vascular addressin cell adhesion molecule 1. Modified after reference [28].

EDARADD recruits TRAF6 and the adaptor protein TAB2 together with TAK1, leading to the activation of the classical NF-κB pathway, similarly to the molecular cascade triggered by RANK [27]. Mutations in EDA, EDAR, EDARADD, TRAF6, IKKγ, I-κBα, RelA or cRel lead to similar skin appendage defects in either man or mice [28]. Even if the downstream effectors of EDA take large place in immune and inflammatory processes, the localized skin appendage expression of EDAR and EDARADD avoids immunodeficiency in patient suffering anhidrotic ectodermal dysplasia. In addition to the NF-κB pathway, the JNK pathway is also induced by EDAR and together these pathways lead to the expression of several target genes (Figure 5.07).

As the phenotype of patients suffering EDA suggests, these TNF family members are crucial for the development of all skin appendages. In addition to sparse hair, few conically shaped teeth and altered sweat gland develop and abnormalities of breast have been reported both in male and female [18]. Although this finding clearly implies that EDA regulates mammary gland morphogenesis, this role has so far only been poorly characterized [17]. Roles of EDA in teeth and HFs have been amply studied and it has been shown that EDA is needed for the enamel knot development. EDA-null mice present a reduced enamel knot, explaining the small and abnormally shaped teeth observed [20]. EDA was also shown to stabilize nascent HF placodes and to be implicated in hair cycling [28]. Thus, loss of EDAR results in significantly less hair and in a catagen acceleration [29]. There is evidence of a crosstalk between Wnt signaling, which plays an important function in HF formation and EDA-EDAR [27, 30]. A regulatory balance seems to take place as EDA signaling activates transcription of Wnt antagonists, thereby inducing a negative feedback on Wnt signaling (Figure 5.07) [27].

5.2.2. TROY, Lymphotoxin and TNF

In addition to the EDA pathway, other TNF family members are implied in skin appendage development.

- #### TROY

In mice, pelage HFs develop in three separate waves during embryogenesis. In mice presenting a defect in EDA signaling, only HFs developing during the first wave are absent. HF morphogenesis from the two subsequent waves is initiated normally, but then gives rise to abnormally shaped hair shafts [25]. This finding led to speculations about the existence of a second pathway, partly redundant with EDAR. The similarity between the ligand-binding domains of TROY and EDAR, and their strikingly similar pattern of expression in developing skin appendages make the TNFR family member TROY a possible candidate for this redundant role [31]. This postulate has been confirmed in 2008, when a study showed that although mice deficient in TROY do not show any skin appendage development impairment, mice lacking both EDA and TROY showed an additional defect in the second wave HFs [32]. The ligand for TROY still remains elusive, with studies showing either

no binding of any known TNF family members [33], or LTα ligation to this receptor [34]. TROY has been shown to activate NF-κB and JNK signaling pathways [31, 34].

- ### *LTβ*

In addition to its role in SLOs development LTβ has also been identified as a downstream target of EDA during HF development. LTβ-deficient mice display a phenotype in skin appendages [35]. They present structurally abnormal hair but no defect in HF development was reported [35]. Surprisingly, neither LTα- nor LTβR-deficient mice present a similar HF defect, indicating a possible novel, unknown receptor for LTβ in HF [35]. In addition to its function in HFs, LTβ is also involved in periderm differentiation, an embryonic superficial layer of cells covering the epidermis before its full maturation [36]. In LTβ-deficient mice, the periderm is detached precociously. It is not known whether LTβR-null mice present such a defect [36].

- ### *TNF*

In 2006, a study showed that TNF is involved in HF cycling, although the HF phenotype observed in TNF-deficient mice was moderate, only with a 1.5 day delay in catagen onset. This suggests that TNF could trigger apoptosis associated with the catagen phase but most probably by cooperating with other pathways [37]. In this same study, the authors showed that K17-null mice develop alopecia in the first week after birth, correlating with hair shaft fragility and untimely apoptosis in the bulb. This phenotype was partly reversed in mice deficient for TNF and K17, suggesting that K17, through its ability to bind TRADD, attenuates TNF-triggered apoptosis [37].

5.3. *RANK, RANKL and OPG in skin appendage development*

5.3.1. *Mammary gland development*

Like HFs described above, mammary glands are patterned during embryogenesis (Figure 5.06), but they continually change their structure throughout the lifetime of reproductively active females (Figure 5.08). After embryogenesis, mammary glands development stops until the release of ovarian hormones at around 3 weeks of age in the mouse. At this time, distal ends of the mammary ducts swell into bulbous structures referred to as terminal end buds (TEBs) that invade the fat pad and branch by bifurcation, resulting in a highly arborated system. During pregnancy, reproductive hormones such as progesterone and prolactin, induce expansion and terminal differentiation of the mammary epithelium into secretory, milk-producing, lobular alveoli. When the pups no longer suckle, involution occurs, the secretory epithelium dies by apoptosis and the gland is remodeled back to a state resembling that of adult nulliparous mice [17, 38].
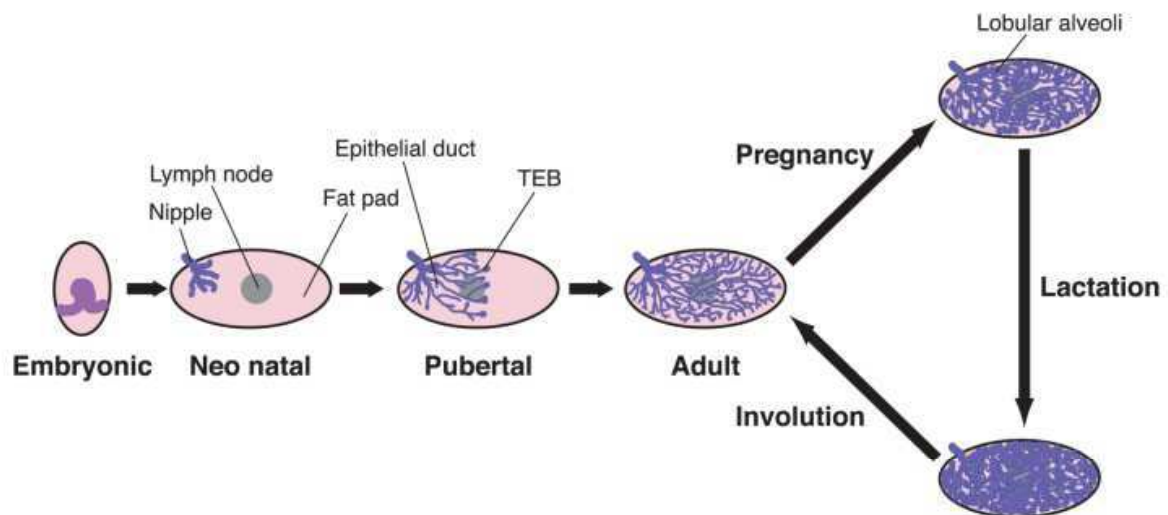
Figure 5.08: Stages of mouse mammary gland development. Schematic representation of the different steps in mammary gland development from embryogenesis to involution after lactation (TEB refers to terminal end buds). After reference [38].

Although RANKL-deficient mice sexually mature and bear youngs, all pups die shortly after birth as a result of an impaired mammary gland development during pregnancy resulting in a lactating defect [39]. In RANKL-deficient mice, the mammary gland develops normally until final hormonal-induced differentiation of mammary epithelium into lobular alveoli, a phenotype resembling progesterone receptor or prolactin receptor deficient mice, highlighting the possible connection between RANKL and pregnancy hormones [39]. In the study of Fata and co-workers RANK was found constitutively expressed throughout the mammary gland. RANKL expression is hormonally-induced in mammary epithelial cells (MECs) and becomes detectable at mid pregnancy and peaks at the first day of lactation [39]. The mammary gland defect in RANKL-knockout mice is characterized by impaired proliferation, enhanced apoptosis, and failure of Akt/PKB activation in MECs, that can be reversed by recombinant RANKL treatment [39]. RANKL was shown to be necessary for cyclin D1 upregulation via IKKα in MECs, which is required for cell proliferation [40]. Ectopic expression of RANKL in mammary epithelium was shown to elicit ductal side branching and alveologenesis [41]. Taken together these studies showed a hormonal regulation of RANKL expression, and a necessary role for this protein in terminal differentiation of mammary epithelium into a milk secreting organ. The hormonal control of RANKL, in addition to its ability to promote cell proliferation and survival, led to the speculation about a possible role of RANK and RANKL in mammary epithelial cancer. This pathological role was recently confirmed by two studies showing a functional contribution of RANKL to mammary tumorigenesis [42, 43]. Thus, the permissive contribution of progesterone and its synthetic derivates to increase, mammary cancer incidence is directly due to RANKL induction and subsequent proliferative changes in MECs [42, 43].

5.3.2. Tooth eruption

As already mentioned above, tooth undergoes complex folding morphogenesis, which lays down the future tooth crown architecture (Figure 5.09). Unlike HFs and mammary glands, teeth do not undergo structural remodeling throughout lifetime, although, in rodents, the incisors continually grow similarly to a HF in anagen.
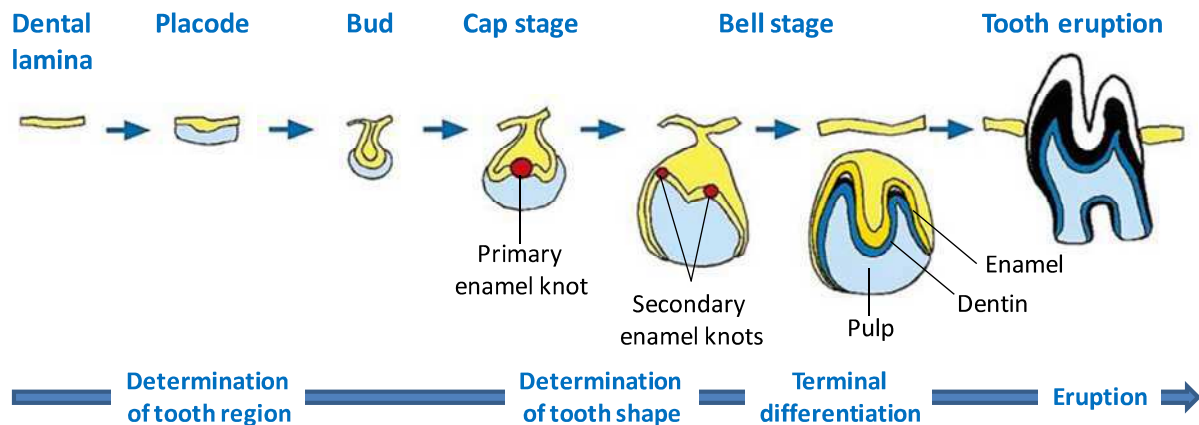
Figure 5.09: Schematic representation of tooth development. After the first developmental stages shared by skin appendages, tooth undergoes embryonic folding that resemble a cap and a bell. Primary and secondary enamel knots play crucial roles in tissue differentiation and tooth shaping. Finally teeth erupt and give rise to the dentition. Yellow represents the tooth epithelium; red the enamel knots; blue the tooth mesenchyme. Modified after reference [20].

Permanent tooth loss and root resorption have been associated to rare bone pathologies linked to mutations in *RANK*, *RANKL* or *OPG* sequences (e.g. familial expansile osteolysis, expansile skeletal hyperphosphatasia and early-onset Paget disease of bone – Chapter 2 Table 2.01) [44-46]. In 1999, it was reported that RANKL-deficient mice do not display any incisor or molar teeth, which was shown to be the result of a defect in tooth eruption into the oral cavity [47]. As extensive bone remodeling of the alveolar crypt is required to open an avenue through the bone of the jaw [48], it was proposed that this impaired tooth eruption in RANKL-deficient mice was due to a failure in osteoclastogenesis [49]. Since then, the mechanisms implied in this physiological process have been more precisely described and the dental follicle, a loose connective tissue sac containing stem cells and surrounding the unerupted tooth, has been shown to be a crucial element during the tooth eruption [50]. The dental follicle regulates both osteoclastogenesis and osteogenesis by tuning the expression of critical genes in both a chronological and a spatial manner. The recruitment of mononuclear cells into the dermal follicle is mediated by monocyte chemoattractant protein-1 (MCP-1) and macrophage colony-stimulating factor-1 (M-CSF) secreted by the dermal follicular cells [51]. Rather than an upregulation of RANKL expression in the dermal follicle, it is the downregulation of OPG expression, induced mainly by M-CSF, that enables osteoclastogenesis [50-52]. Nevertheless, RANKL expression by the

dermal follicle is required, as RANKL-knockout mice, rescued with a RANKL transgene expressed in B and T lymphocytes, still do not display tooth eruption, even if osteoclastogenesis and bone resorption occur in long bones [53].

5.4. *Toward a novel function for RANK, RANKL and OPG in the skin?*

5.4.1. *RANK, RANKL and OPG in the skin*

As described in the previous chapter, RANKL was shown to control T reg cells from the skin [54]. In their study, Loser and co-workers showed that over-expression of RANKL in the epidermal basal layer promotes immune tolerance by increasing the production of T reg cells [54]. Barbaroux and colleagues described strong expression of RANKL by the whole human epidermis under steady-state conditions, with highest levels of expression in the suprabasal population [55]. Loser and co-workers reported that in mouse skin RANKL was barely detectable under steady-state conditions but detected strong RANKL expression in human and mouse epidermis under inflammatory conditions such as ultraviolet exposure or psoriasis (Figure 5.10) [54]. As for RANK, the studies agreed that Langerhans cells express the receptor [54, 55]. With respect to the dermis and the hypodermis, expression of RANK and RANKL was never clearly assessed.
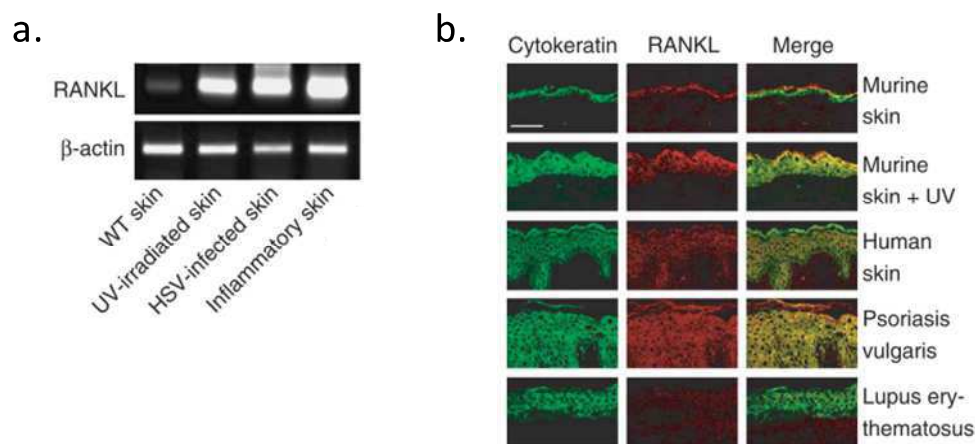
Figure 5.10: RANKL expression in human and mouse skin. (a) RANKL is weakly expressed in untreated wild-type mouse skin (WT skin), whereas a strong expression is detected under inflammatory conditions (from left to right: ultraviolet irradiated skin, herpes simplex virus-1 infected skin and skin from CD40 transgenic mice). (b) Immunofluorescence staining of human and mouse skins using antibodies to cytokeratin and RANKL showing increased RANKL expression under inflammatory conditions. After reference [54].

RANK and RANKL have emerged as important players in epithelial cell growth and differentiation. Thus, these proteins are required for the formation of lactating mammary glands as described above [39] but also for the formation of thymic medullary cells as illustrated in Chapter 2 [56]. In addition, RANKL was shown to be necessary and sufficient for initiating the development of epithelial intestinal microfold cells [57]. These microfold cells provide a portal for efficient sampling

of antigens form the intestinal lumen, a process crucial in intestine where lymphoid tissues need to be inductive sites for both the generation of immune responses and tolerance to antigens present in the intestine, which include those derived from food and commensal flora [57]. RANKL was also shown to be expressed in prostate epithelial cells, with a pattern of expression close to the one depicted by Barbaroux and co-workers in the skin as the expression was higher in luminal cells compared to basal cells [58]. Finally, RANK and RANKL were also shown to be implied in growth and metastasis of prostate [57, 59] and mammary epithelial cancers cells [42, 43].

Thus, as RANK and RANKL affect a wide variety of epithelial cells from different organs, we addressed the question whether RANK, RANKL and OPG have a functionally important role in the epidermal turnover.

5.4.2. RANK, RANKL and OPG in the HF cycle

Given the important roles of RANK, RANKL and OPG in skin appendages development (e.g. mammary gland and teeth), the question about a possible function of these proteins in HF biology arises. Cycling appears to be an autonomous process being able to take place in culture of isolated HF [60]. Nevertheless, the pathways implied in this process are complex with multiple molecules capable to modulate hair cycling (Figure 5.11) but the mechanisms underlying anagen induction are still incompletely understood. Two consensus have with respect to anagen induction: (i) the local balance between hair growth stimulators and inhibitors is crucial and (ii) the bulge, the second hair germ and the dermal papilla are required [12]. The bulge has attracted attention as being a reservoir of adult stem cells, and two main pathways have been described in the activation of bulge stem cells: the bone morphogenic proteins (BMPs) [61] and the Wnt pathway [62]. The first is implied in maintaining the stem cells in a relatively quiescent state, while the second activates them.

Strikingly, many of the molecules known to regulate the HF cycle, are also protagonists of bone remodeling which, in addition, can regulate RANK, RANKL and/or OPG expression (Figure 5.11 and Chapter 1 Table 1.02). Furthermore, OPG is known to be expressed in the bulge [63, 64], supporting a possible important role for these proteins in HF biology.
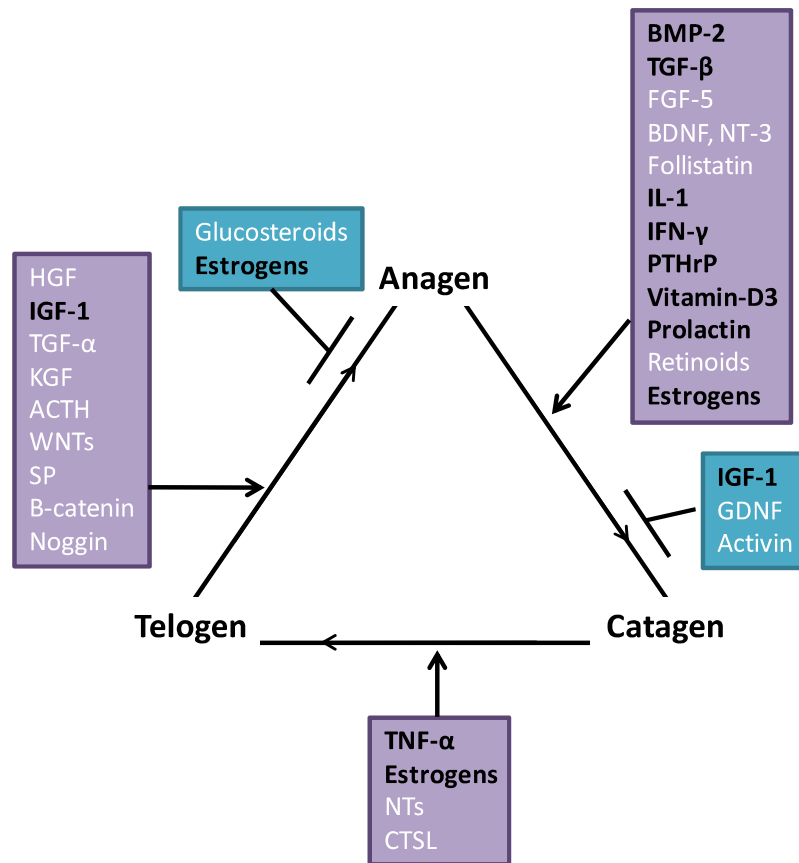
Figure 5.11: Schematic representation of molecules known to influence the HF cycle. Molecules known to induce or to repress the HF progress through the different stages are depicted, molecules in a bold black font are molecules known to regulate RANK, RANKL and/or OPG expression. Abbreviations: ACTH, adrenocorticotrophin; BDNF, brain-derived neurotrophin factor; BMP-2, bone morphogenic protein 2; CTSL, cathepsin-L; FGF-5, fibroblast growth factor 5; HGF, hepatocyte growth factor; IFN-γ, interferon-γ; IGF-1, insulin-like growth factor-1; IL-1, interleukin-1; KGF, keratinocyte growth factor; NTs, neurotrophins; NT-3, neurotrophin-3; PTHrP, parathyroid-related protein; TGF: transforming growth factor; SP, substance P. Modified after reference [60, 65]

Given the importance of RANK in tooth and mammary gland development and that a number of factors involved in hair cycling also regulate RANK signaling, the question of whether RANK plays a role in HF cycling arises. To address this issue we used RANKL-deficient mice and mice over-expressing RANK under the control of the S100A8 promoter active in HF stem cells.

5.5. *Conclusions*

The skin represents a first protection against external physical, chemical and biological aggressions and has attracted recent attention through harboring adult stem cells. Epidermis, dermis and hypodermis constitute the three morphologically distinct layers of the skin. Into the dermis protrudes the HF which is a complex mini-organ undergoing a succession of growing (anagen), regressing (catagen) and resting (telogen) phases throughout lifetime. HFs, along with mammary glands and teeth, are referred to as skin appendages and share early stages of development. Several TNFSF members are required for skin appendage morphogenesis among which EDA, TROY, TNF and LTβ. RANKL is known to be required for lactating mammary gland formation and for tooth eruption. Although RANK and RANKL are respectively expressed in Langerhans and in epidermal keratinocytes, little is known about the possible function of these proteins in the skin ahead of their role in T reg expansion. This is in spite of the fact that RANK and RANKL are required for growth and differentiation of many subtypes of epithelial cells, including thymic medullary cells, intestinal microfold cells and prostate epithelial cells. Additionally, many molecules known to influence the HF cycle are of importance in the bone where they crosstalk with RANK, RANKL or OPG. Finally, OPG is expressed in the bulge but its function there remains unknown. Thus, we examined the role for RANK, RANKL and OPG in the skin.
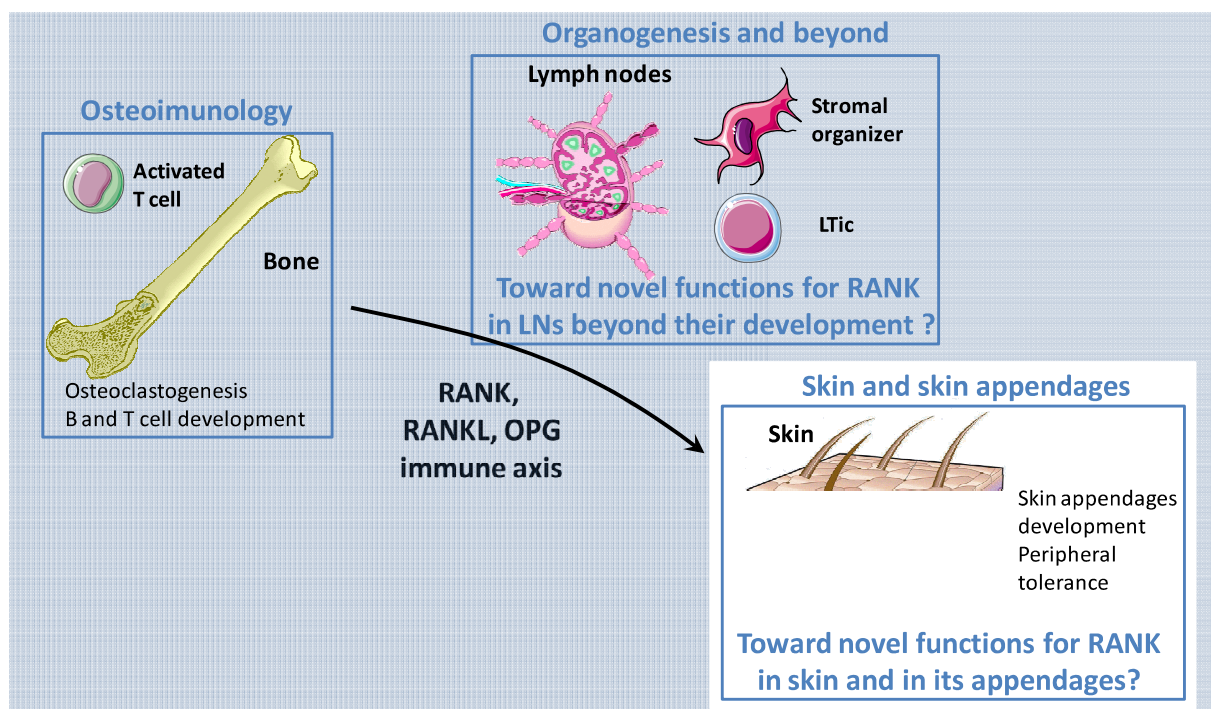
Figure 5.12: The RANK, RANKL and OPG axis: novel functions in the skin and in the hair follicle ? RANK and RANKL are known to be required for the development of skin appendages and for epithelial cells growth and proliferation, we address the question of new possible functions for RANK in the biology of the hair follicle and in the epidermal turnover.

5.6. *Bibliography*

1.   Candi, E., R. Schmidt, and G. Melino, *The cornified envelope: a model of cell death in the skin.* Nat Rev Mol Cell Biol, 2005. **6**(4): p. 328-40.
2.   Potten, C.S., *The epidermal proliferative unit: the possible role of the central basal cell.* Cell Tissue Kinet, 1974. **7**(1): p. 77-88.
3.   Strachan, L.R. and R. Ghadially, *Tiers of clonal organization in the epidermis: the epidermal proliferation unit revisited.* Stem Cell Rev, 2008. **4**(3): p. 149-57.
4.   Blanpain, C. and E. Fuchs, *Epidermal homeostasis: a balancing act of stem cells in the skin.* Nat Rev Mol Cell Biol, 2009. **10**(3): p. 207-17.
5.   Bouwstra, J.A. and M. Ponec, *The skin barrier in healthy and diseased state.* Biochim Biophys Acta, 2006. **1758**(12): p. 2080-95.
6.   Kanitakis, J., *Anatomy, histology and immunohistochemistry of normal human skin.* Eur J Dermatol, 2002. **12**(4): p. 390-9; quiz 400-1.
7.   Dupuy, P., et al., *T-cell receptor-gamma/delta bearing lymphocytes in normal and inflammatory human skin.* J Invest Dermatol, 1990. **94**(6): p. 764-8.
8.   Maricich, S.M., et al., *Merkel cells are essential for light-touch responses.* Science, 2009. **324**(5934): p. 1580-2.
9.   Paus, R. and G. Cotsarelis, *The biology of hair follicles.* N Engl J Med, 1999. **341**(7): p. 491-7.
10.   Standring, S., ed. *Gray's Anatomy: The Anatomical Basis of Clinical Practice*. 40 ed. 2008, Churchill-Livingstone, Elsevier. 1576.
11.   Sumaria, N., et al., *Cutaneous immunosurveillance by self-renewing dermal gammadelta T cells.* J Exp Med, 2011. **208**(3): p. 505-18.
12.   Schneider, M.R., R. Schmidt-Ullrich, and R. Paus, *The hair follicle as a dynamic miniorgan.* Curr Biol, 2009. **19**(3): p. R132-42.
13.   Ito, M., et al., *Hair follicle stem cells in the lower bulge form the secondary germ, a biochemically distinct but functionally equivalent progenitor cell population, at the termination of catagen.* Differentiation, 2004. **72**(9-10): p. 548-57.
14.   Fuchs, E., *Scratching the surface of skin development.* Nature, 2007. **445**(7130): p. 834-42.
15.   Muller-Rover, S., et al., *A comprehensive guide for the accurate classification of murine hair follicles in distinct hair cycle stages.* J Invest Dermatol, 2001. **117**(1): p. 3-15.
16.   Stenn, K.S. and R. Paus, *Controls of hair follicle cycling.* Physiol Rev, 2001. **81**(1): p. 449-494.
17.   Mikkola, M.L. and S.E. Millar, *The mammary bud as a skin appendage: unique and shared aspects of development.* J Mammary Gland Biol Neoplasia, 2006. **11**(3-4): p. 187-203.
18.   Clarke, A., et al., *Clinical aspects of X-linked hypohidrotic ectodermal dysplasia.* Arch Dis Child, 1987. **62**(10): p. 989-96.
19.   Hennighausen, L. and G.W. Robinson, *Signaling pathways in mammary gland development.* Dev Cell, 2001. **1**(4): p. 467-75.
20.   Jernvall, J. and I. Thesleff, *Reiterative signaling and patterning during mammalian tooth morphogenesis.* Mech Dev, 2000. **92**(1): p. 19-29.
21.   Mikkola, M.L., *Genetic basis of skin appendage development.* Semin Cell Dev Biol, 2007. **18**(2): p. 225-36.
22.   Thesleff, I., A. Vaahtokari, and A.M. Partanen, *Regulation of organogenesis. Common molecular mechanisms regulating the development of teeth and other organs.* Int J Dev Biol, 1995. **39**(1): p. 35-50.
23.   Kere, J., et al., *X-linked anhidrotic (hypohidrotic) ectodermal dysplasia is caused by mutation in a novel transmembrane protein.* Nat Genet, 1996. **13**(4): p. 409-16.
24.   Ezer, S., et al., *Ectodysplasin is a collagenous trimeric type II membrane protein with a tumor necrosis factor-like domain and co-localizes with cytoskeletal structures at lateral and apical surfaces of cells.* Hum Mol Genet, 1999. **8**(11): p. 2079-86.

25.   Headon, D.J. and P.A. Overbeek, *Involvement of a novel Tnf receptor homologue in hair follicle induction.* Nat Genet, 1999. **22**(4): p. 370-4.

26.   Headon, D.J., et al., *Gene defect in ectodermal dysplasia implicates a death domain adapter in development.* Nature, 2001. **414**(6866): p. 913-6.

27.   Cui, C.Y. and D. Schlessinger, *EDA signaling and skin appendage development.* Cell Cycle, 2006. **5**(21): p. 2477-83.

28.   Mikkola, M.L., *TNF superfamily in skin appendage development.* Cytokine Growth Factor Rev, 2008. **19**(3-4): p. 219-30.

29.   Fessing, M.Y., et al., *Involvement of the Edar signaling in the control of hair follicle involution (catagen).* Am J Pathol, 2006. **169**(6): p. 2075-84.

30.   van Genderen, C., et al., *Development of several organs that require inductive epithelial-mesenchymal interactions is impaired in LEF-1-deficient mice.* Genes Dev, 1994. **8**(22): p. 2691-703.

31.   Kojima, T., et al., *TROY, a newly identified member of the tumor necrosis factor receptor superfamily, exhibits a homology with Edar and is expressed in embryonic skin and hair follicles.* J Biol Chem, 2000. **275**(27): p. 20742-7.

32.   Pispa, J., et al., *Edar and Troy signalling pathways act redundantly to regulate initiation of hair follicle development.* Hum Mol Genet, 2008. **17**(21): p. 3380-91.

33.   Bossen, C., et al., *Interactions of tumor necrosis factor (TNF) and TNF receptor family members in the mouse and human.* Journal of Biological Chemistry, 2006. **281**(20): p. 13964-13971.

34.   Hashimoto, T., D. Schlessinger, and C.Y. Cui, *Troy binding to lymphotoxin-alpha activates NF kappa B mediated transcription.* Cell Cycle, 2008. **7**(1): p. 106-11.

35.   Cui, C.Y., et al., *Ectodysplasin regulates the lymphotoxin-beta pathway for hair differentiation.* Proc Natl Acad Sci U S A, 2006. **103**(24): p. 9142-7.

36.   Cui, C.Y., et al., *Lymphotoxin-beta regulates periderm differentiation during embryonic skin development.* Hum Mol Genet, 2007. **16**(21): p. 2583-90.

37.   Tong, X. and P.A. Coulombe, *Keratin 17 modulates hair follicle cycling in a TNFalpha-dependent fashion.* Genes Dev, 2006. **20**(10): p. 1353-64.

38.   Wiseman, B.S. and Z. Werb, *Stromal effects on mammary gland development and breast cancer.* Science, 2002. **296**(5570): p. 1046-9.

39.   Fata, J.E., et al., *The osteoclast differentiation factor osteoprotegerin-ligand is essential for mammary gland development.* Cell, 2000. **103**(1): p. 41-50.

40.   Cao, Y., et al., *IKKalpha provides an essential link between RANK signaling and cyclin D1 expression during mammary gland development.* Cell, 2001. **107**(6): p. 763-75.

41.   Fernandez-Valdivia, R., et al., *The RANKL signaling axis is sufficient to elicit ductal side-branching and alveologenesis in the mammary gland of the virgin mouse.* Dev Biol, 2009. **328**(1): p. 127-39.

42.   Gonzalez-Suarez, E., et al., *RANK ligand mediates progestin-induced mammary epithelial proliferation and carcinogenesis.* Nature, 2010. **468**(7320): p. 103-7.

43.   Schramek, D., et al., *Osteoclast differentiation factor RANKL controls development of progestin-driven mammary cancer.* Nature, 2010. **468**(7320): p. 98-102.

44.   Mitchell, C.A., J.G. Kennedy, and R.G. Wallace, *Dental abnormalities associated with familial expansile osteolysis: a clinical and radiographic study.* Oral Surg Oral Med Oral Pathol, 1990. **70**(3): p. 301-7.

45.   Nakashima, T. and H. Takayanagi, *Osteoimmunology: crosstalk between the immune and bone systems.* J Clin Immunol, 2009. **29**(5): p. 555-67.

46.   Nakatsuka, K., Y. Nishizawa, and S.H. Ralston, *Phenotypic characterization of early onset Paget's disease of bone caused by a 27-bp duplication in the TNFRSF11A gene.* J Bone Miner Res, 2003. **18**(8): p. 1381-5.

47.   Kong, Y.Y., et al., *OPGL is a key regulator of osteoclastogenesis, lymphocyte development and lymph-node organogenesis.* Nature, 1999. **397**(6717): p. 315-323.

48.   Wise, G.E. and W. Fan, *Changes in the tartrate-resistant acid phosphatase cell population in dental follicles and bony crypts of rat molars during tooth eruption.* J Dent Res, 1989. **68**(2): p. 150-6.

49.   Kong, Y.Y., et al., *Activated T cells regulate bone loss and joint destruction in adjuvant arthritis through osteoprotegerin ligand.* Nature, 1999. **402**(6759): p. 304-9.

50.   Wise, G.E., *Cellular and molecular basis of tooth eruption.* Orthod Craniofac Res, 2009. **12**(2): p. 67-73.

51.   Heinrich, J., et al., *CSF-1, RANKL and OPG regulate osteoclastogenesis during murine tooth eruption.* Arch Oral Biol, 2005. **50**(10): p. 897-908.

52.   Wise, G.E. and G.J. King, *Mechanisms of tooth eruption and orthodontic tooth movement.* J Dent Res, 2008. **87**(5): p. 414-34.

53.   Kim, N., et al., *Diverse roles of the tumor necrosis factor family member TRANCE in skeletal physiology revealed by TRANCE deficiency and partial rescue by a lymphocyte-expressed TRANCE transgene.* Proc Natl Acad Sci U S A, 2000. **97**(20): p. 10905-10.

54.   Loser, K., et al., *Epidermal RANKL controls regulatory T-cell numbers via activation of dendritic cells.* Nature Medicine, 2006. **12**(12): p. 1372-1379.

55.   Barbaroux, J.B., et al., *Epidermal receptor activator of NF-kappaB ligand controls Langerhans cells numbers and proliferation.* J Immunol, 2008. **181**(2): p. 1103-8.

56.   Rossi, S.W., et al., *RANK signals from CD4(+)3(-) inducer cells regulate development of Aire-expressing epithelial cells in the thymic medulla.* J Exp Med, 2007. **204**(6): p. 1267-72.

57.   Knoop, K.A., et al., *RANKL is necessary and sufficient to initiate development of antigen-sampling M cells in the intestinal epithelium.* J Immunol, 2009. **183**(9): p. 5738-47.

58.   Brown, J.M., et al., *Osteoprotegerin and rank ligand expression in prostate cancer.* Urology, 2001. **57**(4): p. 611-6.

59.   Luo, J.L., et al., *Nuclear cytokine-activated IKK alpha controls prostate cancer metastasis by repressing Maspin.* Nature, 2007. **446**(7136): p. 690-694.

60.   Paus, R. and K. Foitzik, *In search of the "hair cycle clock": a guided tour.* Differentiation, 2004. **72**(9-10): p. 489-511.

61.   Kobielak, K., et al., *Loss of a quiescent niche but not follicle stem cells in the absence of bone morphogenetic protein signaling.* Proc Natl Acad Sci U S A, 2007. **104**(24): p. 10063-8.

62.   Huelsken, J., et al., *beta-Catenin controls hair follicle morphogenesis and stem cell differentiation in the skin.* Cell, 2001. **105**(4): p. 533-45.

63.   Greco, V., et al., *A two-step mechanism for stem cell activation during hair regeneration.* Cell Stem Cell, 2009. **4**(2): p. 155-69.

64.   Morris, R.J., et al., *Capturing and profiling adult hair follicle stem cells.* Nat Biotechnol, 2004. **22**(4): p. 411-7.

65.   Theoleyre, S., et al., *The molecular triad OPG/RANK/RANKL: involvement in the orchestration of pathophysiological bone remodeling.* Cytokine Growth Factor Rev, 2004. **15**(6): p. 457-75.

RESULTS

1. RANK in the regulation of skin homeostasis

1.1. Introduction

The TNF superfamily member RANKL and its functional and decoy receptors, respectively RANK and OPG, are recognized for their functions in osteoclastogenesis and in the immune system. During my doctorate, we investigated the possible roles of this molecular triad in the skin, by focusing on the hair follicle and the epidermis. Indeed, RANK is implicated in the formation of two other skin appendages (tooth and lactating mammary gland), and a striking similarity between the mechanisms regulating hair follicle cycling and osteoclastogenesis exists. In addition, RANK functions in the biology of multiple epithelial cell-type, ranging from mammary tissue to prostate, thymus and intestine.

We studied a murine model deficient for RANKL, in which germline *Rankl* is interrupted by the kanamycin gene and which is characterized by osteopetrosis, lack of all LNs, complete absence of teeth eruption and impaired mammary gland development. Another murin model used for this study, is a mouse over-expressing murine RANK under the control of the human S100A8 (S100 calcium binding protein A8) promoter, active both in osteoclasts precursors and in hair follicle stem cells. RANK gene was modified by the addition of a FLAG epitope in 5' terminus and was inserted around 30 times in the genome.

1.2. <u>Article 1</u>

Receptor Activator of NF-κB (RANK) stimulates the proliferation of epithelial cells of the epidermo-pilosebaceous unit.

<u>Duheron V</u>, **Hess E**, <u>Duval M, Decossas M, Castaneda B, Klöpper JE, Amoasii L, Barbaroux JB, Williams IR, Yagita H, Penninger JM, Choi Y, Lézot F, Groves RW, Paus R, Mueller CG</u>

Proc Natl Acad Sci USA. 108(13):5342-7, 2011.

Receptor activator of NF-κB (RANK) stimulates the proliferation of epithelial cells of the epidermo-pilosebaceous unit

Vincent Duheron[a], Estelle Hess[a], Monique Duval[a], Marion Decossas[a], Beatriz Castaneda[b,c], Jennifer E. Klöpper[d], Leonela Amoasii[a], Jean-Baptiste Barbaroux[e], Ifor R. Williams[f], Hideo Yagita[g], Josef Penninger[h], Yongwon Choi[i], Frédéric Lézot[b], Richard Groves[e], Ralf Paus[d,j], and Christopher G. Mueller[a,1]

[a]Centre National de la Recherche Scientifique, Laboratory of Therapeutic Immunology and Chemistry, Unité Propre de Recherche 9021, Institut de Biologie Moléculaire et Cellulaire, University of Strasbourg, 67084 Strasbourg, France; [b]Institut National de la Santé et de la Recherche Médicale, Unité Mixte de Recherche 872, Cordeliers Research Center, Team 5, Laboratory of Oral Molecular Physiopathology, F-75006 Paris, France; [c]University of Antioquia, Medellin, Colombia; [d]Department of Dermatology, University Hospital Schleswig-Holstein, University of Lübeck, 23562 Lübeck, Germany; [e]St. John's Institute of Dermatology, Division of Genetics and Molecular Medicine, King's College London School of Medicine, London SE1 9RT, United Kingdom; [f]Department of Pathology and Laboratory Medicine, Emory University School of Medicine, Atlanta, GA 30322; [g]Department of Immunology, Juntendo University School of Medicine, Tokyo 113-8421, Japan; [h]Institute of Molecular Biotechnology of the Austrian Academy of Sciences, 1030 Vienna, Austria; [i]Department of Pathology and Laboratory Medicine, University of Pennsylvania School of Medicine, Philadelphia, PA 19104; and [j]School of Translational Medicine, University of Manchester, Manchester M13 9PT, United Kingdom

Receptor activator of NF-κB (RANK), known for controlling bone mass, has been recognized for its role in epithelial cell activation of the mammary gland. Because bone and the epidermo-pilosebaceous unit of the skin share a lifelong renewal activity where similar molecular players operate, and because mammary glands and hair follicles are both skin appendages, we have addressed the function of RANK in the hair follicle and the epidermis. Here, we show that mice deficient in RANK ligand (RANKL) are unable to initiate a new growth phase of the hair cycle and display arrested epidermal homeostasis. However, transgenic mice overexpressing RANK in the hair follicle or administration of recombinant RANKL both activate the hair cycle and epidermal growth. RANK is expressed by the hair follicle germ and bulge stem cells and the epidermal basal cells, cell types implicated in the renewal of the epidermo-pilosebaceous unit. RANK signaling is dispensable for the formation of the stem cell compartment and the inductive hair follicle mesenchyme, and the hair cycle can be rescued by *Rankl* knockout skin transplantation onto *nude* mice. RANKL is actively transcribed by the hair follicle at initiation of its growth phase, providing a mechanism for stem cell RANK engagement and hair-cycle entry. Thus, RANK–RANKL regulates hair renewal and epidermal homeostasis and provides a link between these two activities.

osteoprotegerin | TRANCE | anagen | S100A8

Receptor activator of NF-κB (RANK), a member of the TNF receptor family (TNFRSF11a), was originally identified as a regulator of bone density. Mice deficient in *Rank* or *Rankl* display increased bone density owing to reduced osteoclast formation, but the loss of the RANK ligand (RANKL) decoy receptor osteoprotegerin (OPG) results in lower bone mass because of unchecked RANK activation (1, 2).

RANK has emerged as an important player in epithelial cell growth and differentiation. It is required for the formation of lactating mammary glands (3, 4), thymic medullary epithelial cells (5), and intestinal microfold cells (6) and has been implicated in the growth and metastasis of prostate (7) and mammary epithelial cancers (8, 9). Thus, RANK affects a great variety of epithelial cells of different organs. The skin is the largest epithelial surface, and its epidermo-pilosebaceous unit comprises the interfollicular epidermis (IFE), the hair follicle (HF), and the sebaceous gland. The HF has the particularity of undergoing cycles of growth (anagen), regression (catagen), and relative quiescence (telogen) (10), making it an excellent system for studying epidermal (stem) cells and organ remodeling (11–14). Each HF is composed of a permanent upper portion, which

includes the sebaceous gland and the bulge region, and a temporary lower cycling portion. The local balance of hair growth stimulators and inhibitors is critical for initiation of new hair growth (15–17). Intriguingly, many of these molecular players also operate in bone development and remodeling (e.g., members of the TGF-β superfamily and their antagonists, parathyroid hormones, and hedgehog proteins) (18).

Because *Rank* and *Rankl*-null mice exhibit defects in mammary gland development (3) and in the eruption of teeth (19), which, like HFs, are skin appendages, it raises the question of the role of the RANK–RANKL–OPG triad in HF formation and cycling. The finding that *Opg* is transcribed by the bulge stem cells (20, 21) supports an important role of these proteins in HF biology. However, so far this question has not been investigated.

The IFE is intrinsically linked to the HF through the outer-root sheath, which merges distally the basal layer of IFE and proximally the HF bulge and the HF bulb (10). Like HFs, the IFE undergoes renewal (homeostasis). In this process, keratinocytes of the basal layer divide and terminally differentiate to replace upper-lying cells. RANKL is expressed by the activated IFE, and the epidermal Langerhans dendritic cells carry RANK (22, 23). RANK engagement on Langerhans cells leads to an increase in their cell numbers and to immune response modulation (22, 23). However, the role of RANK in epidermal homeostasis has not been addressed.

We have studied whether RANK plays a functionally important role in the stimulation of epithelial cells of the HF and the IFE. Using *Rankl* knockout (*Rankl*-KO) and *Rank* transgenic (*Rank*-Tg) mice, as well as recombinant RANKL and anti-RANKL mAb, we here present previously unreported evidence that RANK functions in HF growth and in epidermal renewal.

Results

RANK Stimulation Is Dispensable for Normal HF Development but Is Required for HF Anagen. Many molecular regulators of HF cycling also drive HF development (morphogenesis) (17). Therefore, we

first investigated the importance of RANK stimulation in HF morphogenesis. We analyzed the expression of RANK, RANKL, and OPG mRNA by RT-PCR in total skin of wild-type (WT) mice at postnatal day 5 (P5) and P15 and found that the genes were transcriptionally active (Fig. S1A). In situ hybridization of RANK and RANKL mRNA at P5 showed that the genes were transcribed in the IFE and the HF (Fig. S1B). This finding confirms previous data of RANK and RANKL expression in the embryonic IFE and HF (24). We then compared HF morphogenesis of $Rankl^{-/-}$ mice and control littermates. At P5, the back skin HFs of WT mice were in postnatal HF morphogenesis and by P15 began to enter catagen. Exactly the same observation was made in $Rankl^{-/-}$ mice (Fig. S1C), whose postnatal HF morphogenesis and macroscopic hair phenotype appeared indistinguishable from those of WT littermates (25). Furthermore, all four hair types (monotrich, awl, auchene, and zigzag) were found (Fig. S1D), indicating that RANK stimulation is dispensable for HF morphogenesis.

Next, we studied whether absent RANK stimulation affected the HF renewal cycle with entry into the hair growth phase at around P24 in C57BL/6 mice (26). Strikingly, $Rankl^{-/-}$ HFs did not enter anagen by P28 through to P49, whereas WT littermates had long proceeded into anagen or had already reached their second catagen (Fig. 1 A and B and Fig. S2A). Also at P25, there was no sign of anagen initiation, showing a genuine block of HF cycling rather than the occurrence of an abortive, drastically

Fig. 1. RANKL is required for HF anagen. (A) At P28, $Rankl^{-/-}$ HFs are arrested in telogen, whereas WT littermates are in anagen. (B) Schematic representation of HF morphogenesis and cycling in $Rankl^{-/-}$ and controls, and the failure of all $Rankl^{-/-}$ mice to enter anagen. (C) Arrest of $Rank^{-/-}$ HFs in telogen. (D) At 5 d after hair plucking at P19, HFs were in advanced anagen in WT mice but remained in telogen in $Rankl^{-/-}$ mice. Mock-treated WT mice displayed early anagen. (Scale bars, 100 μm; in Insets, 50 μm.) The paraffin-embedded sections were stained with hematoxylin/eosin.

shortened growth phase (Fig. S2B). As expected, given that RANKL is the only ligand for RANK (27), $Rank^{-/-}$ mice also failed to undergo transition from telogen to anagen (Fig. 1C).

Because hair plucking can experimentally provoke hair-cycle activation (28), we tested this stimulus on $Rankl^{-/-}$ mice. Five days after hair plucking, 24-d-old control mice were in advanced anagen, but the $Rankl$-KO animals still remained in telogen (Fig. 1D). Thus, in the absence of RANK stimulation by RANKL, the mouse HF is arrested in first postnatal telogen and is unable to enter its anagen growth phase.

Telogen Arrest in the Absence of RANK Stimulation Does Not Result from Defects of the HF Stem Cell Compartment or from Defective HF Mesenchyme. At least two distinct subpopulations of HF epithelial cells are needed for normal anagen formation, the bulge stem cells (11, 29) and the secondary hair germ (SHG) cells (21, 30). Therefore, we looked for the presence of these cells in the $Rankl^{-/-}$ animals.

Immunofluorescence for CD34, a marker of murine bulge stem cells (31), showed that they were preserved in the $Rankl^{-/-}$ telogen HF (Fig. 2A). Their quantification by flow cytometry revealed that their number was only slightly reduced (Fig. 2B). Immunofluorescence for P-cadherin (21) showed that the SHG was also present (Fig. 2A). Thus, the absence of RANKL does not deplete these cells sufficiently to explain the HF arrest in telogen.

Anagen development also requires inductive signals from the mesenchymal follicular dermal papilla (DP) (32). Therefore, we examined its presence by alkaline phosphatase enzyme histochemistry (33). The enzyme activity in the correct position beneath the HF revealed the presence of morphologically and enzyme-histochemically normal DP in $Rankl^{-/-}$ mice (Fig. 2C), which shows that that the $Rankl^{-/-}$ telogen HF contained all of the cellular elements required for telogen–anagen transition.

We therefore tested whether the hair-cycle arrest can be rescued. We transplanted shaved, 21-d-old $Rankl^{-/-}$ skin, whose HFs were all in telogen, onto age-matched nude mice. Because RANKL is produced during wound healing by neovascularization and by activated epidermal keratinocytes (22, 34), it could be expected that recipient RANKL is synthesized and complements the genetic deficiency. Hair regrowth and anagen development of the grafted skin was monitored. We observed that, by 10 d, both the WT and the $Rankl^{-/-}$ transplanted skin had acquired a dark appearance, a sign of anagen, and, by 3 wk, both transplants presented full hair regrowth (Fig. 2D). Skin cross-sections confirmed that HFs of the $Rankl$-null mice were in anagen. These findings established that the epithelial stem cell compartment and the inductive HF mesenchyme of $Rankl^{-/-}$ HFs are functional.

RANK Is Expressed by HF Epithelial Stem Cells. To better understand how RANK regulates the telogen–anagen transition, we determined the site of RANK expression in telogen HFs. Immunofluorescent labeling localized RANK to the bulge and the SHG (Fig. 3A). Also RANKL and the RANKL decoy receptor OPG were expressed at these sites (Fig. 3A). The immunoreactivity of RANK and RANKL was low, requiring signal amplification, whereas OPG could be visualized without amplification. This finding concurs with published gene profiling results that had shown abundant transcripts of Opg in murine bulge cells (20, 21). RANK, RANKL, or OPG were undetectable in the DP. RT-PCR of CD34$^+$ and P-cadherin$^+$ cells, which were isolated and sorted by FACS (21), confirmed transcriptional activity of $Rank$, $Rankl$, and Opg in the CD34$^+$ bulge and the P-cadherin$^+$ SHG epithelial cells (Fig. 3B).

We then investigated whether RANKL and OPG expression changed during the hair cycle by measuring their mRNA by quantitative RT-PCR in total skin. OPG gene expression was maximal in early to mid-telogen, whereas that of RANKL peaked in early anagen (Fig. 3C). Because RANKL and OPG are soluble proteins, we measured their protein levels by ELISA in the supernatant of a 24-h skin culture. Fig. 3D shows that the

GENETICS

Fig. 2. The HF stem cell and the mesenchymal cell compartment is RANK-signaling independent. (*A*) Identification of CD34$^+$ bulge (B) and P-cadherin$^+$ SHG cells in *Rankl$^{-/-}$* and control telogen HFs by immunofluorescence. Nuclei were colored with DAPI. (Scale bars, 20 μm.) (*B Left*) Flow cytometry of CD34$^+$ bulge cells among keratin 14$^+$ keratinocytes in *Rankl$^{-/-}$* and WT telogen HFs. Arrows point to CD34$^+$ keratin 14$^+$ cells. (*Right*) Graph depicts the percentage of CD34$^+$ and keratin 14$^+$ cells in three KO mice and littermate controls (*$P < 0.05$). (*C*) Identification of follicular DP by their alkaline phosphatase activity. (Scale bars, 20 μm.) (*D*) Restored *Rankl$^{-/-}$* hair renewal after transplantation onto *nude* mice at week 3 and analysis at week 6. A *Rankl$^{-/-}$* skin section shows HFs in anagen. Image is representative for five transplantation experiments. (Scale bar, 100 μm.) The paraffin-embedded section was stained with hematoxylin/eosin.

RANKL and OPG protein levels reflected their mRNA changes with maximal levels of OPG at telogen followed by a peak of RANKL. To uncover the site of RANKL expression during its peak, we performed RT-PCR on separated IFE and dermal HF-associated cells (Fig. 3*E*); it disclosed that RANKL expression was restricted to the HF-associated cells. Anti-RANKL/keratin 14 immunofluorescent labeling of the whole skin revealed RANKL in the lower HF (Fig. 3*F*), and costaining with GATA-3, a marker for the HF inner root sheath (35), showed that RANKL is localized to the inner root sheath and the cuticle layer (Fig. S3*A*). Because RANKL is a soluble protein and the detection at these sites could be the consequence of binding to extracellular components, we visualized its mRNA on sections by in situ hybridization. Again, we saw the RANKL gene activity in the lower HF (Fig. S3*B*). There was no RANKL in the IFE except for some rare cells, in accord with earlier findings (22) (Fig. S3*C*). In anagen skin, RANK was seen in the bulge, the outer root sheath, and the IFE (Fig. 3*G*). Double labeling for RANK with CD34 and integrin α6, both markers for bulge cells (20, 31), validated RANK expression in the anagen bulge stem cells (Fig. S3*D*). Staining of OPG in anagen skin showed the protein in the bulge but not in the lower HF part (Fig. 3*H*). OPG can also be observed in basal keratinocytes (Fig. S3*E*).

Together, these findings showed that RANK, RANKL, and OPG are expressed by bulge and SHG cells. As the hair cycle progresses from telogen to anagen, OPG expression decreases but that of RANKL increases. Thus, at the telogen–anagen transition, more OPG-free RANKL is available to engage RANK and drive the HF stem cells into proliferation.

RANK Stimulation Triggers Anagen Entry. To further address the importance of RANK activation in anagen induction, we used a mouse Tg for *Rank* under the control of the S100A8 gene promoter. This promoter had already been noted as active in the human HF (36) and, recently, was found transcribed in the SHG (21). Immunofluorescent labeling of telogen HFs confirmed that RANK was overexpressed in the SHG (Fig. S4*A*). Endogenous RANK was not seen because its visualization required signal amplification. Expression of the Tg RANK construct in HEK 293T cells showed that RANK was localized at the cell surface and that it activated NF-κB signaling as expected (37) (Fig. S4*B*). We also monitored RANKL and OPG production in these mice by ELISA of skin cultures from weeks 3 to 5. The Tg mice displayed an increase of RANKL, particularly during its peak production at anagen, but showed a reduced OPG level (Fig. S4*C*). Thus, with RANK overexpressed in the HF and a more favorable RANK-activating RANKL/OPG ratio, we expected an increased HF RANK engagement.

Indeed, we saw that the first anagen entry was advanced by 1 or 2 d (Fig. 4 *A* and *C*). Moreover, two rapidly evolving premature anagen cycles occurred at weeks 8 and 11, whereas control littermates were in telogen (Fig. 4 *B* and *C*). Three-month-old Tg mice showed mild alopecia (Fig. S4*D*), similar to other mutant mice with abnormally fast HF cycling (38).

To test whether hair renewal can be prematurely induced in WT mice by RANK stimulation, we injected recombinant RANKL s.c. into 8-wk-old mice in telogen. The functionality of the recombinant RANKL fused to the GST tag was confirmed by NF-κB signaling in RANK-expressing HEK 293T cells (Fig. S4*E*). Control mice received GST only. Hair-cycle analysis 6 d after injection revealed that three of four mice responded to recombinant RANKL-GST by premature anagen (Fig. 4 *D* and *E*). These findings support the importance of RANK stimulation as a critical hair-cycle entry signal.

RANKL Regulates Epidermal Homeostasis. Because *Rank*-Tg animals express more soluble RANKL but less OPG in the skin, we investigated whether this change would affect the IFE. First, we verified epidermal RANK expression in the Tg mice and found that it was expressed by the basal keratinocytes (Fig. S5*A*). We could exclude the detection of Tg RANK because the Ab is directed against an N-terminal peptide, which is absent from the cDNA construct (Fig. S6). It was apparent that the *Rank*-Tg epithelium was greatly thickened (Fig. 5 *A* and *B*). In contrast, the epidermal size of the *Rankl*-KO mice was slightly but significantly reduced (Fig. 5 *A* and *B*). We therefore determined the epidermal renewal rate by using the thymidine analog BrdU. Proliferating BrdU$^+$ keratinocytes were virtually absent in the *Rankl*-null mice but highly abundant in the IFE of the *Rank*-Tg mice (Fig. 5*C*). Quantification of IFE BrdU$^+$ cells by cell counting on sections uncovered a significant reduction for the *Rankl*-KO mice and a highly significant eightfold increase for the Tg mice (Fig. 5*D*). We next analyzed Tg skin for signs of cell activation by measuring the release of TNFα and IL-1β. As shown in Fig. S5*B*, there was a small but significant increase in TNFα and IL-1β in the Tg skin at P21 and P30, respectively. However, there was no dermal CD3$^+$ T-cell infiltration (Fig. S5*C*), and culturing P21 epidermal keratinocytes resulted in three times more cell recovery after 2 wk compared with WT (Fig. S5*D*). This observation supports a cell-autonomous enhanced proliferation in the Tg mice; however, because of the increased inflammatory cytokine production, we cannot formally exclude their contribution to the accelerated epidermal renewal. Except for keratin 14, which extended beyond its normal restriction in the Tg animals and is likely secondary to the high proliferation rate (39, 40), the differentiation of the IFE in both mouse models was normal as judged by the expression of keratin
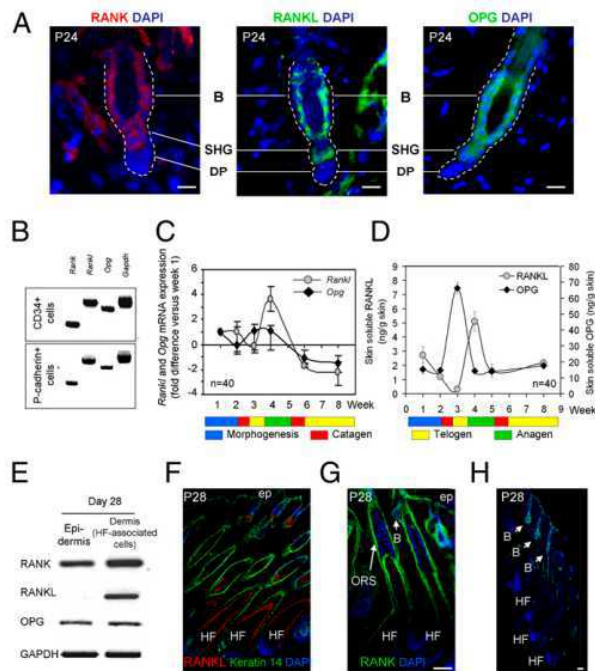
Fig. 3. Expression of RANK, RANKL, and OPG in HF stem cells. (*A*) Localization of RANK, RANKL, and OPG in WT telogen bulge (B) and SHG stem cells by immunofluorescence. Nuclei were colored with DAPI. (Scale bars, 20 μm.) Six mice were analyzed for RANK, RANKL, and OPG. (*B*) RT-PCR of *Rank*, *Rankl*, *Opg*, and *Gapdh* in FACS-sorted CD34+ bulge and P-cadherin+ SHG cells. (*C* and *D*) Measures (mean ± SEM) of *Rankl* and *Opg* gene transcription by quantitative RT-PCR in whole skin (*C*) and of soluble RANKL and OPG by ELISA in skin-organ cultures at the indicated ages (*D*). *n*, number of mice for the analysis, a minimum of six mice per time point. (*E*) RT-PCR of *Rank*, *Rankl*, *Opg*, and *Gapdh* transcripts in the IFE and the HF-associated dermal cells at P28. (*F*) Immunofluorescence of RANKL and keratin 14 on a P28 skin section. Nuclei were colored with DAPI. (*G*) Immunofluorescent labeling for RANK in a P28 skin section with DAPI counterstaining. (*H*) Immunofluorescent labeling for OPG with DAPI coloration in P28 anagen skin. (Scale bars, 50 μm.) ORS, outer root sheath; B, bulge; ep, IFE.

10, loricrin, involucrin, and filaggrin (Fig. S7*A*). Moreover, there was no toluidine blue dye penetration (Fig. S7*B*), demonstrating normal skin barrier function. Finally, we treated Tg mice with anti-RANKL mAb, which, as shown in Fig. 5 *E–G*, resulted in a delay in the hair cycle and a significantly reduced epidermal thickness.

Collectively, these data show that IFE homeostasis occurs normally during anagen when HF RANKL production is high, but that IFE hyperproliferates when RANKL is overproduced.

Discussion

We showed that RANK regulates hair cycling by activating its growth phase: (*i*) although dispensable for HF development, RANK stimulation was required for anagen to normally occur during the fourth week after birth; (*ii*) hair plucking, known to trigger hair renewal, failed to stimulate anagen entry in *Rankl*-null mice; (*iii*) mice with Tg RANK expression in the HF and an altered skin RANKL/OPG ratio displayed advanced hair cycles; and (*iv*) recombinant RANKL induced anagen in WT mice. In addition, we showed that RANK regulates IFE renewal because (*i*) the proliferation rate is reduced in *Rankl*-KO mice but (*ii*) it is increased in the *Rank*-Tg mice and (*iii*) blocking RANKL in *Rank*-Tg mice results in a delay in the hair cycle and a reduced IFE thickness.

Although RANK, RANKL, and OPG are expressed in the IFE and the HF during morphogenesis, we found no visible effect of RANKL on HF and IFE development. This finding, together with the observation that RANK signaling does not affect development of the mammary gland until pregnancy (3), suggests a role of RANK post-embryogenesis. However, embryonic generation of thymic medullary epithelial cells depends on RANKL, yet CD40L can partially compensate after birth (5), suggesting that, if RANK is active in the developing skin, it may be masked by other TNF receptor family members such as Edar or Troy (41–43). Interestingly, lymphotoxin-α—which, like RANKL, functions in lymphoid organ development—also plays a role in HF morphogenesis (44) and is a ligand for Troy (45).

RANK or RANKL were required for the anagen phase of the hair cycle. It is unlikely that the hair-cycle arrest is a reflection of a sickness of these KO mice because they thrive well beyond 6 wk without signs of weakness. Moreover, the hair-plucking experiment was performed on young animals and further demonstrates a genuine block in anagen transition. It remains to be established whether vibrissae hair undergo cycling. The inability to regenerate pelage hair was not the result of defects in the HF stem cell and mesenchymal cell compartment because these cellular elements were present. Indeed, upon transplantation onto a RANKL-proficient environment, *Rankl*−/− skin HFs passed into anagen. The efficiency with which *nude* mice rescued the hair-cycle arrest may be a reflection of the robust RANKL production by activated epidermal keratinocytes or endothelial cells during the healing process (22, 34). In addition, we have found that the anagen HF is an important source of RANKL, and, although *nude* mice lack hair, they have a normal hair telogen–anagen transition.

The expression of RANK, RANKL, and OPG in the HF bulge and SHG supports the importance this protein triad in the control of HF cycling. OPG localization to the bulge and the SHG corroborates previous studies, which have found *Opg* transcription in these cells (20, 21). *Rank* or *Rankl* transcripts were not detected in these studies, probably owing to their low abundance. Indeed, signal amplification was needed to detect RANK and RANKL protein, and soluble RANKL levels were low during telogen. This finding suggests that OPG serves as an autocrine regulator by blocking engagement of RANK by RANKL during telogen.

It is tempting to speculate that, as in the mammary gland (3, 46), HF RANKL is under hormonal control because hair growth is influenced by the endocrine system (47). However, it is unlikely that prolactin or parathyroid hormone related peptide (PTHrp) up-regulate RANKL in the HF because these stimuli antagonize hair renewal and induce catagen in mice (48, 49). However, the *Rankl* promoter contains a number of cell-signaling regulatory elements (NF-κB, Jun/AP-1, vitamin D, and Runx2) (46), allowing it to respond to a multitude of signals known to act on the hair cycle (17, 50, 51). Further work will be necessary to elucidate the impact of these signals on HF RANKL synthesis.

We did not detect any RANK, RANKL, or OPG expression in the DP, which is similar to mammary glands, where stromal cells failed to express RANK or RANKL even after hormonal stimulation (46). However, the mammary gland stromal cells constitutively transcribe *Opg* (46). it is possible that *Opg* is induced in the DP in response to as-yet-unidentified stimuli.

Support for the idea that RANKL and OPG synthesis is subject to changes is provided by their mRNA and protein measures during the hair cycle. It is unlikely that these changes are influenced by tissue injury after the skin excision because RNA extractions were performed immediately on the freshly collected skin, and protein levels closely reflected the mRNA measures. A closer investigation into the site of RANKL production at P28 uncovered that it was synthesized by the lower anagen HF. RT-PCR, mRNA hybridization, and immunofluorescence point to the proliferating matrix and bulb cells as its source, which would concur with RANKL production by activated keratinocytes (22).

Evidence that RANK stimulation by RANKL induces anagen is provided by the precocious anagen phases in mice overexpressing RANK in the HF and in mice administrated with

GENETICS
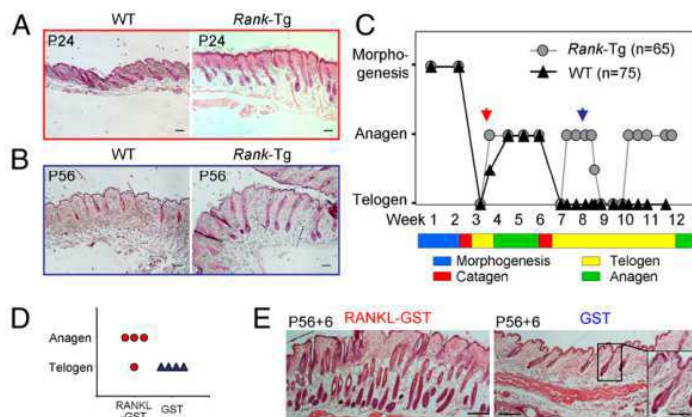
Fig. 4. Precocious anagen entry in *Rank*-Tg mice and in response to recombinant RANKL. (*A*) At P24, WT mice HFs are in anagen II/IIIa, whereas HFs of *Rank*-Tg mice are already in anagen IIIc. (Scale bars, 100 μm.) (*B*) At P56, WT mice HFs are in telogen, whereas HFs of *Rank*-Tg mice are in anagen IV/V. (Scale bars, 100 μm.) (*C*) Schematic representation of hair morphogenesis and the hair-cycle telogen-to-anagen transitions in *Rank*-Tg and control mice. Red arrow points to P24 and blue arrow points to P56, corresponding to images in *A* and *B*. (*D*) At 8 wk, WT mice received two s.c. injections of 100 μg of RANKL-GST or control GST with a 12-h interval. Then, 6 d later, their back skin was analyzed for anagen. Graphic representation that three of four treated mice precociously entered anagen, in contrast to control mice remaining in telogen. (*E*) Image of HFs in anagen of a RANKL-GST–treated mouse, whereas they are in telogen in the GST control mouse. (Scale bars, 100 μm; in *Inset*, 50 μm.) The paraffin-embedded sections were stained with hematoxylin/eosin.

recombinant RANKL. The overexpression of RANK in the SHG may be particularly effective in inducing hair cycling in view of the importance of these cells in anagen entry (21, 30). In addition, there was an increase in RANKL levels and a reduction in OPG. The underlying reasons for the changes in RANKL and OPG synthesis are currently unclear. One possibility may be that the overexpression of RANK in the HF triggers RANKL through a positive feedback loop. Such a loop, not uncommon in the TNF family, may be mediated by NF-κB.

Because the IFE basal-layer keratinocytes also express RANK, we studied the IFE for changes in *Rankl*-KO and *Rank*-Tg animals. We found that, in the *Rankl*$^{-/-}$ mice, epidermal thickness and cell growth were reduced, whereas the epidermis was thickened and cell proliferation was greatly accelerated in the *Rank*-Tg mice. In neither model did we find a marked defect in epidermal differentiation or barrier function, demonstrating that RANK has little impact on this process. The extended keratin 14 expression to suprabasal layers in the Tg animals is likely owing to the hyperproliferation because suprabasal keratin 14 expression is also seen in other mouse models of accelerated epidermal growth (39, 40). We could detect an increase in TNFα and IL-1β production from Tg skin; however, more keratinocytes were recovered after a 15-d culture of primary cutaneous keratinocytes from Tg mice, which suggests a cell-autonomous enhanced keratinocyte proliferation. More work is needed to further clarify the role of these cytokines on keratinocyte activation.

The underlying molecular mechanism for epithelial activation of the epidermo-pilosebaceous unit by RANK is currently un-

clear. Because RANK is a potent NF-κB stimulator and because NF-κB has been implicated in the regulation of HF cycling (52) as well as in epidermal turnover (53), we had first postulated that RANK triggers the NF-κB pathway in skin epithelial cells. However, we could not obtain any evidence for NF-κB activation either in the HF or in the IFE. RANK has also been shown to engage the signaling cascades, implicating JNK, Id-2, Akt, and NFATc1 (54), but, again, we could not observe any evidence that these signaling flows were elicited. Moreover, mice deficient in TRAF6, a signaling module of the NF-κB and JNK pathway, display a phenotype similar to that of *Eda*-null mice but not of *Rankl*$^{-/-}$ animals (55). Therefore, the molecular signaling pathways engaged by RANK in the HF and the IFE remain to be uncovered. Our findings, together with the cyclic renewal of the HF on one side and the continuous homeostasis of the IFE on the other, provide a valuable model system to dissect the signaling pathways triggered by RANK in epithelial (stem) cells.

The herein revealed function of RANK in murine hair-cycle control and epidermal homeostasis further underpins the shared molecular controls of two seemingly distant organs, skin and bone (18), and introduces the RANK–RANKL–OPG triad as a key player in the control of epithelial stem cell biology.

Materials and Methods

Animals. PCR primers for genotyping are listed in Table S1.

Histology/Immunofluorescence. Primary Abs are listed in Table S2.
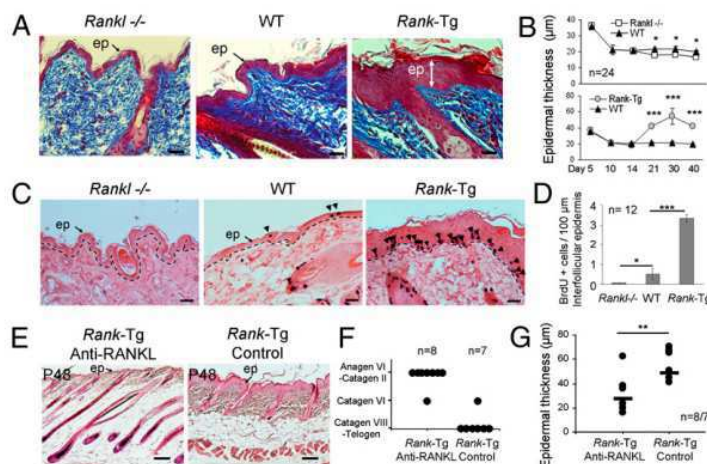
Fig. 5. RANK regulates epidermal homeostasis. (*A*) Different epidermal thickness of skin of 4-wk-old *Rankl*$^{-/-}$, WT, and *Rank*-Tg mice, visualized on fixed, paraffin-embedded sections stained with Masson's trichrome. (Scale bars, 20 μm.) (*B*) Epithelial thickness was measured on 10 randomly chosen images from four mice of each genotype per time point. Data are mean ± SD. (*C*) Identification (arrowheads) of BrdU$^+$ proliferating IFE cells on skin sections stained with eosin. (Scale bars, 20 μm.) (*D*) Graph shows the number of BrdU$^+$ IFE keratinocytes for each mouse. Data are mean ± SD. (*E*) Tg mice received anti-RANKL mAb or were mock-injected (control) every 3 d from P10 to P45. Skins were analyzed for HF cycle and epidermal size on sections stained with hematoxylin/eosin. (Scale bars, 50 μm.) (*F*) Schematic representation of the HF stage of eight treated and seven control mice. (*G*) Epidermal thickness measures of eight treated and seven control Tg mice. (Bars = mean values.) ep, IFE. *$P < 0.05$; **$P < 0.01$; ***$P < 0.001$.

RT-PCR. Classic and real-time PCR primers are listed in Table S3. Detailed experimental protocols for cell proliferation, ELISA, flow cytometry, in situ hybridization, RANK signaling assay, skin cytokine production, primary keratinocyte culture, and epidermal barrier tests are provided in *SI Materials and Methods*.

1. Walsh MC, Choi Y (2003) Biology of the TRANCE axis. *Cytokine Growth Factor Rev* 14: 251–263.
2. Tanaka S, Nakamura K, Takahasi N, Suda T (2005) Role of RANKL in physiological and pathological bone resorption and therapeutics targeting the RANKL–RANK signaling system. *Immunol Rev* 208:30–49.
3. Fata JE, et al. (2000) The osteoclast differentiation factor osteoprotegerin-ligand is essential for mammary gland development. *Cell* 103:41–50.
4. Beleut M, et al. (2010) Two distinct mechanisms underlie progesterone-induced proliferation in the mammary gland. *Proc Natl Acad Sci USA* 107:2989–2994.
5. Akiyama T, et al. (2008) The tumor necrosis factor family receptors RANK and CD40 cooperatively establish the thymic medullary microenvironment and self-tolerance. *Immunity* 29:423–437.
6. Knoop KA, et al. (2009) RANKL is necessary and sufficient to initiate development of antigen-sampling M cells in the intestinal epithelium. *J Immunol* 183: 5738–5747.
7. Luo JL, et al. (2007) Nuclear cytokine-activated IKKα controls prostate cancer metastasis by repressing Maspin. *Nature* 446:690–694.
8. Schramek D, et al. (2010) Osteoclast differentiation factor RANKL controls development of progestin-driven mammary cancer. *Nature* 468:98–102.
9. Gonzalez-Suarez E, et al. (2010) RANK ligand mediates progestin-induced mammary epithelial proliferation and carcinogenesis. *Nature* 468:103–107.
10. Paus R, Cotsarelis G (1999) The biology of hair follicles. *N Engl J Med* 341:491–497.
11. Cotsarelis G (2006) Epithelial stem cells: A folliculocentric view. *J Invest Dermatol* 126: 1459–1468.
12. Fuchs E (2007) Scratching the surface of skin development. *Nature* 445:834–842.
13. Blanpain C, Horsley V, Fuchs E (2007) Epithelial stem cells: Turning over new leaves. *Cell* 128:445–458.
14. Watt FM, Hogan BL (2000) Out of Eden: Stem cells and their niches. *Science* 287: 1427–1430.
15. Morgan BA (2008) A glorious revolution in stem cell biology. *Nat Genet* 40: 1269–1270.
16. Plikus MV, Widelitz RB, Maxson R, Chuong CM (2009) Analyses of regenerative wave patterns in adult hair follicle populations reveal macro-environmental regulation of stem cell activity. *Int J Dev Biol* 53:857–868.
17. Schneider MR, Schmidt-Ullrich R, Paus R (2009) The hair follicle as a dynamic miniorgan. *Curr Biol* 19:R132–R142.
18. Ross FP, Christiano AM (2006) Nothing but skin and bone. *J Clin Invest* 116:1140–1149.
19. Kong YY, et al. (1999) OPGL is a key regulator of osteoclastogenesis, lymphocyte development and lymph-node organogenesis. *Nature* 397:315–323.
20. Morris RJ, et al. (2004) Capturing and profiling adult hair follicle stem cells. *Nat Biotechnol* 22:411–417.
21. Greco V, et al. (2009) A two-step mechanism for stem cell activation during hair regeneration. *Cell Stem Cell* 4:155–169.
22. Loser K, et al. (2006) Epidermal RANKL controls regulatory T-cell numbers via activation of dendritic cells. *Nat Med* 12:1372–1379.
23. Barbaroux JB, Beleut M, Brisken C, Mueller CG, Groves RW (2008) Epidermal receptor activator of NF-κB ligand controls Langerhans cells numbers and proliferation. *J Immunol* 181:1103–1108.
24. Kartsogiannis V, et al. (1999) Localization of RANKL (receptor activator of NFκB ligand) mRNA and protein in skeletal and extraskeletal tissues. *Bone* 25:525–534.
25. Paus R, et al. (1999) A comprehensive guide for the recognition and classification of distinct stages of hair follicle morphogenesis. *J Invest Dermatol* 113:523–532.
26. Müller-Röver S, et al. (2001) A comprehensive guide for the accurate classification of murine hair follicles in distinct hair cycle stages. *J Invest Dermatol* 117:3–15.
27. Bossen C, et al. (2006) Interactions of tumor necrosis factor (TNF) and TNF receptor family members in the mouse and human. *J Biol Chem* 281:13964–13971.
28. Wilson C, et al. (1994) Cells within the bulge region of mouse hair follicle transiently proliferate during early anagen: Heterogeneity and functional differences of various hair cycles. *Differentiation* 55:127–136.
29. Panteleyev AA, Jahoda CA, Christiano AM (2001) Hair follicle predetermination. *J Cell Sci* 114:3419–3431.
30. Jaks V, et al. (2008) Lgr5 marks cycling, yet long-lived, hair follicle stem cells. *Nat Genet* 40:1291–1299.
31. Tumbar T, et al. (2004) Defining the epithelial stem cell niche in skin. *Science* 303: 359–363.
32. Jahoda CA, Reynolds AJ (1996) Dermal-epidermal interactions. Adult follicle-derived cell populations and hair growth. *Dermatol Clin* 14:573–583.
33. Handjiski BK, Eichmüller S, Hofmann U, Czarnetzki BM, Paus R (1994) Alkaline phosphatase activity and localization during the murine hair cycle. *Br J Dermatol* 131: 303–310.
34. Collin-Osdoby P, et al. (2001) Receptor activator of NF-κB and osteoprotegerin expression by human microvascular endothelial cells, regulation by inflammatory cytokines, and role in human osteoclastogenesis. *J Biol Chem* 276:20659–20672.
35. Kaufman CK, et al. (2003) GATA-3: An unexpected regulator of cell lineage determination in skin. *Genes Dev* 17:2108–2122.
36. Schmidt M, et al. (2001) Selective expression of calcium-binding proteins S100a8 and S100a9 at distinct sites of hair follicles. *J Invest Dermatol* 117:748–750.
37. Anderson DM, et al. (1997) A homologue of the TNF receptor and its ligand enhance T-cell growth and dendritic-cell function. *Nature* 390:175–179.
38. Mecklenburg L, Tobin DJ, Cirlan MV, Craciun C, Paus R (2005) Premature termination of hair follicle morphogenesis and accelerated hair follicle cycling in Iasi congenital atrichia (fz^{Ica}) mice points to *fuzzy* as a key element of hair cycle control. *Exp Dermatol* 14:561–570.
39. Hobbs RM, Silva-Vargas V, Groves R, Watt FM (2004) Expression of activated MEK1 in differentiating epidermal cells is sufficient to generate hyperproliferative and inflammatory skin lesions. *J Invest Dermatol* 123:503–515.
40. Pasparakis M, et al. (2002) TNF-mediated inflammatory skin disease in mice with epidermis-specific deletion of IKK2. *Nature* 417:861–866.
41. Mikkola ML (2008) TNF superfamily in skin appendage development. *Cytokine Growth Factor Rev* 19:219–230.
42. Schmidt-Ullrich R, et al. (2006) NF-κB transmits Eda A1/EdaR signalling to activate Shh and cyclin D1 expression, and controls post-initiation hair placode down growth. *Development* 133:1045–1057.
43. Pispa J, Pummila M, Barker PA, Thesleff I, Mikkola ML (2008) Edar and Troy signalling pathways act redundantly to regulate initiation of hair follicle development. *Hum Mol Genet* 17:3380–3391.
44. Cui CY, et al. (2006) Ectodysplasin regulates the lymphotoxin-β pathway for hair differentiation. *Proc Natl Acad Sci USA* 103:9142–9147.
45. Hashimoto T, Schlessinger D, Cui CY (2008) Troy binding to lymphotoxin-α activates NFκB mediated transcription. *Cell Cycle* 7:106–111.
46. Srivastava S, et al. (2003) Receptor activator of NF-κB ligand induction via Jak2 and Stat5a in mammary epithelial cells. *J Biol Chem* 278:46171–46178.
47. Randall VA (2007) Hormonal regulation of hair follicles exhibits a biological paradox. *Semin Cell Dev Biol* 18:274–285.
48. Schilli MB, Ray S, Paus R, Obi-Tabot E, Holick MF (1997) Control of hair growth with parathyroid hormone (7-34). *J Invest Dermatol* 108:928–932.
49. Foitzik K, et al. (2003) Prolactin and its receptor are expressed in murine hair follicle epithelium, show hair cycle-dependent expression, and induce catagen. *Am J Pathol* 162:1611–1621.
50. Li M, et al. (2000) Skin abnormalities generated by temporally controlled RXRα mutations in mouse epidermis. *Nature* 407:633–636.
51. Demay MB, et al. (2007) Role of the vitamin D receptor in hair follicle biology. *J Steroid Biochem Mol Biol* 103:344–346.
52. Zhang Y, et al. (2009) Reciprocal requirements for EDA/EDAR/NF-κB and Wnt/β-catenin signaling pathways in hair follicle induction. *Dev Cell* 17:49–61.
53. Pasparakis M (2009) Regulation of tissue homeostasis by NF-κB signalling: Implications for inflammatory diseases. *Nat Rev Immunol* 9:778–788.
54. Wada T, Nakashima T, Hiroshi N, Penninger JM (2006) RANKL–RANK signaling in osteoclastogenesis and bone disease. *Trends Mol Med* 12:17–25.
55. Naito A, et al. (2002) TRAF6-deficient mice display hypohidrotic ectodermal dysplasia. *Proc Natl Acad Sci USA* 99:8766–8771.

GENETICS

Supporting Information

Duheron et al. 10.1073/pnas.1013054108

SI Materials and Methods

Animals. Mice were kept in a pathogen-free barrier facility following faculty guidelines and within its animal bioethics accord (approval no. AL/01/20/11/08). The $Rankl^{-/-}$ mice were identified by lack of teeth, smaller size, and genomic DNA PCR (Table S1). The $Rank^{-/-}$ mice skin samples were kindly provided by Graham Anderson (University of Birmingham, Birmingham, UK). The $Rank$-Tg mice were genotyped by PCR (Table S1). For skin transplantation, hair was cut and skin was excised, transplanted onto *nude* mice (Harlan), and sutured. A healing spray was applied. Hair plucking was performed on anesthetized mice. At 8 wk, C57BL/6 mice received two s.c. injections of 100 μg of RANKL-GST or control GST in the neck region with a 12-h interval. Anti-RANKL mAb (IK22-5) (1) was injected s.c. into Tg mice every 3 d: 10 μg at P10, 25 μg from P13 to P28, and 50 μg from P31 to P45.

Histology/Immunofluorescence. Dorsal skin was fixed in formalin and embedded in paraffin. Sections (6 μm) were deparaffinized and stained with hematoxylin/eosin or Masson's trichrome (Sigma-Aldrich). Alternatively, skin was frozen in Tissue-Tek O.C.T. Compound (Delta Microscopie), and sections were fixed in acetone, blocked with goat or donkey serum (Sigma-Aldrich), and then incubated overnight at 4 °C with primary Abs (Table S2) diluted in buffered saline. Fluorochrome-labeled secondary Abs (Molecular Probes; Invitrogen) were incubated for 1 h at room temperature. Frozen sections were fixed in formalin before DAPI staining (Molecular Probes; Invitrogen). Tyramide signal amplification (PerkinElmer) was used to visualize RANK and RANKL in WT mice. To reveal endogenous alkaline phosphatase, the frozen sections were incubated with 5-bromo-4-chloro-3-indolyl phosphate (BCIP) and nitroblue tetrasodium (Pierce; Thermo Scientific).

RT-PCR. RNA from sorted bulge and SHG cells (2) was extracted with RNeasy Micro (Qiagen). The cDNA was synthesized and amplified by using the QuantiTect Whole Transcriptome protocol (Qiagen). For epidermal–dermal separation, hair was trimmed with scissors and hair-removal cream (Nair) was applied. After 5 min, the hair-cream emulsion was washed off, and the skin was incubated for 4 h at 37 °C with 1 mg/mL dispase II (Roche Diagnostics). The epidermis was then carefully removed with forceps. Snap-frozen IFE, HF-associated cells (dermis), or whole skin were ground with a pestle and mortar, filled with liquid nitrogen, and placed in dry ice. RNA was extracted from the obtained powder with the Ambion TRI Reagent (Applied Biosystems) and cleaned with RNeasy (Qiagen). The cDNA was synthesized by using ImProm-II RT and oligo(dT)$_{15}$ primer (Promega). Classic and real-time PCR were performed with gene-specific primers (Table S3). The real-time PCR reactions were run using the Eurogentec qPCR MasterMix Plus Low ROX on a Stratagene MX4000 thermal cycler. The CT values of target genes were normalized to GAPDH and β-actin (Applied Biosystems primers). The expression factor was calculated by using the Relative Expression Software Tool (REST; http://www.gene-quantification.de/rest.html).

Cell Proliferation. To visualize proliferating cells, mice were injected i.p. with 1 mg of BrdU (Sigma-Aldrich) at 3 h before they were killed. Dorsal skin tissues were fixed in formalin and embedded in paraffin. Antigen retrieval was in boiling-hot citrate buffer, pH 6.0, for 10 min, and endogenous peroxidase was in-hibited in 3% H_2O_2. The anti-BrdU Ab was incubated overnight at 4 °C. The sections were incubated with goat anti-rat IgG biotin-conjugated secondary Ab at room temperature, followed by horseradish-conjugated ABC complex (Vector Labs). Labeling was revealed with diaminobenzidine-Ni and stopped with distilled water. Sections were counterstained with eosin.

ELISA. Dorsal mouse skin was excised and weighted. It was floated on complete cell-culture medium for 24 h at 37 °C. The cell-free culture medium was sterile-filtered, and soluble RANKL and OPG were measured by ELISA (DuoSet ELISA; R&D Systems). The results were normalized to skin weight.

Flow Cytometry. HF cells were liberated from skin as previously described (2). They were stained for CD34, revealed by an Alexa Fluor 647 goat anti-rat secondary Ab (Molecular Probes; Invitrogen), fixed, permeabilized, and stained for keratin 14, revealed by a FITC donkey anti-rabbit secondary Ab (Molecular Probes; Invitrogen). The cells were analyzed with a FACSCalibur (Becton Dickinson). For sorting, the cells were also labeled for P-cadherin followed by allophycocyanin/streptavidin and sorted on a FACSAria II cell sorter (Becton Dickinson) into $CD34^+$ bulge and P-cadherin SHG cells. Further experimental details for in situ hybridization, RANK signaling assay, skin cytokine production, primary keratinocyte culture, and epidermal barrier test are available in *SI Materials and Methods*.

In Situ Hybridization. In situ hybridization of receptor activator of NF-κB (RANK) and RANK ligand (RANKL) mRNA was performed by using digoxigenin-UTP–labeled sense and antisense mRNA probes, as previously described (1). The signal was developed with 5-bromo-4-chloro-3-indolyl phosphate (BCIP) and nitroblue tetrasodium (Kirkegaard and Perry) for between 1 and 2 d at room temperature in the dark.

RANK Signaling Assay. The murine endogenous and Tg *Rank* cDNA was amplified from WT and *Rank*-Tg skin cDNA and cloned into pCR3.1 (Invitrogen) under the control of the CMV promoter. HEK 293T cells were either transiently transfected with FuGENE (Roche), or a stable cell line was obtained under G418 selection. For the NF-κB signaling assay, the NF-κB1 luciferase reporter vector (Panomics) was transiently transfected, and RANKL-GST was added 24 h later. Luciferase activity was measured 24 h later by following the manufacturer's instructions (Promega).

Skin Cytokine Production. Skin from WT and *Rank*-Tg mice was weighed and floated, hairy side up, on cell-culture medium containing 10% FCS (Invitrogen), antibiotics, and fungicides in a cell-culture incubator for 24 h at 37 °C. The cell-free culture medium was sterile-filtered. TNFα and IL-1-β ELISA were performed with anti-TNFα Abs from BD Biosciences and the DuoSet ELISA kit (R&D Systems) for IL-1β.

Primary Keratinocyte Culture. Hair from 21-d-old WT and *Rank*-Tg mice was removed (Nair) and digested with dispase II (Roche) for 18 h at 4 °C. The epidermis was peeled off and trypsinized (Gibco-Invitrogen) for 30 min at room temperature to liberate basal keratinocytes. These cells were then placed in culture in low-calcium keratinocyte growth medium (CnT 57; CELLnTEC) at an initial cell density of 6×10^3 cells cm^{-2}. Cultures were kept in 5% CO_2/95% humidity at 37 °C for 15 d with medium changed every 4 d. Cells were detached with trypsin and counted.

Epidermal Barrier Test. Killed 8-wk-old Tg and WT mice were shaven, and their skin was cut with scissors at the dorsum. They were then dehydrated in successive steps in methanol and, after rehydration, bathed in 0.01% toluidine blue for 1 min. After washing in water, hair was completely removed with depilation cream (Nair), and mice were photographed.

1. Kamijo S, et al. (2006) Amelioration of bone loss in collagen-induced arthritis by neutralizing anti-RANKL monoclonal antibody. *Biochem Biophys Res Commun* 347: 124–132.
2. Greco V, et al. (2009) A two-step mechanism for stem cell activation during hair regeneration. *Cell Stem Cell* 4:155–169.
3. Mueller CG, et al. (2001) Mannose receptor ligand-positive cells express the metalloprotease decysin in the B cell follicle. *J Immunol* 167:5052–5060.
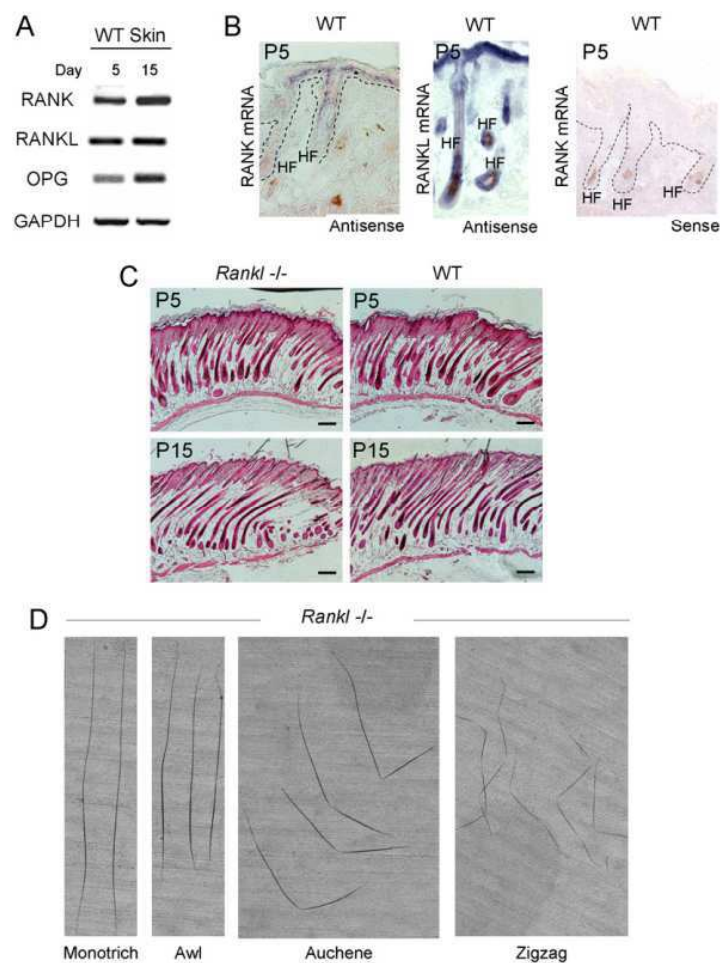
Fig. S1. (*A*) RT-PCR of *Rank*, *Rankl*, *Opg*, and *Gapdh* transcripts in the skin of 5- and 15-d-old mice. (*B*) In situ hybridization for RANK and RANKL mRNA (antisense) or control (RANK sense) at postnatal day 5 (P5). (*C*) Normal hair follicle (HF) morphogenesis of *Rankl*^{−/−} mice, displaying early anagen at P5 and normal hair-cycle entry with catagen II at P15. (Scale bars, 100 μm.) (*D*) Presence of all four hair types (monotrich, awl, auchene, and zigzag) in a 45-d-old *Rankl*^{−/−} mouse.

Fig. S2. (*A*) *Rankl*$^{-/-}$ HFs fail to enter anagen at P40 or P45. WT HFs are in catagen VII at P40 and in the second telogen at P45 (with club hair present). (Scale bars, 100 μm.) (*B*) *Rankl*$^{-/-}$ HFs fail to enter anagen at P25. Back skin of *Rankl*$^{-/-}$ mouse and WT littermate were analyzed for initiation of HF renewal at an age when anagen II is apparent. (Scale bars, 200 μm.) The paraffin-embedded sections were stained with hematoxylin/eosin.

Fig. S3. (*A*) Immunofluorescence of RANKL and GATA-3 of an anagen HF. Nuclei were colored with DAPI. (Scale bar, 30 μm.) (*B*) In situ hybridization for RANKL mRNA (antisense) or control (sense) on P28 anagen skin. (*C*) Identification of a rare RANKL$^+$ cell by anti-RANKL immunolabeling in P28 WT epidermis with DAPI counterstaining. (Scale bars, 10 μm.) Asterisk indicates unspecific staining of the stratum corneum; dashed line indicates the dermo-epidermal junction. (*D*) Skin sections of P28 WT mice show CD34–RANK and integrin α6–RANK double-labeled HF bulge stem cells (arrows). Nuclei were colored with DAPI. Arrows point to the bulge. (Scale bars, 20 μm.) (*E*) Skin section of a P21 WT mouse stained for osteoprotegerin (OPG) shows the protein in the bulge, secondary hair germ (SHG), and basal keratinocytes (arrow). Asterisk indicates unspecific labeling of the stratum corneum. ep, interfollicular epidermis (IFE). (Scale bars, 20 μm.)

Fig. S4. (*A*) Overexpression of RANK (arrowhead) under control of the S100A8 gene promoter in the P-cadherin+ SHG. Nuclei were colored with DAPI. B, bulge. (Scale bar, 20 μm.) (*B*) Tg RANK induces NF-κB signaling. HEK 293T cells were transiently transfected with the *Rank*-Tg expression plasmid and a luciferase expression plasmid under NF-κB control. Cells were stimulated with recombinant RANKL. The NF-κB promoter activity is expressed as the fold increase of luciferase units with respect to cells having received the NF-κB reporter plasmid only. The data are representative of three experiments. (*C*) Measures (mean ± SEM) of soluble RANKL and OPG protein by ELISA in skin-organ cultures, at the indicated ages in *Rank*-Tg and control (WT) mice. (*D*) Three-month-old Rank-Tg mice display mild alopecia compared with control littermates. (*E*) HEK 293T cells stably expressing RANK and transfected with the NF-κB reporter plasmid were stimulated with different concentrations of RANKL-GST. The data are expressed as the fold increase of luciferase units with respect to nonstimulated cells. Data are the mean of triplicates and are representative of three experiments.

Fig. S5. (*A*) Immunolocalization of endogenous RANK to basal keratinocytes in WT and *Rank*-Tg mice. Control was antigen-unspecific goat Ig. Nuclei were colored with DAPI. (Scale bars, 10 μm.) Asterisk indicates unspecific staining of the stratum corneum; dashed lines indicate the dermo-epidermal junction. (*B*) TNFα and IL-1β were measured by ELISA in supernatants of 24-h skin-organ cultures of *Rank*-Tg and WT mice at different ages. The cytokine levels were normalized to skin weight. Each data point represents one mouse, and bars represent the mean value (± SD in vertical bars). **$P < 0.01$. (*C*) Immunolabeling of CD3⁺ T cells (arrows) in skin of WT and *Rank*-Tg mice. Counterstaining was with DAPI. Asterisk indicates unspecific labeling of the stratum corneum; dashed lines indicate the dermo-epidermal junction. The images are representative of at least three mice of each group. (Scale bars, 20 μm.) (*D*) Increased cell recovery of primary epidermal keratinocytes of 3-wk-old *Rank*-Tg mice compared with WT controls at 15 d after seeding into low-calcium keratinocyte growth medium. The data are the mean ± SD of duplicates and are representative of three experiments. **$P < 0.01$.

tattgcccagcaaatgccttcctctttccgcttctcctacctccccacccaaaattttcattctgcacagtgattgccacattcactggttgagaaacagagactgtagcaactctggcagggagaagctgtctctgatggcctgaagctgtgggcagctggccaa

gcctaaccgctataaaaaggagctgcctctcagccctgcatgtctcttgtcagctgtctttcagaagacctggtaagtgggactgtctgggttggctccgcactttgggcttctcttggggagggtcagggaagtggagcagccttcctgagagaggagaga

Exon 1

gaaagctcagggaggtctggagcaaagatactcctggaggtggggagtgaggcagggataaggaaggagagtatcctccagcaccttccagtgggtaagggcacattgtctcctaggctggactttcttgagcagagggtggggtggtaaggaaagtc

tacgggcccccgtgtgtgtgcacatgtctctgtgtgaatggaccctccccttcccacacgtgtatcctatcatcccaccccttccaccagaggccatagccatctgctggtttggttatttgagagtgcaggccaggaccaaggccatcgcttggggcatgaa

Exon 2   M S A L L I L A L V G A A V A D Y K D D D D

tcctctgcgtactgccctggccagatgcaaattccctgccatggggattccccagaaggttctgttttcaggtggggcaagttccgtgggcgatccaccatgtctgcacttctgatcctagctcttgttggagctgcagttgctgactacaaagacgatgacgaca

K L A A A Q V T P P C T Q E R H Y E H L G R C C S R C E P G K Y L S S K C T P T S D S V C L P C G P D E Y L

agctcgcggccgcgcaggtcactcctccatgcacccaggagaggcattatgagcatctcggacggtgttgcagcagatgcgaaccaggaaagtacctgtcctctaagtgcactcctacctccgacagtgtgtgtctgccctgtggccccgatgagtacttg

D T W N E E D K C L L H K V C D A G K A L V A V D P G N H T A P R R C A C T A G Y H W N S D C E C C R R N

gacacctggaatgaagaagataaatgcttgctgcataaagtctgtgatgcaggcaagaagcctggtggcggtggatcctggcaaccacacggcccccgcgtcgctgtgcttgcacggctggctaccactggaactcagactgcgagtgctgccgcaggaac

T E C A P G F G A Q H P L Q L N K D T V C T P C L L G F F S D V F S S T D K C K P W T N C T L L G K L E A H Q

acggagtgtgcacctggcttcggagctcagcatccctgcagctcaacaaggatccggtgtgcacaccctgcctcctggcttcttctcagatgtctttcgtccacagacaaatgcaaaccttggaccaactgcacctccttggaaagctagaagcacacca

G T T E S D V V C S S S M T L R R P P K E A Q A Y L P S L I V L L L F I S V V V V A A I I F G V Y Y R K G G

ggggacaacggaatcagatgtggtctgcagctcttccatgacactgaggagaccacccaaggaggcccaggcttacctgcccagtctcatcgttctgctcctcttcatctctgtggtagtagtggctgccatcatcttcggcgtttactacaggaagggaggga

K A L T A N L W N W V N D A C S S L S G N K E S S G D R C A G S H S A T S S Q Q E V C E G I L L M T R E E K M

aagcgctgacagctaatttgtggaattgggtcaatgatgcttgcagtagtctaagtggaaataaggagtcctcagggggaccgttgtctggttcccactcgagcaacctccagtcagcaagaagtgtgtgaaggtatcttactaatgactcgggaggagaagat

V P E D G A G V C G P V C A A G G P W A E V R D S R T F T L V S E V E T Q G D L S R K I P T E D E Y T D

ggttccagaagacggtgctggagtctgtgggcctgtgtgtgcggcaggtgggccctgggcagaagtcagagattctaggacgttcacactggtcagcaggttgagacgcaaggagacctctcggaggagattcccacagaggtgagtacacggacc

R P S Q P S T G S L L L I Q Q G S K S I P P F Q E P L E V G E N D S L S Q C F T G T E S T V D S E G C D F T

ggccctcgcagccttcgactggttcactgctcctaatccagcagggaagcaaatctataccccattccaggagccccctggaagtggggagaacgacagtttaagccagtgtttcaccgggactgaaagcacggtggattctgagggctgtgacttcactg

E P P S R T D S M P V S P E K H L T K E I E G D S C L P W V V S S N S T D G Y T G S G N T P G E D H E P F P

agcctccgagcagacagactgactctatgcccgtgtccctgaaaagcacctgacaaangaaatagaaggtgacagttgcctccctgggtggtcagctccaactcaacagatggctacacaggcagtgggaacactcctggggaggaccatgaaccctttcc

G S L K C G P L P Q C A Y S M G F P S E A A A S M A E A G V R P Q D R A D E K G A S G S G S S P S D Q P

agggtcctgaaatgtggaccattgccccagtgtgcctacagcatgggcttttccagtgaagcagcagccagcatggcagaggcggggagtacggccccaggacagggctgatgagaagggagcctcagggtccgggagctccccagtgaccagcc

P A S G N V T G N S N S T F I S S G Q V M N F K G D I I V V Y V S Q T S Q E G P G S A E P E S E P V G R P

acctgcctctgtggaacgtgactggaaacagtaactccacgttcatctctgtacgggcaggtgatgaacttcaanggtgacatcatcgtggtgtatgtcagccagacctcgcagggagggggcccgggttccgcagagcccgagtcggagcccgtgggccgccct

V Q E E T L A H R D S F A G T A P R F P D V C A T G A G L Q E Q G A P R Q K D G T S R P V Q E Q G G A

gtgcaggaggagacgctggcacacagagactcctttgcgggcaaccgcgccgcgcgcttcccccgacgtctgtgccaccgggggctgggctgcaggagcagggggcaccccggcagaaggacgggacatcgcggccggtgcaggagcaggggtggggcg

Q T S L H T Q G S G Q C A E Stop

cagacttcactccataccaggggtccggacaatgtgcagaatga

Human *S100A8*

FLAG

Mouse Rank

Fig. S6. Sequence of the mouse *Rank*-Tg construct.

Fig. S7. (A) Immunolocalization of cytokeratin 14, cytokeratin 10, loricrin, involucrin, filaggrin, and DAPI nuclear staining of the skin of *Rankl*^{−/−}, WT, and *Rank*-Tg mice. (Scale bars, 20 μm.) Dashed lines indicate the dermo-epidermal junction. ep, IFE. (B) Epidermal barrier test with toluidine blue. Killed 8-wk-old Tg and WT mice were shaven, and their skin was cut with scissors at the indicated site before the toluidine blue penetration test. Of note, the Tg mouse is in anagen at 8 wk, rendering the skin dark.

Table S1. Genotyping PCR primers

Primer	Sequence (5′ to 3′)
Rankl^{−/−}	Forward: ccaagtagtggattctaaatcctg
	Reverse 1: ggttggacacctgaatgctaatttc (345 bp)
	Reverse 2: attcgcagcgcatcgccttctatcg (575 bp)
Rank-Tg	Forward: atggactacaaagacgatgacgaca
	Reverse: tgccaggaatccaccgccaccag (264 bp)

Table S2. Primary antibodies

Target	Species	Clone or designation	Conjugation	Application	Vendor	Dilution factor
Endogenous						
RANK*	Goat	N20 SC-7626	Purified	IF (Frozen)	Santa Cruz, CliniSciences	1/200
Tg						
RANK	Goat	AF 692	Purified	IF (Frozen)	R&D Systems	1/200
RANKL*	Goat	AF 462	Purified	IF(Frozen)	R&D Systems	1/100
OPG	Mouse	OPG4-1	Ascite	IF(Frozen)	Alexis, Axxora, Coger	1/2,000
CD34	Rat	14-0341	Purified	IF/FACS	eBioscience, CliniSciences	1/150
P-cadherin	Goat	BAF 761	Biotin	IF/FACS	R&D Systems	1/100
						1/20,000
GATA-3	Mouse	HG3-31 SC-268	Purified	IF	Santa Cruz	1/200
Integrin α6	Rat	19765	Purified	IF	Abcam	1/50
Filaggrin	Rabbit	PRB-417P	Purified	IF	Covance, Eurogentec	1/2,000
Keratin 10	Rabbit	PRB-159P	Purified	IF	Covance	1/2,000
Keratin 14	Rabbit	PRB-155P	Purified	IF/FACS	Covance	1/2,000
Loricrin	Rabbit	PRB-145P	Purified	IF	Covance	1/2,000
Involucrin	Rabbit	PRB-140C	Purified	IF	Covance	1/2,000
BrdU	Rat	AbC117-7513	Purified	IHC	AbCys	1/100
CD3ε	Rat	145-2C11	Purified	IHC	BD Biosciences	1/200

IF, immunofluorescence; IHC, immunohistochemistry.
*Signal enhancement with the Tyramide amplification system (Dupont) of endogenous RANK and endogenous RANKL in telogen HFs and epidermis.

Table S3. RT-PCR primers

Primer	Sequence (5′ to 3′)
RANK	Forward: tgc gtg ctg ctc gtt cca
	Reverse: tgc cag gat cca ccg cca cca g (262 bp)
RANKL	Forward: agc atc gct ctg ttc ctg t
	Reverse: tcg tgc tcc ctc ctt tca tc (592 bp)
Real-time PCR	Forward: cag cat cgc tct gtt cct gt
	Reverse: gca gtg agt gct gtc ttc tga
	Probe: tcg agc gca gat gga tcc taa cag aa
OPG	Forward: tga tga gtg tgt gta ttg cag c
	Reverse: tct cta cac tct cgg cat tc (485 bp)
Real-time PCR	Forward: cga gga cca caa tga aca agt g
	Reverse: tgg gtt gtc cat tca atg atg t
	Probe: ctg tgc tgc gca ctc ctg gtg ct
GAPDH	Forward: tcc atg aca act ttg gta tcg tgg
	Reverse: gtc gct gtt gaa gtc aga gga gac (695 bp)

1.3. Conclusions

In this work we have demonstrated, for the first time, a function of RANK in hair cycling and epidermal homeostasis. Mice deficient for RANKL are unable to initiate a new hair follicle growth phase, whereas over-expression of RANK in the hair follicle stem cells and application of recombinant RANKL induces precocious growth. RANK, RANKL and OPG are expressed by hair follicle stem cells, and RANKL expression is upregulated by the hair follicle at the initiation of anagen, providing a mechanism by which RANK engagement of stem cells by RANKL induces anagen entry. Moreover, RANKL-knockout mice display arrested epidermal homeostasis, whereas epidermal growth is accelerated in RANK-transgenic mice. The proliferating epidermal basal cells express RANK. Thus, RANK-RANKL-OPG, previously described for their function in bone, the immune system and in mammary glands, also regulate hair cycling and epidermal homeostasis.

2. RANK in the regulation of lymph node homeostasis

2.1. *Introduction*

During embryogenesis, RANK is required for Lymphoid Tissue inducer cells (LTics) survival and/or proliferation in LN anlagen. Interaction between $LT\alpha_1\beta_2$ expressed by LTics and LTβR displayed by stromal organizer cells induces chemokines and adhesion molecules expression required for LN development. In the absence of either RANK or LTβR signaling, LNs do not form. In addition to its function during embryogenesis, LTβR is also required for B cell follicle organization in the adult. Although some data strongly suggest a similar function for RANK, no comparable study to those conducted with LTβR have been carried with RANK. This led us to address the question of the function of RANK in secondary lymphoid organs post-natally. During our study, we were also attentive to endothelial cells, since RANK is expressed by these cells and has pro-angiogenic activity.

We used the *Rank*-transgenic murine model described in Article 1, which express its transgene in hair follicle stem cells and over-produces hair follicle RANKL. The study (Article 2, under revision for *The Journal of Immunology*) describes a massive hyperplasia of skin-draining LNs and examines the underlying mechanisms for this post-natal LN growth.

2.2. *Article 2*

RANKL induces organized lymph node growth by stromal cell proliferation

Hess E, Duheron V, Decossas M, Lézot F, Berdal A, Bosisio MR, Bridal SL, Choi Y, Yagita H, Mueller CG

J Immunol. Under revision.

RANKL induces organized lymph node growth by stromal cell proliferation

Estelle Hess*, Vincent Duheron*, Marion Decossas*, Frédéric Lézot[†‡], Ariane Berdal[†], Mattéo R. Bosisio[§¶], S.Lori Bridal[§], Yongwon Choi[||], Hideo Yagita[#], Christopher G. Mueller*[,**]

* CNRS, Laboratory of Therapeutic Immunology and Chemistry, UPR9021, IBMC, University of Strasbourg, 67084 France

† INSERM, UMR 872, Cordeliers Research Center, Team 5, Laboratory of Oral Molecular Physiopathology, University of Paris V-VI, 75006 France

‡ INSERM UMR 957, University of Nantes, 44035 France

§ CNRS, UMR 7623, University of Paris VI, 75006 France

¶ Echosens S.A., Paris, France

|| Dept. of Pathology and Laboratory Medicine, University of Pennsylvania School of Medicine, Philadelphia, PA 19104, USA

Department of Immunology, Juntendo University School of Medicine, Tokyo 113-8421, Japan

** Corresponding author: Tel: +33 (0)3 88 41 71 14, Fax. +33 (0)3 88 61 06 80
c.mueller@cnrs-ibmc.unistra.fr

To give a better understanding of the following paper, data not shown in the submitted article are provided as supplemental figures in this manuscript.

Total character count, Figs and table inclusive: estimated 60 000
Running title: Secondary lymphoid organ growth by RANKL

Abstract

RANK (Receptor Activator of NF-κB) and its ligand RANKL are of critical importance for development and regulation of the immune system. We show that mice transgenic for *Rank* in hair follicles (HFs) display massive post-natal growth of skin-draining lymph nodes (LNs). The LN proportions of hematopoietic and the non-hematopoietic stromal cells and their organization are maintained, except for an increase in B cell follicles. The hematopoietic cells are not activated and respond to immunization with foreign antigens and adjuvant. We demonstrate that soluble RANKL is overproduced from the transgenic HFs and that its neutralization normalizes LN size, inclusive area and numbers of B cell follicles. Reticular fibroblastic and vascular stromal cells, known for their critical role in secondary lymphoid organ formation and organization, express RANK and undergo hyperproliferation, which is abrogated by RANKL neutralization. In addition, they express higher levels of CXCL13 and CCL19 chemokines as well as MAdCAM-1 and VCAM-1 cell adhesion molecules in the enlarged LNs. These findings highlight the importance of tissue-derived cues for secondary lymphoid organ homeostasis and identify RANKL as a key molecule for controlling the plasticity of the immune system.

Introduction

The immune system displays an enormous capacity to adapt to environmental changes in order to provide the best-tailored response to a given immune challenge. Secondary lymphoid organs (SLOs) such as LNs play an important part in this quest. They are the anatomical sites where information from the tissue is integrated by the immune cells. Over the last years, it has emerged that non-hematopoietic stromal cells that support the parenchyma of SLOs play a key role in orchestrating the immune response (1, 2). Stroma comprises vascular blood and lymph endothelial cells (BEC and LEC) and fibroblastic reticular cells (FRC), which are interconnected through a micro-conduit system (3). The FRCs consist of reticular cells of the T cell zone (TRC), the sinus marginal zone (MRC) and the B cell follicles, the follicular dendritic cells (FDC) (4-7). Vascular cells regulate entry and exit of lymphocytes (8-11), FRCs function in the homeostasis of T cells and B cells (12, 13) and, together, they provide the necessary structural framework for immune cell encounter and activation (2, 3, 12). During an immune response, stromal cells must adapt to rapid SLO expansion and massive increases in the number of lymphocytes (7, 14), demonstrating enormous plasticity. However, how SLOs accomplish size increase and whether it implies stromal cells is not known.

During embryogenesis, stromal cells interact with lymphoid tissue inducer (LTi) cells and orchestrate SLO development by producing chemokines and adhesion molecules (15-19). They express the lymphotoxin (LT) β R, which is a key molecule in this process (20, 21). Alike LTβR, RANK is a member of the TNF receptor superfamily (TNFRSF11a) and also signals through the classical and the alternative NF-κB pathways (22, 23). RANK is activated by RANKL (TNFSF11 or TRANCE), which is blocked by the soluble decoy receptor osteoprotegerin (OPG) (22, 24). RANK-deficient mice lack most LNs (25-27), which has hampered elucidation of its function in LN development and its immune homeostasis. LTi cells express RANK and RANKL and their numbers and their cluster formation is reduced in RANKL KO mice (27). In addition, RANK stimulates $LT\alpha_1\beta_2$ expression by LTi cells, the ligand for LTβR (28). This has led to the proposal that paracrine RANK-RANKL signaling in LTi cells results in activation of LTβR on stromal cells and subsequent SLO formation. However, the rescue of LN organogenesis in *Rankl*$^{-/-}$ mice by transgenic RANKL expression in B or T cells does not restore LTi cell numbers to normal levels, and the engagement of stromal cell LTβR by an agonistic antibody appears unable to normalize LNs formation (27). Moreover, payers patches and rescued mesenteric LNs of *Rankl*$^{-/-}$ mice are smaller (25, 27) and display disorganized B cell follicles (27, 29). IL-7-rescued *TRAF6*$^{-/-}$ LNs, an adaptor molecule in RANK signaling, lack clearly defined B cell follicles (28). These findings underscore our incomplete knowledge of the pre-, and post-natal functions of RANK in SLO formation and homeostasis.

The HF, one of the defining features of mammals, is a miniorgan of the skin, which periodically regenerates by repetitive cycles of growth (anagen), regression (catagen) and relative quiescence (telogen) (30). It has a specialized association with the immune system as it enjoys a relative immune privilege (31) and shares gene products with the thymus, most commonly exemplified by the *Foxn-1*^{-/-} *nude* mice, which lack hair and thymus. RANK and RANKL are expressed in the thymus and function in the formation of medullary thymic epithelial cells (32-36). RANK also plays an important role for the HF, as RANK stimulation of HF stem cells is required for entry into anagen, which in turn produces soluble RANKL (37).

Here, we present an analysis of a mouse transgenic (Tg) for RANK under the control of the *S100A8* promotor, active in HF stem cells (37) and in macrophages (38). The mouse displays a massive post-natal expansion of skin-draining LNs with an increase in small B cell follicles. The proportions and the organization of hematopoietic and stromal cell populations are well maintained, except for an increase in small B cell follicles. The immune cells are not activated and respond rapidly to immunization. By BM transfers, skin transplantation and genetic rescue experiments, we show that Tg *Rank* expression in the HFs is responsible for LN growth. RANKL is overproduced from the Tg HFs and is responsible for LN growth as RANKL neutralization restores normal organ size. The vascular and reticular fibroblastic cells express RANK and undergo hyperproliferation, which is abrogated by RANKL neutralization. Moreover, the stromal cells show increased transcription of chemokine and cell adhesion molecules, which would contribute to LN growth. Our data show that RANKL functions in SLO homeostasis by stimulating an equilibrated proliferation of all stromal cell subsets, concomitant with increased lymphocyte recruitment.

Materials and Methods

Mice

Animals were kept in a pathogen-free barrier facility, and experimentation was performed in accordance with faculty guidelines and its animal bioethics accord (approval no. AL/01/20/11/08). All mutants were identified by PCR (**Supplemental Table I**), except for CD45.1 mice, which were phenotyped by flow cytometry for the CD45 isoform. For all experiments, mice aged between 6 to 8 wk were used, unless explicitly stated. Ultrasound biomicroscopy was performed with 24 and 47.8 MHz ultrasound system on anesthetized mice (39). For adoptive BM transfer 3-wk-old mice were lethally irradiated with 10 Gy X-rays (Particle accelerator, Saturn 41, General Electrics) and, after 24 h, received i.v. $2x10^6$ BM cells harvested from congenic CD45.1$^+$ WT or CD45.2$^+$ Tg mice. Chimerism was verified every month by assessing the percentage of donor blood leucocytes. For skin transplantation, skin from age-matched mice was transplanted onto the back, below the neck, of 3-wk-old *nude* mice. A healing spray was applied and mice were killed 4 wk after. The *Rank* transgene was backcrossed onto *Msx-2$^{lacZ/lacZ}$* CD1 mice for over 8 generation, which maintained cLN hyperplasia, albeit less pronounced. LN cell numbers were determined at 3 mo of age. To block *in vivo* RANK-RANKL interaction, the neutralizing anti-RANKL antibody IK22-5 (40) was injected s.c. into RANK-Tg mice every 3 d (10 µg at P10, 25 µg from P13 to P28, and 50 µg from P31 to P45).

Isolation of stromal cells and lymphocytes

Stromal cells were isolated and identified using CD31 and podoplanin as markers, as described before (Luther, 2007). Briefly, LNs were collected, capsules were opened and incubated for 30 min at 37°C in RPMI 1640 (Lonza) containing 2% FCS (vol/ vol, Lonza), Dispase, Collagenase D (both from Roche, 1 mg/ ml) and DNase (Sigma Aldrich 40 µg/ ml). Medium containing enzymes was then removed and renewed for another 20 min incubation. Every 10 min, the digest was gently pipetted to break aggregates until no visible fragment remained, the final pipetting was done in presence of 5mM of EDTA. Cells are then passed through a 40 µm mesh and washed twice in RPMI 10% FCS (vol/ vol). DCs were enrichment by an Optiprep gradient (Sigma Aldrich) (41), after collagenase D (1 mg/ ml) LN digestion for 45 min under agitation.

Flow cytometry and cell sorting

Single cell suspensions obtained from different organs were stained with Abs (**Supplemental Table II**) and analyzed on FACSCalibur (Becton Dickinson) using CellQuest and FlowJo softwares. Cells were sorted on a FACSVantage SE (Becton Dickinson). Regulatory T cells were labeled for Foxp3 following the manufacturer's recommendations (eBioscience).

Immunofluorescence and histochemistry

LNs were frozen in Tissue-Tek O.C.T. Compound (EMS, Electron Microscopie Science) and sections prepared. After fixation in cold acetone, and blocking with goat serum (Sigma-Aldrich), they were incubated with primary Ab and, if necessary, followed by secondary Ab detection (**Supplemental Table II**). Images were acquired with the Zeiss, Axiovert 200M microscope and the AxioVision Rel.4.8 software. Quantification of area and number of B cell follicles was done on images using the ImageJ software. Beta-galactosidase activity was revealed as previously described (42).

RT-PCR

RNA was extracted from snap-frozen and ground LNs with the Ambion TRI Reagent (Applied Biosystems) and cleaned with Rneasy Mini kit (Qiagen). RNA from sorted stromal subsets was extracted with RNeasy Micro kit (Qiagen). cDNA was synthesized by oligo(dT)$_{15}$ primers and ImProm-II RT (Promega). PCR were performed using Promega GoTaq amplification mix and Eurogentec qPCR MasterMix Plus Low ROX. Gene-specific primers used are listed in **Supplemental Table I**. qRT-PCR was run on a Stratagene MX4000 thermal cycler and CT values of target genes were normalized to GAPDH, HPRT and/ or β-actin. The expression factor was calculated by using the Relative Expression Software Tool (REST; http://mmm.gene-quantification.de/rest.html).

BrdU incorporation assay

Mice were injected i.p. with 0.5 mg of BrdU (Sigma-Aldrich) diluted in PBS and given BrdU in drinking water (0.8 mg/ ml). CD45$^-$ and CD45$^+$ cells were isolated from LNs, and the incorporation of BrdU measured by flow cytometry using the BrdU flow kit (BD Pharmingen). Stromal subsets were additionally identified using CD31 and podoplanin as markers.

Immunization

Twelve-wk-old mice received s.c. injections of 200 µg chicken OVA with either 5 µg LPS (Sigma-Aldrich), IFA or 25 µg CpG (Invivogen). A boost was administrated 2 wk later. Before and every 5 d after, chicken OVA-reactive serum IgG was measured by direct ELISA. For Ab affinity measures mice received s.c. injections of 50 µg NP$_{30}$-KLH (Biosearch Technologies) in 5 µg/ ml LPS (Sigma-Aldrich). A boost was administrated at 10 d. Serum anti-NP IgG was determined every 5 d by direct ELISA on plates coated with NP$_3$-BSA or NP$_{30}$-BSA (Biosearch Technologies). Titers were determined as highest serum dilution that gave a value of $\geq$3 SD above the average reading for secondary controls. Relative affinity was determined as the titer NP3/ titer NP30 (43).

Statistical analysis

An unpaired two-tailed Student's *t*-test was used to determine statistically significant differences. *P* values of less than 0.05 were considered statistically significant. GraphPad Prism version 5 for Windows (Graphpad software) was used for statistical data analysis.

Results

Rank-Tg mice display a prominent post-natal LN growth

Mice overexpressing murine *Rank* under control of the *S100A8* promoter, show a massive hyperplasia of skin-draining LNs (inguinal, axial, brachial and superficial paratoid), while internal LNs (mesenteric [m] or para-aortic), spleen or thymus showed no such growth (**Fig. 1***A*). Cell counting revealed an 8-10 fold increase in hematopoietic cell numbers of the cutaneous (c) LNs, whereas the counts for mLNs, spleen, thymus, blood and BM were unchanged or even slightly reduced (**Fig. 1***B* **and Table I**). To find out whether the SLO hyperplasia was acquired post-natally, we assessed cLN cell numbers 1 wk after birth and at different time points thereafter. Growth started after post-natal wk 2 and reached a plateau at wk 13 (**Fig. 1***C*). To determine its onset more accurately, we used *in vivo* ultrasound imaging, which measures LN size in young mice more accurately than cell counting or organ weighing (39). It fixed the start of inguinal LN growth at post-natal day (P) 24 (**Fig. 1***D*). Thus, *Rank*-Tg mice display a prominent post-natal growth of their cLNs.

Conserved LN architecture with a notable increase in small B follicles

To investigate whether cLN hyperplasia was accompanied by an abnormal over-representation of a hematopoietic cell lineage, we determined the proportion of the CD11b$^+$ granulo-myeloid lineage, as well as B220$^+$ B cells and CD3$^+$ T cells by flow cytometry in cLNs, mLNs and spleen of Tg and control animals. There was a significant increase in CD11b$^+$ cells in both LN-types and the spleen of mutant mice (**Fig. 2***A*). An over-representation of these cells has also been noted in the BM (44) and is most likely secondary to transgene expression in this lineage (44, 45) (data not shown - Supplemental Figure 3). More restrictively, there was an increase in the proportion of B cells and a reduction of T cells in cLNs, but not in mLNs or spleen. B cells do not express the transgene [(45) and data not shown - Supplemental Figure 4], suggesting that the change in B/ T cell proportions was the result of the abnormal LN size. There was little alteration in B cell hematopoiesis as the number of splenic transitional type 1 and type 2 B cells remained relatively stable in comparison to a strong reduction of mature B cells (**Table II**), suggesting a reinforced recruitment of mature B cells to the cLNs. We therefore visually inspected B cell organization in the cLNs by staining sections for B220. We saw normal B cell organization into follicles of the paracortex, clearly delineated from the T cell-rich area, but noted an increase of small B cell follicles (**Fig. 2***B*, see also **Fig. 5***C*). All B cell follicles comprised stromal CD35$^+$ FDCs (**Fig. 2***B*). To assess whether cLN hyperplasia led to changes in the proportions of stromal cell subsets, given their central role in SLO development and organization (2, 4, 46), we compared percentage and distribution of FRCs, BECs and LECs in cLNs of Tg vs WT animals. The cells were identified on the basis of podoplanin and CD31 expression after gating on CD45$^-$ cells (12). FRCs and BECs were present in normal proportions but the percentage of LECs showed a slight decrease (**Fig. 2***C*). All stromal subsets were normally distributed, with FRCs

dispersed around cortical BECs, and LECs juxtaposed to B cell follicles (**Fig. 2D**). Thus, the cLN cell composition and its architecture showed remarkably little alteration for such an important growth, except for an increase in the number of B cells and their follicles.

The expanded immune compartment of the cLNs is not activated and responds to immunization

To address the question of whether the hematopoietic cells of the Tg mouse cLNs were dysfunctional, we studied its cutaneous immune response. Skin-, and blood-derived DCs, purified from brachial and axial LNs and identified on the basis of I-A/ CD11c expression (41, 47), showed low CD86 levels but normally upregulated this activation marker in response to a s.c. CpG injection (**Fig. 3A**). T cells of cLNs, mLN or spleen were resting but responded to CpG by CD62L loss and CD44 upregulation (**Fig. 3B**). Also, B cells showed no signs of activation in non-immunized Tg mice (**Fig. 3C**), and s.c. immunisation by OVA with LPS, CpG or IFA provoked an efficient humoral immune response (**Fig. 3D**). Antibody affinity maturation in response to immunisation with 4-hydroxy-3-nitrophenyl-acetyl (NP)-KLH in LPS proceeded faster in the Tg animals than in control mice (**Fig. 3E**). To test for a possible rupture in self tolerance, we assessed the presence of serum auto-antibodies against actin, rheumatoid factor and DNA in non-immunized and immunized Tg mice. However, no such antibodies were detected (data not shown). In addition, there was no significant difference between the animals in the number of B cells in the autoimmune-sensitive salivary glands (WT $30\pm12\text{x}10^3$ vs Tg $35\pm9\text{x}10^3$, n=8). In accord with these results, the proportion of FoxP3$^+$ regulatory T cells was not markedly altered in cLNs, mLNs or spleen of Tg compared to WT mice (data not shown - Supplemental Figure 5). Since stromal cells can contribute to peripheral tolerance by expression of tissue-restricted peripheral tissue antigens (PTAs) by Aire (5, 48-50), which is under positive control by RANK in the thymus (32-35), we evaluated whether stromal cells contributed to tolerance by Aire upregulation in the Tg mouse cLNs. We measured Aire mRNA by quantitative (q) RT-PCR of whole-cLN RNA. No difference in Aire expression between Tg and WT mice was seen (data not shown - Supplemental Figure 5), and the stromal-subset-restricted expression of Mlana and tyrosinase PTAs (49, 50) was also conserved (data not shown - Supplemental Figure 5). Therefore, the post-natal LN growth has no discernable negative influence on its immune cells and peripheral tolerance mechanisms need not be reinforced to ensure self-tolerance.

LN growth is associated with the transgenic HF

To understand the mechanisms for the organized cLN expansion, we investigated the contribution of the *Rank*-transgene in the CD11b$^+$ granulo-myeloid cell lineage by performing adoptive BM transfers. Lethally-irradiated 3-wk-old Tg mice were reconstituted with BM of congenic CD45.1$^+$ C57BL/6 mice. The reciprocal transfer was also done. Three months later, cLN cell numbers were determined. The BM transfers were complete, as all hematopoietic cells, including the CD11b$^+$ lineage, were of donor origin (**Supplemental Fig. 1A and B**), but the WT>Tg chimeras developed LN hyperplasia to the same extend as control Tg>Tg animals (**Fig. 4A**). Reciprocally, Tg BM could not transfer LN

growth to WT mice. These findings demonstrate that *Rank*-transgene expression by the granulo-myeloid cell linage is not responsible for cLN growth. We determined whether the radio-resistant stromal cells expressed the *Rank*-transgene by performing RT-PCR on cLNs recovered from WT>Tg chimeras. The transgene was no longer expressed, demonstrating that the cLN stroma is not transgenic for *Rank* (**Supplemental Fig. 1C**). We then considered the possibility, that cLN growth is conveyed by *Rank*-transgene expression in the HF (37). To address this issue, we first transplanted Tg or WT skin from 3-wk-old donors onto the backs of age-matched *nude* mice. Seven wks later, cell numbers of brachial, axial LNs and inguinal LNs were determined. As the inguinal LN are not expected to drain from the graft, its cell counts served as internal control for natural LN size and inter-experimental variations. Although there was only a small difference, presumably owing to the limited graft size, we found a significant increase for Tg skin recipients compared to WT skin, indicating that LN growth is associated with *Rank*-transgene expression in the HFs (**Fig. 4B**). We verified this conclusion by reducing transgene expression in HFs. This was done by crossing the transgene onto *Msx-2$^{lacZ/lacZ}$* mice, which have a shortened anagen phase (51), and are therefore expected to express lower levels of the *Rank* transgene (**Supplemental Fig. 1D**). This mutant gene combination resulted in a strongly reduced cLN growth (**Fig. 4C**). To exclude the possibility that Msx-2 affected the organ size through a local expression, we stained brachial LNs of *Rank* Tg x *Msx-2$^{lacZ/+}$* animals for β-galactosidase. The *lacZ* gene activity was not detected in the LNs, whereas, as expected (51), it was found at the base of the HFs (**Fig. 4D**). Taken together, these findings support the conclusion that *Rank*-transgene expression in the HF is necessary and sufficient for skin-draining LN hyperplasia.

RANKL induces cLN growth

To identify the signal conveyed by the anagen HF and responsible of cLN growth, we considered RANKL as a probable candidate because (i) the anagen HF is an important source of soluble RANKL (37), (ii) soluble RANKL is a small (>10 kDa) globular protein, which can be expected to have direct access to LN stroma through its conduit system (3, 52, 53), and (iii) RANKL is known to play a critical role in SLO formation (25-27). To verify whether RANKL levels would concord with this idea, we measured soluble RANKL and OPG release from Tg and WT skin at different time points during HF morphogenesis and cycling. We confirmed that RANKL was highest at anagen when OPG levels were low (37) and found significantly higher levels of RANKL released from the Tg skin at P14 and during anagen compared to WT (**Supplemental Fig. 2A and B**). We then directly tested the role of RANKL by s.c. administration of a RANKL-blocking mAb to Tg mice from P10 to wk 6. Littermate controls received control Ab. Cutaneous LNs and spleen were weighed, cell numbers determined and the B/ T cell proportion assessed. As hypothesized, the RANKL neutralizing mAb restored cLN weight and cell numbers to near WT levels (**Fig. 5A**), and the increase in the proportion of B cells was inversed (**Fig. 5B**). Also, the number of B cell follicles was reduced and their size restored (**Fig. 5C**). RANKL-neutralization did not lead to a loss of cell numbers in the spleen

(**Supplemental Fig. 2C**), nor were B or T cells activated, as assessed by plasmocyte and memory T cell proportions (**Supplemental Fig. 2D and E**). The anti-RANKL treatment provoked a diminution in body weight (WT 17.7±0.5 g, Tg 18.7±1.1 g, treated Tg 12.1±1.6 g, n=12), most probably attributable to perturbation of bone homeostasis (25, 26). These data show that RANKL induces LN growth, inclusive augmentation of small B cell follicles.

RANKL activates chemokine synthesis and proliferation of SLO stroma
In view of their central role in coordinating lymphoid organ growth during development (2, 4-6), we regarded the LN stromal cells as likely RANKL cell targets. To address this possibility, we determined whether *Rank* was expressed by stromal cells by performing RT-PCR on RNA from FRCs, LECs and BECs, which were flow-cytometry-sorted from WT and Tg animals using podoplanin and CD31 as markers. *Rank* was transcriptionally active in all stromal subsets (**Fig. 6A**), suggesting that skin-derived RANKL could directly activate the cLN stroma. Since chemokines and cell adhesion molecules are expressed by stroma and play an important role in SLO growth (9, 46), we tested whether these type of molecules were upregulated in the stromal cells. We performed qRT-PCR on the sorted stromal cells, pooled from cLNs of 6-wk-old WT and Tg animals. Among the different genes tested (**Supplemental Table I**), we found that in the Tg mice FRCs transcribed more CXCL13 mRNA, and that BECs and LECs increased CCL19, MAdCAM-1 and VCAM-1 mRNA synthesis (**Fig. 6B**). This suggests that cLN growth is the consequence of RANK-stimulated expression of chemokines and cell adhesion molecules. In the light of the almost unchanged stromal cell proportion of the enlarged cLNs, together with the finding that RANKL induces medullary thymic epithelial cell proliferation (35), we next asked the question of whether stromal cells proliferated in response to RANK-stimulation. To this end, we measured stromal cell division by BrdU incorporation in 6-wk-old WT and Tg mice, which were untreated or received the anti-RANKL mAb. Mice were given the nucleotide analogue during 6 d, and BrdU incorporation into stromal cell DNA was measured by flow cytometry. We saw that already the WT non-hematopoietic cells had a reasonable proliferation rate, but, in the Tg mice, it was greatly increased. Strikingly, when RANKL was neutralized, the proportion of BrdU$^+$ stroma of the Tg mice fell to WT levels (**Fig. 6C**). In contrast, the proportion of BrdU$^+$ hematopoietic cells was similar between WT and Tg animals and there was no change after administration of the RANKL-blocking mAb. We next analyzed the FRCs, LECs and BECs separately. All 3 stromal cell subsets proliferated faster in the Tg, and again, the higher BrdU incorporation was abrogated when RANKL was neutralized (**Fig. 6D**). To address the question of whether the RANKL also affected stromal cell viability, we performed pulse-chase experiments. The cell renewal rate was monitored by measuring the percentage of BrdU$^+$ cells at 2 and 9 wks after the BrdU labeling period. We found that the loss of the BrdU label from the stromal subsets was not delayed in the Tg mice, indicating that RANKL stimulated stromal cell division without altering their

viability (**Supplemental Fig. 2F**). This shows that RANKL provokes cLN growth by inducing the proliferation of its vascular and reticular fibroblastic stromal cells.

Discussion

In this study we have shown that RANK-stimulation results in the proliferation of LN stromal subsets and their expression of chemokine and adhesion molecules, culminating in LN growth. LN organization was preserved, with a notable increase in small B cell follicles. RANK-stimulation did not provoke an immune activation; no auto-reactivity could be detected and the immune cells responded rapidly and strongly to immunization by foreign antigens.

Although recognized as an important regulator of immunity, the lack of almost all SLOs in *Rank* or *Rankl* KO mice has hampered elucidation of the function of RANK in development and homeostasis of the immune system. We have therefore studied a *Rank*-Tg mouse, which displayed greatly-oversized skin-draining LNs, while other SLOs, spleen, thymus or BM were normal. LN growth occurred post-natally and, at its plateau, their combined lymphocyte number largely surpassed that of the spleen. Otherwise, we could not detect other major abnormalities of the immune system, except for a general over-representation of *Rank*-Tg CD11b$^+$ cells, presumably attributable to the cell survival action of RANK (54-56). A condition that resembles this phenotype is found in a mouse Tg for IL-7 (57). There, increased LTi cell numbers led to SLO growth and ectopic SLO formations. Dissimilar to the IL-7 Tg mouse model, however, is that the here-described SLO expansion appeared much more prominent and no ectopic SLOs could be found. In spite of the massive cLN size expansion of the *Rank*-Tg mice, the hematopoietic and stromal cell composition of the cLN and their organization were remarkably well-conserved. The only notable alteration was an increase in the number of small B cell follicles and a rise in the proportion of B cells. These observations concord with findings that small B cell follicles are more frequent in large LNs (14). Support for a role of RANK-signaling in regulating peripheral immune cell numbers stems from a study of *Opg$^{-/-}$* mice, where LN B and T cell numbers were likewise augmented (58). In the *Opg$^{-/-}$* mice, the B cell compartment was particularly boosted in the spleen, which was attributed to an accelerated B cell development (58). We did not find a prominent rise in splenic transitional type 1 or type 2 B cells, discarding the possibility that the additional cLN B cells derive from accelerated B cell hematopoiesis. Instead, the higher B cell proportion is likely due to a reinforced recruitment of mature B cells.

The greatly-expanded SLO size could have been the consequence of a dysfunctional hematopoietic cell compartment. However, T cells, B cells or DCs showed no signs of activation and no autoantigen-reactivity could be detected. Moreover, LN-purified T cells did not spontaneously proliferate in culture, as has been described for a different model of SLO hyperplasia (59), and transfer of cLN CD4$^+$ T cells into *Rag*-2 KO mice did not result in abnormal expansion (data not shown -

Supplemental Figure 6). The cLN immune cells of the *Rank*-Tg animals were not anergic, as they responded to immunization with foreign antigen and adjuvant. The immune responses elicited from the Tg mice were not greatly superior to those of WT mice, although a more rapid Ab affinity maturation was detected, which may reflect more available B and T cells or a more accessible FDC network. Given the positive relation between RANKL and Aire expression in the thymus (32-35), and although LN Aire appears to contribute to peripheral T cell tolerance (50, 60), we could not reveal such association between RANKL and Aire in the cLNs of the Tg animals. As the exact identity of the Aire[+] stromal subset is not fully resolved (5), we had preferred to measure Aire mRNA in the whole LN. It remains a possibility that this has masked variations in Aire mRNA levels in a stromal subset.

By performing BM transfer, skin transplantation and genetic rescue experiments, we determined that the SLO growth signal originated in the *Rank*-Tg HF. This finding provides an explanation to why only skin-draining LNs were affected and is in accord with initiation of LN growth at the start of the HF anagen phase at P24. Moreover, the growth plateau is likely due to loss of HF transgene expression, as the mouse develops alopecia (37). It is interesting to note that the post-natal period, during which skin-draining LN expansion surpasses body growth, occurs during HF morphogenesis and the first HF anagen phase (39). This is suggestive of a naturally-operating link between HF development/ renewal and cLN growth, an association which appears to be amplified in the Tg mouse. We considered the possibility that DCs mediate the HF-LN link, however, in analogy to dermatopathic lymphadenopathy (61), more numerous, long-lived or mature DCs would principally lead to an expanded T cell zone. This was not seen, and the proportion of DCs and their maturation status was unchanged. Since shortening of anagen by loss of Msx-2 abrogated LN growth, we deduced that the signal arises during the anagen phase of the hair cycle. The high levels of soluble RANKL produced by the Tg anagen HF incited us to propose the concept that HF RANKL conveys cLN growth. In fact, not only is the levels of HF RANKL higher in the mutant animal, but the skin also undergoes additional anagen phases, leading to a prolonged RANKL release. The underlying reason for the rise in HF RANKL is currently unclear. One possibility may be the existence of a self-amplifying RANK-RANKL loop, similar to what was seen for thymic epithelial cells (36). The precocious anagen phases result from RANK-mediated activation of the HF stem cells, which control HF cycling (37). Another argument in favor of RANKL as mediator of SLO growth is that RANKL is a small globular protein, which can be expected to have unobstructed assess to all stromal cells through their conduits (3). Indeed, RANKL neutralization by a blocking mAb restored normal LN size, B/ T cell ratio and follicle area and numbers. We cannot formally exclude the possibility that blocking RANKL from other sources contributed to normalization, however skin RANKL was assuredly affected, since abnormal HF cycling and epidermal dysplasia were corrected (37). The observed loss of B cells and the reduction of FRC proliferation beyond WT levels in the anti-RANKL-treated Tg mice is likely due to blocking RANKL produced by the MRCs (7). Among other potential

SLO RANKL sources, we can exclude T cells, which synthesize RANKL only when activated (55), since they were resting. Interestingly, it has recently been reported that tumor regulatory T cells are a source of RANKL (62). Whether LN regulatory T cells constitutively produce RANKL is not known. Although the mAb was administrated s.c., bone homeostasis was affected, as the treated mice displayed growth retardation. However, a disturbed hematopoietic cell output by reduction of BM niches (63) was not seen as spleen cell numbers were not diminished. In a different model of skin RANKL overexpression by *Rankl* transgenesis under control of the keratin 14 promotor, cLN hyperplasia was not reported (64). While this difference may suggest that factors other than an increased output of skin RANKL are implicated in cLN growth, the cardinal difference between the two mouse models is that the Tg RANKL is not soluble and therefore cannot freely reach the draining LNs. Moreover, Tg RANKL is overexpressed in cells, which naturally produce OPG (37), so that most RANKL may be blocked by OPG. As proposed by the authors, it is likely that the Tg RANKL principally affects the Langerhans cells.

To identify the cellular RANKL target, we envisioned LTi cells and stromal cells as candidates. The LTi cells express RANK (27, 65) and boosting their numbers through IL-7 led to SLOs expansion (57). However, the proportion of LTi cells was not altered in the cLNs and we could not detect an increase in IL-7 synthesis by FRCs, the predominant IL-7 source in SLOs (12) (data not shown - Supplemental Figure 4 and 7). LTi cells of the Tg mice did not overexpress RANK (data not shown - Supplemental Figure 4), and we can also rule out *Rank* transgene expression by the radio-resistant stromal cells, as its RNA was no longer detectable in cLNs after WT>Tg BM transfer. However, all stromal subsets expressed endogenous RANK. It is known that endothelial cells (66-68) and mesenchymal cells (54, 69) can express RANK, but whether their SLO counterpart likewise carries RANK had not been studied. RANKL-stimulated LN stroma upregulated chemokine and cell adhesion molecules, but more strikingly, FRCs, LECs and BECs showed a dramatic hyperproliferation in the Tg mice, which was fully abolished by RANKL-neutralization. Owing to podoplanin co-expression, it was not possible to differentiate between TRCs and MRCs within the FRC population by this method. However, if only MRCs carried RANK one would expect its enrichment by proliferation in response to RANKL. This was not seen, as judged by the unchanged qRT-PCR measures of *Rankl* mRNA, which is specific to MRCs (7) (data not shown - Supplemental Figure 7). Whether FDCs also express RANK is difficult to determine, owing to technical challenges in obtaining a sufficiently homogeneous cell population. A RANK-mediated FDC proliferation would certainly offer the simplest explanation for the increase in B cell follicles. Indeed, the RANK gene was found expressed in a transcriptome study of FDCs (70) (C. Berek, personal communication). However, in keeping with the idea that MRCs may be FDC precursors (7), it remains a possibility that RANK-stimulation of MRC translates into simultaneous cell proliferation and FDC differentiation. Robust stromal cell proliferation and synthesis of chemokine/ leukocyte adhesion molecules would

result in SLO growth. It remains to be determined whether reduction of lymphocyte egress rates could also contribute (11). While the loss of LECs is suggestive of alteration of egress rates in the hyperplastic LNs, the stable blood cell counts argue against this possibility (71).

The underlying molecular mechanisms of SLO stroma stimulation by RANKL remain to be clarified. It was found that RANK ligation on vascular cells stimulates angiogenesis and ICAM-1 as well as VCAM-1 expression (67, 68, 72). In an artificial SLO-like cell system, high fluid pressure activates stromal cell chemokine synthesis (73). This invites speculation on the existence of an interlinked direct RANK action on endothelial cells and reticular fibroblasts. Importantly, LTβR and TNFR signaling are mandatory for FDC formation and maintenance (74, 75), and LTβR-signaling contributes to SLO growth in response to viral infection (14). Also, CXCL13 and MAdCAM expression on BEC are increased upon LTβR engagement (9). An upregulation of LTβR mRNA on FRCs was not seen (data not shown - Supplemental Figure 7), however, the higher CXCL13 and CCL19 levels would stimulate $LT\alpha_1\beta_2$ synthesis by B and T cells, resulting in reinforced LTβR signaling (76, 77). Therefore, the possibility that LTβR signaling plays a part in cLN growth cannot be excluded, but elucidation of the precise roles of RANK and LTβR in SLO homeostasis is complicated by the findings that LTβR stimulates RANK and RANKL expression (36, 78). It would be of interest to test the effect of RANKL-neutralization in the model of viral-induced SLO growth (14). Our results, together with the current understanding of RANK and LTβR actions, raise the question of whether RANK and LTβR are partially redundant in function and difference only arise through variations in spatial-temporal ligand availabilities.

The ability of activated T cells to release high amounts of RANKL (79, 80) invites the idea that during an immune response, T cells sustain SLO expansion and contribute to tertiary lymphoid tissue formation through RANKL. Conversely, CD40-stimulate B cells release OPG, which would keep RANKL in check (81). The question of whether RANK-directed therapy can find novel applications for boosting of the immune system or, on the contrary, in treatment of inflammatory diseases now merits close examination. Our results support the idea that tissue-derived RANKL (i.e. from pre-, and neo-natal skin) contributes to lymphoid tissue formation and growth by stimulating stromal cell proliferation. In view of their important cLN size with preservation of a normal immune status as well as stromal and hematopoietic cell compositions, the *Rank* Tg mouse should make a valuable tool to study rare stromal subsets, such as EpCam^{+} cells (48). Our results highlight the importance of environmental cues for immune regulation (82) by uncovering the role of HF-derived RANKL in LN growth via stroma stimulation.

References

1. Junt, T., E. Scandella, and B. Ludewig. 2008. Form follows function: lymphoid tissue microarchitecture in antimicrobial immune defence. *Nat. Rev. Immunol.* 8:764-775.
2. Mueller, S. N., and R. N. Germain. 2009. Stromal cell contributions to the homeostasis and functionality of the immune system. *Nat. Rev. Immunol.* 9:618-629.
3. Lammermann, T., and M. Sixt. 2008. The microanatomy of T-cell responses. *Immunol. Rev.* 221:26-43.
4. Roozendaal, R., and R. E. Mebius. 2011. Stromal cell-immune cell interactions. *Annu. Rev. Immunol.* 29:23-43.
5. Fletcher, A. L., D. Malhotra, and S. J. Turley. 2011. Lymph node stroma broaden the peripheral tolerance paradigm. *Trends Immunol.* 32:12-18.
6. Luther, S. A., T. K. Vogt, and S. Siegert. 2011. Guiding blind T cells and dendritic cells: A closer look at fibroblastic reticular cells found within lymph node T zones. *Immunol. Lett.*:in press.
7. Katakai, T., H. Suto, M. Sugai, H. Gonda, A. Togawa, S. Suematsu, Y. Ebisuno, K. Katagiri, T. Kinashi, and A. Shimizu. 2008. Organizer-like reticular stromal cell layer common to adult secondary lymphoid organs. *J. Immunol.* 181:6189-6200.
8. Palframan, R. T., S. Jung, G. Cheng, W. Weninger, Y. Luo, M. Dorf, D. R. Littman, B. J. Rollins, H. Zweerink, A. Rot, and U. H. von Andrian. 2001. Inflammatory chemokine transport and presentation in HEV: a remote control mechanism for monocyte recruitment to lymph nodes in inflamed tissues. *J. Exp. Med.* 194:1361-1373.
9. Browning, J. L., N. Allaire, A. Ngam-Ek, E. Notidis, J. Hunt, S. Perrin, and R. A. Fava. 2005. Lymphotoxin-beta receptor signaling is required for the homeostatic control of HEV differentiation and function. *Immunity* 23:539-550.
10. Pham, T. H., P. Baluk, Y. Xu, I. Grigorova, A. J. Bankovich, R. Pappu, S. R. Coughlin, D. M. McDonald, S. R. Schwab, and J. G. Cyster. 2009. Lymphatic endothelial cell sphingosine kinase activity is required for lymphocyte egress and lymphatic patterning. *J. Exp. Med.* 207:17-27.
11. Schwab, S. R., and J. G. Cyster. 2007. Finding a way out: lymphocyte egress from lymphoid organs. *Nat. Immunol.* 8:1295-1301.
12. Link, A., T. K. Vogt, S. Favre, M. R. Britschgi, H. Acha-Orbea, B. Hinz, J. G. Cyster, and S. A. Luther. 2007. Fibroblastic reticular cells in lymph nodes regulate the homeostasis of naive T cells. *Nat. Immunol.* 8:1255-1265.
13. Kosco, M. H., E. Pflugfelder, and D. Gray. 1992. Follicular dendritic cell-dependent adhesion and proliferation of B cells in vitro. *J. Immunol.* 148:2331-2339.
14. Kumar, V., E. Scandella, R. Danuser, L. Onder, M. Nitschke, Y. Fukui, C. Halin, B. Ludewig, and J. V. Stein. 2011. Global lymphoid tissue remodeling during a viral infection is orchestrated by a B cell-lymphotoxin-dependent pathway. *Blood* 115:4725-4733.
15. Cupedo, T., and R. E. Mebius. 2005. Cellular interactions in lymph node development. *J. Immunol.* 174:21-25.
16. Honda, K., H. Nakano, H. Yoshida, S. Nishikawa, P. Rennert, K. Ikuta, M. Tamechika, K. Yamaguchi, T. Fukumoto, T. Chiba, and S. I. Nishikawa. 2001. Molecular basis for hematopoietic/mesenchymal interaction during initiation of Peyer's patch organogenesis. *J. Exp. Med.* 193:621-630.
17. Cupedo, T., M. F. Vondenhoff, E. J. Heeregrave, A. E. De Weerd, W. Jansen, D. G. Jackson, G. Kraal, and R. E. Mebius. 2004. Presumptive lymph node organizers are differentially represented in developing mesenteric and peripheral nodes. *J. Immunol.* 173:2968-2975.
18. White, A., D. Carragher, S. Parnell, A. Msaki, N. Perkins, P. Lane, E. Jenkinson, G. Anderson, and J. H. Caamano. 2007. Lymphotoxin a-dependent and -independent signals regulate stromal organizer cell homeostasis during lymph node organogenesis. *Blood* 110:1950-1959.
19. Coles, M. C., H. Veiga-Fernandes, K. E. Foster, T. Norton, S. N. Pagakis, B. Seddon, and D. Kioussis. 2006. Role of T and NK cells and IL7/IL7r interactions during neonatal maturation of lymph nodes. *Proc. Natl. Acad. Sci. USA* 103:13457-13462.

20. Tumanov, A. V., D. V. Kuprash, and S. A. Nedospasov. 2003. The role of lymphotoxin in development and maintenance of secondary lymphoid tissues. *Cytokine. Growth. Factor. Rev.* 14:275-288.

21. Browning, J. L. 2008. Inhibition of the lymphotoxin pathway as a therapy for autoimmune disease. *Immunol. Rev.* 223:202-220.

22. Wada, T., T. Nakashima, N. Hiroshi, and J. M. Penninger. 2006. RANKL-RANK signaling in osteoclastogenesis and bone disease. *Trends Mol. Med.* 12:17-25.

23. Dejardin, E., N. M. Droin, M. Delhase, E. Haas, Y. Cao, C. Makris, Z. W. Li, M. Karin, C. F. Ware, and D. R. Green. 2002. The lymphotoxin-beta receptor induces different patterns of gene expression via two NF-kappaB pathways. *Immunity* 17:525-535.

24. Walsh, M. C., and Y. Choi. 2003. Biology of the TRANCE axis. *Cytokine Growth Factor Rev.* 14:251-263.

25. Kong, Y. Y., H. Yoshida, I. Sarosi, H. L. Tan, E. Timms, C. Capparelli, S. Morony, A. J. Oliveira-dos-Santos, G. Van, A. Itie, W. Khoo, A. Wakeham, C. R. Dunstan, D. L. Lacey, T. W. Mak, W. J. Boyle, and J. M. Penninger. 1999. OPGL is a key regulator of osteoclastogenesis, lymphocyte development and lymph-node organogenesis. *Nature* 397:315-323.

26. Dougall, W. C., M. Glaccum, K. Charrier, K. Rohrbach, K. Brasel, T. De Smedt, E. Daro, J. Smith, M. E. Tometsko, C. R. Maliszewski, A. Armstrong, V. Shen, S. Bain, D. Cosman, D. Anderson, P. J. Morrissey, J. J. Peschon, and J. Schuh. 1999. RANK is essential for osteoclast and lymph node development. *Genes. Dev.* 13:2412-2424.

27. Kim, D., R. E. Mebius, J. D. MacMicking, S. Jung, T. Cupedo, Y. Castellanos, J. Rho, B. R. Wong, R. Josien, N. Kim, P. D. Rennert, and Y. Choi. 2000. Regulation of peripheral lymph node genesis by the tumor necrosis factor family member TRANCE. *J. Exp. Med.* 192:1467-1478.

28. Yoshida, H., A. Naito, J. Inoue, M. Satoh, S. M. Santee-Cooper, C. F. Ware, A. Togawa, and S. Nishikawa. 2002. Different cytokines induce surface lymphotoxin-alphabeta on IL-7 receptor-alpha cells that differentially engender lymph nodes and Peyer's patches. *Immunity* 17:823-833.

29. Knoop, K. A., N. Kumar, B. R. Butler, S. K. Sakthivel, R. T. Taylor, T. Nochi, H. Akiba, H. Yagita, H. Kiyono, and I. R. Williams. 2009. RANKL is necessary and sufficient to initiate development of antigen-sampling M cells in the intestinal epithelium. *J. Immunol.* 183:5738-5747.

30. Schneider, M. R., R. Schmidt-Ullrich, and R. Paus. 2009. The hair follicle as a dynamic miniorgan. *Curr. Biol.* 19:R132-142.

31. Paus, R., B. J. Nickoloff, and T. Ito. 2005. A 'hairy' privilege. *Trends Immunol.* 26:32-40.

32. Rossi, S. W., M. Y. Kim, A. Leibbrandt, S. M. Parnell, W. E. Jenkinson, S. H. Glanville, F. M. McConnell, H. S. Scott, J. M. Penninger, E. J. Jenkinson, P. J. Lane, and G. Anderson. 2007. RANK signals from CD4+3- inducer cells regulate development of Aire-expressing epithelial cells in the thymic medulla. *J. Exp. Med.* 14:14.

33. Akiyama, T., Y. Shimo, H. Yanai, J. Qin, D. Ohshima, Y. Maruyama, Y. Asaumi, J. Kitazawa, H. Takayanagi, J. M. Penninger, M. Matsumoto, T. Nitta, Y. Takahama, and J. Inoue. 2008. The tumor necrosis factor family receptors RANK and CD40 cooperatively establish the thymic medullary microenvironment and self-tolerance. *Immunity* 29:423-437.

34. White, A. J., D. R. Withers, S. M. Parnell, H. S. Scott, D. Finke, P. J. Lane, E. J. Jenkinson, and G. Anderson. 2008. Sequential phases in the development of Aire-expressing medullary thymic epithelial cells involve distinct cellular input. *Eur. J. Immunol.* 38:942-947.

35. Hikosaka, Y., T. Nitta, I. Ohigashi, K. Yano, N. Ishimaru, Y. Hayashi, M. Matsumoto, K. Matsuo, J. M. Penninger, H. Takayanagi, Y. Yokota, H. Yamada, Y. Yoshikai, J. Inoue, T. Akiyama, and Y. Takahama. 2008. The cytokine RANKL produced by positively selected thymocytes fosters medullary thymic epithelial cells that express autoimmune regulator. *Immunity* 29:438-450.

36. Mouri, Y., M. Yano, M. Shinzawa, Y. Shimo, F. Hirota, Y. Nishikawa, T. Nii, H. Kiyonari, T. Abe, H. Uehara, K. Izumi, K. Tamada, L. Chen, J. M. Penninger, J. I. Inoue, T. Akiyama, and

M. Matsumoto. 2011. Lymphotoxin Signal Promotes Thymic Organogenesis by Eliciting RANK Expression in the Embryonic Thymic Stroma. *J. Immunol.* 186:5047-5057.

37.   Duheron, V., E. Hess, M. Duval, M. Decossas, B. Castaneda, J. E. Klöpper, L. Amoasii, J. B. Barbaroux, I. R. Williams, H. Yagita, J. M. Penninger, Y. Choi, F. Lezot, R. Groves, R. Paus, and C. G. Mueller. 2011. Receptor Activator of NF-kB (RANK) stimulates the proliferation of epithelial cells of the epidermo-pilosebaceous unit. *Proc. Natl. Acad. Sci. USA* 108:5342-5347.

38.   Lagasse, E., and I. L. Weissman. 1997. Enforced expression of Bcl-2 in monocytes rescues macrophages and partially reverses osteopetrosis in op/op mice. *Cell* 89:1021-1031.

39.   Bosisio, M. R., C. Maisonneuve, S. Gregoire, A. Kettaneh, C. G. Mueller, and S. L. Bridal. 2009. Ultrasound biomicroscopy: A powerful tool probing murine lymph node size in vivo. *Ultrasound Med. Biol.* 35:1209-1216.

40.   Kamijo, S., A. Nakajima, K. Ikeda, K. Aoki, K. Ohya, H. Akiba, H. Yagita, and K. Okumura. 2006. Amelioration of bone loss in collagen-induced arthritis by neutralizing anti-RANKL monoclonal antibody. *Biochem. Biophys. Res. Commun.* 347:124-132.

41.   Ruedl, C., P. Koebel, M. Bachmann, M. Hess, and K. Karjalainen. 2000. Anatomical origin of dendritic cells determines their life span in peripheral lymph nodes. *J. Immunol.* 165:4910-4916.

42.   Aioub, M., F. Lezot, M. Molla, B. Castaneda, B. Robert, G. Goubin, J. R. Nefussi, and A. Berdal. 2007. Msx2 -/- transgenic mice develop compound amelogenesis imperfecta, dentinogenesis imperfecta and periodental osteopetrosis. *Bone* 41:851-859.

43.   Matsumoto, M., S. F. Lo, C. J. Carruthers, J. Min, S. Mariathasan, G. Huang, D. R. Plas, S. M. Martin, R. S. Geha, M. H. Nahm, and D. D. Chaplin. 1996. Affinity maturation without germinal centres in lymphotoxin-alpha-deficient mice. *Nature.* 382:462-466.

44.   Castaneda, B., Y. Simon, J. Jacques, E. Hess, Y. W. Choi, C. Blin-Wakkach, C. Mueller, A. Berdal, and F. Lezot. 2010. Bone resorption control of tooth eruption and root morphogenesis: involvement of the receptor activator of NF-kappaB (RANK). *J. Cell. Physiol.* 226:74-85.

45.   Lagasse, E., and I. L. Weissman. 1992. Mouse MRP8 and MRP14, two intracellular calcium-binding proteins associated with the development of the myeloid lineage. *Blood* 79:1907-1915.

46.   Mebius, R. E. 2003. Organogenesis of lymphoid tissues. *Nat. Rev. Immunol.* 3:292-303.

47.   Jakubzick, C., M. Bogunovic, A. J. Bonito, E. L. Kuan, M. Merad, and G. J. Randolph. 2008. Lymph-migrating, tissue-derived dendritic cells are minor constituents within steady-state lymph nodes. *J Exp Med.* 205:2839-2850.

48.   Gardner, J. M., J. J. Devoss, R. S. Friedman, D. J. Wong, Y. X. Tan, X. Zhou, K. P. Johannes, M. A. Su, H. Y. Chang, M. F. Krummel, and M. S. Anderson. 2008. Deletional tolerance mediated by extrathymic Aire-expressing cells. *Science* 321:843-847.

49.   Cohen, J. N., C. J. Guidi, E. F. Tewalt, H. Qiao, S. J. Rouhani, A. Ruddell, A. G. Farr, K. S. Tung, and V. H. Engelhard. 2010. Lymph node-resident lymphatic endothelial cells mediate peripheral tolerance via Aire-independent direct antigen presentation. *J. Exp. Med.* 207:681-688.

50.   Fletcher, A. L., V. Lukacs-Kornek, E. D. Reynoso, S. E. Pinner, A. Bellemare-Pelletier, M. S. Curry, A. R. Collier, R. L. Boyd, and S. J. Turley. 2010. Lymph node fibroblastic reticular cells directly present peripheral tissue antigen under steady-state and inflammatory conditions. *J. Exp. Med.* 207:689-697.

51.   Ma, L., J. Liu, T. Wu, M. Plikus, T. X. Jiang, Q. Bi, Y. H. Liu, S. Muller-Rover, H. Peters, J. P. Sundberg, R. Maxson, R. L. Maas, and C. M. Chuong. 2003. 'Cyclic alopecia' in Msx2 mutants: defects in hair cycling and hair shaft differentiation. *Development* 130:379-389.

52.   Gretz, J. E., C. C. Norbury, A. O. Anderson, A. E. Proudfoot, and S. Shaw. 2000. Lymph-borne chemokines and other low molecular weight molecules reach high endothelial venules via specialized conduits while a functional barrier limits access to the lymphocyte microenvironments in lymph node cortex. *J. Exp. Med.* 192:1425-1440.

53.   Roozendaal, R., T. R. Mempel, L. A. Pitcher, S. F. Gonzalez, A. Verschoor, R. E. Mebius, U. H. von Andrian, and M. C. Carroll. 2009. Conduits mediate transport of low-molecular-weight antigen to lymph node follicles. *Immunity* 30:264-276.

54. Anderson, D. M., E. Maraskovsky, W. L. Billingsley, W. C. Dougall, M. E. Tometsko, E. R. Roux, M. C. Teepe, R. F. DuBose, D. Cosman, and L. Galibert. 1997. A homologue of the TNF receptor and its ligand enhance T-cell growth and dendritic-cell function. *Nature* 390:175-179.

55. Wong, B. R., R. Josien, S. Y. Lee, B. Sauter, H. L. Li, R. M. Steinman, and Y. Choi. 1997. TRANCE (tumor necrosis factor [TNF]-related activation-induced cytokine), a new TNF family member predominantly expressed in T cells, is a dendritic cell-specific survival factor. *J. Exp. Med.* 186:2075-2080.

56. Cremer, I., M. C. Dieu-Nosjean, S. Marechal, C. Dezutter-Dambuyant, S. Goddard, D. Adams, N. Winter, C. Menetrier-Caux, C. Sautes-Fridman, W. H. Fridman, and C. G. Mueller. 2002. Long-lived immature dendritic cells mediated by TRANCE-RANK interaction. *Blood* 100:3646-3655.

57. Meier, D., C. Bornmann, S. Chappaz, S. Schmutz, L. A. Otten, R. Ceredig, H. Acha-Orbea, and D. Finke. 2007. Ectopic lymphoid-organ development occurs through interleukin 7-mediated enhanced survival of lymphoid-tissue-inducer cells. *Immunity* 26:643-654.

58. Yun, T. J., M. D. Tallquist, A. Aicher, K. L. Rafferty, A. J. Marshall, J. J. Moon, M. E. Ewings, M. Mohaupt, S. W. Herring, and E. A. Clark. 2001. Osteoprotegerin, a crucial regulator of bone metabolism, also regulates B cell development and function. *J. Immunol.* 166:1482-1491.

59. Willerford, D. M., J. Chen, J. A. Ferry, L. Davidson, A. Ma, and F. W. Alt. 1995. Interleukin-2 receptor alpha chain regulates the size and content of the peripheral lymphoid compartment. *Immunity* 3:521-530.

60. Lee, J. W., M. Epardaud, J. Sun, J. E. Becker, A. C. Cheng, A. R. Yonekura, J. K. Heath, and S. J. Turley. 2007. Peripheral antigen display by lymph node stroma promotes T cell tolerance to intestinal self. *Nat. Immunol.* 8:181-190.

61. Shamoto, M., M. Shinzato, B. Qian, S. Hosokawa, and M. Ishibashi. 1999. Paracortical hyperplasia of superficial lymph nodes in a new mutant strain of hairless rats (ISh): a lesion similar to human dermatopathic lymphadenopathy. *Pathol. Int.* 49:305-309.

62. Tan, W., W. Zhang, A. Strasner, S. Grivennikov, J. Q. Cheng, R. M. Hoffman, and M. Karin. 2011. Tumour-infiltrating regulatory T cells stimulate mammary cancer metastasis through RANKL-RANK signalling. *Nature* 470:548-553.

63. Kollet, O., A. Dar, S. Shivtiel, A. Kalinkovich, K. Lapid, Y. Sztainberg, M. Tesio, R. M. Samstein, P. Goichberg, A. Spiegel, A. Elson, and T. Lapidot. 2006. Osteoclasts degrade endosteal components and promote mobilization of hematopoietic progenitor cells. *Nat. Med.* 12:657-664.

64. Loser, K., A. Mehling, S. Loeser, J. Apelt, A. Kuhn, S. Grabbe, T. Schwarz, J. M. Penninger, and S. Beissert. 2006. Epidermal RANKL controls regulatory T-cell numbers via activation of dendritic cells. *Nat. Med.* 12:1372-1379.

65. Schmutz, S., N. Bosco, S. Chappaz, O. Boyman, H. Acha-Orbea, R. Ceredig, A. G. Rolink, and D. Finke. 2009. Cutting edge: IL-7 regulates the peripheral pool of adult ROR gamma+ lymphoid tissue inducer cells. *J. Immunol.* 183:2217-2221.

66. Collin-Osdoby, P., L. Rothe, F. Anderson, M. Nelson, W. Maloney, and P. Osdoby. 2001. Receptor activator of NF-kappa B and osteoprotegerin expression by human microvascular endothelial cells, regulation by inflammatory cytokines, and role in human osteoclastogenesis. *J. Biol. Chem.* 276:20659-20672.

67. Kim, H. H., H. S. Shin, H. J. Kwak, K. Y. Ahn, J. H. Kim, H. J. Lee, M. S. Lee, Z. H. Lee, and G. Y. Koh. 2003. RANKL regulates endothelial cell survival through the phosphatidylinositol 3'-kinase/Akt signal transduction pathway. *Faseb J.* 17:2163-2165.

68. Min, J. K., Y. M. Kim, E. C. Kim, Y. S. Gho, I. J. Kang, S. Y. Lee, Y. Y. Kong, and Y. G. Kwon. 2003. Vascular endothelial growth factor up-regulates expression of receptor activator of NF-kappa B (RANK) in endothelial cells. Concomitant increase of angiogenic responses to RANK ligand. *J. Biol. Chem.* 278:39548-39557.

69. Rifas, L., S. Arackal, and M. N. Weitzmann. 2003. Inflammatory T cells rapidly induce differentiation of human bone marrow stromal cells into mature osteoblasts. *J. Cell. Biochem.* 88:650-659.

70. Wilke, G., G. Steinhauser, J. Grun, and C. Berek. 2010. In silico subtraction approach reveals a close lineage relationship between follicular dendritic cells and BP3(hi) stromal cells isolated from SCID mice. *Eur. J. Immunol.* 40:2165-2173.

71. Mandala, S., R. Hajdu, J. Bergstrom, E. Quackenbush, J. Xie, J. Milligan, R. Thornton, G. J. Shei, D. Card, C. Keohane, M. Rosenbach, J. Hale, C. L. Lynch, K. Rupprecht, W. Parsons, and H. Rosen. 2002. Alteration of lymphocyte trafficking by sphingosine-1-phosphate receptor agonists. *Science* 296:346-349.

72. Min, J. K., Y. M. Kim, S. W. Kim, M. C. Kwon, Y. Y. Kong, I. K. Hwang, M. H. Won, J. Rho, and Y. G. Kwon. 2005. TNF-related activation-induced cytokine enhances leukocyte adhesiveness: induction of ICAM-1 and VCAM-1 via TNF receptor-associated factor and protein kinase C-dependent NF-kappaB activation in endothelial cells. *J. Immunol.* 175:531-540.

73. Tomei, A. A., S. Siegert, M. R. Britschgi, S. A. Luther, and M. A. Swartz. 2009. Fluid flow regulates stromal cell organization and CCL21 expression in a tissue-engineered lymph node microenvironment. *J. Immunol.* 183:4273-4283.

74. Gommerman, J. L., and J. L. Browning. 2003. Lymphotoxin/light, lymphoid microenvironments and autoimmune disease. *Nat. Rev. Immunol.* 3:642-655.

75. Endres, R., M. B. Alimzhanov, T. Plitz, A. Futterer, M. H. Kosco-Vilbois, S. A. Nedospasov, K. Rajewsky, and K. Pfeffer. 1999. Mature follicular dendritic cell networks depend on expression of lymphotoxin beta receptor by radioresistant stromal cells and of lymphotoxin beta and tumor necrosis factor by B cells. *J. Exp. Med.* 189:159-168.

76. Ansel, K. M., V. N. Ngo, P. L. Hyman, S. A. Luther, R. Forster, J. D. Sedgwick, J. L. Browning, M. Lipp, and J. G. Cyster. 2000. A chemokine-driven positive feedback loop organizes lymphoid follicles. *Nature* 406:309-314.

77. Luther, S. A., A. Bidgol, D. C. Hargreaves, A. Schmidt, Y. Xu, J. Paniyadi, M. Matloubian, and J. G. Cyster. 2002. Differing activities of homeostatic chemokines CCL19, CCL21, and CXCL12 in lymphocyte and dendritic cell recruitment and lymphoid neogenesis. *J. Immunol.* 169:424-433.

78. Vondenhoff, M. F., M. Greuter, G. Goverse, D. Elewaut, P. Dewint, C. F. Ware, K. Hoorweg, G. Kraal, and R. E. Mebius. 2009. LTbetaR signaling induces cytokine expression and up-regulates lymphangiogenic factors in lymph node anlagen. *J. Immunol.* 182:5439-5445.

79. Wong, B. R., J. Rho, J. Arron, E. Robinson, J. Orlinick, M. Chao, S. Kalachikov, E. Cayani, F. S. Bartlett, 3rd, W. N. Frankel, S. Y. Lee, and Y. Choi. 1997. TRANCE is a novel ligand of the tumor necrosis factor receptor family that activates c-Jun N-terminal kinase in T cells. *J. Biol. Chem.* 272:25190-25194.

80. Takayanagi, H., K. Ogasawara, S. Hida, T. Chiba, S. Murata, K. Sato, A. Takaoka, T. Yokochi, H. Oda, K. Tanaka, K. Nakamura, and T. Taniguchi. 2000. T-cell-mediated regulation of osteoclastogenesis by signalling cross-talk between RANKL and IFN-gamma. *Nature* 408:600-605.

81. Yun, T. J., P. M. Chaudhary, G. L. Shu, J. K. Frazer, M. K. Ewings, S. M. Schwartz, V. Pascual, L. E. Hood, and E. A. Clark. 1998. OPG/FDCR-1, a TNF receptor family member, is expressed in lymphoid cells and is up-regulated by ligating CD40. *J. Immunol.* 161:6113-6121.

82. Matzinger, P., and T. Kamala. 2011. Tissue-based class control: the other side of tolerance. *Nat. Rev. Immunol.* 11:221-230.
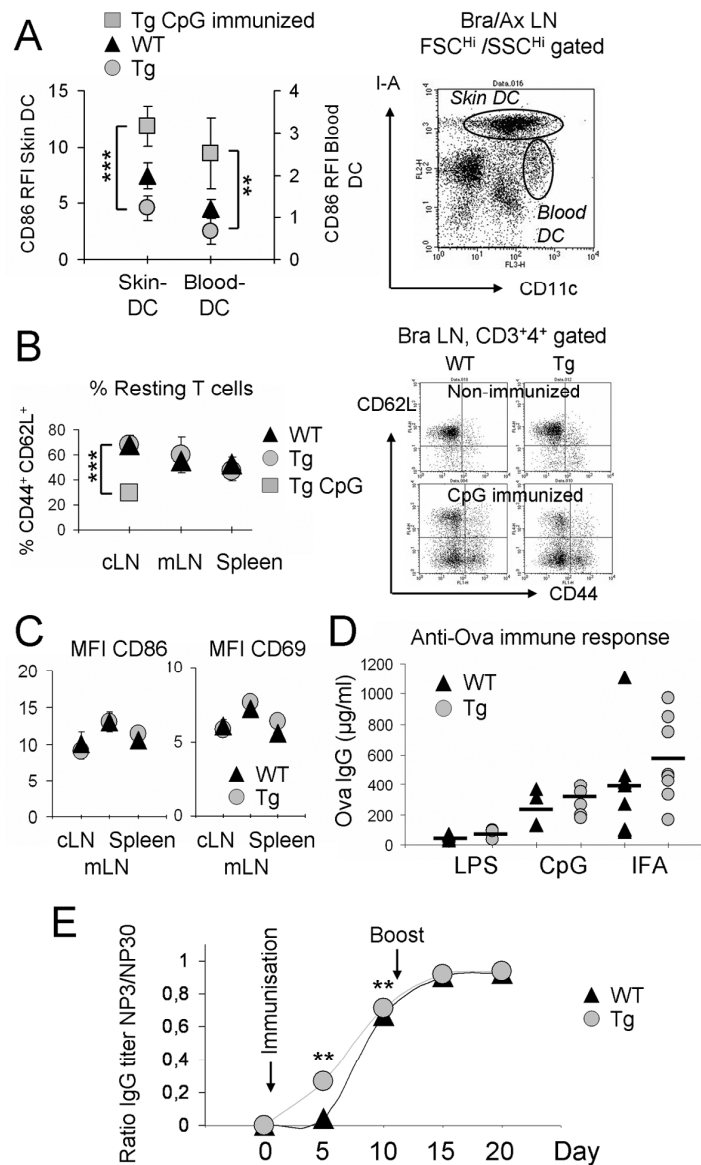
Figures
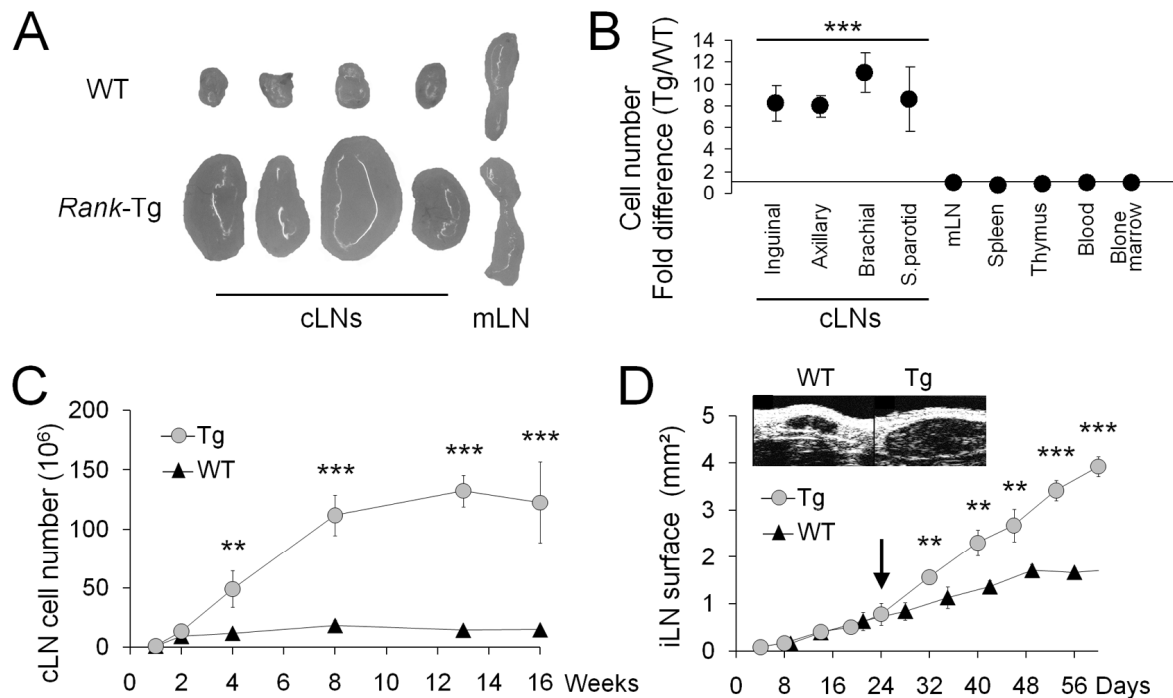
Figure 1. Post-natal cLN hyperplasia in *Rank*-Tg mice

A, Representative photographs of cutaneous (c) LNs (left to right: inguinal [i], axial, brachial and superficial parotid LN) and a mesenteric (m) LN from 12-wk-old WT and *Rank*-Tg mice. *B*, Fold difference in cell numbers of cLNs, mLNs, spleen, thymus, blood and BM in 12-wk-old *Rank*-Tg vs WT mice. *C*, cLN cell numbers from wk 1 to 16 in *Rank*-Tg and WT mice. *D*, iLN surface area measured by ultrasound in *Rank*-Tg and WT mice from postnatal day 4 to 58. Insets show an iLN ultrasound image of 12-wk-old WT and Tg mice. Data in *B* are from 11 mice, collected in three experiments; in *C* and *D*, data are the mean ± SD from 6 mice/ genotype for each time point. **P<0.01, ***P<0.001.
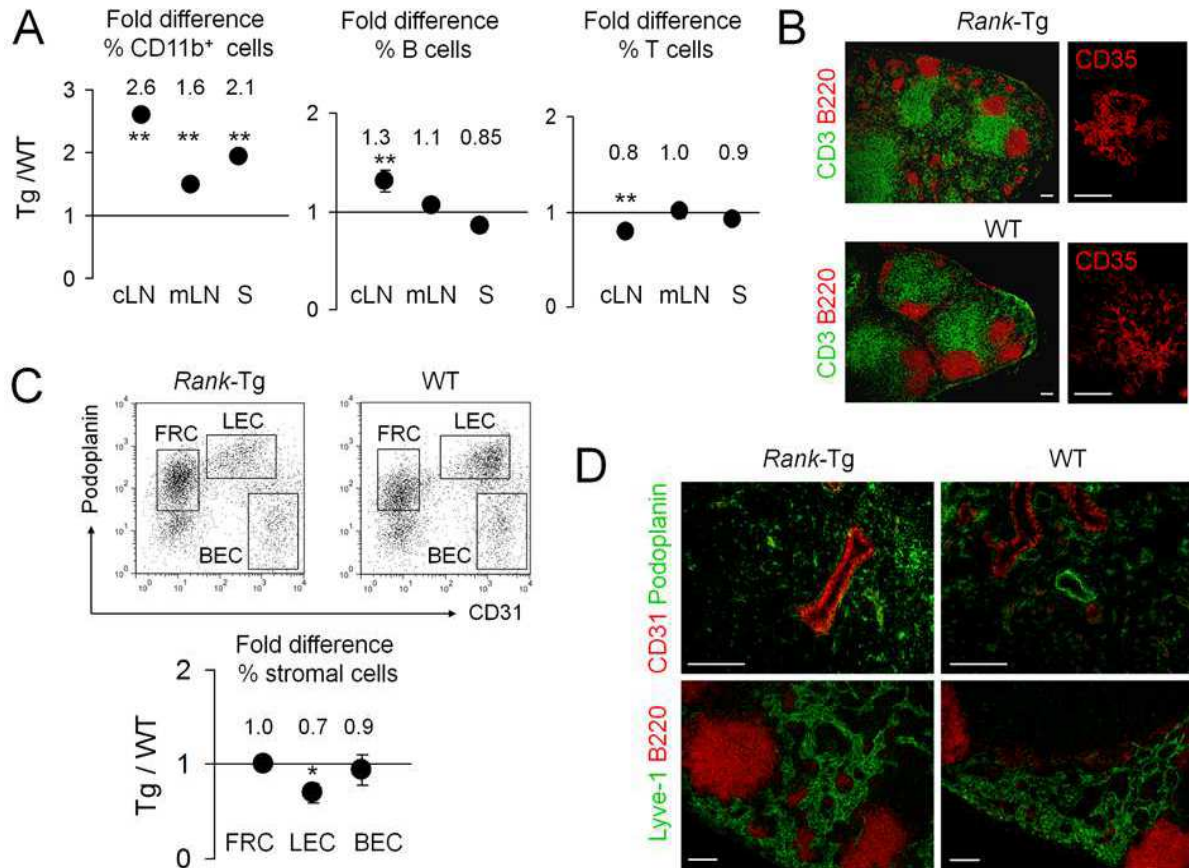
Figure 2. The enlarged cLNs display a well-conserved cell composition and organ architecture

A, Cell lineage proportions in cLN, mLN and spleen of CD11b$^+$ granulo-myeloid cells, B220$^+$ B cells and CD3$^+$ T cells in *Rank*-Tg vs WT mice were identified by flow cytometry. (*n*=11/ genotype) *B*, Representative images of T cell zone and B cell follicle organization (CD3 and B220 staining) and presence of FDCs in follicles (CD35 staining) in cLNs of *Rank*-Tg and WT mice. Scale bar 100 μm. *C*, Identification of cLN the CD45$^-$ FRC, LEC and BEC stromal cell subsets by flow cytometry using podoplanin and CD31 cell surface markers. Lower graph depicts their proportions in cLNs of *Rank*-Tg vs WT mice. The data are from *n*=11-14 mice, accumulated in 4 experiments. *D*, Representative images showing BECs/ FRCs (CD31/ podoplanin) and LECs/ B cells (Lyve-1/ B220) distribution on cLN sections. Scale bar 100 μm. All data are the mean ± SD. *P<0.05, **P<0.01.

Figure 3. The cLN immune cells are resting but respond rapidly to immunization

A, CD86 expression levels of skin-, and blood-derived DCs, purified from brachial and axial LNs in non-immunized WT and *Rank*-Tg mice, as well as in *Rank*-Tg mice 4 d after a s.c. immunization boost with CpG. The graph shows the mean ± SD of 3 animals/ genotype performed in duplicates. The flow cytometry dot blot depicts the gate setting for I-A^{Hi} CD11c$^+$ skin DCs and for I-A$^+$ CD11c^{Hi} blood-derived DCs. *B*, Percentage of CD44 and CD62L-expressing activated helper T cells in cLNs, mLN or spleen in WT, *Rank*-Tg and in *Rank*-Tg mice 4 d after a s.c. immunization boost with CpG. The data is the mean ± SD of at 6-8 animals/ genotype. The flow cytometry dot plots depict a representative analysis of CD62L and CD44 expression of non-immunized and CpG immunized WT and Tg helper T cells from brachial LNs. *C*, CD86 and CD69 expression levels of B220$^+$ B cells in cLNs, mLNs and spleen from WT and *Rank*-Tg mice. The data is the mean ± SEM of 5 animals/ group. *D*, Serum anti-OVA IgG levels in WT and *Rank*-Tg mice, measured after a s.c. immunization boost with OVA in LPS, CpG or IFA. Each data point is for one animal and the bars are the mean values. *E*, High affinity anti-4-hydroxyl-3-nitrophenyl-acetyl (NP) IgG levels after s.c. immunizations of NP$_{30}$ conjugated to KLH in LPS. Serum anti-NP IgG was by ELISA for NP$_3$-BSA or NP$_{30}$-BSA, and the relative affinity was determined as the titer NP$_3$/ titer NP$_{30}$. The data are the mean ± SEM of 7 mice/ group. **$P<0.01$, ***$P<0.001$.
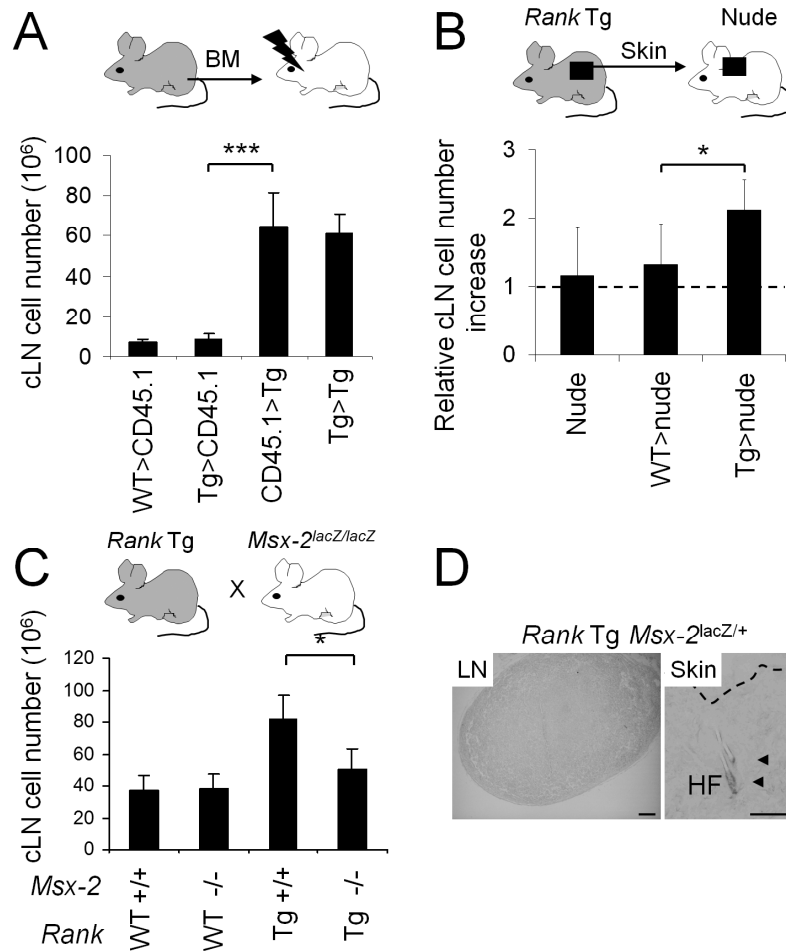
Figure 4. Tg RANK overexpression in HF induces cLN hyperplasia

A, Analysis of cell numbers in cLNs (brachial, inguinal and axial) after adoptive BM transfers, as indicated. The data are from 3 mice/ group compiled from 7 different experiments. *B*, Relative cLN cell number increase of brachial and axial LNs, normalized to inguinal LNs in *nude* mice and after skin grafting of the indicated skin genotype. The data are from 3 mice/ group compiled from 3 different experiments. *C*, cLN cell numbers in WT, *Msx-2* $^{LacZ/LacZ}$, *Rank*-Tg and *Rank*-Tg x *Msx-2*$^{LacZ/LacZ}$ mice. The data are from 8 mice/ group from 4 experiments. *D*, Representative β-galactosidase staining in a brachial LN and the skin of *Rank*-Tg x *Msx-2* $^{LacZ/+}$ mice. Arrow heads point to β-galactosidase enzymatic reactivity of hair follicle (HF) matrix cells. Dashed line indicates the dermo-epidermal junction. Scale bar 100µm. All data are the mean ± SD. *P<0.05, ***P<0.001.
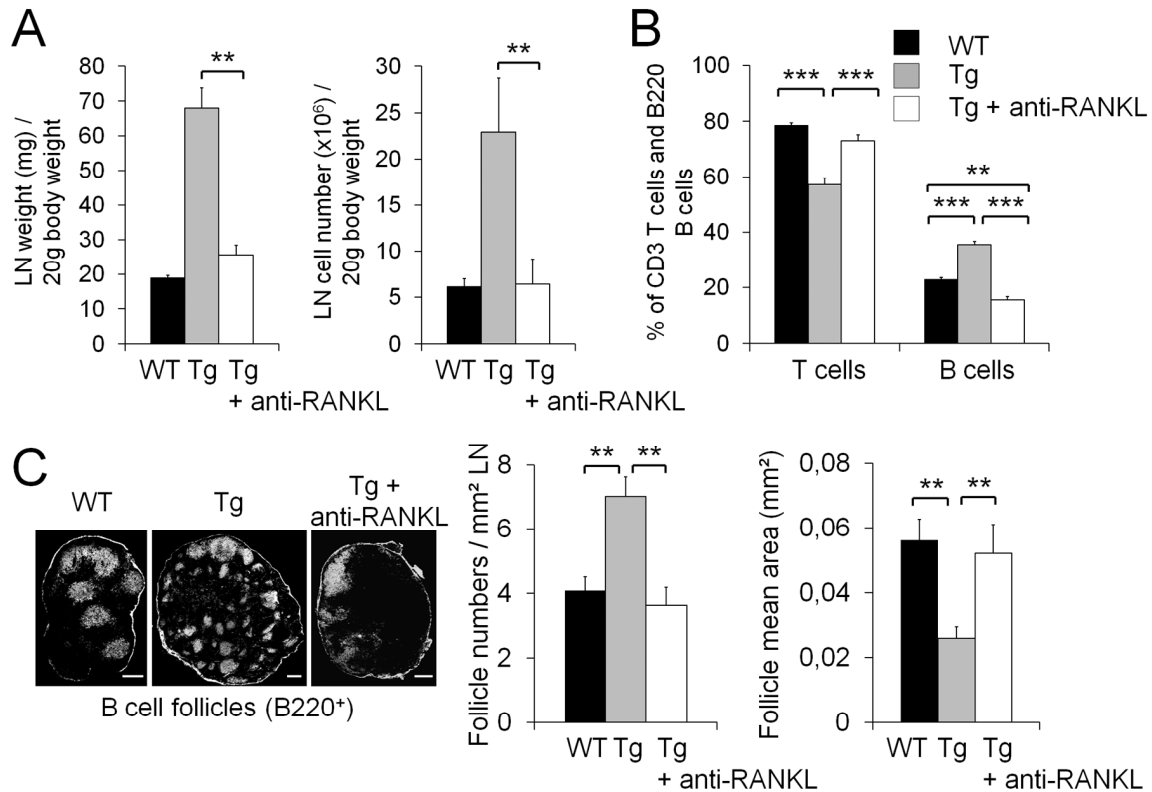
Figure 5. RANKL induces cLN growth

A, Weight and cell numbers of cLNs, normalized to body weight, of WT, control Ig-administered *Rank*-Tg mice and *Rank*-Tg mice, treated with anti-RANKL blocking mAb from P10 to 6-wk of age. *B*, Percentage of T and B cells in cLNs of WT, control Ig-administered *Rank*-Tg mice and *Rank*-Tg mice, treated with anti-RANKL blocking mAb. *C*, Left: Representative visualization of B cell follicles in WT, control Ig-administered *Rank*-Tg mice and *Rank*-Tg mice, treated with anti-RANKL blocking mAb by immunofluorescence on axial LN sections. Bars represent 200 µm. Right: B cell follicles visualized on B220-stained axial LN cross sections were counted and their area quantified using the ImageJ software. All data are the mean ± SEM of 9 mice/ group acquired in 3 separate experiments. **$P<0.01$, ***$P<0.001$.
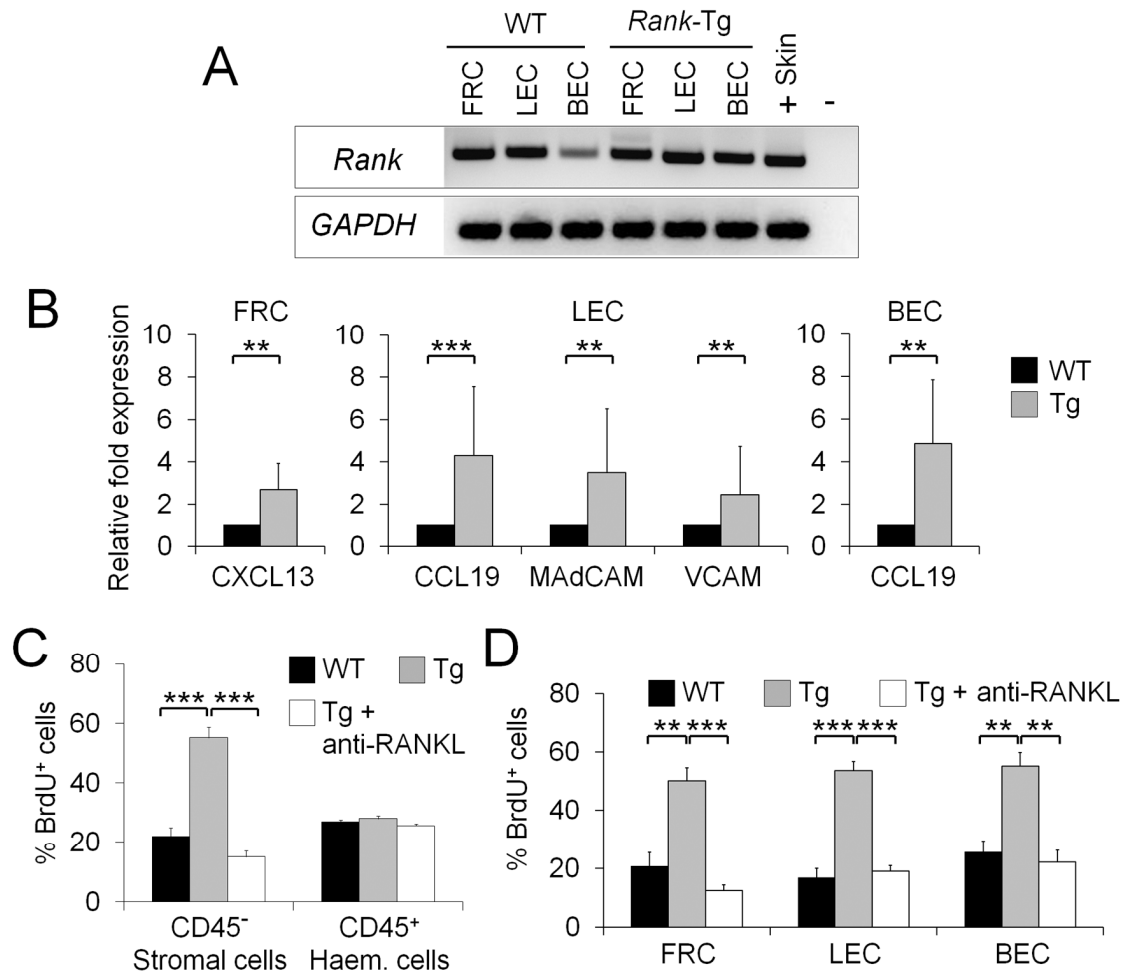
Figure 6. RANKL activates stromal cell proliferation and chemokine/ adhesion molecule expression

A, RT-PCR analysis of *Rank* and *GAPDH* mRNA expression by stromal subsets from cLNs of WT and *Rank*-Tg, flow cytometry-sorted on the basis of podoplanin/ CD31 expression (see Fig. 2*C*). Skin cDNA served as positive and water as negative controls. Image is representative of 4 separate experiments with 15 pooled WT and 5 pooled Tg mice. *B*, mRNA expression of chemokines and adhesion molecules in stromal subsets from WT and *Rank*-Tg mice in flow cytometry-sorted stromal subsets. The measures were done by qRT-PCR and are depicted as the fold increase with respect to WT. The data are the mean ± SEM of 4 independent experiments performed in duplicate with 15 pooled WT mice and 5 pooled *Rank*-Tg mice. *C*, BrdU incorporation by flow cytometry of CD45$^-$ cLN stromal and CD45$^+$ hematopoietic cells from WT, control Ig-administered *Rank*-Tg mice and *Rank*-Tg mice treated with anti-RANKL blocking mAb. *D*, BrdU incorporation by the cLN stromal subsets from WT, control Ig-administered *Rank*-Tg mice and *Rank*-Tg mice treated with anti-RANKL blocking mAb. Data in *C* and *D* are the mean ± SEM of 6-9 mice per group, obtained by flow cytometry using podoplanin/ CD31 markers to identify the subsets. **$P<0.01$, ***$P<0.001$.

Tables

Table I. Absolute cell numbers in organs

Cell numbers (10^6)	Cutaneous LNs	Mesenteric LNs	Spleen	Thymus	Blood	Bone Marrow
Rank-Tg (n=11)	196 ± 39	6.3 ± 3.1	76 ± 14	96 ± 44	5.6 ± 4.8	5.6 ± 4.8
WT (n=8)	22 ± 3	7.2 ± 1.6	105 ± 20	125 ± 44	6.2 ± 4.0	6.2 ± 4.0
	P<0.001	NS.	*P*<0.01	NS.	NS.	NS.

Cell numbers of organ and blood cell suspensions from 12-wk-old Tg and WT animals were counted in a hemacytometer. The data is the mean ± SD. NS = non significant.

Table II. Absolute cell numbers of hematopoietic cell types

Cell numbers (10^6)	Organ	CD3$^+$ T cells	CD11b$^+$ Macrophages	B220$^+$ B cells	Mature B IgD^{Mod}IgM^{Mod}	T2 B IgD^{Hi}IgM^{Hi}	T1/MZ B IgD^{Lo}IgM^{Hi}
Rank-Tg (n=11)	cLNs[a]	53.9 ± 17.7	2.7 ± 1.2	65.4 ± 30			
WT (n=8)		8.5 ± 3.1	0.2 ± 0.06	5.6 ± 2.3			
		p<0.001	p<0.001	p<0.001			
Rank-Tg (n=11)	Mesenteric LN	3.3 ± 1.4	0.08 ± 0.07	2.3 ± 1.3			
WT (n=8)		4.3 ± 1.1	0.07 ± 0.06	2.4 ± 0.5			
		NS	NS	NS			
Rank-Tg (n=11)	Spleen	16.4 ± 4.7	4.4 ± 2	36.1 ± 9.5	28 ± 12	2.6 ± 1.6	8.8 ± 4.5
WT (n=8)		25.4 ± 6.1	3.3 ± 0.6	57 ± 13	39 ± 9	3.6 ± 0.6	7.4 ± 3.4
		p<0.001	NS	p<0.002	p<0.03	p<0.05	NS
Rank-Tg (n=11)	Blood (mL^{-1})	2.2 ± 1.3	1.4 ± 1.0	2.9 ± 2.2			
WT (n=8)		1.7 ± 0.7	1.0 ± 0.4	2.7 ± 1.5			
		NS	NS	NS			

[a] Cutaneous (c) LNs were inguinal, axial, brachial and superficial paratoid, except for B cells and macrophages, where cell numbers were determined without brachial LNs.

Cell numbers of organs and blood cell suspensions were counted in a hemacytometer and analyzed for T cells, macrophages, B cells and B cell subsets by flow cytometry. The total number was determined using the percentage composition of the different cell types. The data is the mean ± SD. Statistic analysis was done by the Student's *t*-test, NS = non-significant.
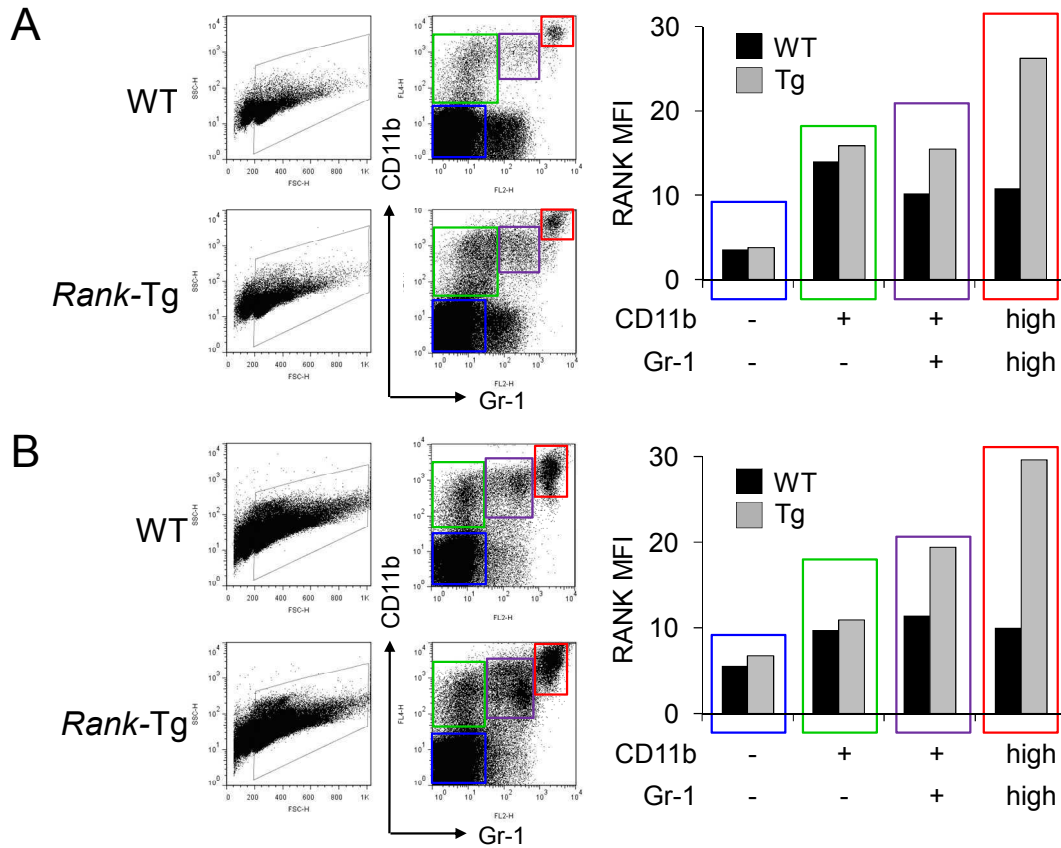
Supplementary figures
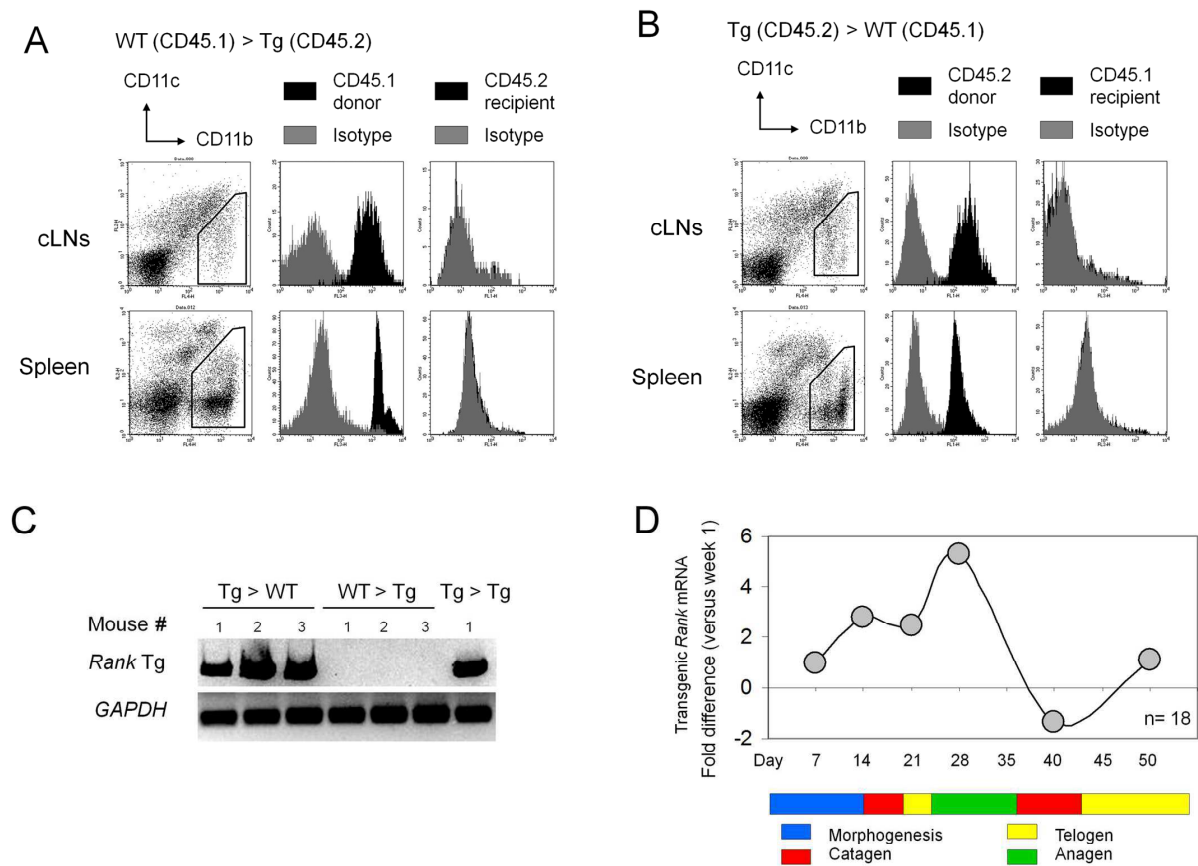
Supplemental Figure 1. Verification of adoptive BM transfer and skin transgenic *Rank* mRNA expression

A and *B*, Flow cytometry analysis of host or donor origin of CD11b$^+$ cells in cLNs and spleen was performed in *Rank*-Tg (*A*) and WT (*B*) recipient mice, 3 mo after adoptive BM transfer, representative of 5 mice/ group. *C*, RT-PCR for Tg *Rank* and *GAPDH* on total cLN RNA in the indicated chimeras, 3 mo after adoptive transfers. *D*, Skin transgenic *Rank* mRNA expression in *Rank*-Tg mice from postnatal day 7 to 50 was determined by qRT-PCR. The expression level is expressed as fold difference versus day 7 and is the mean of 3 mice/ time point. The HF morphogenesis and the HF cycle phases are indicated below the graph.
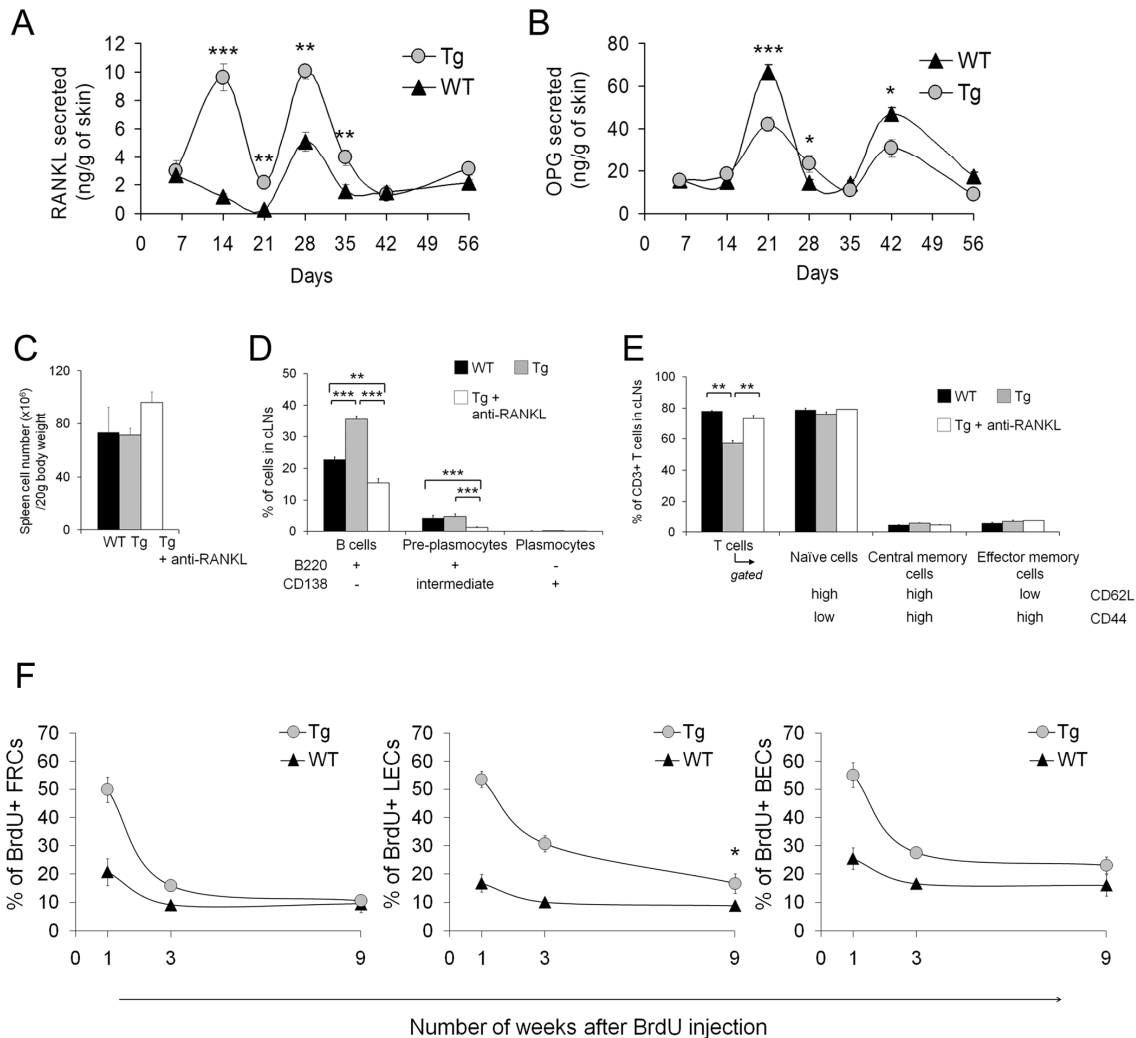
Supplemental Figure 2. Skin RANKL and OPG release, verification of the effect of RANKL-blocking on splenic cell numbers and on cLN immune cell activation as well as analysis of stromal cell viability

The level of soluble RANKL (*A*) and OPG (*B*) after a 24 h skin organ culture was determined by ELISA from mice of the indicated ages. The values are the mean ± SD (at least 5 mice per group) and were normalized for skin weight. *C*, Spleen cell number, normalized to body weight, were determined for WT control, mock-treated *Rank*-Tg mice and *Rank*-Tg mice administered with anti-RANKL blocking mAb. The graph data is the mean ± SEM of 6 animals/ group, of 3 different experiments. (*D* and *E*) Percentage of B cell plasmocytes (*D*) and memory T cells (*E*) in cLNs of WT, control Ig-administered *Rank*-Tg mice and *Rank*-Tg mice, treated with anti-RANKL blocking mAb, was determined by flow cytometry. The data are the mean ± SEM of 6 animals/ group, collected in 3 experiments. *F*, Percentage of BrdU incorporation by the cLN stromal subsets (FRC, LEC and BEC) from WT and *Rank*-Tg mice for 6 d, at 6 wk of age, followed by a chase period, measured by flow cytometry using podoplanin/ CD31 markers to identify the stromal subsets. The percentage of BrdU$^+$ cells was monitored 2 and 8 wks after BrdU labeling. The data are the mean ± SEM of 6 mice/ group, accumulated in 3 experiments. *$P<0.05$, **$P<0.01$, ***$P<0.001$.

Supplemental Figure 3. RANK expression in the CD11b⁺ cell population in cLNs and spleen

RANK expression by CD11b+ granulo-myeloid cells in cLNs (A) and spleen (B) from WT and *Rank*-Tg mice was determined by flow cytometry. CD11b Gr-1 staining was performed on large cells, electronically gated as shown on the left. The graph depicts the RANK expression level on the different subsets, highlighted by color boxing and is representative for 6 experiments.
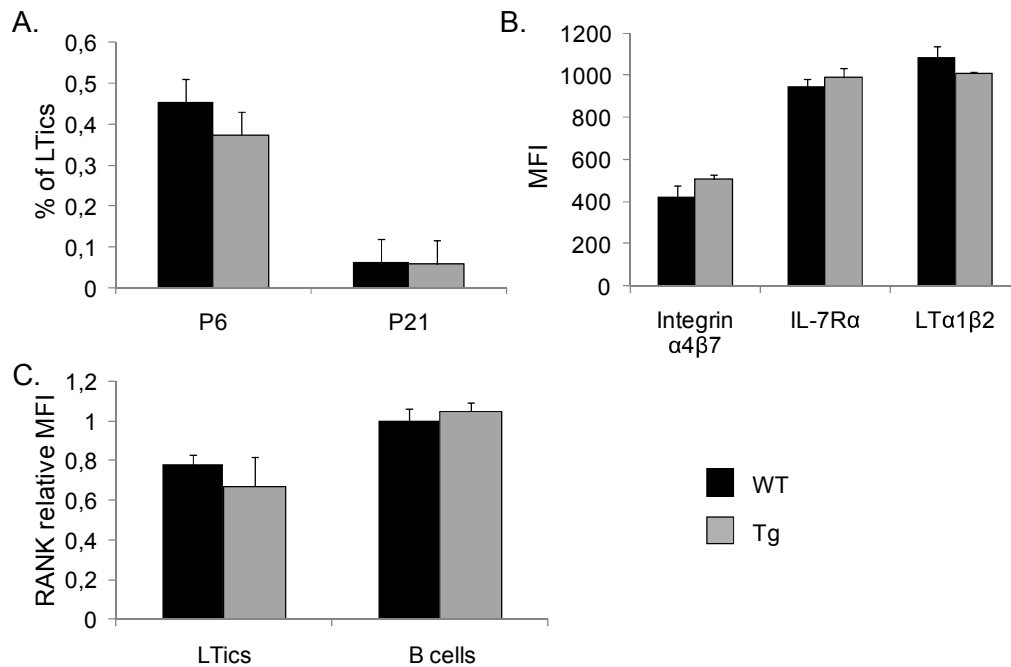
Supplemental Figure 4. Normal LTics population in *Rank*-Tg mice and no transgene expression in LTics and in B cells.

A, Flow cytometry analysis of CD3⁻CD4⁺IL-7Rα⁺α4βv⁺ LTics in P6 and P21 cLNs (brachial, inguinal and axial). The data are the result of 3 different experiments. *B*, Flow cytometry analysis of integrin α4β7, IL-7Rα and LTα1β2 expression by LTics from P6 mice cLNs. The data are representative of 3 mice per group. *C*, Flow cytometry analysis of RANK expression by LTics from P6 mice cLNs and CD19⁺ B cells from 6 wk mice. The data are representative of at least 3 mice per group.
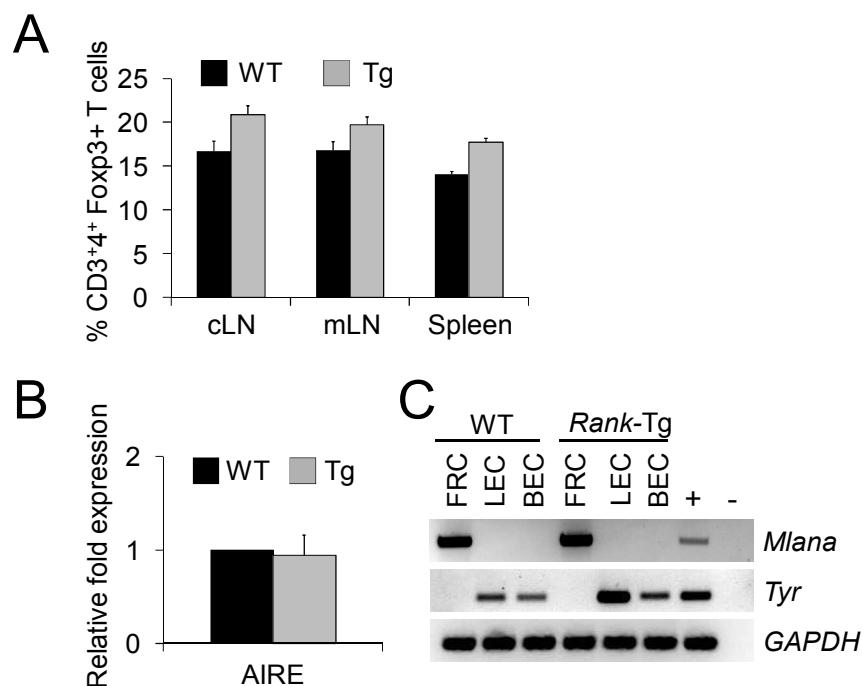
Supplemental Figure 5. Preserved tolerance in hyperplasic cLN

(A) Proportion of FoxP3^{+} regulatory T cells among CD3^{+}CD4^{+} T cells in cLNs, mLNs and spleen from 6 to 15-wk-old WT and *Rank*-Tg mice. The data are the mean ± SD of at least 9 animals per group. (B) qRT-PCR on whole cLNs from 6-wk-old *Rank*-Tg and WT mice was performed to assess *Aire* expression. The data is the mean ± s.e.m of 8 mice/ group and is expressed as the relative fold increase vs WT. (C) Transcriptional analysis for the genes encoding Mlana and Tyrosine peripheral T cell antigens, as well as GAPDH, by RT-PCR on FACS-sorted stromal subsets from 6-wk-old *Rank*-Tg and WT mice. Whole cLN cDNA served as positive control, while water was the negative control. The image is representative of 4 separate experiments with 15 pooled WT and 5 pooled Tg mice.
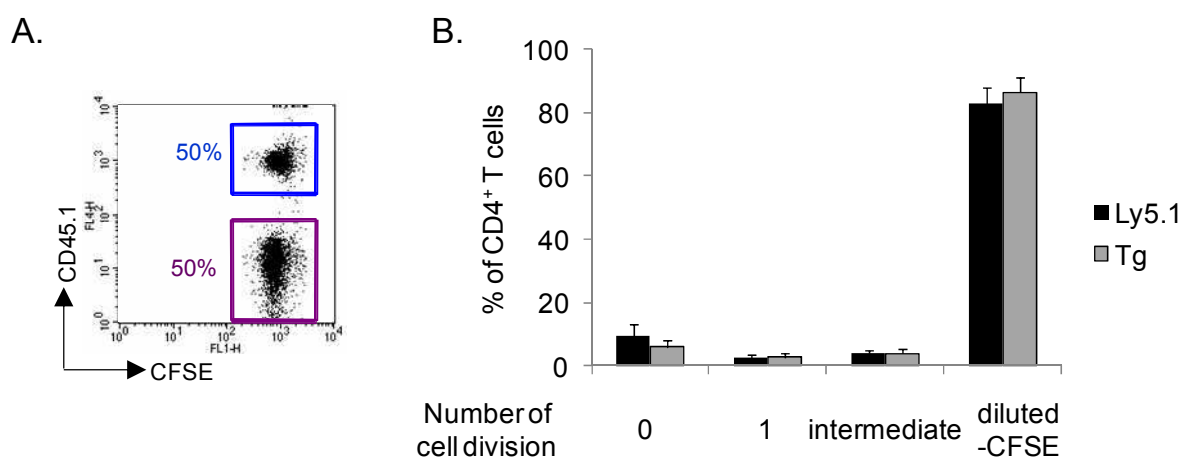
Supplemental Figure 6. Normal CD4+ T cells proliferation after transfer in a lymphopenic environment.

A, Flow cytometry analysis of the Ly5.1 and *Rank*-Tg CFSE^{+}CD3^{+}CD4^{+} cells transferred in 4 wk *rag2^{-/-}* mice. *B*, Flow cytometry analysis of the CD3^{+}CD4^{+} cells recovered 7 days after the transfer into the *rag2^{-/-}* mice. The data are representative of at least three mice per group.
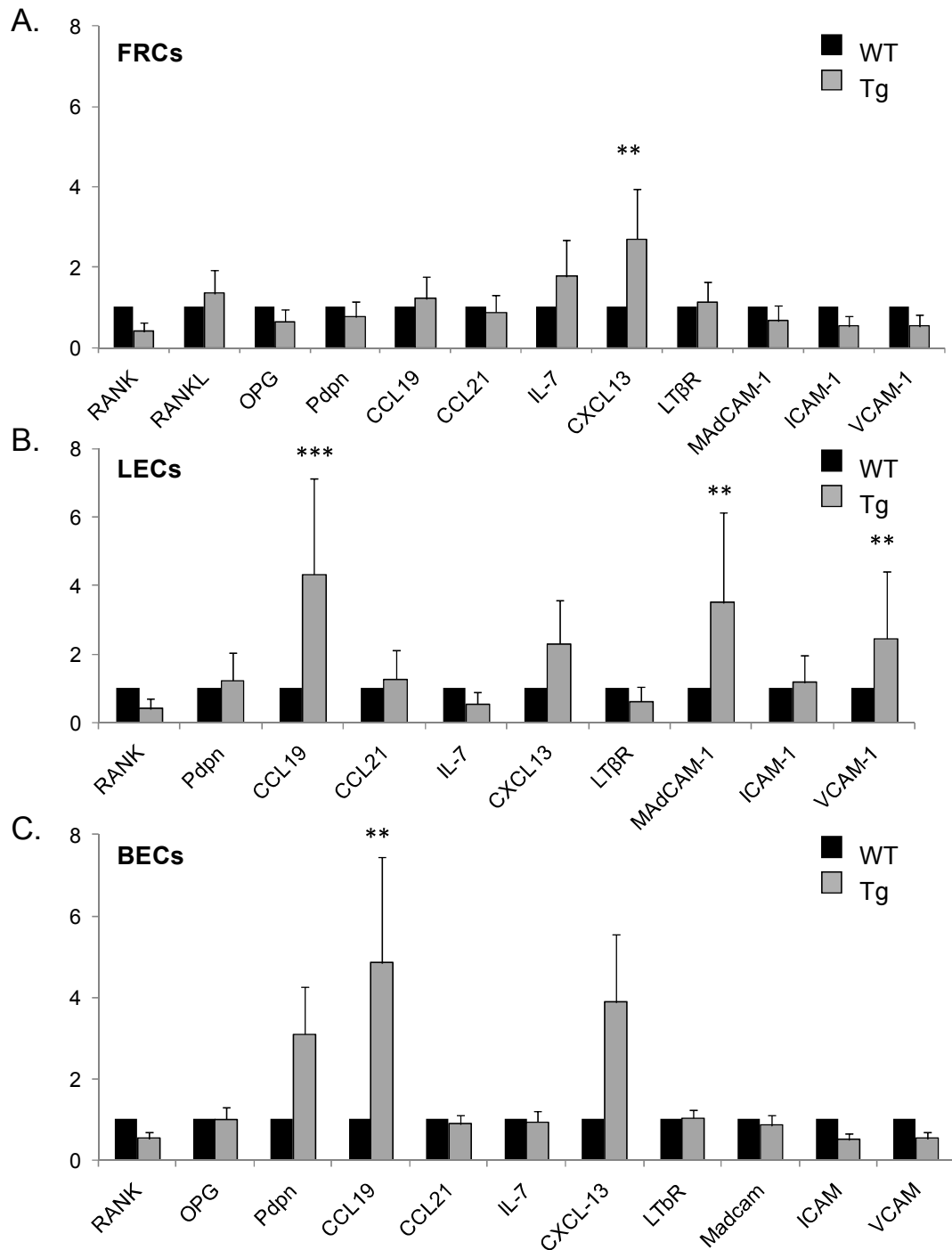
Supplemental Figure 7 RANK, RANKL, OPG, chemokines and adhesion molecule expression by stromal cells subsets.

mRNA expression of chemokines and adhesion molecules in stromal subsets from WT and *Rank*-Tg mice in flow cytometry-sorted stromal subsets (a: FRCs, b:LECs, c: BECs). The measures were done by qRT-PCR and are depicted as the fold increase with respect to WT. The data are the mean ± SEM of 4 independent experiments performed in duplicate with 15 pooled WT mice and 5 pooled *Rank*-Tg mice. **$P<0.01$, ***$P<0.001$.

Supplementary tables

Supplemental Table I. PCR primers

Gene	Primer	Application
Genotyping		
Rank-Tg	forward : atggactacaaagacgatgacgaca reverse : tgccaggaatccaccgccaccag (264 bp)	PCR-genotyping
Msx-2 $^{lacZ/lacZ}$	forward : gtcttcgcttgagagttgcca reverse : gtcggacatgagcgcctc (WT 225 bp) reverse : ggcaaagcgccattcgccattcaggc (*LacZ*) (Mutant 300 bp)	PCR-genotyping
RT-PCR/qPCR		
β-actin	forward: atgagctgcctgacggccaggtcatc reverse: tggtaccaccagacagcactgtgttg (192 bp)	qPCR
GAPDH	forward: tgacgtgccgc tggagaaa reverse: agtgtagcccaagatgcccttcag (98 bp)	qPCR / RT-PCR
HPRT	forward: cttgctggtgaaaaggacctct reverse: aagtactcattatagtcaagggcat (111 bp)	qPCR
CCL19 *	forward: ctgcctcagattatctgccat reverse: tcattagcacccccccagagt (105 bp)	qPCR
CCL21 *	forward: ccctggacccaaggcagt reverse: aggcttagagtgcttccggg (162 bp)	qPCR
CXCL13 *	forward: gtattctggaagcccattacac reverse: aacttgcgagcagcacgatttag (184 bp)	qPCR
ICAM-1 *	forward: cactgccttggtagaggtgactga reverse: gttacttggctcccttccgagac (171 bp)	qPCR
IL-7 *	forward: cgatgaattggacaaaatgacagg reverse: aacttgcgagcagcacgatttag (126 bp)	qPCR
LT-βR *	forward: aaatcccccagagccagga reverse: ggtgccgcttgagcagagt (146 bp)	qPCR
MAdCAM *	forward: gacccatagaaaggagattccagta reverse: tgagcccagtggagactgc (125 bp)	qPCR
OPG *	forward: cgaggaccacaatgaacaagtg reverse: tgggttgtccattcaatgatgt (73 bp)	qPCR
Podoplanin*	forward: gggttttggggagcgtttg reverse: gaggtgccttgccagtagattca (176 bp)	qPCR
Rank *	forward: tgcgtgctgctcgttcca reverse: accgtccgagatgctcataat (85 bp)	*qPCR*
Rankl *	forward: cagcatcgctctgttcctgt reverse: gcagtgagtgctgtcttctga (73 bp)	*qPCR*
VCAM-1 *	forward: agcagagacttgaaatgcctgtga reverse: ggtgattcgcagcccgta (178 bp)	qPCR
AIRE	forward: ccaagggagcccaggtca reverse: tggcacacggcacactca (136 bp)	qPCR
Mlana	forward: ctgctgaagaggccgcaggg reverse: ggagcgttgggaaccacggg (232 bp)	*RT-PCR*
Tyr	forward: attgattttgcccatgaagc reverse: ggcaaatccttccagtgtgt (453 bp)	*RT-PCR*
Rank-Tg	forward: atgtctcttgtcagctgtctt reverse: agcttgtcgtcatcgtctt (131 bp)	qPCR / RT-PCR

* Genes tested for upregulation in the stromal subsets of cLNs

Supplemental Table II. Primary antibodies

Target	Species	Clone or designation	Conjugation	Appli-cation	Vendor	Dilution
BrdU	mouse IgG1	B44	FITC	FC¤	Becton Dickinson	1/10
CD3	armenian hamster IgG1	145-2C11	PerCP	FC	BD-Pharmingen	1/200
CD3 Secondary Ab	rabbit IgG goat IgG	polyclonal/A0452 polyclonal/A11070	Unconjugated A488	IHC¤	Dako Molecular Probes	1/50 1/500
CD4	rat IgG2a	RM4-5	PE and PerCP -Cy5.5	FC	BD-Pharmingen	1/200
CD11b	rat IgG2b	M1/70	APC	FC	BD-Pharmingen	1/1000
CD11c	armenian hamster IgG1	HL3	Biotin Streptavidin PerCP	FC	BD-Pharmingen	1/400 1/300
CD31	rat IgG2a	390	PE	FC, IHC	Biolegend	1/1000
CD35	rat IgG2a	8C12	Biotin TSA* (A546)	IHC	BD-Pharmingen Perkin Elmer	1/100
CD44	rat IgG2b	IM7	FITC and APC	FC	BD-Pharmingen	1/400
CD45	rat IgG2b	30-F11	APC	FC	BD-Pharmingen	1/1000
CD45.1	mouse IgG2a	A20	Biotin Streptavidin PerCP	FC	e-Bioscience BD-Pharmingen	1/500 1/300
CD45.2	mouse IgG2a	104	FITC	FC	e-Bioscience	1/500
CD45R	rat IgG2a	RA3-6B2	FITC and APC	FC	BD-Pharmingen	1/300
CD45R	rat IgG2a	RA3-6B2	Biotin Streptavidin A546	IHC	BD-Pharmingen Molecular Probes	1/100 1/500
CD62L	rat IgG2a	MEL-14	PE and APC	FC	BD-Pharmingen	1/400
CD69	armenian hamster IgG1	H1-2F3	PE	FC	BD-Pharmingen	1/400
CD86	rat IgG2a	GL1	PE	FC	BD-Pharmingen	1/200
CD138	rat IgG2a	281.2	APC	FC	BD-Pharmingen	1/400
Gr-1	rat IgG2b	RB6-8C5	PE	FC	BD-Pharmingen	1/1000
I-A I-E	rat IgG2a	2G9	PE	FC	BD-Pharmingen	1/1000
Lyve-1	rat IgG1	ALY7	A488	IHC	e-Bioscience	1/100
Foxp3	rat IgG2a	FJK-16s	APC	FC	e-Bioscience	1/200
Podoplanin Secondary Ab	syrian hamster IgG goat IgG	8.1.1 polyclonal/107065142	Unconjugated Biotin Streptavidin A488	FC, IHC	Biolegend Jackson IR Molecular Probes	1/100 1/300 1/500
RANK Secondary Ab	goat IgG donkey IgG	polyclonal/AF462 polyclonal/705065147	Unconjugated Biotin Streptavidine PerCP	FC	R&D Systems Jackson IR BD-Pharmingen	1/100 1/100 1/300

¤ FC: Flow Cytometry, IHC: Immunohistochemistry

* Signal enhancement with the Tyramide Signal Amplification System (TSA; Perkin Elmer)

2.3. *Conclusions*

The lack of LNs in RANKL and RANK deficient mice renders the task of elucidating the possible function of RANK in LNs beyond the development difficult. We therefore took advantage of the murine *Rank*-transgenic model, which over-produces endogenous hair follicle RANKL. These mice display a massive post-natal growth of skin-draining LNs but conserved proportions of hematopoietic and stromal cells, along with a conserved general organization. Nevertheless, although T and B cells normally segregate into different zones, there was an increase of small B cell follicles. The hematopoietic cells are not activated and respond normally to foreign antigens and adjuvant, thus hyperplasia observed is not the result of an inflammation. Bone marrow transfer after a lethal irradiation and skin graft experiments support that *Rank*-transgene expression in hair follicles is necessary and sufficient for skin-draining LNs hyperplasia. Neutralization of RANKL (most likely the soluble RANKL released by the transgenic hair follicles) normalizes LNs size, including area and number of B cell follicles. We show that reticular fibroblastic and vascular stromal cells, which express RANK, hyperproliferate in our transgenic model and that RANKL neutralization abrogate this hyperproliferation. Moreover, these stromal cells express higher levels of CXCL13 and CCL19 chemokines and MAdCAM-1 and VCAM-1 cell adhesion molecules in the hyperplasic LNs. Hence, skin-derived RANKL activates stromal cells to proliferate and to express molecules known in organ development and inflammation. This work highlighted a novel function for RANK-RANKL in LNs, beyond development, by identifying RANKL as a molecule controlling the plasticity of LNs, and underlined the importance of tissue-derived cues for secondary lymphoid organ homeostasis.

CONCLUSIONS

AND

PERSPECTIVES

Conclusions and perspectives

1. *Objectives of the thesis*

RANK, RANKL and OPG are widely expressed throughout the body and are thus implicated in several biological processes. Hence, these proteins are key regulators of bone homeostasis and are also implicated in several immunological functions such as dendritic cell biology and central tolerance. The functions of RANK in these two biological systems allowed the discovery of the mechanism underlying bone loss during chronic inflammation and the emergence of a new field of research: osteoimmunology. In addition, RANK and RANKL are crucial for the development of LNs. The development of these organs relies on close interactions between stromal organizer cells and LTics. While $LT\alpha_1\beta_2$-$LT\beta R$ is essential for the maturation of stromal organizer cells and for chemokines expression, RANK-RANKL is required for LTics proliferation and/or survival. $LT\beta R$ was found to be required for the maintenance of the microarchitecture of B cell follicles and evidence of a similar role for RANK has been described but was never clearly addressed. RANK is implicated in the survival and proliferation of endothelial cells and in their expression of adhesion molecules. Endothelial cells belong to the LN stroma and are thus important for LN functions during steady state and inflammation. The functions of RANK in endothelial cells biology along with the similitudes between RANK and $LT\beta R$ during LN development and possibly for the maintenance of its architecture led us to address the functions of RANK in LNs.

During my doctorate we also addressed the function of RANK in the skin. RANK and RANKL are required for growth and differentiation of many subtypes of epithelial cells such as the mammary and prostate epithelial cells, the thymic medullary cells and the intestinal microfold cells. Thus, we asked the question of a possible role of RANK and RANKL in the continuous epidermal turnover of the skin, which is the largest epithelial surface of the body. In addition, RANK is implicated in the development of two skin appendages: the teeth and the mammary glands. The hair follicle (HF) is another skin appendage and many molecules known to influence its cycle are also important in the bone biology and regulate RANK, RANKL or OPG expression. Hence, we also addressed the possible function of RANK in HF cycling.

To address these questions two murine models were used: RANKL-deficient mice and mice over-expressing RANK in HF stem cells and in granulo-myeloid lineage (*Rank*-Tg mice). Both mice were used to study the function of RANK in the skin homeostasis. The study of RANK function relied on the transgenic model.

2. *RANK in the regulation of skin homeostasis*

In addition to the bone and the immune system, we demonstrated that RANK is implicated in another biological system: the skin. We established for the first time that RANK acts as a regulator of hair cycling and epidermal homeostasis.

Although RANKL-deficient mice display normal HF morphogenesis, these animals were unable to initiate a new growth phase (anagen). Anagen entry after RANKL-deficient skin transplantation onto a RANKL-proficient environment and after s.c. injection of RANKL on resting wild-type skin, along with its expression by the anagen HF demonstrated the requirement of RANKL for HF anagen. RANK, RANKL and OPG are expressed by the HF stem cells supporting the importance of these proteins for the HF cycling. The previously reported strong expression of OPG in the bulge could be related to a possible function of OPG as an autocrine regulator of anagen entry by blocking RANK-RANKL interaction. Hence, soluble levels of OPG were higher at telogen. In addition to this possible direct regulation, an indirect mechanism could also take place. In the bone system, estradiol and IGF-1 (insulin growth factor 1) were respectively found to increase and to decrease the expression of OPG. Estradiol is known to antagonize the entry in anagen, whereas IGF-1 is known to induce it. Hence, part of the HF regulatory process by these proteins could rely on their modified expression of OPG (Figure 1). Nevertheless, further experiments are needed to confirm this possible function and the signals regulating RANKL expression in the HF remain elusive.
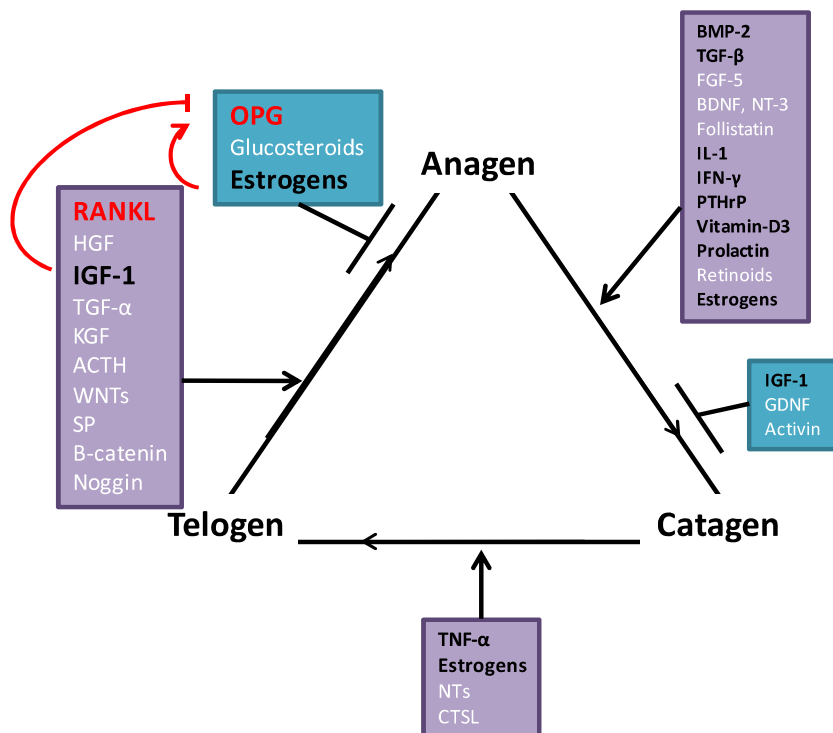
Figure 1: Schematic representation of the proposed mechanism of anagen entry. Molecules known to induce or to repress HF progress through the different stages are depicted, molecules in a bold black font are molecules known to regulate RANK, RANKL and/or OPG expression. RANKL is required for anagen entry and OPG may be a negative regulator of this process. In addition, like in the bone system, IGF-1 and estrogens could respectively decrease and increase OPG expression.

RANKL-deficient mice present a diminished epidermal thickness associated with a reduced cell growth, whereas *Rank*-Tg mice display a thickened epidermis and an accelerated cell proliferation, suggesting a role for RANK in epidermal renewal. RANK was not associated with epidermal differentiation or barrier function as no such defects were found in the two murine models studied. A slight and transient upregulation of IL-1β and TNFα was found in the skin of *Rank*-Tg animals. Although we could not exclude an implication of these pro-inflammatory cytokines in epidermal proliferation, this expression did not trigger local or distant immune cell activation. Moreover RANK expression by basal-layer keratinocytes along with the increase in the number of keratinocytes recovered after 15 days of primary keratinocytes culture of *Rank*-Tg mice suggest a cell-autonomous enhanced keratinocyte proliferation.

Thus, RANK-RANKL-OPG, previously described for their function in the bone, the immune system and in the mammary glands, also regulate hair cycling and epidermal homeostasis.
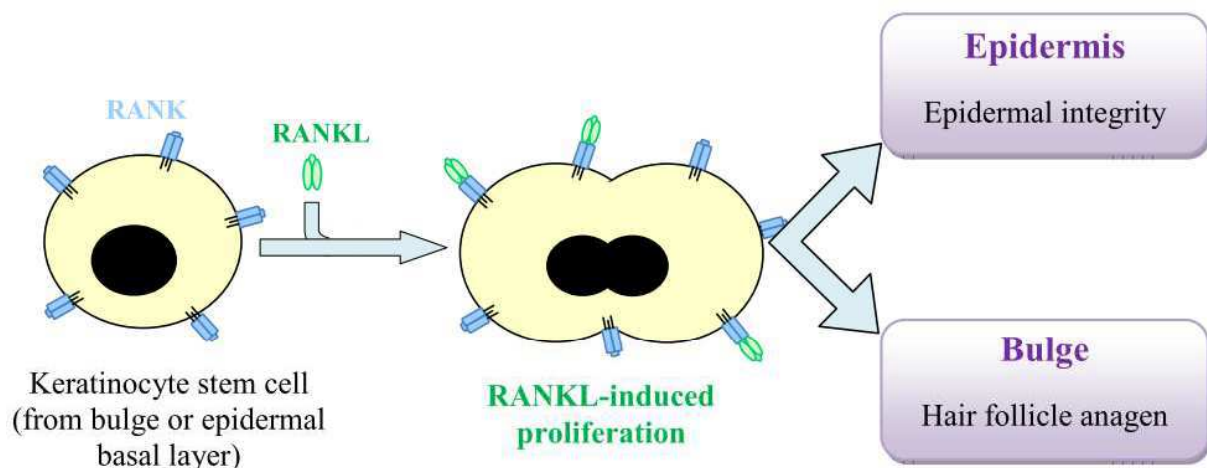
Figure 2: Schematic representation of RANKL-induced proliferation in the skin. RANKL induces the proliferation of RANK-expressing keratinocytes from the bulge and from the epidermal basal layer. RANK-RANKL function in the skin to maintain the epidermal integrity and to induce telogen-anagen transition.

3. *RANK in the regulation of lymph node homeostasis*

We showed that RANK-RANKL functions in the LNs beyond their development. In our model RANK-stimulation results in the proliferation of LN stromal subsets and their expression of chemokines and adhesion molecules, resulting in LN growth.

Given the lack of LNs in RANK- and RANKL-deficient mice, we took advantage of the murine model over-expressing RANK in the skin and in the granulo-myeloid lineage. *Rank*-Tg mice display an important post-natal growth of skin-draining LNs but normal other SLOs. Hence, cell counting revealed an 8-10 fold increase in hematopoietic cell number in cutaneous LNs (cLNs), whereas mesenteric LNs, spleen, thymus, blood and bone marrow displayed unchanged or even slightly reduced cell counts. *In vivo* ultrasound imaging allowed determining precisely the onset of LN

growth at P24. This phenotype closely resemble the one described in the IL-7 Tg murine model [1]. In these mice SLOs growth along with ectopic SLOs formation was reported and was linked to an increased number of LTics. Our RANK-Tg model is nevertheless dissimilar from this previously described hyperplasia given that the SLOs expansion is much more prominent and was not associated to ectopic SLOs formation.

Hyperplasic LNs from RANK-Tg mice display a generally conserved proportion of hematopoietic and stromal cells. Nevertheless, a slight decrease in lymphatic endothelial cells was found along with an increase in *Rank*-Tg CD11b$^+$ and B cell numbers. The increased number of CD11b$^+$ cells was most probably the result of a survival effect of the transgene expressed in this population [2, 3]. The increased B cell proportion was likely due to a higher recruitment of mature B cells as B cell populations in the spleen were found normal thereby discarding a possible accelerated B cell hematopoiesis. T and B cells segregate normally but an increase in small B cell follicles located in the paracortex was observed.

The hematopoietic cells from RANK-transgenic mice are not activated and respond normally to foreign antigens and adjuvant, thus hyperplasia observed was not the result of an inflammation. Bone marrow transfer experiments after a lethal irradiation were performed and allowed us to eliminate the possible implication of the transgene expression in the granulo-myeloid lineage. Skin graft experiment and genetic rescue experiments supported that the LN growth signal originates from the anagen *Rank*-Tg HFs. Hence, the anagen Tg HF express higher RANKL level most probably due to a RANK-RANKL positive feed-back loop in this miniorgan similarly to what has been already observed in thymic epithelial cells [4]. The high level of soluble RANKL produced by the Tg anagen HF and the additional anagen phases observed in *Rank*-Tg animals results in a prolonged RANKL release and leads us to propose that RANKL was the signal required for LN growth. Hence, neutralization of soluble RANKL was sufficient to normalize skin-draining LNs size, B/T cell ratio and the area and number of B cell follicles. We cannot exclude that the blockade of endogenous LN RANKL also contributed to the observed normalization. Nevertheless, skin RANKL was affected as abnormal HF cycling and epidermal dysplasia were corrected upon RANKL neutralization.

In this study we also showed that reticular fibroblastic and vascular stromal cells express RANK. In our *Rank*-Tg model, these endogenous RANK-expressing stromal cells hyperproliferate and RANKL neutralization abolished this hyperproliferation. We do not know yet if this mechanism was direct or indirect but LTics do not seem implied as their proportion is not increased in *Rank*-Tg mice. The decrease of the lymphatic endothelial cell proportion could also participate in the hyperplasia observed by a decreased egress of lymphocytes, nevertheless the normal number of blood lymphocytes argues against this hypothesis. Hence, the model we propose to explain the mechanism underlying the massive increase of skin-draining LN size is that RANKL-induced proliferation of stromal cells in association with an increased synthesis of chemokines and adhesion molecules results in LN growth (Figure 3).

This study showed a novel function for RANK-RANKL in LNs beyond their development and identified RANKL as a molecule controlling the plasticity of LNs. It also highlighted the importance of a tissue-derived cue for SLO biology.
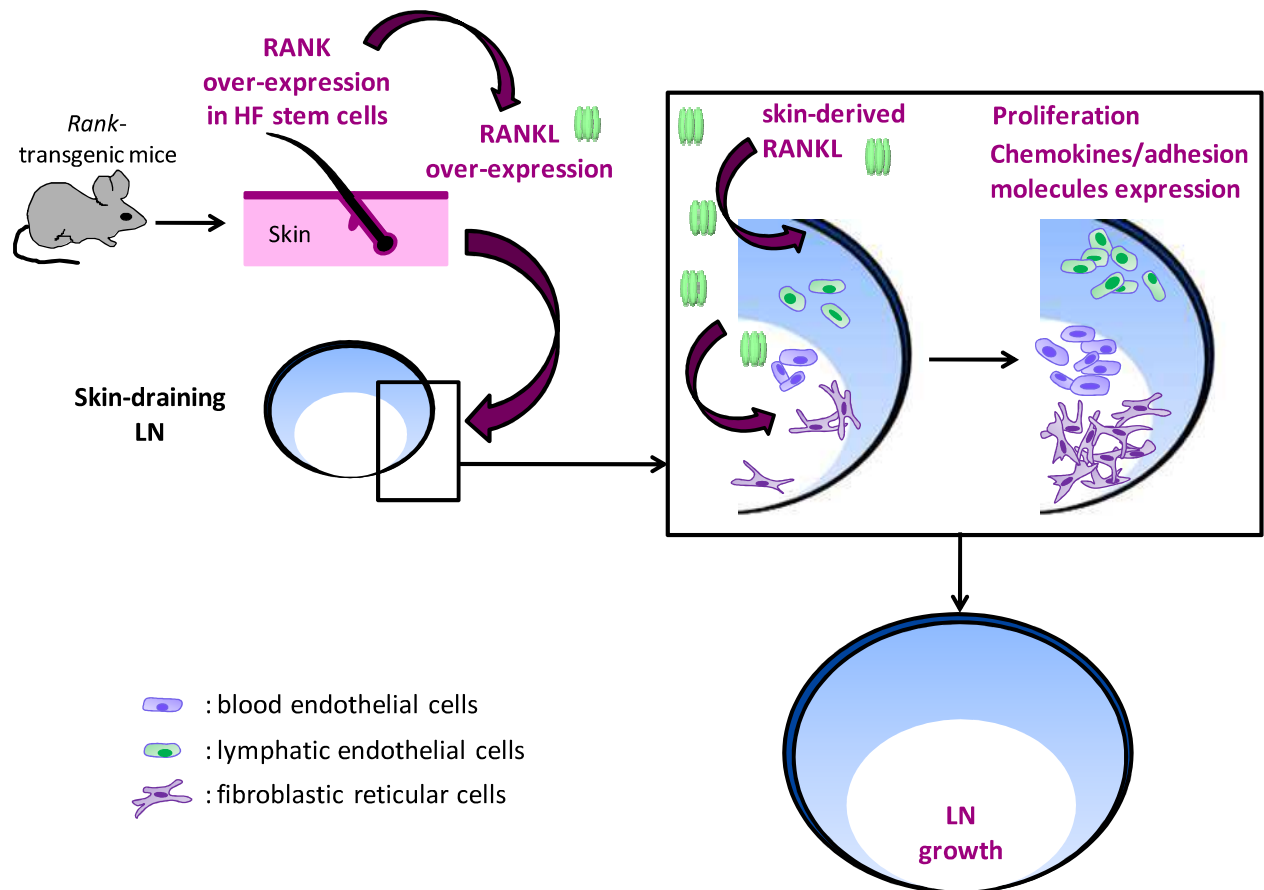

Figure 3: Model of the mechanism underlying the skin-draining LNs hyperplasia in *Rank*-Tg mice. *Rank*-Tg mice over-express RANK in HF stem cells leading to a positive feedback loop inducing soluble RANKL over-expression. Skin-derived RANKL induces LN stromal cells proliferation and chemokine and adhesion molecule expression resulting in the organ growth.

4. *Discussion and perspectives*

During my doctorate, we uncovered functions of RANK-RANKL in the LNs and in the skin. Hence, one could propose the existence of an integrative function of the molecular triad RANK-RANKL-OPG across the body, from primary lymphoid organ (bone marrow), to potential immune effector sites (skin) by passing through SLOs (LNs) (Figure 4). In addition to the already described crosstalk between the bones and the immune system, our work also shows a crosstalk mediated by RANKL between the skin and its associated LNs. Skin-derived RANKL can influence the local LN plasticity without any associated immune activation. This finding shows that tissue-derived cues can be important regulators for SLO homeostasis and function. Indeed, in order to elicit the best-suited

response a model of immune responses governed not only by the type of pathogen inducing it but also by the tissue-derived signals has been proposed [5].

Our results could indicate that such tissue-derived signals could be important for LNs even with no associated inflammation. One could argue against our proposal that our model is mainly based on the study of a transgenic mouse, however the RANKL-responding cells, e.g. LN stromal cells, do not express the transgene and as shown by the bone marrow transfer experiment and the skin grafts, an ectopical expression of the transgene is responsible of the observed phenotype. A possible naturally-occurring link between HF development and renewal and skin-draining LNs may take place. Indeed, during HF morphogenesis and the first HF anagen phase, the skin-draining LN expansion surpasses body growth [6].
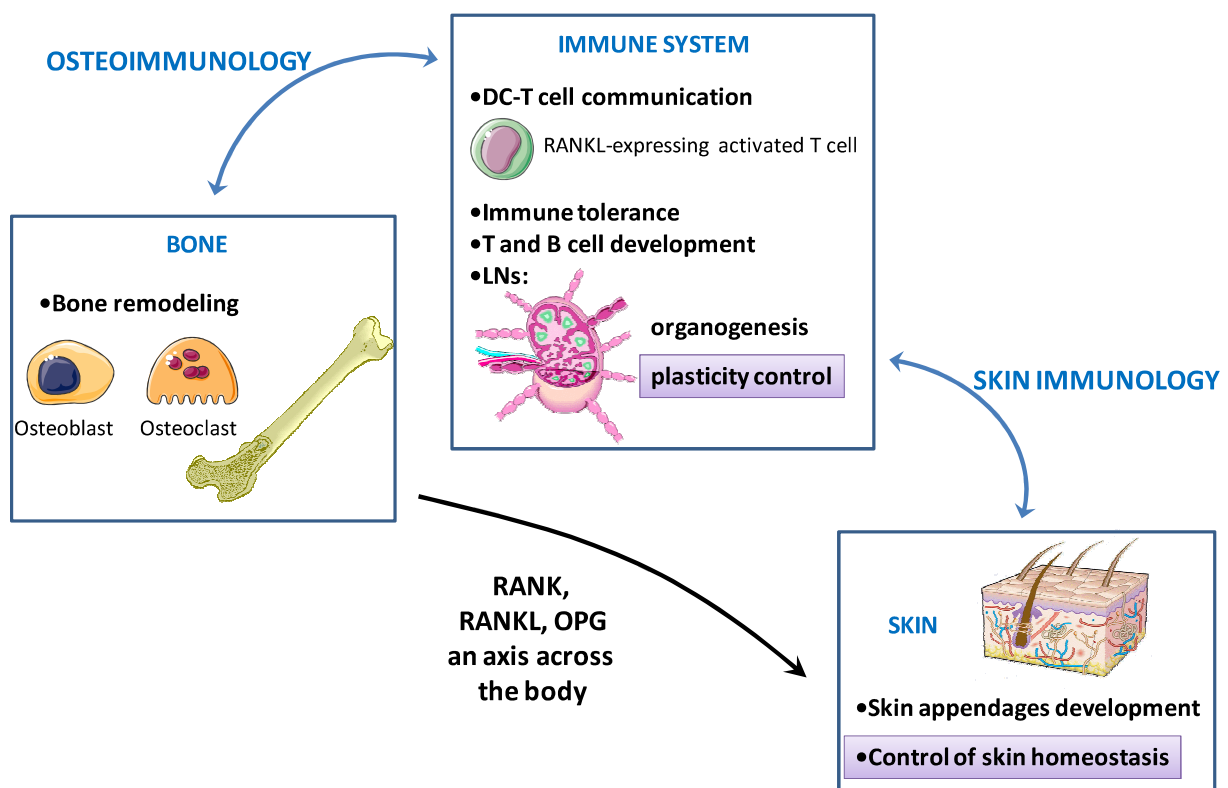
Figure 4: RANK-RANKL-OPG, an axis across the body. RANK, RANKL and OPG are key regulators of bone homeostasis and RANKL is produced by activated T cells. This molecular triad allowed to explain the crosstalk between this two biological systems leading to the term osteoimmunology. In addition, we provided evidence of a new function for RANK in LNs beyond their development and in skin homeostasis. We highlighted another likely RANKL-mediated crosstalk between two other biological systems: the skin and the skin-draining LNs. One could therefore coin this crosstalk "RANKL-mediated" skin immunology.

The precise mechanism underlying the RANKL-mediated proliferation of stromal cells remains to be elucidated. Whether this effect is direct or indirect is at the moment unknown. We tried to address this question *in vitro* by a stromal cell proliferation assay but these experiments were hampered by a high basal rate of proliferation of fibroblastic stromal cells and an elevated mortality of endothelial cells. Nevertheless, some clues can let us suppose that this mechanism is rather direct: all

stromal subsets tested express RANK and LTics, which rely on RANKL for their survival and proliferation, are not found augmented in *Rank*-Tg LNs. In addition, bone marrow transfer experiments after a lethal irradiation showed that the LTics of *Rank*-Tg origin are not required for the LN hyperplasia. Additional data are needed to clarify this point and we are currently addressing if there is a possible NF-κB2 signaling signature typical for RANK signaling in stromal cells. Nevertheless, this experiment will not exclude a possible redundant function between RANK and LTβR, which also signals through the alternative NF-κB pathway. To formally exclude this possible redundancy, a conditional RANK knockout model for instance in fibroblastic reticular cells would be of interest.

The finding that RANKL can mediate the proliferation of LN stromal cells and their expression of chemokines and adhesion molecules could be of interest during an immune response by providing an additional mechanism of LN expansion. Indeed, RANKL is continuously expressed in LNs by the marginal reticular cells and by activated T cells. One way to address this function during immune response could be to neutralize RANKL during a viral-induced SLO growth. It was previously reported that blockade of RANK signaling in vivo resulted only in a slightly reduced CD4^{+} T cell response to lymphocytic choriomeningitis virus (LCMV), which is mainly due to its functional redundancy with CD40 in the immune system [7]. Thus, LCMV infection could be a model to address the function of RANKL in the expansion of LNs by its neutralization without hampering the immune response. In addition, this experiment could also allow to address the function of RANKL in adult LTics survival, as these cells were found to be required for the restoration of lymphoid microanatomy after the destruction of the fibroblastic reticular meshwork from the T cell zone during the infection by cytotoxic T lymphocytes [8].

Finally, another possible implication of this new function for RANKL would be its role in the development of tertiary lymphoid tissues (TLTs). While SLOs are arising during embryogenesis and are genetically preprogrammed, TLTs are an accumulation of lymphoid cells that arise in the adult in response to environmental stimuli during chronic inflammation and which are not restricted to precise anatomical locations (Figure 5a) [9]. TLTs can develop upon inflammation induced by autoimmune pathologies such as rheumatoid arthritis, Hashimoto's thyroiditis, Grave's disease and Sjogren's syndrome. In addition these structures can also arise during microbial infection and chronic allograft rejection. TLTs are referred to as lymphoid organs because of their similitudes with SLOs in their cellular composition and compartmentalization. Hence, compartmentalized B and T cell zones, lymphatic vessels, functional PNAd-expressing HEVs, FDCs and germinal centers were reported in these structures [10]. More recently, FRCs and conduit networks were also observed in TLTs [11]. The physiological events which induce the formation of these structures under chronic inflammation remain unclear but same key players in SLO development are involved in this process. Thus, in mice lymphoid neogenesis can be inhibited by LTβR-Ig, and transgenic expression of CCL19, CCL21 or CXCL13 chemokines can lead to the development of TLTs[10]. In addition the key molecules

implicated in SLO development were reported in human TLTs [12]. Nevertheless, implication of LTics in this process still remains controversial and the possible source of LTα1β2 could also be provided by NK, B or T cells. Another unsolved question is the identity of the possible mesenchymal precursor giving rise to the stromal subsets which is yet still unknown. One proposed mechanism is that activated fibroblast could give rise to the stromal subsets as they share some features with stromal organizer cells, such as extracellular matrix synthesis and expression of cytokines and chemokines [9]. Due to its function in LN development and in LN expansion, RANKL could be implicated in the formation of these structures (Figure 5a). Hence, in rheumatoid arthritis, TLTs were reported in the synovial membrane and one could speculate that the infiltrate of RANKL-expressing activated T cells could provide a signal for the induction and/or expansion of TLTs (Figure 5b). A RANKL-neutralizing study in an autoimmune murine model developing TLTs would provide information about this possible function of RANKL. TLTs induce deleterious effects in autoimmune pathologies be perpetuating the inflammation. Thus, RANKL neutralization treatment could be considered in such pathologies.
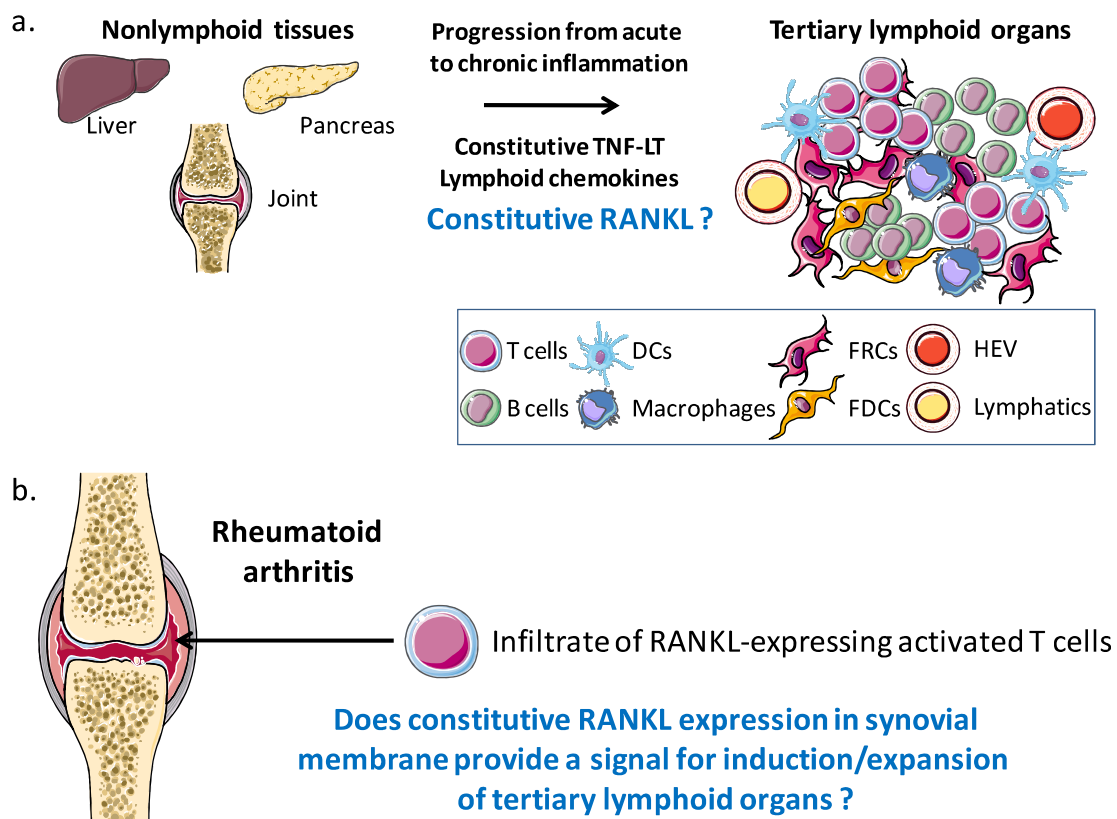
Figure 5: RANKL possible function in TLTs induction/expansion. (a) Proposed developmental process of TLTs in nonlymphoid tissues. Modified after [10, 11]. (b) Possible function for RANKL in the induction and/or expansion of TLTs associated with rheumatoid arthritis.

5. *Bibliography*

1.   Meier, D., et al., *Ectopic lymphoid-organ development occurs through interleukin 7-mediated enhanced survival of lymphoid-tissue-inducer cells.* Immunity, 2007. **26**(5): p. 643-54.

2.   Wong, B.R., et al., *TRANCE (tumor necrosis factor [TNF]-related activation-induced cytokine), a new TNF family member predominantly expressed in T cells, is a dendritic cell-specific survival factor.* J Exp Med, 1997. **186**(12): p. 2075-80.

3.   Anderson, D.M., et al., *A homologue of the TNF receptor and its ligand enhance T-cell growth and dendritic-cell function.* Nature, 1997. **390**(6656): p. 175-179.

4.   Mouri, Y., et al., *Lymphotoxin signal promotes thymic organogenesis by eliciting RANK expression in the embryonic thymic stroma.* J Immunol, 2011. **186**(9): p. 5047-57.

5.   Matzinger, P. and T. Kamala, *Tissue-based class control: the other side of tolerance.* Nat Rev Immunol, 2011. **11**(3): p. 221-30.

6.   Bosisio, M.R., et al., *Ultrasound biomicroscopy: a powerful tool probing murine lymph node size in vivo.* Ultrasound Med Biol, 2009. **35**(7): p. 1209-16.

7.   Bachmann, M.F., et al., *TRANCE, a tumor necrosis factor family member critical for CD40 ligand-independent T helper cell activation.* J Exp Med, 1999. **189**(7): p. 1025-31.

8.   Scandella, E., et al., *Restoration of lymphoid organ integrity through the interaction of lymphoid tissue-inducer cells with stroma of the T cell zone.* Nat Immunol, 2008. **9**(6): p. 667-75.

9.   Ruddle, N.H. and E.M. Akirav, *Secondary lymphoid organs: responding to genetic and environmental cues in ontogeny and the immune response.* J Immunol, 2009. **183**(4): p. 2205-12.

10.   Drayton, D.L., et al., *Lymphoid organ development: from ontogeny to neogenesis.* Nat Immunol, 2006. **7**(4): p. 344-53.

11.   Link, A., et al., *Association of T-zone reticular networks and conduits with ectopic lymphoid tissues in mice and humans.* Am J Pathol, 2011. **178**(4): p. 1662-75.

12.   Timmer, T.C., et al., *Inflammation and ectopic lymphoid structures in rheumatoid arthritis synovial tissues dissected by genomics technology: identification of the interleukin-7 signaling pathway in tissues with lymphoid neogenesis.* Arthritis Rheum, 2007. **56**(8): p. 2492-502.

ANNEX

Annex:
RANK in the control of tooth eruption and root morphogenesis

Bone resorption control of tooth eruption and root morphogenesis: involvement of the receptor activator of NF-κB (RANK)

Castaneda B, Simon, Jacques J, **Hess E**, Choi Y, Blin-Wakkach C, Mueller CG, Berdal A, Lézot F.

This article is the result of a collaboration with the Laboratory of oral and molecular physiopathology at the Cordeliers Research Center in Paris. Using the *Rank*-transgenic model which overexpresses RANK both in hair follicle and in osteoclast precursors, their team addressed the impact of an excessive bone resorption on tooth growth. In this collaboration, we characterized the expression of the transgene in the granulo-myeloid lineage.

Bone Resorption Control of Tooth Eruption and Root Morphogenesis: Involvement of the Receptor Activator of NF-κB (RANK)

BEATRIZ CASTANEDA,[1,2] YOHANN SIMON,[1] JAIME JACQUES,[1] ESTELLE HESS,[3] YONG-WONG CHOI,[4] CLAUDINE BLIN-WAKKACH,[5] CHRISTOPHER MUELLER,[3] ARIANE BERDAL,[1] AND FRÉDÉRIC LÉZOT[1]*

[1] INSERM UMR 872, Cordeliers Research Center, Team 5, Laboratory of Oral Molecular Physiopathology, Paris, France

[2] Faculty of Odontology, Department of Basic Studies, University of Antioquia, Medellin, Colombia

[3] CNRS, UPR 9021, Laboratory of Therapeutic Immunology and Chemistry, IBMC, University of Strasbourg, Strasbourg, France

[4] Department of Pathology and Laboratory Medicine, Abramson Family Cancer Research Institute, University of Pennsylvania School of Medicine, Philadelphia, Pennsylvania

[5] INSERM U576, Laboratory of Regulation of Immune and Inflammatory Reactions, L'Archet Hospital, Nice, FranceThe authors have declared that no conflict of interest exists.

Activation of the receptor activator of NF-κB (RANK) is a crucial step in osteoclastogenesis. Loss- and gain-of-function mutations in the *Rank* gene cause, respectively, osteopetrosis and several forms of extensive osteolysis. Tooth and alveolar bone alterations are associated with these pathologies but remain to be better characterized. The aim of the present study was to establish the tooth and alveolar bone phenotype of a transgenic mouse model of RANK over-expression in osteoclast precursors. Early tooth eruption and accelerated tooth root elongation were observed subsequent to an increase in osteoclast numbers surrounding the tooth. The final root length appeared not to be affected by RANK over-expression, but a significant reduction in root diameter occurred in both control and root-morphogenesis-defective *Msx2* null mutant mice. These results indicate that root length is independent of the surrounding bone resorption activity. In contrast, root diameter is sensitive to the activity of alveolar bone osteoclasts. These data suggest that early eruption and thin root are phenotypic features that could be associated with extensive osteolytic pathologies.

J. Cell. Physiol. 226: 74–85, 2010. © 2010 Wiley-Liss, Inc.

The receptor activator of NF-κB (RANK) is a member of the tumor necrosis factor receptor superfamily (precisely TNFRSF11A) and was originally shown to be crucial for osteoclastogenesis and lymph node development (Dougall et al., 1999; Li et al., 2000). Its ligand, known as RANKL, ODF, OPGL, Ly109l, or TRANCE, is a member of the tumor necrosis factor superfamily (TNFSF11) and plays important roles in differentiation and activation of lymphocytes, dendritic cells, and osteoclasts (Kong et al., 1999; Kim et al., 2000; Barbaroux et al., 2008). Osteoprotegerin (OPG, also called TNFRSF11B) acts as a soluble decoy receptor and competes with RANK for binding to RANKL (Yasuda et al., 1998a,b). Mutations in the human genes for *Rankl* and *Opg* have been associated with bone pathologies such as autosomal recessive, osteoclast-poor forms of osteopetrosis for *Rankl* (OMIM #259710; Sobacchi et al., 2007), and juvenile Paget disease for *Opg* (OMIM #239000; Dunn et al., 1979; Cundy et al., 2002; Whyte et al., 2002; Chong et al., 2003). With respect to *Rank*, 12 mutations have been reported to date in the OMIM database, which can be classified into two groups according to their effects on RANK function. Loss-of-function mutations always cause severe osteoclast-poor osteopetrosis (OMIM #612301; Guerrini et al., 2008). Gain-of-function mutations, corresponding to tandem duplications in the exon 1 sequence, have been found in three seemingly distinctive disorders with autosomal-dominant inheritance: familial expansile osteolysis (FEO, OMIM #174810;

Osterberg et al., 1988; Wallace et al., 1989; Hughes et al., 1994, 2000; Johnson-Pais et al., 2003), expansile skeletal hyperphosphatasia (ESH; Whyte et al., 2000; Whyte and Hughes, 2002), and early-onset Paget disease of bone (PDB2, OMIM #602080; Nakatsuka et al., 2003). Clinically, these diseases are characterized by uncontrolled bone remodeling, with the presence of many and often enlarged osteoclasts, accompanied by areas of active bone formation. Premature permanent tooth loss and root external resorption have been described in these pathologies as consequences of the increased osteoclast activity (Mitchell et al., 1990; Nakatsuka

CONTROL OF TOOTH GROWTH BY BONE RESORPTION

75

et al., 2003). However, a fine analysis of growth alterations of the complex formed by tooth and alveolar bone has, so far, not been done. Therefore, the main objective of the present study was to analyze, using an animal model, the impact of RANK gain of function on the growth of the complex formed by tooth and alveolar bone. The growth of this complex entails a finely orchestrated increase in dental and periodontal tissue volume accompanied by modeling of surrounding alveolar bone. Cell–cell communication in dental and periodontal morphogenesis and bone modeling has been studied extensively in a tooth-toward-bone direction. Several studies have analyzed alveolar bone modeling during tooth eruption, showing the production by dental/periodontal cells of various cytokines tied to the recruitment of monocyte/osteoclast precursors, their differentiation into osteoclasts, and finally bone resorption (reviewed by Wise, 2009). In contrast, the impact of bone cells on tooth growth has rarely been investigated. What little data there are amount to indirect evidence based on dental phenotypes associated with osteopetrosis (reviewed by Helfrich, 2005).

The RANK gain-of-function model used in this study is a transgenic mouse over-expressing RANK in the monocytic lineage. The impact of RANK over-expression on tooth growth was analyzed with respect to tooth eruption and root formation processes. Root formation corresponds to a graded invagination, in the adjacent dental mesenchyme, of fused inner and outer enamel epitheliums (Ten Cate, 1994). The formed epithelial lamina, called Hertwig epithelial root sheath (HERS), separates the mesenchyme into two parts: the inner dental pulp and the outer dental follicle. Interactions between epithelial cells of the HERS and these mesenchymal cells enable, on the one hand, the differentiation of both root dentin-secreting odontoblasts from the dental pulp (Bosshardt and Nanci, 2004) and cementum-secreting cementoblasts from the follicle (Hammarströn, 1997; Suzuki et al., 2002; Zeichner-David et al., 2003). On the other hand, differentiation of the HERS cells ends with fragmentation of the sheath into a mass of numerous cells which lines the newly formed root dentin, called Malassez rests (Kat et al., 2003).

The results presented here provide evidence that RANK over-expression induces earlier onset of tooth eruption and accelerated root elongation leading to a significant reduction of the final root diameter. These data constitute new phenotypic features that may be associated with extensive osteolytic pathologies.

Materials and Methods
Animal generation and sampling

All experiments were performed in accordance with the French National Consultative Bioethics Committee for Health and Life Science, following the ethical guidelines for animal care. Staff trained to perform in vivo studies carried out all experiments.

Rank transgenic (RTg) mice were generated by heterologous recombination of a cassette containing 1.5 kb of the human myeloid-related protein 8 (*Mrp8*) gene promoter (Lagasse and Weissman, 1997) and the coding sequence of the mouse *Rank* gene. This promoter was previously shown to drive expression in immature myeloid cells of the bone marrow, myeloid cells in the splenic red pulp and marginal zone, monocytes, and blood neutrophils (Lagasse and Weissman, 1992, 1994). Comparative analysis of bone marrow cell populations between wild-type (WT) and RTg mice showed a significant increase in the pre-monocyte/macrophage population (CD11b$^+$ Gr1^{int}) in RTg mice (Supplementary Fig. 1A,B), contrasting with the apparent absence of modulation of the pre-granulocyte population (CD11b$^+$ Gr1^{hi}). RANK expression was not detected in other non-macrophage bone marrow cells such as the B-lymphocytes (B220$^+$) (Supplementary Fig. 1C).

Thirty-two copies of the cassette were inserted in tandem in the *Rank* transgenic line used in this study. Genotype was ensured by PCR with the following primers:

5′ *Rank* transgene: ATGGACTACAAAGACGATGACGAC;
3′ *Rank* transgene: TGCCAGGATCCACCGCCACCA.

The RTg mice initially made on a C57/BL6 background had been backcrossed for at least nine generations onto the CD1 Swiss genetic background for these experiments.

Msx2 gene knock-in (KI) mutant mice were generated by in-frame insertion of the bacterial *lacZ* gene into the coding sequence of the *Msx2* gene, replacing the latter, as previously described (Lallemand et al., 2005). *Msx2* null mutant mice were obtained by mating heterozygous animals. Genotyping was performed by PCR with the following primers:

5′ *Msx2*: GTCTTCGCTTGAGAGTTGCCA;
3′ *Msx2*: GTCGGACATGAGCGCCTC;
3′ *LacZ*: GGCAAAGCGCCATTCGCCATTCAGGC.

RTg males heterozygous for the *Msx2* gene mutation were mated (using a CD1 Swiss genetic background) with females heterozygous for *Msx2* gene mutation in order to compare *Msx2* expression (β-galactosidase staining in heterozygous) between control and RTg mice, and to obtain *Msx2* null mutant mice carrying or lacking the *Rank* transgene.

Mice were studied at 3, 7, 14, 21, 28, and 105 days with at least three animals in each experimental group for a total of 87 animals.

Rankl$^{+/-}$ mice had been generated by homologous recombination (Odgren et al., 2003). Genotyping was done by PCR using the following primers:

5′ *Rankl*: CCAAGTAGTGGATTCTAAATCCTG;
3′ *Rankl*: CCAACCTGTGGACTTACGATTAAAG;
3′ insert: ATTCGCAGCGCATCGCCTTCTATC.

Bone marrow analysis

Tibia and femur bones of 4- and 12-week-old WT and RTg mice were flushed in phosphate-buffered saline (PBS) containing 2% fetal calf serum and 0.05 mM EDTA. The bone marrow cells were dispersed and labeled with antibodies specific for CD11b-APC (eBioscience, Frankfurt, Germany), Gr-1-FITC (eBioscience), CD11c-PE (BD Biosciences, San Jose, CA), B220-APC (BD Biosciences), and anti-RANK (R&D Systems, Lille, France), followed by rabbit-anti-goat-biotin (Southern Biotechnology Associates, Birmingham, AL) and streptavidin–PE. The cells were analyzed by flow cytometry on a FACS Calibur (Becton-Dickinson, Le Pont de Claix, France) and using CellQuest Pro software.

Osteoclast differentiation from purified monocytes

For osteoclast differentiation, 5×10^4 sorted monocytes were seeded in a 48-well plate in αMEM medium supplemented with 5% fetal calf serum in the presence of 25 ng/ml M-CSF and 50, 100, or 200 ng/ml RANKL (Tebu, le Perray en Yvelines, France). After 6 days of culture, cells were stained for TRAP activity and counted.

Alveolar bone microdissection

After sacrifice, half-mandibles were collected and soft tissues, including muscles and gingival epithelium, removed under a stereomicroscope by using forceps and scalpels as previously described (Aïoub et al., 2007). Molars were then extracted with forceps and the integrity of the extracted teeth checked to prevent contamination of alveolar bone samples by dental tissue (mainly epithelium). The alveolar bone was then collected with forceps and directly immerged in Tri-Reagent solution (Euromedex, Souffelweyersheim, France) for RNA extraction following the manufacturer's instructions. The absence of dental tissue

76

C A S T A N E D A   E T   A L.

TABLE 1. PCR conditions and primer sequences

Gene	Size (bp)	Annealing T (°C)	Elongation time (sec)	Forward primer (5'–3')	Reverse primer (5'–3')
Rank^{Tg}	181	52	30	ATGTCTCTTGTCAGCTGTCTT	GCTCATAATGCCTCTCCTG
Rank	458	55	30	CCATCATCTTCGGCGGCGTTTACT	ACTGTCGTTCTCCCCCACTT
Rankl	592	57	30	CAGCATCGCTCTGTTCCTGT	TCGTGCTCCTTTCATC
Opg	457	59	30	TGATGAGTGTGTGTATTGCAGC	CCCAGGCAAACTGTCCACCAA
Tnfα	132	53	30	CCCCAAAGGGATGAGAAGTT	CACTTGGTGGTTTGCTACGA
Pthrp	113	53	30	GCAGTTAGAGGCGCTGATTC	ACGGAGTAGCTGAGCAGGAA
Tgfβ1	136	53	30	CAACAATTCCTGGCGTTACC	GCTGAATCGAAAGCCCTGTA
IIIα	131	56	30	TCAAGATGGCCAAAGTTCCT	TGAGCCATAGCTTGCATCAT
Runx2	300	53	30	GGACGAGGCAAGAGTTTCAC	TGCCTGCCTGGGATCTGTAA
Oc	257	56	30	CTCACTCTGCTGGCCCTG	CCGTAGATGCGTTTGTAGGC
Bsp	454	56	30	GACCAGGAGGCGGAGGCAGA	CTTCGGGCGGTGGGGTTGTC
Ctsk	150	53	30	GAACGAGAAAGCCCTGAAGA	ACCAACACTGCATGGTTCAC
Trap	67	56	30	TGCCTACCTGTGTGGACATGA	CACATAGCCCACACCGTTCTC
18S	155	53	30	AAACGGCTACCACATCCAAG	CCTCCAATGGATCCTCGTTA
Gapdh	824	55	30	TTCCAGTATGATTCCACTCA	CTGTAGCCATATTCATTGTC
Krt2	378	56	30	CAACAAGCGCACGTCTGCGG	GGCCAGGTCCTCTCGGCACT
Krt19	470	56	30	TGTTTTCCGCGCACCCAGCA	TGTCGGCCTCCACGCTCAGA
CD19	72	56	30	CCATCGAGAGGCACGTGAA	TCCATCCACCAGTTCTCAACAG
CD3e	495	56	30	ACTGGAGCAAGAATAGGA	AGGAGAGGAAAGGAACTG
F4/80	509	56	30	AGATGGGGGATGACCACACTTC	TGTTCAGGGCAAACGTCTCG
c-fms	57	56	30	GACTTCGCCCTCAGCTTGG	TCCCCAGACCCCTCATGTT
CD11b	398	56	30	TGGGCAGGTGGAGCCTTCCT	CACTGCCACCGTGCCCTCTG
CD11c	75	56	30	CTGAGAGCCCAGACGAAGACA	TGAGCTGCCCACGATAAGAG

(epithelium) contamination was ensured by PCR (Supplementary Fig. 2) with sets of primers for keratins (*Krt*) 2 and 19 (Table 1).

RT-PCR analysis

RT-PCR was performed in a two-step protocol using Superscript II enzyme (Gibco BRL, Cergy-Pontoise, France) for the reverse transcription step and Eurobiotaq (Eurobio, Courtaboeuf, France) for the PCR step, according to manufacturers' instructions and as previously described (Lézot et al., 2008). The primers used for PCR analysis are listed in Table 1. Primers of each pair were chosen to anneal to two different exons to ensure that potential genomic DNA contamination did not interfere with the analysis. The PCR-amplified fragments were separated by a 2% agarose gel and photographed with Bio-Rad Gel Doc XR (Bio-Rad, Marnes-la-Coquette, France). Specificity of the amplified fragments was ensured by correct fragment size and by Southern blot analysis using specific probes, as previously described (Lézot et al., 2010). The specificity of the amplified fragments was also validated through the use of these primers in real-time PCR. To ensure that the PCR was done in the linear range, all PCRs were performed starting with 0.5 and 1 μl of cDNA and the obtained bands on the gel were quantified by using the Visiomic software (Genomic S.A., Archamps, France).

Microradiographs, histological analyses, and tartrate-resistant acid phosphatase (TRAP) activity assays

After chloral anesthesia, intra-cardiac perfusion was performed with a fixative solution containing 4% paraformaldehyde (Sigma, la Verpillière, France) in PBS, pH 7.4. Post-fixation was ensured by immersion of heads in the fixative solution overnight at 4°C. After rinsing in PBS, the half-heads (cut along the sagittal axis) were microradiographed on High Resolution Film SO-343 (Kodak Professional, Paris, France) using a microfocal X-ray generator (Tubix, Paris, France) at a focal distance of 56 cm for 20 min (power setting: 12 mA and 15 kV). The half-heads were then processed for histological analysis by decalcification at 4°C for up to 2 months (depending on the age of the samples) in a pH 7.4 PBS solution containing 4.13% EDTA (Sigma) and 0.2% paraformaldehyde. After extensive washing in PBS, the samples were dehydrated in increasing concentrations of ethanol and toluene and were finally embedded in paraffin (Paraplast plus, Sigma). Serial frontal sections of the half-heads were made with a microtome (RM 2145; Leica,

Rueil-Malmaison, France). The 8-μm-thick sections were deparaffinized and rehydrated before being either stained according to a modified Van Gieson protocol (Lézot et al., 2008, 2010) or subjected to a tartrate-resistant acid phosphatase (TRAP) activity assay as previously described (Aïoub et al., 2007).

β-Galactosidase, BrdU, and PCNA immunohistochemistry

Immunohistochemistry of β-galactosidase was performed on paraffin frontal sections of *Msx2/LacZ* heterozygous mouse heads. Sections were deparaffinized, hydrated, and endogenous peroxidases were inhibited by incubation for 20 min in a freshly made solution of 3% H_2O_2 in PBS. Sections were then washed in PBS and incubated for 1 h in a blocking solution of PBS containing 10% of normal swine serum (S-4000; Vector Laboratories, Paris, France) and 1% of bovine serum albumin (Sigma). Anti-β-galactosidase polyclonal antibody (R1064P; Acris GmbH, Herford, Germany) was then applied to the sections at a dilution of 1:1,000 overnight at 4°C. After washing in PBS, sections were sequentially incubated with goat anti-rabbit IgG coupled to horseradish peroxidase (HRP) (PO448; Dako, Trappes, France) at a dilution of 1:200. Staining was revealed with a liquid DAB+ substrate chromogen system (K3468; Dako) and the sections were counterstained with hematoxylin.

Proliferating cell nuclear antigen (PCNA) immunohistochemistry was conducted on paraffin frontal sections of RTg and WT mouse heads. Tissue sections were quenched for endogenous peroxidases as described above. After incubation in the blocking solution for 1 h, mouse monoclonal (PC10) anti-PCNA (ab29; Abcam, Paris, France) was applied overnight at 4°C to the sections at a dilution of 1:200. Tissue sections were then incubated with a biotinylated goat anti-mouse IgG antibody (PO 447; Dako) at a dilution of 1:200. Staining was developed with a liquid DAB+ substrate chromogen system (K3468; Dako), and the slides were mounted without counterstaining. Negative controls were obtained by omitting primary antibodies.

To determine proliferation using 5-bromo-2-deoxy-uridine (BrdU, B5002; Sigma) incorporation, mice were injected IP with BrdU (50 μg/g of body weight) 12 h before sacrifice. To visualize the BrdU incorporation, tissue sections were deparaffinized, hydrated, and the DNA was denatured by incubation for 1 h in 2 N HCl solution. After washing in water and in PBS buffer, potential non-specific staining was blocked by a short treatment with

CONTROL OF TOOTH GROWTH BY BONE RESORPTION   77

proteinase K (20 μg/ml; Sigma). After rinsing in washing buffer, the sections were incubated in blocking solution for 30 min and then overnight at 4°C with monoclonal anti-BrdU antibody (Bu20a; Dako). The secondary antibody detection system described above for PCNA was used to visualize anti-BrdU antibody binding. Staining was developed with a liquid DAB+ substrate chromogen system (K3468; Dako).

Microcomputed tomography (micro-CT) scanner imaging

A micro-CT scanner (desktop Skyscan 1172, Aartselaar, Belgium) was used to provide three-dimensional images of mouse mandibles. This system is based on a cone beam X-ray source. A spatial resolution producing voxels that measure 6.7 μm on a side was used. Acquisition parameters were 80 kV and 100 mA with an exposure time of 4 sec. A 0.25° rotation step was operated between two exposures. A total of five exposures were obtained for each angle, and means were calculated. For each mode, a 0.5 mm aluminum filter was installed in the beam path to cut off the softest X-rays and increase the accuracy of the primary images. These settings allowed a head to be scanned in 3.5 h. Cross-sectional images were reconstructed using a classical Feldkamp cone-beam algorithm with NRecon[R] software (SkyScan). Additional software, Data Viewer[R] (SkyScan), allowed visualization of the cross-sectional images in three dimensions. Three-dimensional reconstructions were achieved using CTAn[R] software (Micro Photonics, Inc., Allentown, PA). All three-dimensional reconstructions were realized using the same conditions and, particularly, the same threshold for WT and RTg mice.

Results
Transgenic mouse model of RANK over-expression

The transgenic mouse model used in this study was constructed with the human myeloid related protein-8 (hMrp8/S100A8) gene promoter to drive over-expression of the mouse receptor RANK in monocyte–macrophage cell lineages. In order to ensure that the induced over-expression was occurring in alveolar bone cells but not in adjacent dental epithelial cells, Rank transgene (Rank[Tg]) expression was analyzed by RT-PCR in 14-day-old mouse alveolar bone and dental epithelium. As expected, transgene expression was detected in alveolar bone of Rank transgenic (RTg) mice but not in adjacent dental epithelium (Fig. 1A). To associate expression of the transgene in alveolar bone with an increase in the number of Rank-expressing cells, in situ hybridization with Rank probes was performed on 14-day-old WT (Fig. 1B,D) and RTg (Fig. 1C,E) mouse mandible frontal sections. In both, WT and RTg mice, Rank transcripts were detected in the alveolar bone along the lateral and basal regions of the forming first molar mesial root (Fig. 1B–D). However, the RTg mouse displayed an increased number of stained cells and higher staining levels within these cells (Fig. 1C,E) compared to WT (Fig. 1B,D). No staining was detected in the root dental epithelium. To confirm that the increased number of Rank-expressing cells in the alveolar bone of the RTg mouse corresponds to an increase in the number of cells from monocyte–macrophage lineages, RT-PCRs with primers specific for different cell lineages were performed (Supplementary Fig. 2). The results confirmed that only the monocyte–macrophage lineages were affected by RANK over-expression (Supplementary Figs. 1 and 2). Interestingly, no significant difference in the number of osteoclasts formed in vitro from purified monocytes of WT and RTg mice was observed whatever the RANKL concentration used (Supplementary Fig. 2). These results suggest that the increased number of osteoclasts observed in the alveolar bone of the RTg mouse was due to an increased number of precursors already present in the bone marrow (Supplementary Fig. 1).
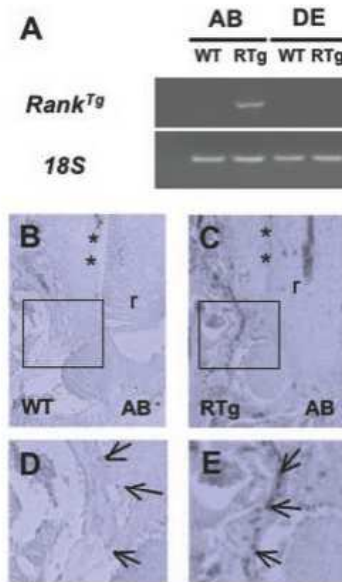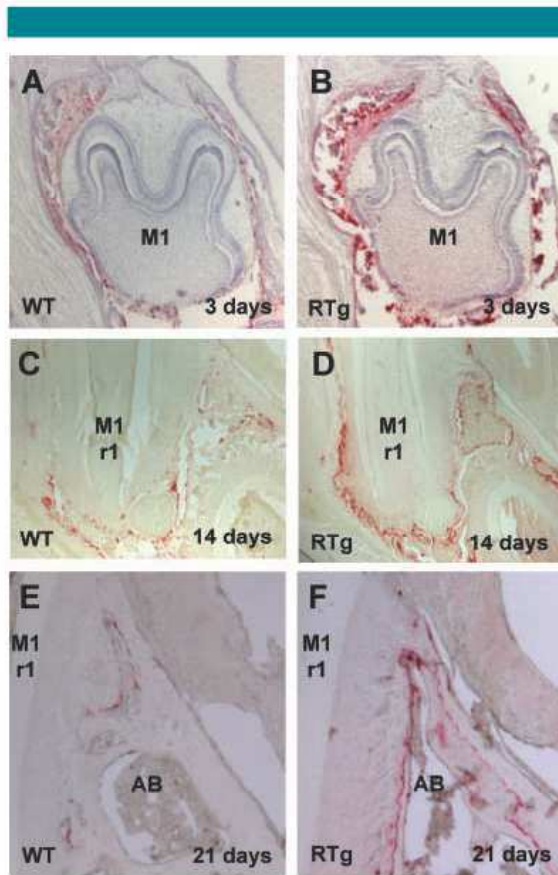

Fig. 1. A: RT-PCR analysis of Rank transgene (Rank[Tg]) expression in 14-day-old mouse alveolar bone (AB) and dental epithelium (DE) using primers specific to the transgene. Expression was detected only in the alveolar bone of transgenic mouse (RTg). B–E: In situ hybridization analysis of Rank expression patterns in 14-day-old WT and RTg mouse mandibles. In both mice, Rank transcripts were detected in the alveolar bone (AB) along the forming first molar root (r); however, an increased number of stained cells and higher Rank expression level were observed in the RTg mouse (arrows in D and E). No staining was observed in the dental root epithelium (stars in B and C). D and E correspond to the squares in B and C, respectively.

The frequency of TRAP-positive cells was investigated in order to substantiate the impact of RANK over-expression on the number of osteoclasts. Irrespective of the age tested (3, 14, and 21 days), the number of TRAP-positive osteoclasts was strongly increased in the alveolar bone of RTg mice as compared to WT mice (Fig. 2 and Table 2). Despite this increase, the normal periodontal distribution of pre-osteoclasts and osteoclasts observed during dento-alveolar complex growth was conserved: that is, at 3 days, TRAP-positive cells (mainly pre-osteoclasts) were present all around the tooth (Fig. 2A,B), whereas at 14 and 21 days (Fig. 2C–F), the expression was observed in more limited areas of the bone crypt. The increase in the number of pre-osteoclasts and osteoclasts is in accord with augmentation of the bone marrow pre-monocyte–macrophage population in the RTg mouse.

Impact of RANK over-expression on tooth eruption and dental root elongation

To determine the impact of RANK over-expression on growth of the dento-alveolar complex, a comparative analysis of WT and RTg mouse mandibular molar morphology was performed at 3, 5, 7, 11, 14, 17, 21, and 28 days.
Microradiograph and microscan analyses. The overall pattern of odontogenesis was followed by microradiography. No difference between WT and RTg mice appeared at 3 and 7 days (Fig. 3A–D). At 21 days, when the first molar roots of WT and RTg mice had finished their elongation, no difference in molar root length was apparent; however, RTg mouse molar roots were narrower than those of WT mice (Fig. 3E,F).

elongation in the RTg mouse. Quantitative data for root length and diameter at 3, 14, and 21 days are presented in Table 2.

Histological analyses. No differences between RTg and WT mouse mandibular first molar sections were found by histological analysis through day 7 (Fig. 4A–D). At day 14, the first molar of the RTg mouse showed premature eruption (red arrow) as compared to the first molar of the WT mouse (blue arrow) (Fig. 4E,F). Moreover, the roots of the RTg mouse first molar were longer and narrower (Fig. 4E,F). However, the overall process of root dentinogenesis seemed to be similar in the two genotypes. The size of the pulp chamber of the RTg first molar was reduced (Fig. 4E,F). At day 28, no significant difference in the length of the mandibular first molar mesial root was noticed between WT and RTg mice, but the root was narrower in the transgenic mouse (Fig. 4G,H). Moreover, partial closure of the mesial root pulp chamber in the apical area was occasionally seen in the RTg mouse (Fig. 4H).

Impact of RANK over-expression on dental epithelial cell proliferation and differentiation

To establish a link between accelerated root elongation and increased proliferation of dental epithelial cells of the HERS, PCNA expression and BrdU incorporation were compared by immunohistochemistry at 14 days. Both PCNA and BrdU staining were detected in epithelial cells of the HERS apex area and in adjacent periodontal cells (Fig. 5). The number of stained HERS cells was increased in the RTg mouse (Fig. 5B,D,F,H) as compared to the WT mouse (Fig. 5A,C,E,G). With respect to the periodontal cells, an increase in the number of BrdU-stained cells was observed in the RTg mouse (Fig. 5E–H), whereas no significant difference was seen in PCNA staining (Fig. 5A–D). The discrepancy between the BrdU and PCNA staining can be explained by the fact that PCNA reveals the number of proliferating cells at an instant (t) whereas BrdU shows the number of cells that have been proliferating over a period of time ($\Delta t = 12$ h in the present study). Regarding the periodontal cells, this difference suggests that the number of proliferating cells was not increased, but that the proliferation cycle was accelerated. Concerning the pulp, no difference was observed between WT and RTg mice for both PCNA and BrdU staining (Fig. 5A–D). Comparative quantification of dental and periodontal cell proliferation between WT and RTg mice at 3 and 14 days is presented in Table 2.
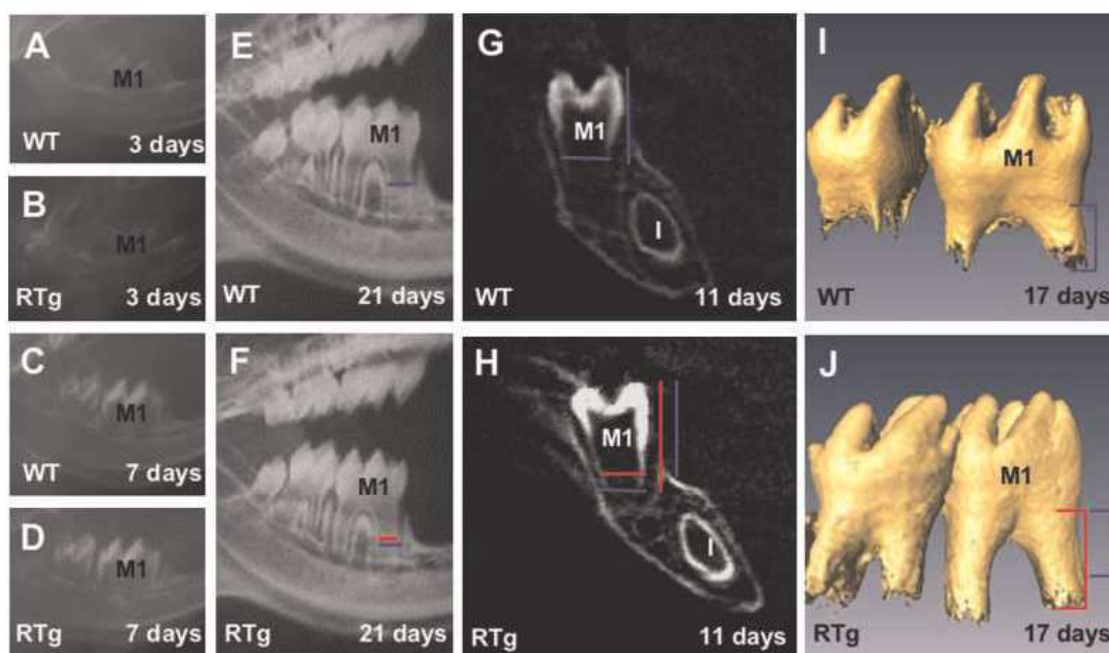
To further characterize the association between accelerated root elongation and earlier differentiation of the HERS cells, *Msx2* expression in heterozygous *Msx2/LacZ* reporter mice was compared between 14-day-old animals over-expressing RANK or not (Fig. 6A,B). The *Msx2* homeobox gene was chosen because its expression pattern in HERS cells has been fully described at all stages of the molar root elongation process (Yamashiro et al., 2003) and because the *Msx2* null mutation induces severe defects in the root elongation process (Fig. 6E). Figure 6B shows that *Msx2* expression in HERS cells of a 14-day-old RTg mouse corresponds to a later stage of the root elongation process (17 days, see in Supplementary Fig. 3) as compared to an age-matched control mouse (Fig. 6A). Indeed, in the RTg mouse, HERS disruption was more advanced, displaying an increased number of rests of Malassez, as shown by strong *Msx2* staining. Moreover, the size of the apical HERS was reduced, as evidenced by the reduced number of epithelial cells stained for *Msx2* in the apical area. These data are consistent with earlier differentiation of HERS cells in the RTg mouse.

Relationship between RANK activation and dental root morphology

To deepen our understanding of the relationship between root elongation timing and root thickness, the impact of RANK over-

Fig. 2. A–F: Comparative analysis of TRAP staining around the mandibular first molar of the WT (A,C,E) and RTg (B,D,F) mice. A large increase in numbers of TRAP-positive cells was observed in the RTg mouse. They were distributed all around the tooth at 3 days (A vs. B) and in more restricted areas of the alveolar bone crypt associated with root growth at 14 days (C vs. D) and at 21 days (E vs. F). M1, first molar crown; M1r1, first molar mesial root; AB, alveolar bone.

Comparative analysis of mouse mandible root shape was performed by more sensitive microscans. Frontal sections at 11 days showed an increase in root length (448.03 ± 9.39 μm for RTg vs. 364.13 ± 15.41 μm for WT) together with a decrease in root diameter (Fig. 3G,H). Three-dimensional reconstructions of 17-day-old WT (Fig. 3I) and RTg (Fig. 3J) mouse molars, generated using the same conditions, including the same threshold, showed a significantly advanced molar root

TABLE 2. Summary of RANK over-expression on root morphology, osteoclast number, and dental cell proliferation

	3 days	14 days	21 days
Osteoclast number (TRAP)	1.5	2	1.5
Root morphology			
Length	1	1.25	1
Diameter	1	0.4	0.7
Proliferation (BrdU/PCNA)			
HERS	1	1.3	Undetermined
Dental pulp	1	1	Undetermined
Dental follicle	1	≥2	Undetermined

Each result corresponds to the ratio (RTg mean value)/(WT mean value).

CONTROL OF TOOTH GROWTH BY BONE RESORPTION   79

Fig. 3. Microradiographic comparative analysis of mandibular molar growth between WT (A,C,E) and RTg (B,D,F) mice. At 3 and 7 days, no difference was observed (A–D). At 21 days, the first molar roots appeared narrower in RTg mice as compared to WT animals (red and blue lines in E and F). Comparative analysis of microscan (2D) frontal sections of 11-day-old WT (G) and RTg (H) mouse mandibular first molar mesial root shapes. The RTg mouse root appeared narrower and longer than that of WT (red vs. blue lines in G and H). Microscan three-dimensional comparative analysis of 17-day-old WT (I) and RTg (J) mouse mandibular first molar root length. The RTg mouse displayed longer roots than WT (red vs. blue line in I and J).

expression on mesial root morphology was analyzed in 21-day-old control ($Msx2^{+/+}$) and $Msx2$ null mutant ($Msx2^{-/-}$) mice (Fig. 6C–F). The $Msx2^{-/-}$ mouse root (Fig. 6E) presents many morphological defects, including a reduction of the length compared to the WT mouse root (Fig. 6C). The $Msx2^{-/-}$ mouse is, therefore, an appropriate complementary model with which to analyze the impact of RANK over-expression on root formation. In both $Msx2^{+/+}$ and $Msx2^{-/-}$ mice, RANK over-expression had no impact on mandibular first molar mesial root length at 21 days, but it induced a significant reduction of the root diameter (Fig. 6C–F).

To validate the relationship between RANK activity and root diameter, the morphology of the mandibular first molar mesial root was compared between 21-day-old WT, RTg, and $Rankl$ heterozygous ($Rankl^{+/-}$) mice using microradiography (Fig. 6G–I). $Rankl$-deficient mice ($Rankl^{-/-}$) present a severe form of osteopetrosis due to the absence of RANK activation (Kim et al., 2000). $Rankl^{+/-}$ mice were chosen here as a model of moderate RANK loss of function (Odgren et al., 2003). The data show that reduced RANK stimulation as a consequence of RANKL haplo-insufficiency (Fig. 6I) has an opposite effect on root diameter compared to RANK over-activation due to RANK over-expression (Fig. 6G), with the $Rankl^{+/-}$ mouse molar having an increased root diameter (Fig. 6J) compared to that of WT. Taken together, these results demonstrate that alveolar bone resorption activity plays a determining role in root morphogenesis in addition to dental-cell intrinsic determinants (Fig. 6K). Indeed, the results of experiments combining an $Msx2$ gene null mutation and RANK over-activation are consistent with a model in which the final root

length is genetically determined (independent of alveolar bone resorption activity), whereas the final root diameter is dependent on the surrounding alveolar bone resorption activity during growth (Fig. 6K).

Effect of RANK over-expression on alveolar bone modeling and remodeling

To determine the impact of RANK over-expression on alveolar bone modeling and remodeling, the transcriptional activity of genes of differentiating and mature osteoclasts and osteoblasts was assessed by RT-PCR in WT and RTg mice at 14 days and 3.5 months.

In 14-day-old mice, during alveolar bone modeling, expression levels of functional osteoclast markers such as $Trap$ and Cathepsin K ($Ctsk$) were higher in the transgenic mouse alveolar bone (Fig. 7A, Supplementary Table 1), in agreement with a previously described increase in TRAP staining (Fig. 2D) and secondary to the increase in $Rank$ expression due to the transgene (Fig. 7A, Supplementary Table 1). In contrast, expression levels of $Rankl$ and $Tnf\alpha$, two inducers of osteoclastogenesis, were higher in WT mouse alveolar bone than in RTg mouse bone (blue stars in Fig. 7A, Supplementary Table 1). These differences can be explained by the fact that the mandibular first molar of the WT mouse underwent eruption at 14 days whereas the molar of the RANK over-expressing mouse was post-eruptive (Fig. 7B, Supplementary Table 1). The observation that expression of $Runx2$, the main osteoblastogenesis regulating factor, increases in RTg mice concomitantly with a decrease of osteocalcin (Oc) and bone
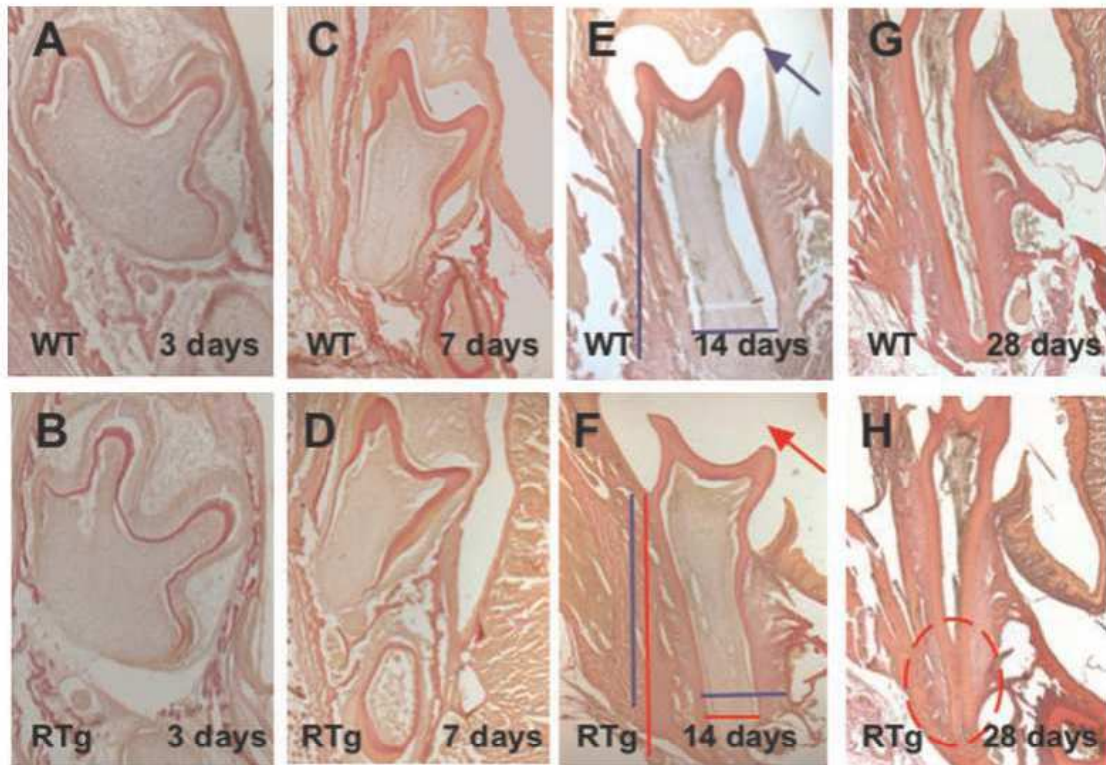
80 CASTANEDA ET AL.

Fig. 4. Histological comparative analysis of mandibular first molar growth between WT (A,C,E,G) and RTg (B,D,F,H) mice. At 3 and 7 days, no significant difference was observed. At 14 days, the RTg mouse molar was fully erupted (red arrow in F) in contrast to the WT mouse molar (blue arrow in E). Moreover, the mesial root appeared longer and narrower in the RTg mouse (red lines F) than in the WT mouse (blue lines in E and F). At 28 days, a partially closed mesial root pulp chamber was observed in certain RTg mice (circle in H).
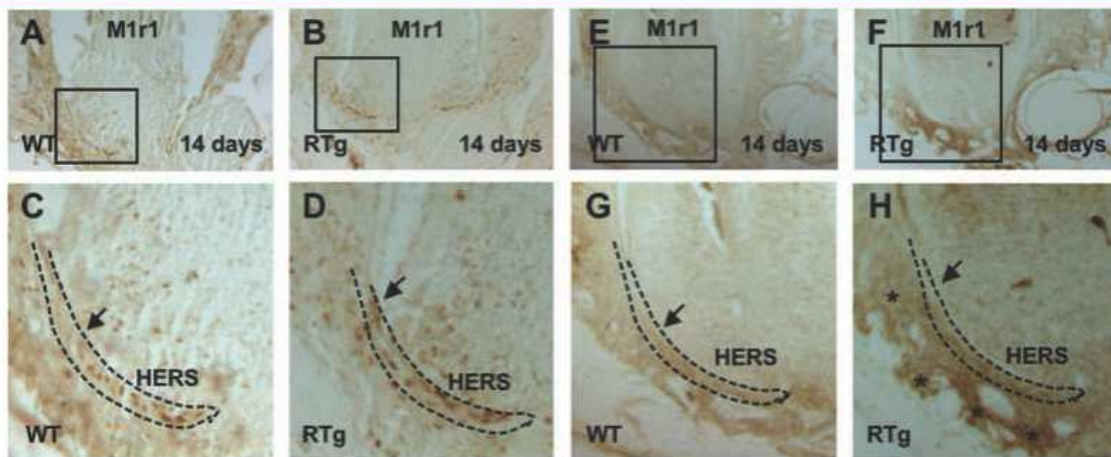
Fig. 5. Comparative analysis of proliferation of mouse first molar mesial root epithelial cells between 14-day-old WT (A,C,E,G) and RTg (B,D,F,H) mice using staining for PCNA (A–D) and BrdU incorporation (E–H). PCNA staining revealed extensive proliferation activity within HERS in the RTg mouse (B,D) as compared to WT (A,C), as shown by the relative positions of the last stained cells (arrows in C and D). BrdU staining was similar to PCNA-staining in terms of epithelial cell proliferation, as evidenced by the relative position of the last stained cells of the HERS (arrows in G and H). BrdU staining also showed a strong proliferation zone in the adjacent mesenchymal cells in the RTg mouse (F and star in H) compared to WT (E,G). C, D, G, and H correspond, respectively, to enlargement of the squares in A, B, E, and F. M1r1, first molar mesial root.

CONTROL OF TOOTH GROWTH BY BONE RESORPTION   81
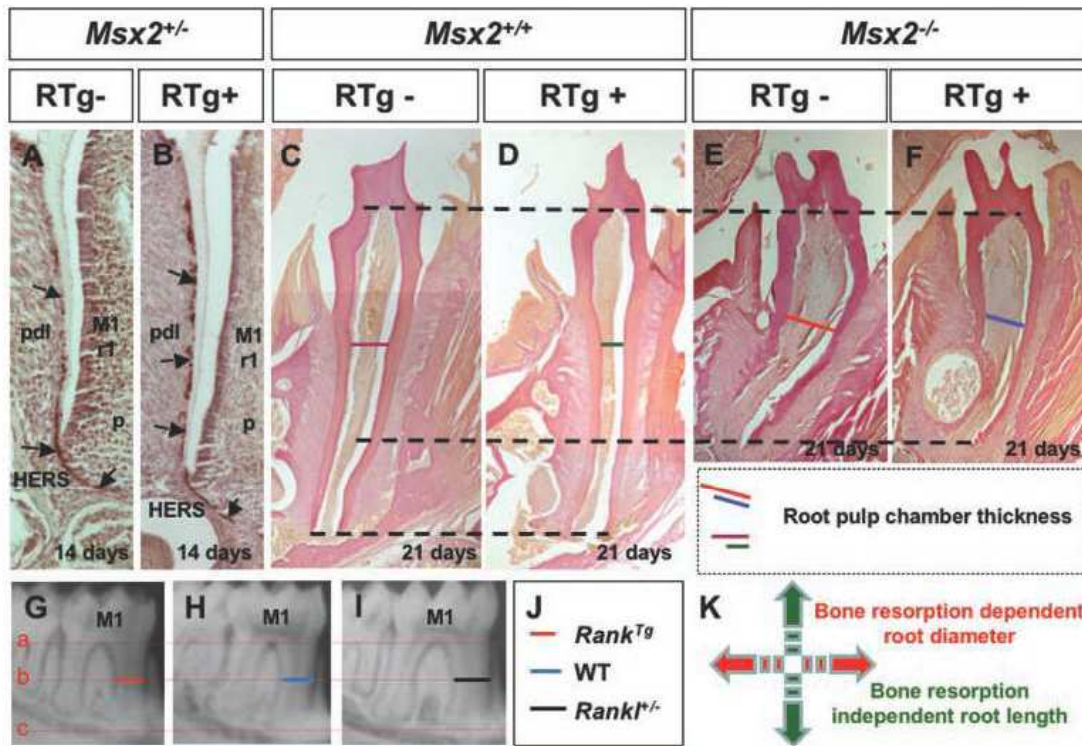
Fig. 6.   A,B: Analysis of the impact of RANK over-expression on *Msx2* homeobox gene expression pattern in 14-day-old mouse mandibular first molar root using the heterozygous *Msx2/LacZ* reporter mouse (*Msx2*$^{+/-}$). No significant difference in the *Msx2* expression pattern was observed in the root epithelium (arrows in A and B) according to the noticeable root elongation stage difference between WT and RTg mice. However, in the RTg mouse, a higher labeling intensity is evident in the HERS and Malassez epithelial cells (arrows in B) as compared to the WT mouse (arrows in A). Labeling is also observed in cells of the periodontal ligament (pdl) and the dental pulp (p). C–F: Analysis of the impact of RANK over-expression on the morphology of the mandibular first molar mesial root at 21 days. At this age, both control mouse (*Msx2*$^{+/+}$; C,D) and *Msx2* null mutant (*Msx2*$^{-/-}$; E,F) molars have terminated their eruption and root elongation. The *Msx2*$^{-/-}$ mouse (E) presented a reduced root length and a more curved shape compared to the WT mouse (C). RANK over-expression had no effect on the final root length in both genetic backgrounds (*Msx2*$^{+/+}$ and *Msx2*$^{-/-}$) but induced an important decrease of the root diameter, as shown by comparison of the root pulp chamber thickness (lines in C–F). G–J: Microradiographic comparative analysis of the first molar mesial root diameter between 21-day-old RTg, WT, and *Rankl*$^{+/-}$ mice. A decrease in the root diameter was observed in the RTg mouse (red lines in G and J), whereas an increase was observed for the *Rankl*$^{+/-}$ mouse (black lines in I and J) compared to the WT control (blues line in H and J). Lines a, b, and c were used for tooth alignments and measurements. K: Schematic representation of differential controls of the root developmental axis. Control of root length appears to be independent of bone resorption whereas root width is dependent on the latter.

sialoprotein (*Bsp*), two mature osteoblast markers, is consistent with this explanation (Fig. 7A, Supplementary Table 1).
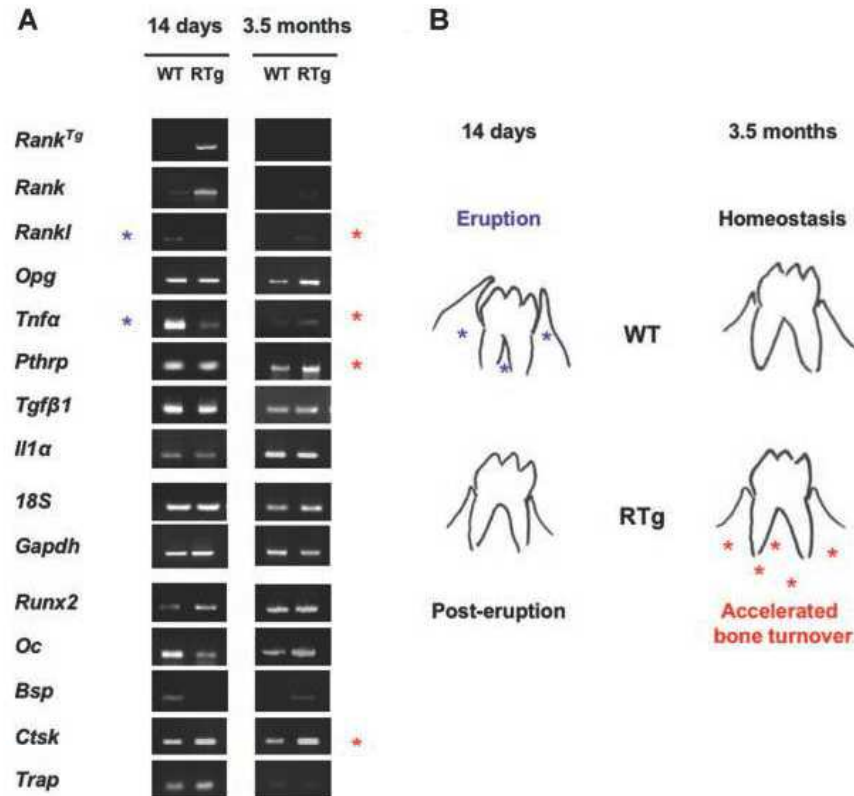
At 3.5 months, RTg mouse alveolar bone presented increased expression of most osteoclastogenesis activators (*Rankl, Tnfα, Pthrp*) but also of *Ctsk*, a mature osteoclast marker (red stars in Fig. 7A, Supplementary Table 1). These data suggest that alveolar bone resorption was increased in the RTg mouse. Interestingly, the expression levels of both Runx2 and mature osteoblast markers were mildly increased in the RTg mouse (Fig. 7A, Supplementary Table 1), evidence of accelerated bone turnover (Fig. 7B, Supplementary Table 1). Osteoprotegerin (*Opg*) expression levels were increased in RTg mouse alveolar bone (Fig. 7A, Supplementary Table 1), which may reflect a potential compensatory response to increased bone resorption.

Discussion

In humans, constitutive activation of RANK is responsible for three seemingly distinctive disorders with autosomal-dominant inheritance: FEO (OMIM #174810; Osterberg et al., 1988; Wallace et al., 1989; Hughes et al., 1994, 2000; Johnson-Pais et al., 2003), ESH (Whyte et al., 2000; Whyte and Hughes, 2002), and early-onset Paget disease of bone (PDB2, OMIM #602080; Nakatsuka et al., 2003). Tandem duplications in the first exon, 18 bp for FEO, 15 bp for ESH, and 27 bp for PBD2, increase the length of the RANK signal peptide and alter its normal cleavage, which is believed to cause over-activation of the NF-κB pathway (Whyte and Hughes, 2002; Nakatsuka et al., 2003). Such over-activation of the RANK signaling pathway causes higher osteoclastic activity and, therefore, increases bone turnover. Stimulation of osteoblasts is also observed with a variable occurrence and associated with widening of the long bones and early deafness (Whyte, 2006). Surprisingly, no impact on the immune system has been reported to date. Early tooth loss was also observed in some cases associated with idiopathic external resorption, localized at either the apical or cervical levels (Mitchell et al., 1990; Hughes et al., 1994; Whyte, 2006).

So far, no data are available which address the mechanisms that link these genetic mutations with the phenotype of the

82   CASTANEDA ET AL.

Fig. 7. A: Comparative analysis of osteoclastogenesis and osteoblastogenesis stimulatory factor expression levels in alveolar bone between WT and RTg mice. At 14 days, WT mouse alveolar bone presented a higher expression level of *Rankl* and *Tnfα* (blue star). *Pthrp*, *Opg*, *Tgfβ1*, and *Il1α* seemed not to be modulated. In contrast, expression levels of the mature osteoclast markers, namely *Trap* and *Ctsk*, were higher in the RTg mouse. Concerning osteoblastogenesis, the expression level of *Runx2* was higher in the RTg mouse. Conversely, the expression levels of mature osteoblast markers (*Oc* and *Bsp*) were higher in WT mouse alveolar bone. All of these data reflect the difference in eruption stage between RTg and WT mouse, as represented in (B). At 3.5 months, the expression level of most osteoclastogenesis activators (*Rankl*, *Pthrp*, *Tnfα*, red star) and mature osteoclast markers (*Ctsk*) were increased in the RTg mouse alveolar bone, suggesting increased bone resorption, as represented by a red star in (B). RANK expression is at the limit of detection at 3.5 months in RTg mouse alveolar bone and the transgene expression is not detected by classical RT-PCR. This is evidence of an important reduction of transgene expression levels in adult bone compared to growing bone (14 days).

complex structure formed by tooth and alveolar bone. A transgenic mouse model of RANK over-expression in osteoclast cell lineage precursors was used here as a physiopathological model for RANK pathway activation. RANK over-expression induced a large increase in the number of TRAP-positive cells in the alveolar bone at all ages, as schematically represented in Figure 8. Two peaks correspond to the established stages of monocyte recruitment, days 3–5, and tooth eruption, days 9–14 (Volejnikova et al., 1997; Wise, 2009). Interestingly, the increase in TRAP-positive cells followed the normal spatial patterns that these cells (pre-osteoclasts and osteoclasts) adopt during the growth of the complex formed by tooth and alveolar bone (Wise and Fan, 1989; Volejnikova et al., 1997; Heinrich et al., 2005). Growth of this complex implies coordination between alveolar bone modeling and tooth volumetric growth (for review, see Boughner and Hallgrímsson, 2008). The molecular modalities of this coordination have been, in part, deciphered with respect to recruitment and activation of osteoclasts by dental and periodontal cells (for review, see Wise, 2009). The role of RANKL/RANK in this coordinative process (Rani and MacDougall, 2000; Ohazama et al., 2004; Heinrich et al., 2005;

Liu et al., 2005; Wise and Yao, 2006) would explain the increase in TRAP-positive cell numbers (osteoclasts) observed in the *Rank* transgenic (RTg) mouse alveolar bone. A consequence of the increased numbers of osteoclasts in the RTg mouse was to induce premature tooth eruption and accelerate root elongation (Fig. 8).

Interactions between epithelial cells of the HERS and mesenchymal cells of both the dental pulp and outer dental follicle are essential for root formation. These interactions involve many signaling molecules such as Sonic Hedgehog (Nakatomi et al., 2006; Khan et al., 2007), Wnt family member 10a (Yamashiro et al., 2007; Lohi et al., 2009), and bone morphogenetic protein (BMP) family members 2, 3, 4, and 7 (Mouri et al., 2003; Yamamoto et al., 2004; Kémoun et al., 2007; Hosoya et al., 2008), as well as their receptors Patched2, ActR-I, BMPR-IB, and BMPR-II, respectively (Nakatomi et al., 2006; Kémoun et al., 2007; Hosoya et al., 2008), and transcription factors *Dlx2*, *Msx2*, and *Gli1* (Lézot et al., 2000; Yamashiro et al., 2003; Nakatomi et al., 2006). The accelerated tooth root elongation observed in the RTg mouse corresponded to an increase in proliferation of the outer HERS and adjacent follicular cells (Fig. 9), whereas cell proliferation in the dental

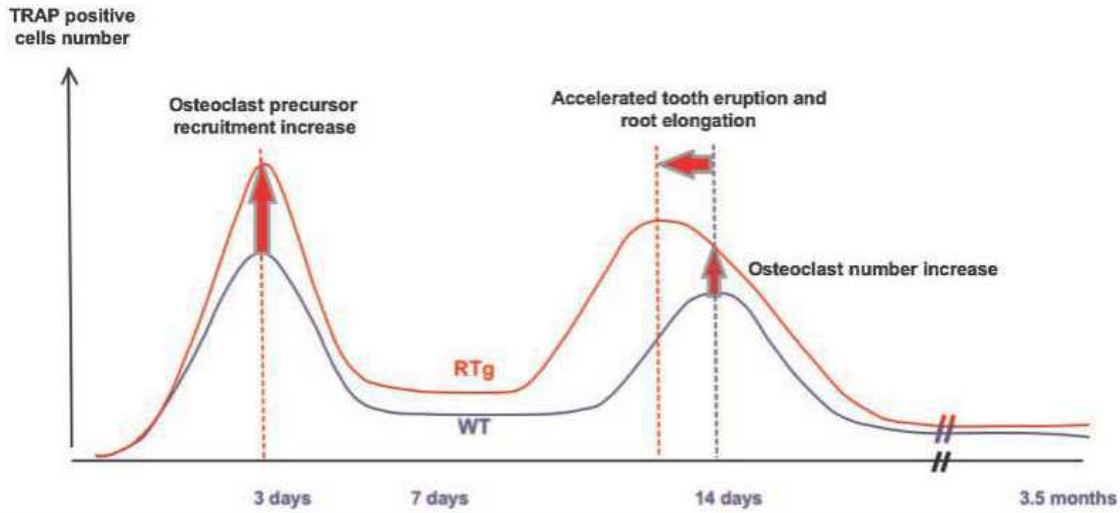## CONTROL OF TOOTH GROWTH BY BONE RESORPTION

Fig. 8.   Schematic representation (derived from Wise, 2009) of the impact of RANK over-expression in alveolar bone modeling and remodeling. At 3–7 days, RTg mouse alveolar bone presents an increase in TRAP-positive cells. At 9–14 days, the RTg mouse exhibits earlier tooth eruption and root elongation, secondary to an earlier and a higher increase in TRAP-positive cells.

pulp appeared unchanged. An earlier onset of HERS differentiation was associated with the increased proliferation of these cells (Fig. 9), as evidenced by the comparative analysis of the pattern of *Msx2* expression in control and RTg mice

(Supplementary Fig. 3). Final root lengths of control and RTg mice were similar, suggesting that interactions between epithelial and mesenchymal cells necessary for root elongation are not fundamentally affected by RANK over-expression but
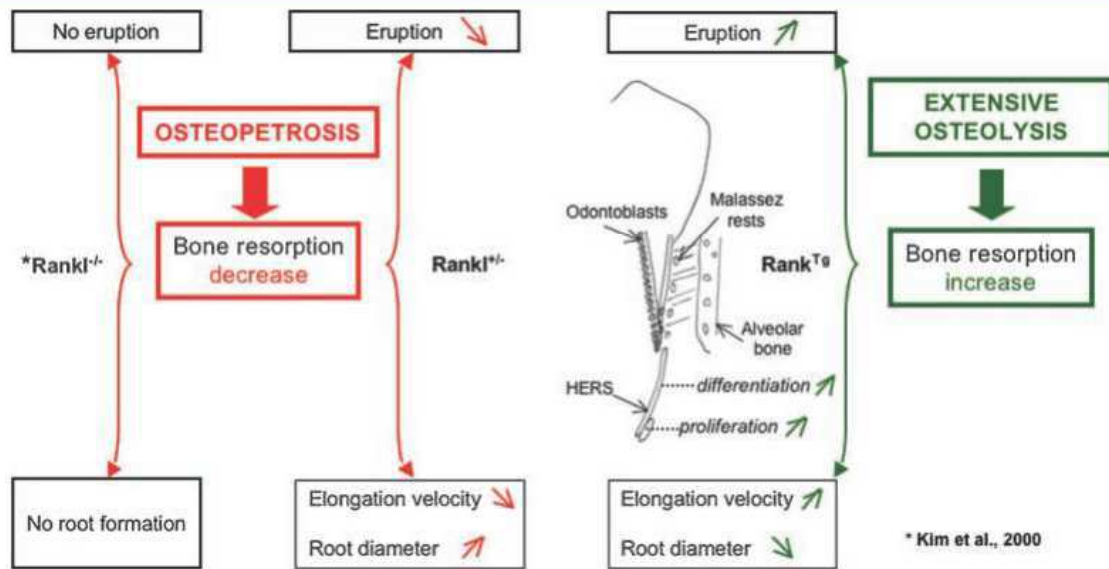

Fig. 9.   Schematic representation of the impact of bone resorption activity levels on dental root elongation and final root diameter. Left side: In severe forms of osteopetrosis (for instance, *Rankl*$^{-/-}$), the absence of bone resorption blocks both eruption and root elongation. Middle: When bone resorption is decreased, as observed in mild forms of osteopetrosis (*Rankl*$^{+/-}$), the eruption is delayed, the root elongation velocity is decreased, and the final root diameter is increased. Right side: In contrast, when bone resorption is increased, as observed in extensive osteolysis pathologies (*Rank*^{Tg}), eruption occurs earlier, root elongation velocity is increased, and the final root diameter is decreased. The increased velocity of root elongation corresponds to an increased rate of Hertwig epithelial root sheath (HERS) cell proliferation and differentiation.

CASTANEDA ET AL.

take place earlier. This hypothesis is supported by the observation in RTg mice of normal final thicknesses of both root dentin (Fig. 3) and cementum (data not shown), indicating that the processes of odontoblast and cementoblast differentiation are unaffected. Interestingly, the accelerated tooth root elongation, secondary to RANK over-expression, induced a significant decrease in the root diameter in both $Msx2^{+/+}$ and $Msx2^{-/-}$ mice. This smaller diameter can be traced to an abnormally thin dental pulp.

The $Msx2^{-/-}$ mouse is an exemplary model for root anomalies (Aïoub et al., 2007). The phenotype includes an important reduction of root length, as shown in Figure 6. The fact that, in the $Msx2^{-/-}$ mouse, RANK over-activation also induced a decrease in the root diameter, without affecting the final root length, argues that final length and diameter are two independent root morphogenetic parameters. Final root length appears to be independent of the level of alveolar bone resorption activity; rather it is determined by genetic factors, as exemplified by the different root lengths in $Msx2^{+/+}$ and $Msx2^{-/-}$ mice. In contrast, root diameter appears to be dependent on the level of alveolar bone resorption activity (Fig. 9). This was clearly demonstrated here, considering RANK activation as the key determinant of bone resorption. Indeed, RANK over-expression induced a decrease in root diameter, whereas, conversely, RANKL haplo-insufficiency induced an increase in root diameter (Fig. 9). The inverse relationship between alveolar bone resorption level and root diameter established here could explain the root defects associated with osteoclast diseases (reviewed by Helfrich, 2005).

Comparative analysis of RTg and WT adult mouse alveolar bones revealed increased expression of osteoclastogenesis activators (*Rankl*, *Pthrp*, and *Tnfα*) and cathepsin K genes in the RTg mouse. Such an expression increase reflected both osteolytic and inflammatory bone status. Indeed, the RANKL/RANK interaction is an important element of immune system cell–cell communication implicated in the immune response that may be over-activated in RTg mice. Interestingly, up-regulation of *Opg* gene expression was also observed in the alveolar bone of adult *Rank* transgenic mice. Such modulation could constitute a negative retro-control to the RANK signaling over-activation. Such an auto-regulatory loop of RANK signaling through OPG has been described in long bones (reviewed by Helfrich, 2005). Increased OPG expression levels would be a determinant for the absence of dental resorption observed in the present study, despite the hyperactivity of periodontal osteoclasts. The presence of such a regulatory loop remains to be clarified in patients presenting RANK over-activation, with evident consequences for a therapeutic approach.

Conclusion

Our analysis of an animal model of RANK over-activation revealed the presence of an early onset of tooth eruption and a decrease in dental root diameter. This dental phenotype constitutes potential supplementary criteria to achieve an earlier diagnosis of extensive osteolytic genetic pathologies. This animal model is an important resource for deciphering the molecular mechanisms of dental and bone cell interactions during growth and maintenance of the dento-alveolar complex, and for researching targeted therapy in local and systemic disorders involving RANK signaling pathways.

Acknowledgments

Literature Cited

Aioub M, Lézot F, Molla M, Castaneda B, Robert B, Goubin G, Néfussi JR, Berdal A. 2007. Msx2−/− transgenic mice develop compound amelogenesis imperfect, dentinogenesis imperfect and periodontal osteopetrosis. Bone 41:851–859.

Barbaroux JB, Beleut M, Brisken C, Mueller CG, Groves RW. 2008. Epidermal receptor activator of NF-kappaB ligand controls Langerhans cells numbers and proliferation. J Immunol 181:1103–1108.

Bosshardt DD, Nanci A. 2004. Hertwig's epithelial root sheath, enamel matrix proteins, and initiation of cementogenesis in porcine teeth. J Clin Periodontol 31:184–192.

Boughner JC, Hallgrimsson B. 2008. Biological space–time and the temporal integration of functional modules: A case study of dento-gnathic developmental timing. Dev Dyn 237:1–17.

Chong B, Hegde M, Fawkner M, Simonet S, Cassinelli H, Coker M, Kanis J, Seidel J, Tau C, Tuysuz B, Yuksel R, Love D, Cundy T. 2003. Idiopathic hyperphosphatasia and TNFRSF11B mutations: Relationships between phenotype and genotype. J Bone Miner Res 18:2095–2104.

Cundy T, Hegde M, Naot D, Chong B, King A, Wallace R, Mulley J, Love DR, Seidel J, Fawkner M, Banovic T, Callon KE, Grey AB, Reid IR, Middleton-Hardie CA, Cornish J. 2002. A mutation in the gene TNFRSF11B encoding osteoprotegerin causes an idiopathic hyperphosphatasia phenotype. Hum Mol Genet 11:2119–2127.

Dougall WC, Glaccum M, Charrier K, Rohrbach K, Brasel K, De Smedt T, Daro E, Smith J, Tometsko ME, Maliszewski CR, Armstrong A, Shen V, Bain S, Cosman D, Anderson D, Morrissey PJ, Peschon JJ, Schuh J. 1999. RANK is essential for osteoclast and lymph node development. Genes Dev 13:2412–2424.

Dunn V, Condon VR, Rallison ML. 1979. Familial hyperphosphatasemia: Diagnosis in early infancy and response to human thyrocalcitonin therapy. Am J Roentgen 132:541–545.

Guerrini MM, Sobacchi C, Cassani B, Abinum M, Kilic SS, Pangrazio A, Moratto D, Mazzolari E, Clayton-Smith J, Orchard P, Coxon FP, Helfrich MH. 2008. Human osteoclast-poor osteopetrosis with hypogammaglobulinemia due to TNFRSF11A (RANK) mutations. Am J Hum Genet 83:64–76.

Hammarström L. 1997. Enamel matrix, cementum development and regeneration. J Clin Periodontol 24:658–668.

Heinrich J, Bsoul S, Barnes J, Woodruff K, Abboud S. 2005. CSF-1, RANKL and OPG regulate osteoclastogenesis during murine tooth eruption. Arch Oral Biol 50:897–908.

Helfrich MH. 2005. Osteoclast diseases and dental abnormalities. Arch Oral Biol 50:115–122.

Hosoya A, Kim JY, Cho SW, Jung HS. 2008. BMP4 signaling regulates formation of Hertwig's epithelial root sheath during tooth root development. Cell Tissue Res 333:503–509.

Hughes AE, Shearman AM, Weber JL, Barr RJ, Wallace RG, Osterberg PH, Nevin NC, Mollan RA. 1994. Genetic linkage of familial expansile osteolysis to chromosome 18q. Hum Mol Genet 3:359–361.

Hughes AE, Ralston SH, Marken J, Bell C, MacPherson H, Wallace RGH, Van Hul W, Whyte MP, Nakatsuka K, Hovy L, Anderson DM. 2000. Mutations in TNFRSF11A, affecting the signal peptide of RANK, cause familial expansile osteolysis. Nat Genet 24:45–48.

Johnson-Pais TL, Singer FR, Bone HG, McMurray CT, Hansen MF, Leach RJ. 2003. Identification of a novel tandem duplication in exon 1 of the TNFRSF11A gene in two unrelated patients with unrelated patients with familial expansile osteolysis. J Bone Miner Res 18:376–380.

Kat PS, Sampson WJ, Wilson DF, Wiebkin OW. 2003. Distribution of the epithelial rests of Malassez and their relationship to blood vessels of the periodontal ligament during rat tooth development. Aust Orthod J 19:207–286.

Kémoun P, Laurencin-Dalicieux S, Rue J, Farges JC, Gennero I, Conte-Auriol F, Briand-Mesange F, Gadelorge M, Arzate H, Narayanan AS, Brunel G, Salles JP. 2007. Human dental follicle cells acquire cementoblast features under stimulation by BMP-2/-7 and enamel matrix derivatives (EMD) in vitro. Cell Tissue Res 329:283–294.

Khan M, Seppala M, Zoupa M, Cobourne MT. 2007. Hedgehog pathway gene expression during early development of the molar tooth root in the mouse. Gene Expr Patterns 7:239–243.

Kim N, Odgren PR, Kim DK, Marks SC, Choi Y. 2000. Diverse roles of the tumor necrosis factor family member TRANCE in skeletal physiology revealed by TRANCE deficiency and partial rescue by a lymphocyte-expressed TRANCE transgene. Proc Natl Acad Sci USA 97:10905–10910.

Kong YY, Yoshida H, Sarosi I, Tan HL, Timms E, Capparelli C, Morony S, Oliveira-dos-Santos AJ, Van G, Itie A, Khoo W, Wakeham A, Dunstan CR, Lacey DL, Mak TW, Boyle WJ, Penninger JM. 1999. OPGL is a key regulator of osteoclastogenesis, lymphocyte development and lymph-node organogenesis. Nature 397:315–323.

Lagasse E, Weissman IL. 1992. Mouse MRP8 and MRP14, two intracellular calcium-binding proteins associated with the development of the myeloid lineage. Blood 79:1907–1915.

Lagasse E, Weissman IL. 1994. bcl-2 inhibits apoptosis of neutrophils but not their engulfment by macrophages. J Exp Med 179:1047–1052.

Lagasse E, Weissman IL. 1997. Enforced expression of Bcl-2 in monocytes rescues macrophages and partially reverses osteopetrosis in op/op mice. Cell 89:1021–1031.

Lallemand Y, Nicola MA, Ramos C, Bach A, Cloment CS, Robert B. 2005. Analysis of Msx1–Msx2 double mutants reveals multiple roles for Msx genes in limb development. Development 132:3003–3014.

Lézot F, Davideau JL, Thomas B, Sharpe P, Forest N, Berdal A. 2000. Epithelial Dlx-2 homeogene expression and cementogenesis. J Histochem Cytochem 48:277–284.

Lézot F, Thomas B, Greene SR, Hotton D, Yuan ZA, Castaneda B, Bolaños A, Depew M, Sharpe P, Gibson CW, Berdal A. 2008. Physiological implications of DLX homeoproteins in enamel formation. J Cell Physiol 216:688–697.

Lézot F, Thomas BL, Blin-Wakkach C, Castaneda B, Bolanos A, Hotton D, Sharpe PT, Heymann D, Carles GF, Grigoriadis AE, Berdal A. 2010. Dlx homeobox gene family expression in osteoclasts. J Cell Physiol 223:779–787.

Li J, Sarosi I, Yan XQ, Morony S, Capparelli C, Tan HL, McCabe S, Elliott R, Scully S, Van G, Kaufman S, Juan SC, Sun Y, Tarpley J, Martin L, Christensen K, McCabe J, Kostenuik P, Hsu H, Fletcher F, Dunstan CR, Lacey DL, Boyle WJ. 2000. RANK is the intrinsic hematopoietic

CONTROL OF TOOTH GROWTH BY BONE RESORPTION   85

cell surface receptor that controls osteoclastogenesis and regulation of bone mass and calcium metabolism. Proc Natl Acad Sci USA 97:1566–1571.

Liu D, Yao S, Pan F, Wise GE. 2005. Chronology and regulation of gene expression of RANKL in the rat dental follicle. Eur J Oral Sci 113:404–409.

Lohi M, Turcker AS, Sharpe PT. 2010. Expression of Axin2 indicates a role for canonical Wnt signaling in development of the crown and root during pre- and postnatal tooth development. Dev Dyn 239:160–167.

Mitchell CA, Kennedy JG, Wallace RG. 1990. Dental abnormalities associated with familial expansile osteolysis: A clinical and radiographic study. Oral Surg Oral Med Oral Pathol 70:301–307.

Mouri Y, Shilba H, Mizuno N, Noguchi T, Ogawa T, Kurihara H. 2003. Differential gene expression of bone-related proteins in epithelial and fibroblastic cells derived from human periodontal ligament. Cell Biol Int 27:519–524.

Nakatomi M, Morita I, Eto K, Ota MS. 2006. Sonic hedgehog signaling is important in tooth root development. J Dent Res 85:427–431.

Nakatsuka Y, Nishizawa Y, Ralston SH. 2003. Phenotypic characterization of early onset Paget's disease of bone caused by a 27-bp duplication in the TNFRSF11A gene. J Bone Miner Res 18:1381–1385.

Odgren PR, Kim N, MacKay CA, Mason-Savas A, Choi Y, Marks SC, Jr. 2003. The role of RANKL (TRANCE/TNFSF11), a tumor necrosis factor family member, in skeletal development: Effects of gene knockout and transgenic rescue. Connect Tissue Res 44:264–271.

Ohazama A, Courtney JM, Sharpe PT. 2004. Opg, Rank, Rankl in tooth development: Co-ordination of odontogenesis and osteogenesis. J Dent Res 83:241–244.

Osterberg PH, Wallace RG, Adams DA, Crone RS, Dickson GR, Kanis JA, Mollan RA, Nevin NC, Sloan J, Toner PG. 1988. Familial expansile osteolysis: A new dysplasia. J Bone Joint Surg 70:255–260.

Rani CS, MacDougall M. 2000. Dental cells express factors that regulate bone resorption. Mol Cell Biol Res Commun 3:145–152.

Sobacchi C, Frattini A, Guerrini MM, Abinun M, Pangrazio A, Susani L, Bredius R, Mancini G, Cant A, Biship N, Grabowski P, Del Fattore A, Messina C, Errigo G, Coxon FP, Scott DI, Teti A, Rogers MJ, Vezzoni P, Villa A, Helfrich MH. 2007. Osteoclast-poor human osteopetrosis due to mutations in the gene encoding RANKL. Nat Genet 39:960–962.

Suzuki M, Inoue T, Shimono M, Yamada S. 2002. Behavior of epithelial root sheath during tooth root formation in porcine molars: TUNEL, TEM, and immunohistochemical studies. Anat Embryol (Berl) 206:13–20.

Ten Cate AR. 1994. Oral histology. Development, structure, and function. St Louis, MO: Mosby-Year Book. 532 pp.

Volejnikova S, Laskari M, Marks SC, Jr., Graves DT. 1997. Monocyte recruitment and expression of monocyte chemoattractant protein-1 are developmentally regulated in remodeling bone in the mouse. Am J Pathol 150:1711–1721.

Wallace RG, Barr RJ, Osterberg PH, Mollan RA. 1989. Familial expansile osteolysis. Clin Orthop Rel Res 248:265–277.

Whyte MP. 2006. Paget's disease of bone and genetic disorders of RANKL/OPG/RANK/NF-kappaB signaling. Ann N Y Acad Sci 1068:143–164.

Whyte MP, Hughes AE. 2002. Expansile skeletal hyperphosphatasia is caused by a 15-base pair tandem duplication in TNFRSF11A encoding RANK and is allelic to familial expansile osteolysis. J Bone Miner Res 17:26–29.

Whyte MP, Mills BG, Reinus WR, Podgornik MN, Roodman GD, Gannon FH, Eddy MC, McAlister WH. 2000. Expansile skeletal hyperphosphatasia: A new familial metabolic bone disease. J Bone Miner Res 15:2330–2344.

Whyte MP, Obrecht SE, Finnegan PM, Jones JL, Podgornik MN, McAlister WH, Mumm S. 2002. Osteoprotegerin deficiency and juvenile Paget's disease. New Engl J Med 347:175–184.

Wise GE. 2009. Cellular and molecular basis of tooth eruption. Orthod Craniofac Res 12:67–73.

Wise GE, Fan W. 1989. Changes in the tartrate-resistant acid phosphatase cell population in dental follicles and bony crypts of rat molars during tooth eruption. J Dent Res 68:150–156.

Wise GE, Yao S. 2006. Regional differences of expression of bone morphogenetic protein-2 and RANKL in the rat dental follicle. Eur J Oral Sci 114:512–516.

Yamamoto H, Cho SW, Kim EJ, Kim JY, Fujiwara N, Jung HS. 2004. Developmental properties of the Hertwig's epithelial root sheath in mice. J Dent Res 83:688–692.

Yamashiro T, Tummers M, Thesleff I. 2003. Expression of bone morphogenetic proteins and Msx genes during root formation. J Dent Res 82:172–176.

Yamashiro T, Zheng L, Shitaku Y, Saito M, Tsubakimoto T, Takada K, Takano-Yamamoto T, Thesleff I. 2007. Wnt10a regulates dentin sialophosphoprotein mRNA expression and possibly links odontoblast differentiation and tooth morphogenesis. Differentiation 75:452–462.

Yasuda H, Shima N, Nakagawa N, Yamaguchi K, Kinosaki M, Mochizuki S, Tomoyasu A, Yano K, Goto M, Murakami A, Tsuda E, Morinaga T, Higashio K, Udagawa N, Takahashi N, Suda T. 1998a. Osteoclast differentiation factor is a ligand for osteoprotegerin/osteoclastogenesis-inhibitory factor and is identical to TRANCE: RANKL. Proc Natl Acad Sci USA 95:3597–3602.

Yasuda H, Shima N, Nakagawa N, Mochizuki SI, Yano K, Fujise N, Sato Y, Goto M, Yamaguchi K, Kuriyama M, Kanno T, Murakami A, Tsuda E, Morinaga T, Higashio K. 1998b. Identity of osteoclastogenesis inhibitory factor (OCIF) and osteoprotegerin (OPG): A mechanism by which OPG/OCIF inhibits osteoclastogenesis in vitro. Endocrinology 139:1329–1337.

Zeichner-David M, Oishi K, Su Z, Zakartchenko V, Chen LS, Arzate H, Bringas P, Jr. 2003. Role of Hertwig's epithelial root sheath cells in tooth root development. Dev Dyn 228:651–663.

Supplementary figures
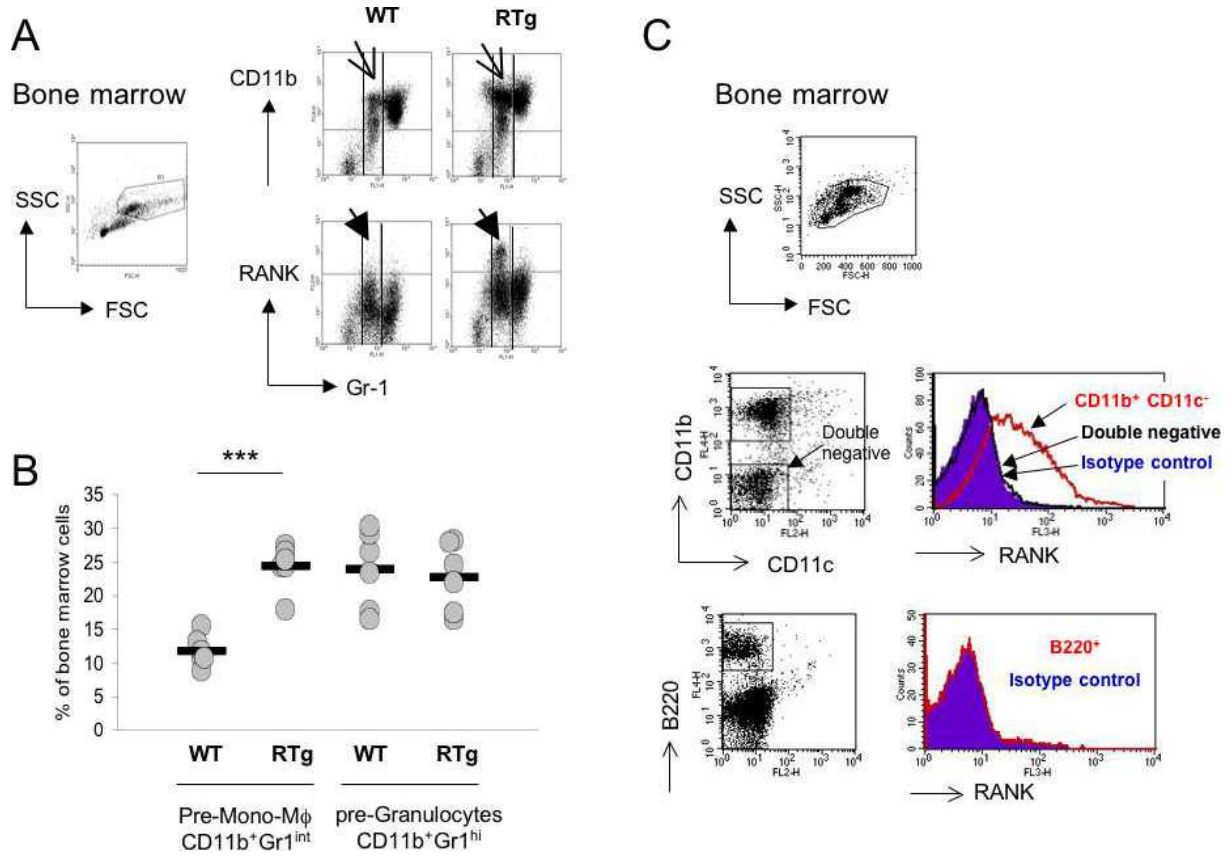
Supplementary figure 1: Bone marrow osteoclast-lineage precursors over-express RANK.

A. Bone marrow cells from WT and RTg mice were gated for large cells and expression of the myeloid cell marker CD11b, the granulocytic cell marker Gr-1 and RANK at the cell surface analyzed by flow-cytometry. Upper arrows point to a $CD11b^+Gr-1^-$ cell population over-represented in the RTg mice; lower arrows point to over-expression of RANK by the $CD11b^+Gr1^-$ pre-osteoclastic cell linage in the RTg mice. B. The percentage of $CD11b^+Gr-1^-$ cells is significantly increased in the bone marrow of RTg mice (*** $p<0.001$). Each data point corresponds to one mouse. The horizontal bar is the mean.
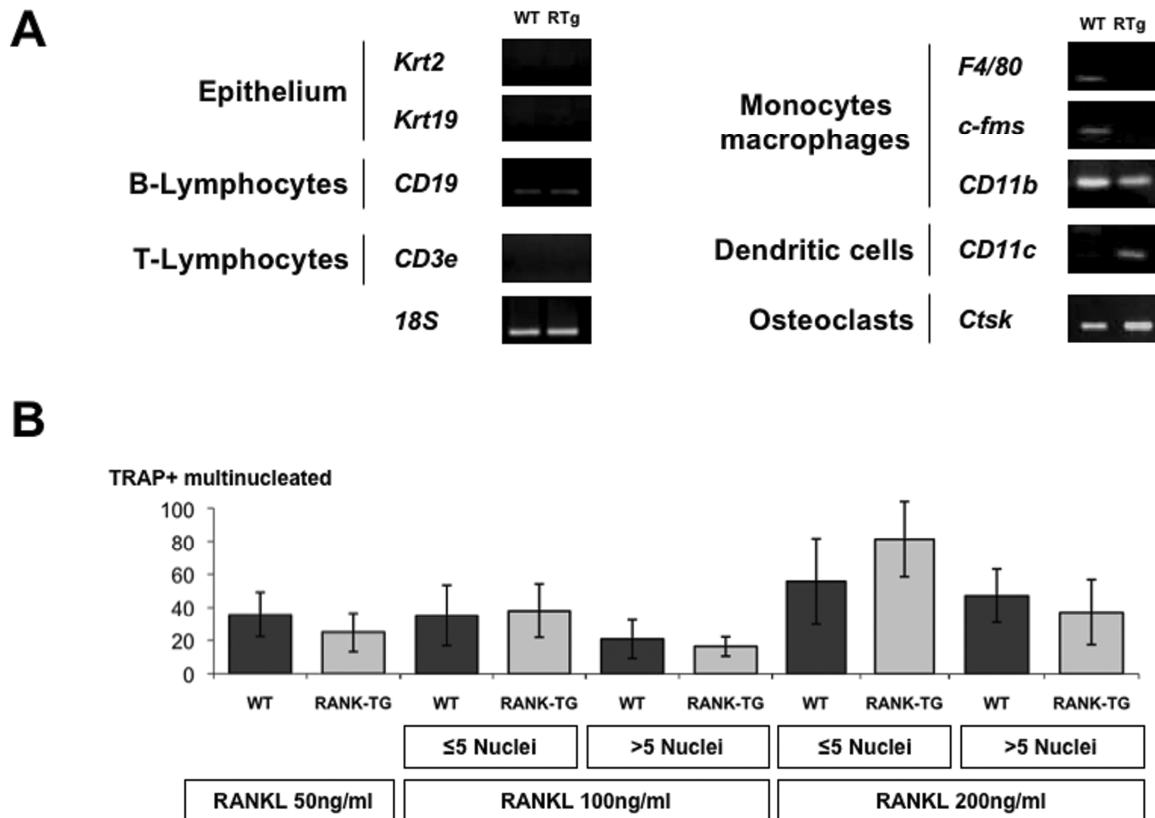
Supplementary figure 2: Normal alveolar bone cell lineages and osteoclast differentiation in RKTg mice.

A. RT-PCR performed on alveolar bone from WT and RTg mice to assess the presence of different cell lineages. B. Purified monocytes of WT and RTg mice were cultured in presence of different RANKL concentration and assessed for their differentiation into multinucleated TRAP+ osteoclasts.

The receptor activator of NF-κB (RANK) is known to control bone mass and development of the skin appendages. This, and its function in epithelial cell biology in general, incited us to investigate the role of RANK in skin and hair follicles (HFs). We show that mice deficient in RANK or RANK-ligand (RANKL) are unable to initiate a new growth phase of the hair cycle and display arrested epidermal homeostasis. Transgenic mice overexpressing RANK in the HF and administration of recombinant RANKL activate the hair cycle and epidermal growth. RANK is expressed by HF stem cells and RANKL is actively transcribed by the growing HF supporting a role of RANK-activation of stem cells for hair cycle entry.

In addition to its function in bone and skin, RANK is required for development of lymph nodes (LNs), a feature shared with lymphotoxin β receptor (LTβR). However, LTβR is further involved in the maintenance of LN organization, which had not been demonstrated for RANK. We therefore addressed the question of the function of RANK in LNs beyond development. For this, we took advantage of the transgenic mice overexpressing RANK in the HF, as they displayed a massive post-natal growth of skin-draining LNs. They displayed conserved proportions of hematopoietic and stromal cells, but an increase in the number of small B cell follicles. We showed that skin-derived RANKL induces LN stromal cell proliferation and expression of chemokines and adhesion molecules, resulting in the LN growth. This work highlighted an additional function for RANK-signaling in LNs, namely its control of LN plasticity, and underlines the importance of tissue-derived cues for secondary lymphoid organ homeostasis.

Le récepteur activant NF-κB (RANK) est connu pour son rôle dans le contrôle de la masse osseuse mais aussi dans le développement des appendices de la peau. RANK est également impliqué dans la biologie des cellules épithéliales, amenant ainsi à poser la question de son rôle dans la plus grande surface épithéliale du corps, à savoir la peau, et dans les follicules pileux (FP). Nous avons montré que les souris déficientes pour RANK ou RANK-ligand (RANKL) sont incapables d'initier une nouvelle phase du cycle pileux et qu'elles présentent une homéostasie de l'épiderme altérée. D'autre part, la surexpression de RANK dans les cellules souches des FP de souris transgéniques ainsi que l'administration de RANKL activent le cycle pileux et la croissance de l'épiderme. Les cellules souches du FP expriment RANK et RANKL est activement transcrit par le FP en croissance mettant en évidence le rôle de RANK dans l'activation des cellules souches pour l'entrée dans le cycle pileux.

En plus de sa fonction dans l'os et dans la peau, RANK est aussi requis pour le développement des ganglions lymphatiques (GL). Cette fonction est partagée avec le récepteur de la lymphotoxine β (LTβR) mais ce dernier est, de plus, impliqué dans le maintien de l'organisation du GL. Nous avons donc essayé d'apporter des éléments de réponse à la question de la possible fonction de RANK dans le GL après son développement. Pour ce faire, nous avons étudié des souris sur-exprimant RANK dans le FP, ces dernières développant une hyperplasie massive des GL drainant la peau. Ces GL hyperplasiques présentent des proportions de cellules hématopoïétiques et stromales normales mais une augmentation marquée du nombre de petits follicules B. Nous avons montré que le RANKL dérivé de la peau induit la prolifération des cellules stromales ainsi que l'expression de chemokines et de molécules d'adhésion, déclenchant ainsi la croissance du GL. Ces travaux ont permis de décrire une nouvelle fonction de RANK dans le GL, à savoir le contrôle de sa plasticité, et soulignent l'importance des signaux dérivés des différents tissus de l'organisme pour l'homéostasie des organes lymphoïdes secondaires.